

**Anaerobic Membrane Bioreactors under Extreme Conditions  
Mesophilic and Thermophilic Degradation of Phenol at High Salinity**

Muñoz Sierra, Julian

**DOI**

[10.4233/uuid:ca48d813-716b-43d9-b410-48462b7a7939](https://doi.org/10.4233/uuid:ca48d813-716b-43d9-b410-48462b7a7939)

**Publication date**

2022

**Document Version**

Final published version

**Citation (APA)**

Muñoz Sierra, J. (2022). *Anaerobic Membrane Bioreactors under Extreme Conditions: Mesophilic and Thermophilic Degradation of Phenol at High Salinity*. [Dissertation (TU Delft), Delft University of Technology]. <https://doi.org/10.4233/uuid:ca48d813-716b-43d9-b410-48462b7a7939>

**Important note**

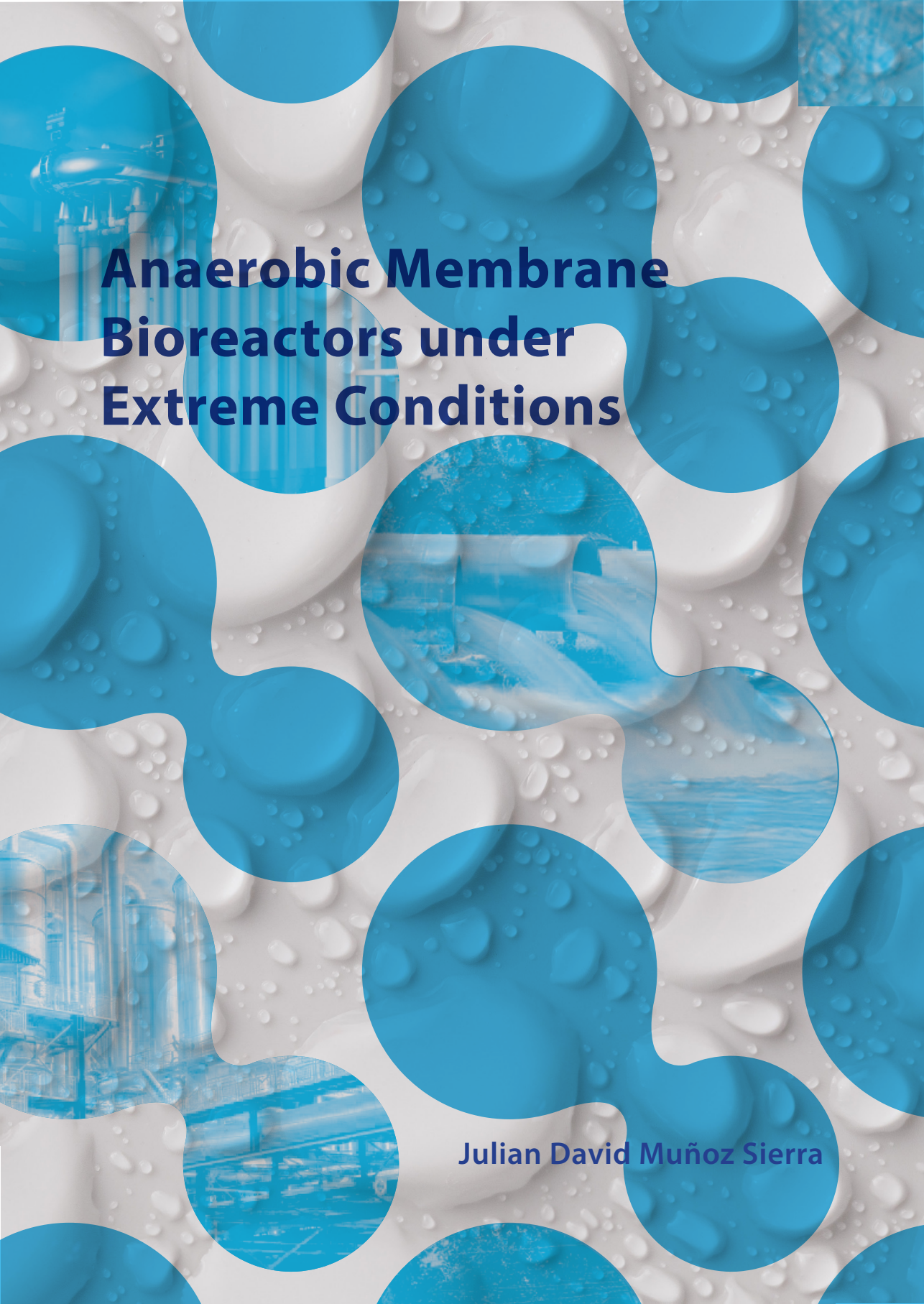
To cite this publication, please use the final published version (if applicable).  
Please check the document version above.

**Copyright**

Other than for strictly personal use, it is not permitted to download, forward or distribute the text or part of it, without the consent of the author(s) and/or copyright holder(s), unless the work is under an open content license such as Creative Commons.

**Takedown policy**

Please contact us and provide details if you believe this document breaches copyrights.  
We will remove access to the work immediately and investigate your claim.



# **Anaerobic Membrane Bioreactors under Extreme Conditions**

**Julian David Muñoz Sierra**

# **ANAEROBIC MEMBRANE BIOREACTORS UNDER EXTREME CONDITIONS**

Mesophilic and Thermophilic Degradation of Phenol at High Salinity



# **ANAEROBIC MEMBRANE BIOREACTORS UNDER EXTREME CONDITIONS**

Mesophilic and Thermophilic Degradation of Phenol at High Salinity

## **Proefschrift**

ter verkrijging van de graad van doctor  
aan de Technische Universiteit Delft,  
op gezag van de Rector Magnificus prof.dr.ir. T.H.J. van der Hagen,  
voorzitter van het College voor Promoties,  
in het openbaar te verdedigen op donderdag 20 januari 2022 om 15:00 uur

door

**Julian David MUÑOZ SIERRA**

Professional Doctorate in Engineering, Bioprocess Engineering,  
Technische Universiteit Delft, Nederland,  
geboren te Medellín, Colombia.

Dit proefschrift is goedgekeurd door de promotoren.

Samenstelling promotiecommissie bestaat uit:

Rector Magnificus	voorzitter
Prof.dr.ir. J.B van Lier	Technische Universiteit Delft, promotor
Dr.ir. H.L.F.M Spanjers	Technische Universiteit Delft, promotor

Onafhankelijke leden:	
Prof.dr. D. Stuckey	Imperial College London, United Kingdom
Dr. C.M. Plugge	Universiteit Wageningen, the Netherlands
Prof.dr.ir. I.Y. Smets	Katholieke Universiteit Leuven, Belgium
Prof.dr.ir. M.K. de Kreuk	Technische Universiteit Delft
Prof.dr. J.M. Lema	University of Santiago de Compostela, Spain
Prof.dr.ir. L.C. Rietveld	Technische Universiteit Delft, reservelid

This research was supported by the Dutch Technology Foundation (STW, Project No.13348), which is part of the Netherlands Organization for Scientific Research (NWO), partly funded by the Dutch Ministry of Economic Affairs. This research was co-sponsored by Evides Industriewater B.V and Paques B.V.

Keywords: AnMBR, high salinity, thermophilic, phenol, chemical wastewater, anaerobic treatment

Cover design: Proefschrift-aio.nl & J.D. Muñoz Sierra

Printed by Proefschrift-aio.nl

DOI 10.4233/uuid:ca48d813-716b-43d9-b410-48462b7a7939

ISBN 978-94-6384-284-6

Copyright © 2021 by J.D. Muñoz Sierra

All rights reserved. No part of the material protected by this copyright notice may be reproduced or utilized in any form or by any means, electronic or mechanical, including photocopying, recording, or by any information storage or retrieval system, without written permission from the author.

An electronic version of this dissertation is available at

<http://repository.tudelft.nl/>.

To my beloved Family





“...time was not passing...it was turning in a circle...”

Gabriel García Márquez, *One Hundred Years of Solitude*



# Preface

The origin of my dissertation, “Anaerobic Membrane Bioreactors under extreme conditions” lies in my passion for water technologies, my resilience, and my adaptability capacity. As the world moves further into fast-growing industrialization and generating a large amount of wastewater, there will be a greater need in the future to access energy-efficient technologies for water reuse and reclamation. It was part of my job to contribute to the state of the art of the development of AnMBRs for their potential application in treating chemical wastewaters under extreme conditions. I hope researchers and industry make use of the findings to do what we all should be doing, finding solutions to make the life of our future generations better.

I was engaged in writing a project research proposal for the STW Water technology call of 2013, that was formulated together with my supervisors, Dr. ir. Henri Spanjers, and Prof. dr. ir. Jules van Lier. The BioXtreme project was granted at the beginning of 2014. This project was very ambitious, but fortunately, I managed to answer most of the formulated questions, which I could not fit all in this book.

I would like to thank my supervisors for their guidance and support during this trajectory. I also thank you both, Dr. Marjet Oosterkamp and MSc. Victor Garcia, for fully trusting me leading the research and the BioXtreme team, and for being always willing to support and discuss ideas. I thank especially the visiting researchers Dr. Wei Wang, Dr. Daniel Cerqueda Garcia, and Dr. Carlos Lafita who kindly contributed to my work. To the project committee group, thank you for sharing your points of view on my research decisions and outcomes. All colleagues and staff from the Department of Water Management thank you for your wonderful cooperation. It was always fruitful to bat around ideas about my research and life with you. Last but not least, my family and Sandra, you kept me all the time motivated towards the completion of my dissertation. This journey without your love and unconditional support would not have been plausible.

This book is written to fulfill my goal to become a scientific researcher, a Doctor. I would like to invite you to provide any feedback that could contribute to my future research. Feedback truthfully made my research process and each of the chapters of this dissertation of better quality.

Utrecht, the Netherlands, March 2020



# Contents

<b>Preface</b>	<b>ix</b>
<b>Summary</b>	<b>xiii</b>
<b>Chapter 1</b>	
General Introduction	3
<b>Chapter 2</b>	
Trace metals leaching by sodium in AnMBR	33
<b>Chapter 3</b>	
Phenol conversion in AnMBR at high salinity	55
<b>Chapter 4</b>	
Effects of large salinity fluctuations on phenol conversion in AnMBR	83
<b>Chapter 5</b>	
Comparative performance of UASB and AnMBR treating phenolic wastewater at high salinity	111
<b>Chapter 6</b>	
Upward temperature shifts in mesophilic AnMBR treating saline phenolic wastewater	137
<b>Chapter 7</b>	
Feasibility of thermophilic phenol conversion in AnMBR at high salinity	169
<b>Chapter 8</b>	
Conclusions and Outlook	199
<b>Acknowledgments</b>	<b>211</b>
<b>Publications</b>	<b>213</b>
<b>About the author</b>	<b>217</b>



# Summary

Industrial wastewaters generated in chemical industries are often characterized by extreme conditions, such as the presence of complex, recalcitrant, and toxic aromatic compounds, high temperature, and high salinity. The mentioned conditions predominantly occur when chemical industries reduce process water use or strive for closing water loops. For wastewaters with extreme characteristics, conventional wastewater technologies have limitations. However, granular sludge-based or membrane-assisted anaerobic bio-treatment offers many advantages such as in-reactor augmentation of the required microbial species and long sludge retention times, ensuring high metabolic conversion rates per unit of reactor volume, besides low investment costs and low or negligible energy use. Frequently, auto-immobilization or stable anaerobic sludge granulation cannot be guaranteed under extreme conditions. Thus, the application of anaerobic membrane bioreactor (AnMBR) technology for pre-treating industrial wastewaters could offer an alternative solution with several advantages, such as full retention of specific and slow-growing microbial communities, effluents free of suspended solids, and system compactness.

The purpose of this thesis is to investigate the applicability of the AnMBR technology for the treatment of chemical wastewater under extreme conditions by studying the impact of high and fluctuating salinity, and high temperature on the conversion of phenol. Phenol was selected as a model aromatic compound because it is commonly found in chemical wastewaters, while it is also a known inhibitor for the anaerobic conversion process. Moreover, this thesis provides additional understanding of the AnMBR operation, including assessment of membrane resistance to filtration, microbial population dynamics under the different conditions. Three laboratory-scale AnMBRs and one upflow anaerobic sludge blanket (UASB) reactor were used to carry out the experiments at varied salinity, phenol concentration and temperature. Different operating conditions were tested to determine the limitations and robustness of the AnMBR and UASB reactor configurations. The high salinity, expressed as sodium concentration, varied between  $6 \text{ gNa}^+\cdot\text{L}^{-1}$  and  $37 \text{ g Na}^+\cdot\text{L}^{-1}$ . Influent phenol concentrations from  $0.1 \text{ gPh}\cdot\text{L}^{-1}$  up to  $5 \text{ gPh}\cdot\text{L}^{-1}$  were applied. The AnMBR operational temperature was mainly set to the mesophilic range at  $35^\circ\text{C}$ , but experiments were also performed in the hypermesophilic ( $40\text{-}45^\circ\text{C}$ ) and thermophilic ( $50\text{-}55^\circ\text{C}$ ) range.

During the start-up of the AnMBRs, the high salinity had a strong effect on biomass methanogenic activity. The applied high salinity resulted in sodium accumulation in the biomass, resulting in cation exchange and solubilization of trace metals, which became prone to wash-out. Consequently, the COD removal rate and the biomass particle size decreased. This study showed that doubling the supply of trace metals was required to distinctly increase the COD removal rate in the AnMBRs. In addition, the effects of long-term salinity increase were studied, focusing on phenol conversion, membrane filtration performance, and microbial community composition in the AnMBR. The increase in salinity adversely affected the transmembrane pressure, likely due to particle size reduction and the presence of small fines. Relative abundance of phenol-degrading bacteria increased upon adaptation of the microbial community to high salinity, which resulted in increased phenol conversion rates. Batch tests showed that, in addition to appropriate trace metals supplementation, a potassium to sodium ratio of 0.05 is required for improving COD removal.

Results showed that the AnMBR could overcome a gradual step-wise salinity increase to 20 gNa<sup>+</sup>·L<sup>-1</sup>. However, in practice, strong salinity fluctuations frequently occur, which can be attributed to process operation dynamics, cleaning, or water recycling. Therefore, the impact of high and fluctuating salinity on the anaerobic phenol conversion and membrane filtration in an AnMBR was also investigated. A step-wise increase in sodium concentration from 20 to 37 gNa<sup>+</sup>·L<sup>-1</sup> reduced the phenol and COD removal efficiencies to 86% and 84%, whereas large fluctuations between 8 and 35 gNa<sup>+</sup>·L<sup>-1</sup> decreased the efficiencies to 42% and 28%, respectively. However, the AnMBR was able to overcome the impact of the salinity fluctuations, maintaining and recovering phenol and COD conversion rates, even though microbial population richness and diversity were substantially reduced. Moreover, the resulting reduction in biomass particle size led to increased transmembrane pressures, exceeding 400 mbar, and the membrane resistance to filtration increased to 25 x 10<sup>12</sup> m<sup>-1</sup>. Based on these results, a comparison was made between the long-term performance of an AnMBR and a UASB under step-wise salinity increase and high specific phenol loading rates. The AnMBR exhibited a higher process stability and better performance than the UASB for the treatment of the synthetic phenolic wastewater over a range of 16–26 gNa<sup>+</sup>·L<sup>-1</sup>. At 26 gNa<sup>+</sup>·L<sup>-1</sup> and a phenol concentration of 3 gPh·L<sup>-1</sup>, the UASB biomass deflocculated, likely due to calcium wash-out, eventually leading to reactor failure. High salinity considerably decreased the biomass particle size in both reactors, but full biomass retention was ensured in the AnMBR. Additionally, as indicated by higher species evenness, the AnMBR showed higher methanogenic activity than the UASB.

In addition to high salinity and the presence of inhibitive substances, high temperature is a frequently encountered challenging extreme characteristic of industrial chemical wastewaters. Therefore, the susceptibility of an AnMBR to step-wise temperature shifts by 5°C from 35 °C to 55 °C was examined, and its bioconversion capacity treating phenol-containing wastewater at 16 gNa<sup>+</sup>·L<sup>-1</sup> was evaluated. Results showed that the phenol conversion process was less susceptible to the temperature increase than methanogenesis. Moreover, membrane filtration was negatively affected by the temperature increase coinciding with a 77% biomass particle size decrease and a higher content of microbial protein-like substances. Under mesophilic and hypermesophilic conditions (42-45°C), the specific phenol conversion capacity of the AnMBR at high salinity was higher compared to thermophilic conditions. However, because the operation at 55°C was only carried out during a short period, it remained unclear whether a stable phenol degrading methanogenic consortium can develop under thermophilic conditions. For that reason, the maximum conversion capacity of an AnMBR during long-term operation at 55°C, treating phenol-containing wastewater at 18 gNa<sup>+</sup>·L<sup>-1</sup> was assessed. COD and phenol removal efficiencies of about 95% were achieved. However, after exceeding a phenol loading rate of 20 mgPh.gVSS<sup>-1</sup>·d<sup>-1</sup>, the reactor phenol concentration increased, leading to deterioration of methanogenesis. Furthermore, the hydrogenotrophic methanogenic activity was a factor 2.3 higher than the acetoclastic methanogenic activity. Correspondingly, hydrogenotrophic methanogens were enriched while the acetoclastic Methanosaeta species were reduced.

This Ph.D. thesis shows the feasibility of the AnMBR as a reliable technology for the treatment of phenol-containing wastewaters under extreme conditions. The robustness exhibited to fluctuations in salinity, high phenol concentrations, and hypermesophilic conditions, provides a solid basis for further research and potential application.







1

# 1

## General Introduction



## 1.1. Introduction

### 1.1.1. Background

Global scarcity of freshwater is a large and rapidly growing problem. Water stress is projected to increase with the rise in global temperatures as a result of climate change. Increasing awareness of the need for sustainability during the last decades has encouraged actions towards solving environmental issues with a local or global impact. The United Nations have agreed that global development will be guided by a set of sustainable development goals (SDGs) (UN 2015). Important actions for achieving these goals are amongst others: promoting industries to recycle and reduce waste, changing the way of disposing of toxic waste and pollutants, encouraging water efficiency, and supporting treatment technologies for clean water and sanitation. Furthermore, global data on industrial water withdrawal (Figure 1.1) indicates that industry is a major consumer of water, which is estimated to be about 19% as a global average in relation to other sectors (Ritchie and Roser 2017, Vítězová et al. 2020). In industrialised countries, like the Netherlands, the industrial sector is responsible for up to 85-90% of the annual national water withdrawal (Aquastat 2019).

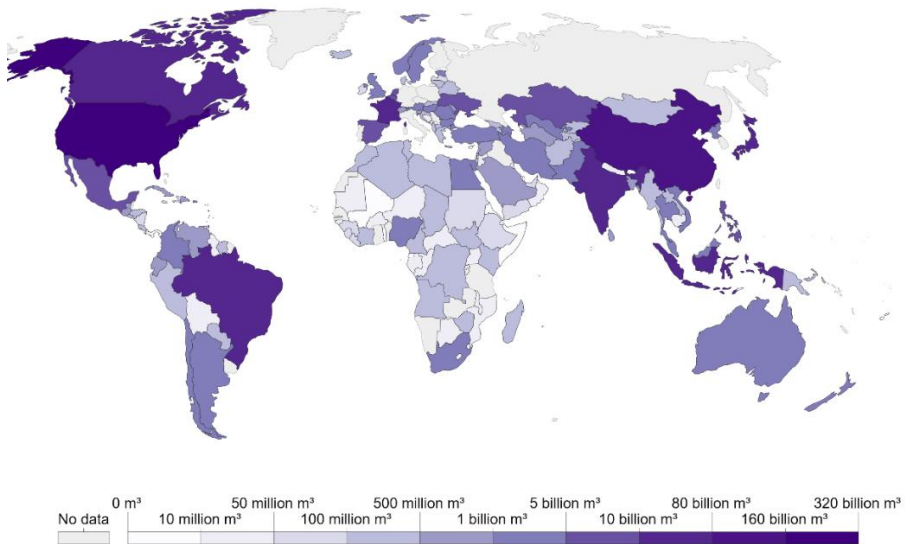


Figure 1.1 Industrial Water Withdrawal 2010 (Ritchie and Roser 2017)

The industrial water demand is increasing, especially in fast-developing economies, where a high amount of industrial wastewater is discharged by chemical industries (Kong et al. 2019b). Industrial water demand in 2025 is forecasted to double the level of the year 2000. Industrial activities are responsible for polluting adjacent surface water and ground water because of the inefficient management of water resources at the industrial premises. The massive production of synthetic organic chemicals intensifies the release of slowly biodegradable, refractory, or hazardous

compounds into the environment. Chemical and petrochemical industries have been identified as the primary producer of these types of wastes (Mishra et al. 2019, Tian et al. 2020).

Frequently, high-strength chemical wastewater streams are generated, which can severely pollute water bodies. Uncontrolled discharge of such wastewaters is prohibited, and if not treatable with current technologies they generally are further concentrated and subsequently incinerated at high costs and with a huge energy loss. Chemical wastewaters differ in strength, organic materials, pH, salinity, temperature, and biodegradability from other industrial sectors such as food processing. While many industrial wastewaters can be treated by biological processes, several compounds present in these chemical streams can be refractory or even toxic to microorganisms. The petrochemical waste streams often contain aromatic compounds such as phenols, terephthalates, aniline, formaldehyde, benzaldehydes, benzene, and toluene (Kleerebezem and Macarie 2003, Razo-Flores et al. 2006).

Up to date, there is still a lack of applications in the industrial sector that demonstrate proper biological treatment of these chemical streams because of toxicity, inhibition, low biodegradability, high energy demand, or overall non-feasibility. Among the state of the art biological wastewater treatment technologies, anaerobic digestion is considered a reliable and cost-effective biotechnology (Lettinga 2005, Lettinga 2014). Anaerobic treatment technologies have a high potential for the saving or even recovery of (biochemical) energy in the treatment of high-strength industrial wastewaters. Anaerobic processes are receiving renewed attention, owing to the ongoing concerns over increasing energy prices and greenhouse gas emissions, especially within the biorefinery (Zhen et al. 2019), waste to resources (Khan et al. 2016), and circular economy concepts (Song et al. 2018).

In the past decades, high-rate anaerobic reactors have been developed, which achieved a very competitive level in the industrial wastewater sector due to a i) high degree of reduction in sludge production, ii) high energy efficiency, and iii) small footprint. A sludge bed reactor is the most applied anaerobic treatment technology worldwide, with more than 4500 of these high-rate anaerobic reactors currently in operation (van Lier et al. 2020). This technology relies on the ability to retain a high concentration of biomass due to the formation of a dense sludge bed that consists of well settleable methanogenic sludge granules (Ozgun et al. 2013). The cases in which its implementation has not been successful mainly concern wastewater streams that are characterised by extreme conditions. Such extreme wastewater characteristics include high suspended solids, high temperature, high fat, oil, and grease (FOG) content, drastic fluctuations in organic load, high salinity, and presence of toxicity. Under extreme conditions, biomass granulation or immobilization cannot be guaranteed, leading to biomass washout, and thus biological activity and reactor loading capacity are reduced (Derehi et al. 2012). However, high-rate reactors equipped with membrane-based biomass retention, denominated anaerobic membrane bioreactors (AnMBR), offer an alternative and promising solution. This is particularly important in cases where established technologies, i.e., high-rate granular sludge bed reactor systems, such as UASB, EGSB, and IC, may fail, or where very high effluent water quality is required for water recycling (Cornelissen et al. 2001, van Lier et al. 2001, van Lier et al. 2015).

### 1.1.2. Anaerobic membrane bioreactors (AnMBRs) as the technology to overcome extreme conditions

In the upcoming years, chemical wastewater streams will become more extreme because water management policies encourage the reduction in industrial water footprint, stimulating water reuse and resource recovery (Dereli et al. 2012, Kong et al. 2019b, Lin et al. 2013). Sharp fluctuations in pH, temperature, organic loading, and salinity are often due to process operation changes, cleaning, and maintenance activities (Kleerebezem 1999, Kleerebezem et al. 1997, van Lier et al. 2020, Vyrides and Stuckey 2017). Particularly for the extreme industrial wastewaters, membrane assisted bio-treatment such as the AnMBR, offers several advantages. AnMBRs produce high-quality effluents free of suspended solids, simplifying effluent upgrading techniques. AnMBRs achieve complete retention of biomass, regardless of the biomass settling or granulation properties. They can also augment specialized microbial communities that can degrade specific pollutants in the wastewater at maximized sludge retention, ensuring high metabolic conversion per unit of reactor volume. Furthermore, AnMBRs combine the anaerobic degradation process in bioreactors with direct solids–liquid separation by a membrane (ultra) filtration, and its compactness allows installation even inside buildings (Figure 1.2).



Figure 1.2 Industrial AnMBR (Memthane®, courtesy Biothane) at a food company; left: external crossflow membrane skid, right: anaerobic mixed tank bioreactor.

Even though AnMBR technology implementation started to emerge in the early 2000s, the application of this technology is still in its development stage (Liao et al. 2006, Lin et al. 2013), requiring more research and industrial application (Skouteris et al. 2012, Stuckey 2012). Increased research interest in AnMBR is attributed to i) the reduction in membrane module costs, ii) increased industrial water reuse, iii) increasingly stringent water discharge requirements, iv) interest in reduced energy demands and environmental impacts, and v) interest in recovering resources (Smith et al. 2012). New reactor configurations have been researched to make the technology more energy-efficient, which could increase its commercial applicability (Maaz et al. 2019). In addition, AnMBR design and operation have not yet reached maturity, and further research is needed to maximize

process efficiency (Robles et al. 2018). As a result, the number of published scientific papers about AnMBR and AnMBR for industrial applications has noticeably increased during the last ten years (Figure 1.3. ). Note that even though published research on industrial wastewater treatment with AnMBRs is relatively modest, in terms of full-scale applications, industrial AnMBRs are the majority. The latter might be explained by the fact that industrial flows are generally small and of interest for a specific industry only. Most of the existing full-scale AnMBR plants are being applied to food processing wastewater streams, but the number of applications in the non-food sector is currently growing (van Lier et al. 2015).

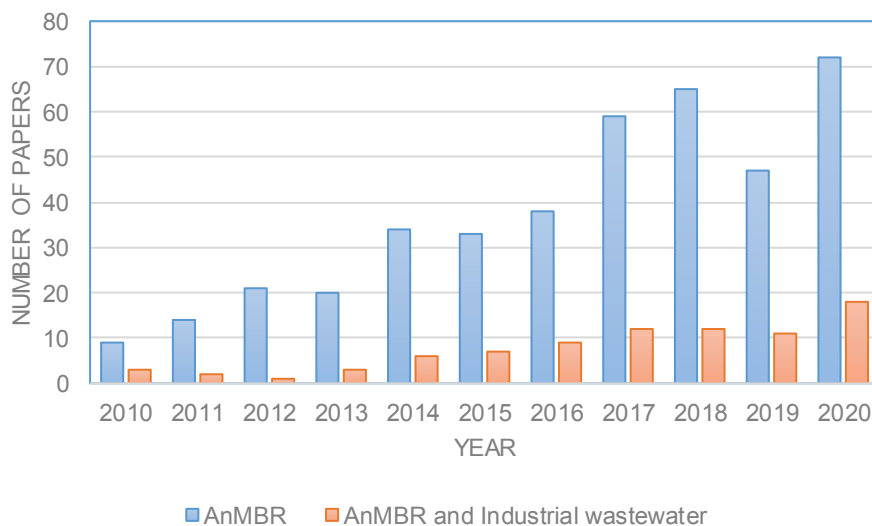


Figure 1.3 Indicative number of scientific papers of AnMBRs for industrial applications over the past ten years (search via Science Direct).

Recent studies have shown that AnMBR can be used to treat wastewaters from different industries such as pulp and paper (Gao et al. 2016, Gao et al. 2011, Gao et al. 2010, Lin et al. 2011); coal and coke (Van Zyl et al. 2008, Yun et al. 2019), textile and tannery (Baêta et al. 2013, Umaiyakunjaram and Shanmugam 2016, Yurtsever et al. 2020, Yurtsever et al. 2017, Zhang et al. 2018), pharmaceutical (Chen et al. 2020, Chen et al. 2018, Hu et al. 2018, Huang et al. 2018, Kaya et al. 2017, Ng et al. 2015, Svojítka et al. 2017); and chemical (Bhattacharyya et al. 2013, Kong et al. 2019a, Li et al. 2020, Wang et al. 2014, Wang et al. 2019, Wang et al. 2017a) (Table 1.1).

Pulp and paper industries generate varieties of wastewaters depending on the type of the pulping process, the type of paper and the pulped material. Gao et al. (2016) used a submerged AnMBR to treat high strength thermo-mechanical pulping pressate wastewater and obtained  $83\pm 4\%$  of chemical oxygen demand (COD) removal efficiency. Because of the variability of industrial wastewaters, Gao et al. (2010) demonstrated that high pH shocks can induce breakage of sludge flocs, partial inhibition, and deteriorated membrane filtration in an AnMBR for pulping pressate



wastewater. Moreover, Gao et al. (2011) showed that thermomechanical pulping pressate can be treated by using an AnMBR at operating temperatures of 37, 45 and 55 °C to achieve a COD removal efficiency of 76–83%. White water treatment is feasible in AnMBRs with organic removal of about 90% (Lin et al. 2011).

Coke wastewater is a toxic industrial effluent that contains high concentrations of ammonia, cyanide, thiocyanate, and phenols. Yun et al. (2019) treated low-grade coal wastewater in an AnMBR by adding yeast waste as a cosubstrate. Methanogenesis was completely suppressed without the addition of cosubstrate due to the presence of recalcitrant compounds (4-methyl-phenol, 1,2-benzenediol, phenol, and 4-methyl-1,2-benzenediol). Notably, some studies have focused on the aerobic degradation of these compounds after anaerobic and anoxic treatment steps (Zhao et al. 2009, Zhao et al. 2010). Likewise, Van Zyl et al. (2008) applied a submerged AnMBR to treat wastewater from a fuel synthesis process from coal. The system was operated at an organic loading rate (OLR) of up to 25 kgCOD·m<sup>-3</sup>·d<sup>-1</sup>. The results showed that a COD conversion to methane of more than 98% can be obtained. These results indicate that AnMBRs can have high loading rates and high treatment efficiencies for petrochemical wastewater.

In the textile industry, various processes are used and many of them generate wastewater. Textile wastewater contains organic compounds such as starch, surfactants, softeners, fixers, and dyes. Baêta et al. (2013) showed that a submerged AnMBR had a better degradation performance than a UASB reactor, achieving COD removal efficiencies in the range of 73-94%. Tanneries are also considered a major contributor to chemical wastewater discharges, which normally are also saline. For example, Umayyakunjaram and Shanmugam (2016) treated high suspended solids raw tannery wastewater in a submerged AnMBR of 80 L. Results showed a COD removal efficiency of about 90%, which suggest the potential of AnMBR for treating raw tannery wastewater, reducing the costs of chemicals for flocculation and chemical sludge disposal. Furthermore, Yurtsever et al. (2017) also showed promising results with azo-dye wastewater, with an average COD removal efficiency of 86%, and a complete decolorization (>99%) in an AnMBR at different solids retention times (SRTs). Furthermore, in another effort to treat textile wastewater containing azo-dye remazol brilliant violet (RBV)-5R, Yurtsever et al. (2020) investigated the performance of an anaerobic dynamic membrane bioreactor, in which the cake layer on a support medium act as the actual membrane (Ersahin et al. 2012, Ersahin et al. 2014). Almost complete color (>99%) and high COD (95–97%) removal efficiencies were obtained by using nylon support of 20, 53, and 100 µm at relatively high fluxes (5-35 Lmh). In a comparative study, Zhang et al. (2018) found a 20% higher COD removal efficiency of an AnMBR treating dyeing wastewater compared to a sludge-bed based reactor configuration with a similar biomass concentration.

Other examples include pharmaceutical industrial processes that generate wastewater containing refractory organic compounds and inorganic salts. Chen et al. (2020) operated two AnMBRs with OLRs increasing from 1.5-7.0 with industrial pharmaceutical wastewater, achieving stable COD removal efficiencies of 89±2% and 94±2%, without and with biochar addition respectively. Also, halogenated organic compounds (AOX) were removed on average at about 56.2 – 61.5%. In another study, simulating chemical synthesis pharmaceutical wastewater, Chen et al. (2018) observed average total removal efficiencies of m-cresol and isopropyl alcohol of 95% and 96%, respectively,

with a pilot-scale AnMBR at different hydraulic retention times (HRTs). Among pharmaceutical wastewater, one of the main pollutants is tetrahydrofuran (THF), and is highly toxic. Hu et al. (2018) observed COD and THF removal efficiencies of 95% and 98%, respectively, when the HRT of a pilot AnMBR was longer than 24 h. Furthermore, Huang et al. (2018) operated an AnMBR to treat wastewater containing antibiotics, in which the highest removal efficiencies of amoxicillin, ceftriaxone, cefoperazone, and ampicillin were  $73 \pm 4\%$ ,  $48 \pm 2\%$ ,  $79 \pm 4\%$ , and  $35 \pm 3\%$ , respectively. The obtained total COD removal efficiency was 87 and 94% at HRTs of 24 and 48 h, respectively. Ng et al. (2015) bioaugmented an AnMBR with coastal sediment to treat saline pharmaceutical wastewater, obtaining higher total COD removal efficiency of approximately 60% compared to 46% of the control AnMBR, at an OLR of  $13 \text{ kgCOD}\cdot\text{m}^{-3}\cdot\text{d}^{-1}$  and HRT of 30 h. Svojitka et al. (2017) tested a pilot AnMBR treating wastewater and waste organic solvents originating from pharmaceutical and chemical industries. Varying COD removal efficiencies of about 78% were observed when the AnMBR was operated with pharmaceutical wastewater components as the sole carbon source. COD removal of up to 97% was obtained by adding methanol whereas low performance was observed with the waste organic solvents as co-substrate.

Recalcitrant solvents such as *N,N*-Dimethylformamide (DMF) are widely used as a water-miscible polar solvent in a wide variety of chemical industries. Kong et al. (2019a) successfully treated high-strength DMF-containing wastewater with an AnMBR achieving up to 95% COD removal efficiency, corresponding to a maximum of 96% removal of DMF. The high performance was achieved at OLRs of  $3.14\text{--}6.54 \text{ kg COD}\cdot\text{m}^{-3}\cdot\text{d}^{-1}$  and HRT of 24 h. Furthermore, Li et al. (2020) compared the same AnMBR with a UASB treating similar DMF containing wastewater, showing that the increase in OLR significantly limited the hydrolysis of DMF resulting in a decreased performance in both reactors.

Wang et al. (2014) investigated the performance of an AnMBR for removing five different polycyclic musks (PCMs), which are common active ingredients of personal care and household cleaning products. Stable removal over 95% was achieved for each PCM. Also with chemical wastewater streams, Wang et al. (2017a) applied an AnMBR equipped with ceramic membranes to treat phenolic wastewater, containing mainly phenol and quinoline. The reactor achieved 99% of phenol, 98% of quinoline, and 88% of COD removal, showing a quick establishment of phenol- and quinolone-degrading consortia in the AnMBR. The removal efficiency of phenol exceeded 40% when the wastewater permeated through the membrane cake layer. Moreover, in a follow-up study, removal efficiencies higher than 99% were achieved for both compounds, with an overall COD removal of 95% (Wang et al. 2019).

This recent interest in AnMBR treatment of chemical wastewater is encouraging, as historically, the chemical industry has preferred aerobic treatment over anaerobic treatment, if considering biological treatment at all. The introduction of anaerobic advanced treatment technology will reduce the energy costs for chemical wastewater treatment (McCarty et al. 2011, Nguyen et al. 2020). And as reviewed by Dvořák et al. (2016), both from research and the industrial community, there is an interest to boost the development of the AnMBR as a solution for treating industrial chemical wastewater. Apparently, there is an urgent need for cost-effective treatment techniques for the recovery of process waters under extreme conditions for water reuse and recycling. In fact, the

absence of such a treatment technique hinders the development of cleaner production in the chemical industry.

### 1.1.3. Extreme conditions in chemical wastewaters

Extreme industrial wastewater characteristics negatively impact the anaerobic reactor process performance. Also, under extreme conditions, adequate retention of slow-growing biomass is essential for successful anaerobic high-rate treatment. In particular, difficulties are typically associated with the high organic strength of chemical wastewaters, and the three most critical extreme conditions identified are related to salinity, the toxic compounds load, and high temperature (Sipma et al. 2010).

#### 1.1.3.1. High salinity

Chemical, textile, pharmaceutical, and petroleum industries are considered the primary producers of highly saline wastewater (Lefebvre and Moletta 2006, Ng et al. 2005, Yang et al. 2013, Zhao et al. 2020). Wastewater streams with saline and hypersaline characteristics are estimated to be approximately 5% of the world's total industrial effluents (Lefebvre et al. 2007, Praveen et al. 2015). A high concentration of salts exhibits severe effects on the environment and the performance of wastewater treatment techniques such as filtration, photocatalysis, Fenton, MBR, UASB, etc (Srivastava et al. 2021). Limited information is available on the anaerobic degradation of wastewater components under saline and hypersaline conditions (Le Borgne et al. 2008). Inorganic salts in chemical wastewaters are mainly in the form of sodium chloride (NaCl). High concentrations of sodium chloride negatively impact the biodegradation process, mainly attributed to the sodium ions (Guerrero et al. 1997, Rinzema et al. 1988, Vallero et al. 2003b, Vallero et al. 2004). At high concentrations, sodium could readily disturb the activity of microorganisms and hamper their metabolism (Chen et al. 2008).

Previous studies indicated that high sodium concentrations can reduce the efficiency of an anaerobic treatment (Lefebvre et al. 2007, Vallero et al. 2003a) and can induce the disintegration of flocs or granules, leading to operational challenges such as biomass washout in granular sludge bed reactors (Ismail et al. 2008, Pevero et al. 2007). At high salinity, granule strength is reduced by the exchange of calcium with sodium ions (Ismail et al. 2010, Jeison et al. 2008a). Ismail et al. (2010) observed a five-fold increase in calcium concentration in the bulk liquid with an exposure of thirty days to a sodium concentration of  $20 \text{ gNa}^+\cdot\text{L}^{-1}$ . As a consequence, the observed loss in granule strength also reduced the biomass particle size (Jeison and van Lier 2007a). De Vrieze et al. (2016a) also suggested that an increase in conductivity to  $45 \text{ mS}\cdot\text{cm}^{-1}$  caused granular sludge disintegration and biomass washout. Jeison et al. (2008a) observed that a high sodium concentration over  $7 \text{ gNa}^+\cdot\text{L}^{-1}$  in a UASB resulted in a decrease and inhibition of acetoclastic methanogens. Other studies, such as that of Aslan and Şekerdağ (2016), showed that COD removal considerably decreased at about  $20 \text{ gNa}^+\cdot\text{L}^{-1}$ , when treating saline wastewater in a UASB reactor. De Vrieze et al. (2016b) also reported a low COD removal of  $4.9 \pm 0.8\%$  at  $20 \text{ gNa}^+\cdot\text{L}^{-1}$  and, thereby, a severe inhibition of methanogenesis in CSTR digesters. Studies have suggested that reduction in sodium susceptibility over time is likely to be expected due to long-term acclimation and growth of halo-tolerant species in the methanogenic sludge. Here, also attention to the trace metals (TM) content, fractionation,

Table 1.1 Progress on AnMBRs treating industrial chemical wastewater.

Industry	T [°C]	Wastewater	Influent COD/OLR [g/L]/[kg COD/m <sup>3</sup> d]	COD removal efficiency [%]	Flux [L/m <sup>2</sup> h]	HRT [d]/SRT [d]	Configuration/T type of membrane	Reactor volume [L]	Ref.
Pulp and paper	35±1	White water (thermochemical pulping pressate wastewater)	4.3-5.1 / 2.0-3.5	83±4	4.5-8.6	N.A / N.A	Submerged / Hollow-fiber PVDF	6.0	(Gao et al. 2016)
			2.8-3.4 / 2.4±0.4	30-90	5.2±0.5	N.A / 280	Submerged / Flat sheet PVDF	10.0	(Gao et al. 2010)
	37±1	White water (thermochemical pulping pressate wastewater)	2.8-3.5 / 2.6-4.8	90	4.8-9.1	N.A / 280	Submerged / Flat sheet PVDF	10.0	(Lin et al. 2011)
			2.1-3.6 / 2.6±0.5	53-83	5.7-6.9	N.A / 350	Submerged / Flat sheet PVDF	10.0	(Gao et al. 2011)
Coal and coke, petrochemical	35±1	Low grade coal wastewater + glucose / yeast waste	2.0 / 1.0	0-58	0.14	1.0 / N.A	Submerged / Hollow fiber PVDF	2.0	(Yun et al. 2019)
			18 / <25	98	1.5-4.5	1.3/175	Submerged / Flat sheet	23.0	(Van Zyl et al. 2008)
	35	Azo dye remazol yellow gold RNL + ethanol	N.A/0.5-0.6	73-94	0.18	1.0 / N.A	Submerged / Hollow fiber	3.25	(Baeta et al. 2013)

N.A	glucose/yeast extract Industrial high suspended solids raw tannery wastewater	11.2-12.9/6.0	28-90	6.8	1.66 / N.A	Submerged / Flat sheet PVDF	80.0	(Umaiya kumar and Shanmug am 2016) (Yurtseve et al. 2017) (Yurtseve et al. 2020) (Zhang et al. 2018)
N.A	Azo dye Remazol Brilliant Violet 5R (RBV-5R) and glucose	2.0 / 1.0	86	4.22- 8.51	2.1 ± 0.13 / inf, 60,30	Submerged / Flat sheet PES	5.7	
33±2	Azo dye Remazol Brilliant Violet 5R (RBV-5R)	1.0 / N.A	95-97	5.0 – 35.0	N.A / inf.	Submerged / Flat sheet Nylon mesh	4.0	
34±1	Industrial high chroma- dye wastewater	1.5-9/1.3-1.5	70	5.0	1.0 / N.A	Submerged / Flat sheet Ceramic	3.0	
32±2	Industrial pharmaceutical wastewater with high organic matter, AOX, and salinity.	1.5-7.0/1.5-7.0	89-94	2.3	1.0 / N.A	Submerged/ Hollow fiber PVDF	5.5	(Chen et al. 2020)
35 ± 1	Pharmaceutical wastewater containing m-cresol and isopropyl alcohol.	4.2-5.1/N.A	81-96	4.6-18.3	0.5-2.0 / N.A	Submerged / Hollow Fiber PVDF	4400	(Chen et al. 2018)
35 ± 1	Tetrahydrofuran pharmaceutical wastewater + glucose β-lactams antibiotics pharmaceutical wastewater	4.3-5.1/2.2-9.9	95	N.A	0.5-2.0 / N.A	Submerged / Hollow Fiber PVDF	4400	(Hu et al. 2018)
		4.4-5.1/2.4-4.5	87-94	N.A	1.0-2.0 / 250	Sidestream / Hollow fiber PVDF	180	(Huang et al. 2018)

35	Etodolac chemical synthesis wastewater from the pharmaceutical industry	20-23/0.3-0.5	85-90	0.9-3	N.A / inf.	Submerged / Flat Sheet PES, Hollow Fiber PP	4.0	(Kaya et al. 2017)
35	Saline pharmaceutical wastewater	16.3/1.7-13	46-60	6	1.28 / 100	Submerged / Hollow Fiber PVDF	10.0	(Ng et al. 2015)
35-37	Industrial pharmaceutical wastewater + methanol + waste organic solvents	1.5-44/0.6-14	44-94	8.4	1.7-5.0/120 - 450	Sidestream / Tubular Ceramic	50.0	(Svojitka et al. 2017)
35	Acrylic acid, acetic acid, maleic acid, isopropanol, and formaldehyde.	85/1.5 – 3.4	99	0.13	25.0 / N.A	Submerged / Flat Sheet	25.0	(Bhattacharya et al. 2013)
35	Solvent wastewater with N, N-dimethylformamide.	2.0/3.1 -10.2	23-96	N.A	0.3 – 1.0 / N.A	Submerged / Flat sheet CPE	7.0	(Li et al. 2020)
35	Solvent wastewater with N, N-dimethylformamide.	1.9-2.0/3.1 - 10.2	14-95	3.0 - 9.1	0.3 – 1.0 / N.A	Submerged / Flat sheet CPE	7.0	(Kong et al. 2019a)
35	Polycyclic musks (PCMs) wastewater (HHCB, AHTN, AHDI, ATTII, DPMD)+ glucose	N.A/N.A	84±2	2.4	4.0 / 150	Sidestream / Tubular Ceramic	30.0	(Wang et al. 2014)
35 ± 1	Phenol and quinoline containing wastewater	2.5/1.75	88	N.A	2.0 / N.A	Sidestream / Tubular ceramic	6.2	(Wang et al. 2017a)
35 ± 1	Phenol and quinoline containing wastewater	3.5/4.1	95	4.3	2.0 / N.A	Sidestream / Tubular ceramic	6.2	(Wang et al. 2019)

and speciation is required (Fermoso et al. 2009, van Hullebusch et al. 2016) because their bioavailability under high salinity should be guaranteed for the well-functioning of the anaerobic conversion process (Osuna et al. 2004). In addition, Gagliano et al. (2017) found that a potassium concentration of  $0.7 \text{ gK}^+\cdot\text{L}^{-1}$  alleviates the negative effect of  $20 \text{ gNa}^+\cdot\text{L}^{-1}$  in a UASB.

In AnMBRs, the presence of small particle sized sludge has a substantial influence on cake layer compaction, increasing the overall membrane resistance to filtration (Hemmelmann et al. 2013, Jeison et al. 2009a). Hemmelmann et al. (2013), studying the treatment of protein-containing saline wastewater at  $25 \text{ gNa}^+\cdot\text{L}^{-1}$ , suggested that full biomass retention provided by membrane filtration enables efficient bioconversion, but membrane filtration may be restricted to low fluxes, because biomass develops as single cells. In this regard, Yang et al. (2014) suggested that high sodium concentrations promote the formation of a more compact gel layer. Moreover, Yurtsever et al. (2016) showed that salinity induces the formation of large molecules, which are detected as foulants in the gel/cake layer and which may originate from biomass soluble microbial products (SMPs). Vyrides and Stuckey (2011) inferred that the cake layer was the main cause of increased membrane resistance of an AnMBR under saline conditions ( $13.8 \text{ gNa}^+\cdot\text{L}^{-1}$ ).

### 1.1.3.2. Fluctuating salinity

In most of the conducted researches, a gradual increase in salinity was investigated. Song et al. (2016) showed that a step-wise increase in the sodium concentration beyond  $4 \text{ gNa}^+\cdot\text{L}^{-1}$  reduced the COD removal efficiency to values below 80%. Similarly, by sequentially duplicating the salinity from 0 to  $16 \text{ gNa}^+\cdot\text{L}^{-1}$ , a decrease in the COD removal efficiency from 96% to 78% was observed (Chen et al. 2019). Jeison et al. (2008b) treating saline acidified wastewater from 6 to  $24 \text{ gNa}^+\cdot\text{L}^{-1}$ , found a severe accumulation of propionate at  $24 \text{ gNa}^+\cdot\text{L}^{-1}$ . Propionate oxidizers have less adaptation potential to high sodium concentrations (Feijoo et al. 1995).

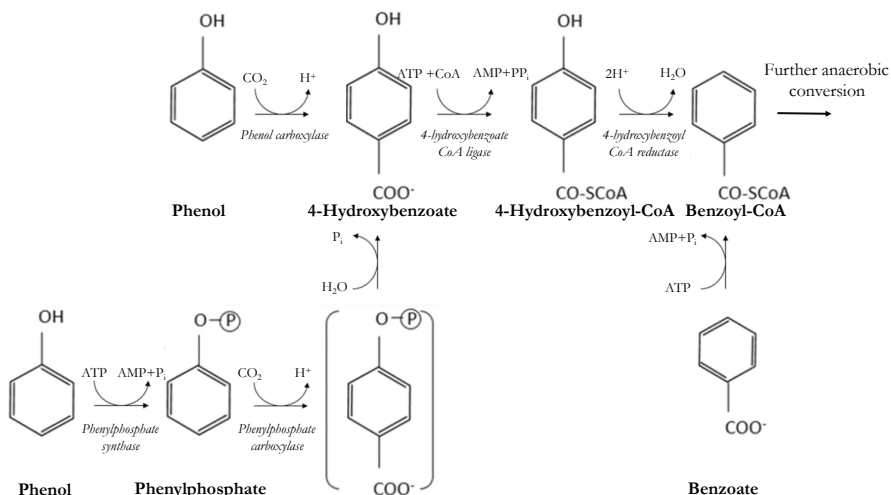
In industrial settings, salinity fluctuations may occur owing to process dynamics, cleaning activities, or water recycling (Vyrides 2015). Vyrides et al. (2010) investigated the performance of a submerged AnMBR reactor by addition of osmolytes after consecutive step-wise increase/decrease of the salinity from  $0.08 \text{ gNa}^+\cdot\text{L}^{-1}$  to  $13.8 \text{ gNa}^+\cdot\text{L}^{-1}$ . Their results showed that a decrease in salinity improved the performance of the reactor. Praveen et al. (2015) suggested that once a microbial community is acclimated to a certain salt concentration, it can be rapidly lost if the concentration is changed. Salt concentrations higher than  $10 \text{ g}\cdot\text{L}^{-1}$  induce disintegration of cells because of plasmolysis and dehydration (Wood 2015). Biological reactions need to yield sufficient energy to the microorganisms for osmotic adaptation and survival in a high salinity environment (Lay et al. 2010). The addition of several compatible solutes was found to alleviate sodium inhibition and contribute to fast osmotic adaptation, whereas the osmolyte glycine betaine was found to be the most effective (Vyrides and Stuckey 2009).

Additionally, forward osmosis-AnMBR technology with transient salinity accumulation and decrease within each cycle has gained interest, with potential applications in both industrial and municipal wastewater treatment (Lutchmiah et al. 2014, Schneider et al. 2021, Vinardell et al. 2020).

### 1.1.3.3. Toxicity

Chemical wastewaters are often laden with toxic compounds that are (partly) biodegradable (e.g., formaldehyde, cyanide, phenols, chlorophenols, aromatics) or inert, such as heavy metals (Sipma et al. 2010). These wastewaters are often also loaded with salts and may contain refractory aromatic compounds (Ferrer-Polonio et al. 2016). Phenolic compounds are toxic organics that are widely present in industrial wastewater streams such as those coming from coal gasification, coke, pulp-paper manufacturing, pharmaceutical and oil-refining (Wang et al. 2017a, Wang et al. 2017c). Phenol is an aromatic compound that has served as a reference model for treating chemical wastewaters in various studies. Phenol is a key intermediate in the anaerobic conversion of many aromatics (Busca et al. 2008, Fuchs 2008). Anaerobic biomass exhibits tolerance towards phenol (Fang and Chan 1997). Some phenol-degrading bacteria can utilize phenol at a low concentration as their carbon source. However, as the concentration increases, the effect of its biotoxicity also increases, thus the growth and bioconversion capacity will be progressively inhibited (Hou et al. 2019).

A.



B.

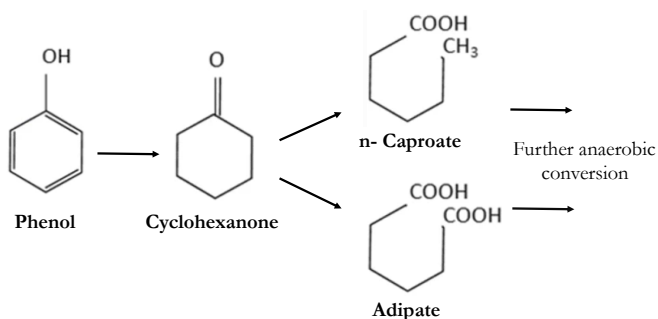


Figure 1.4 Anaerobic phenol conversion pathways. A. Via 4-hydroxybenzoate. B. Via n-caproate



Anaerobic phenol degradation pathways have been described either via 4-hydroxybenzoate or via n-caproate (Tomei et al. 2021). Strict anaerobic bacteria, are able to convert phenol directly to 4-hydroxybenzoate by a 4-hydroxybenzoate carboxylase (Huang et al. 1999). Phenol can also be converted to phenylphosphate by an ATP-dependent phenylphosphate synthase, followed by a para-carboxylation to 4-hydroxybenzoate by a phenylphosphate carboxylase of anaerobic denitrifying bacteria (Tschuch and Fuchs 1989). In both pathways, the 4-hydroxybenzoate is activated to a CoA-thioester and finally reduced to benzoyl-CoA for further anaerobic conversion (Schink et al. 2000, Tomei et al. 2021). In the carboxylic acid route, phenol is first reduced to cyclohexanone and then to n-caproate, which is  $\beta$ -oxidised to fatty acids. Previous studies inferred that this pathway occurs under thermophilic conditions (Evans and Fuchs 1988, Fang et al. 2006). However, Hoyos-Hernandez et al. (2014) have demonstrated that thermophilic phenol degradation is also possible via the benzoate conversion pathway.

In the last decade, anaerobic technologies such as the UASB reactor, anaerobic sequencing batch reactor (AnSBR), anaerobic fluidized bed reactor (AFBR), anaerobic hybrid reactors (AHR) (De Amorim et al. 2015, Franchi et al. 2020, Ramakrishnan and Surampalli 2013, Rosenkranz et al. 2013, Wang et al. 2011a, Wang et al. 2017b) and, more recently, the AnMBRs were applied to treat wastewaters containing phenolic compounds under mesophilic conditions (this thesis).

Wang et al. (2011a) investigated a UASB reactor for treating coal gasification wastewater at 37°C, and obtained maximum COD and total phenols removal of 55–60% and 58–63%, respectively. Rosenkranz et al. (2013) obtained phenol conversion rates up to 31 mgPh-VSS<sup>-1</sup>d<sup>-1</sup> in synthetic phenol-containing wastewater by a mesophilic AnSBR. Similarly, Franchi et al. (2020) obtained COD removal efficiencies higher than 90% in an AnSBR. De Amorim et al. (2015) investigated an AFBR system and achieved phenol and COD removal efficiencies in the range of 85–99%. Wang et al. (2017b) reported stable biomass activities of the phenolics degraders and methanogens at influent total phenols (TPh: phenol, catechol, resorcinol, and hydroquinone) concentrations in the range of 100–500 mgTPhL<sup>-1</sup>. However, other studies reported inhibition of phenol conversion at a concentration of 600 mgPhL<sup>-1</sup> in the reactor, and minor biogas production at 895 mgPhL<sup>-1</sup> (Madigou et al. 2016). Moreover, Poirier et al. (2016) observed that the stability of the anaerobic digestion process is reduced by phenol concentrations above concentrations of 1 gPhL<sup>-1</sup>. Wang et al. (2020) indicated that sludge granule size is directly correlated to higher conversion rates, because mass transfer resistance will reduce the phenol concentrations towards the core of the granules, diminishing phenol toxicity. Although the researched anaerobic reactors exhibited high removal of phenol during stable operation, the fluctuations in phenol concentration, as well as shifting the operational temperature to a higher level were identified as the major obstacles for achieving performance robustness (Levéen et al. 2012, Wang and Han 2012).

#### 1.1.3.4. High temperature

Anaerobic processes are commonly operated at about 35 °C, which is considered the optimum of the mesophilic temperature range. However, there are good reasons why it would be helpful to be able to operate at higher temperatures, i.e. thermophilic conditions reaching 55 °C when treating hot industrial wastewaters. Particularly when process water recovery is pursued, cooling and heating of the industrial effluent then can be minimized, leading to energy savings. Moreover, at high

temperatures, reaction rates are higher, and the viscosities of the biomass suspension and the permeate are lower, potentially leading to higher membrane fluxes (Stuckey 2012). However, an increased reaction rate at elevated temperature is particularly of interest for completely mixed reactors, where the HRT equals the SRT. In sludge retention systems, such as sludge bed reactors and AnMBRs, the actual retention of active biomass will predominantly determine the conversion capacity. For chemical wastewaters containing phenolic compounds, earlier studies indicated that thermophilic anaerobic operation could improve the bioconversion rate, as well as the methane yield when compared to mesophilic operation (Ramakrishnan and Surampalli 2013, Wang et al. 2011b). Wang et al. (2011b) compared UASB reactors under mesophilic and thermophilic conditions and determined that thermophilic operation improves about 30% the overall degradation of phenolic compounds including aerobic post-treatment. Similarly, Ramakrishnan and Surampalli (2013) showed that in an anaerobic hybrid reactor thermophilic conversion of phenolic wastewater is superior to mesophilic in terms of methane yield and effluent quality. In contrast, Fang et al. (2006) showed that the phenol degradation rate at 55°C was substantially lower than under mesophilic conditions in a UASB reactor. Few studies have been conducted on continuous flow reactors comparing thermophilic and mesophilic phenol degradation even though chemical industries are often discharging hot waste streams.

Adequate retention of anaerobic biomass by (auto-)immobilization is the main challenge in treating industrial wastewater at both high temperature and high salinity in sludge bed reactors. The prevalence of poor settling characteristics and dispersed biomass at high temperatures hamper effective sludge retention in comparison with mesophilic conditions (Dereli et al. 2012). Furthermore, the phenol conversion capacity of thermophilic microbial consortia is usually low and develops slowly (Fang et al. 2006, Levén and Schnürer 2005). Apparently, under thermophilic conditions, AnMBR is considered a promising application for different types of wastewaters (Duncan et al. 2017).

Particularly the simultaneous occurrence of toxicity, high salinity, and thermophilic conditions increases the need to combine membrane separation with anaerobic treatment to prevent biomass washout, which is considered a prerequisite to achieve a high-quality effluent and potentially better performance robustness (Lin et al. 2013). However, previous research indicated that thermophilic conditions can result in the formation of very fine particles, that will lead to cake layer compaction on the membranes of both submerged and side stream AnMBR configurations (Jeison et al. 2009b, Jeison and van Lier 2007b, 2008). As a result, very low membrane fluxes were attained, challenging the economic feasibility of AnMBR. Despite their potentials (van Lier 2008), thus far, full-scale anaerobic membrane bioreactors (AnMBRs) are not yet applied to high-temperature chemical wastewater treatment (Duncan et al. 2017).

A breakthrough in wastewater treatment can be achieved when AnMBR technology is able to overcome the adverse impact of extreme conditions. However, there are still several challenges that must be overcome before this technology can be implemented (Table 1.2). Essential for future development is a better understanding of how bioconversion and filtration performance are affected by the most challenging extreme conditions in chemical wastewater, i.e., high salinity, high temperature, and toxicity.

Table 1.2 Benefits and challenges of AnMBRs under high salinity and salinity fluctuations, high temperature, and toxicity.

Extreme condition	Effect on anaerobic process	Benefits of AnMBRs	Challenges of AnMBRs
<b>High salinity and salinity fluctuations</b>	<ul style="list-style-type: none"> <li>▪ Reduced biological activity mainly due to plasmolysis, cations, sodium inhibition of acetoclastic methanogens, and propionate oxidizers.</li> <li>▪ Biomass decay</li> <li>▪ Long adaptation time</li> <li>▪ Poor granule stability/strength, low settleability, calcium leach out.</li> <li>▪ Fluctuations may impact the stability and robustness of the sludge retention and reactor performance.</li> </ul>	<ul style="list-style-type: none"> <li>▪ Microorganisms are retained in the reactor regardless of settling/granulation properties.</li> <li>▪ Long sludge retention times (SRT) may improve the adaptation of microorganisms to salinity.</li> <li>▪ Full biomass retention may promote bioaugmentation of halophilic microorganisms capable of growth in a wide range of high salinity levels.</li> </ul>	<ul style="list-style-type: none"> <li>▪ Bacterial decay products due to osmotic pressure stress, and single-cell biomass development affect filtration performance.</li> <li>▪ Fluctuations may increase the SMPs production, and impact membrane filtration.</li> <li>▪ Formation of a more compact cake/gel layer.</li> </ul>
<b>High temperature</b>	<ul style="list-style-type: none"> <li>▪ Biomass granulation and immobilization is hampered</li> <li>▪ Thermophilic reactors have lower biomass production.</li> <li>▪ Thermophilic biomass has faster kinetics including a higher cell decay rate.</li> <li>▪ Product and substrate inhibition are frequently more pronounced.</li> <li>▪ Long adaptation needed when using mesophilic sludge as inoculum.</li> </ul>	<ul style="list-style-type: none"> <li>▪ Full biomass retention independent from granulation.</li> <li>▪ Higher rates of reaction. Overall conversion rates can be higher owing to reduced particle size and thus less mass transfer limitation</li> <li>▪ Advanced treatment when treated water is to be reused in the industrial processes.</li> <li>▪ The viscosity of reactor broth and permeate is lower at high temperatures, enabling lower energy consumption for mixing, and possibly leading to higher water fluxes over the membrane.</li> </ul>	<ul style="list-style-type: none"> <li>▪ Membrane fouling propensity when using mesophilic sludge as inoculum.</li> <li>▪ A compact cake layer may cause lower fluxes when compared to mesophilic conditions.</li> <li>▪ Formation of precipitates (solubility change) that could affect the filtration.</li> <li>▪ Thermophilic wastewater treatment is hardly applied in full-scale AnMBR.</li> </ul>
<b>Toxicity</b>	<ul style="list-style-type: none"> <li>▪ Long acclimatization times required if microorganisms needed for conversion of the toxicant grow slowly or are easily washed out.</li> <li>▪ Inhibition of SMA might be masked by mass transfer limitation when biofilms/granules are applied</li> <li>▪ Increased biomass decay</li> <li>▪ Biomass loss</li> </ul>	<ul style="list-style-type: none"> <li>▪ Bioaugmentation of specialized microorganisms by applying an absolute barrier: no specific washout.</li> <li>▪ Bacteria retention in the reactor is regardless of their settling/granulation properties. This may provide a better response to toxic shock loads.</li> <li>▪ No biomass loss, long SRTs for biomass adaptation are possible.</li> </ul>	<ul style="list-style-type: none"> <li>▪ Suspended (floc) biomass systems are more susceptible to toxicants than biofilm or granular sludge-based systems.</li> <li>▪ Securing long-term stability and robustness (also for sludge bed systems).</li> </ul>

Four main problems should be investigated before further implementation is possible:

- The toxic effect of aromatic compounds on the flocculent or suspended AnMBR biomass may be more pronounced than in granular sludge-based reactors. On the contrary, AnMBR provides full retention of biomass, which means that microorganisms with specific metabolic functions to degrade these types of compounds are fully retained in the system.
- Only limited knowledge exists about the degradation of aromatics and the impact of these compounds on the anaerobic biomass under high salinity conditions in an AnMBR. In practice, salinity will fluctuate, even though the reactor will also act as a buffer, which adds an additional challenge: robustness of degradation.
- There is little research on the thermophilic degradation of aromatics. If thermophilic conditions can be applied without negative effect on degradation, this will eliminate the need to cool the incoming effluent and heat the reclaimed process water.
- The fouling potential of AnMBR during the treatment of aromatics under high salinity and thermophilic conditions is unknown. As a consequence of polymeric substances production and single-cell growing bacteria accumulating in the reactor broth, higher fouling propensities are expected. However, considering the extreme conditions of the target chemical industrial effluents, presumably the attainable bioconversion capacity will be the critical factor, and not the achievable membrane flux.

The above described challenges explain why there is reluctance in the chemical industry to employ AnMBR as a core of the treatment process. Especially under extreme conditions, the attainable maximum bioconversion capacity is inherently crucial, while the link between bioconversion and filtration performance should be better understood to ensure successful implementation.

Until now, little research has been done on the use of membrane bioreactors for the anaerobic treatment of industrial saline phenol-containing wastewater, characterised by either a constant or (largely) fluctuating salinity level. Related to high salinity level, the fate and role of trace metals (TM), their partitioning and speciation, as well as bioavailability, is also not well understood. Indeed, no TM partitioning or bioavailability studies have been reported in AnMBRs. Moreover, the application of thermophilic AnMBRs for such hot phenolic streams have not been studied at all, neither the temperature susceptibility of the phenol conversion process linked to microbial community structure analysis. Although thermophilic operation will bring operational energy benefits when treating high-temperature chemical industrial wastewaters, so far it remains unclear whether the conversion capacity of the reactor will be higher than at mesophilic operation. Therefore, further research is required that will advance the understanding of the effect of extreme conditions in AnMBR for the treatment of chemical wastewaters under extreme conditions.

## 1.2. Aim of this thesis

This research aimed to investigate the impact of extreme conditions on the bioconversion of aromatic compounds in AnMBRs. The research made use of synthetic wastewater, simulating industrial chemical wastewater streams, and aimed for opening up a new niche market for AnMBR applications. In particular, phenol is selected as a model compound, because it is considered an intermediate in the anaerobic conversion of a wide variety of aromatics. Thereby, the goal is to research the treatment of synthetic phenol-containing wastewater under high and fluctuating salinity conditions and high temperatures. The latter research objective followed from our industrial project partners' interest to gain insights into the treatment using AnMBR of phenolic wastewater under the mentioned combined conditions.

Monitoring the microbial community dynamics and biomass properties during short- and long-term experiments adds knowledge to link these aspects to the reactor performance, i.e., bioconversion capacity and membrane filtration. The performed research increases the understanding of the influence of different extreme conditions. Findings are compared with granular sludge bed-based high-rate anaerobic reactors (UASB), elucidating the added benefits of the AnMBR. This thesis examine the following questions:

- What is the impact of high salinity (sodium concentration) on trace metals availability and methanogenic activity in the AnMBR?
- What is the impact of high salinity and fluctuations in salinity on the conversion capacity, biomass properties, and membrane filtration?
- What are the differences in stability and performance between an AnMBR and a granular sludge bed reactor like UASB, for treating highly saline phenolic wastewaters?
- What are the effects of shifting from mesophilic to thermophilic AnMBR operation on membrane filtration, microbial community structure, and biomass characteristics?
- What is determining the phenol conversion capacity of the AnMBR under thermophilic operation?

In order to answer these questions, several long-term experiments were performed in AnMBRs under the studied extreme conditions. The conclusions of the experiments are translated into a future outlook for the anaerobic treatment of industrial chemical wastewater under extreme conditions.

### 1.3. Outline of the thesis

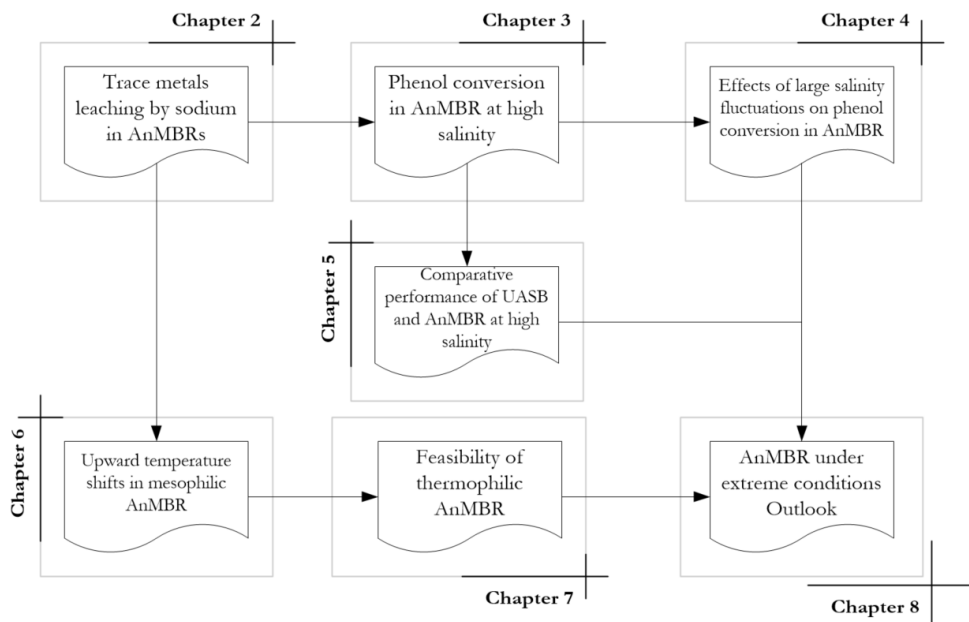


Figure 1.5. The schematic structure of the thesis.

The outline of the thesis is presented in Figure 1.5, which describes the research flow and how the chapters are related. The chapters in this thesis are structured as follows:

**Chapter 2** investigates the effects of high salinity and trace metal supplementation on biomass methanogenic activity during the start-up of two AnMBRs. The accumulation of sodium and trace metals speciation in the bulk liquid and biomass matrix was investigated. The implications on the biomass particle size and COD removal of the AnMBRs are presented. Doubling trace metals supplementation was introduced in the reactors to increase their bioavailability and improve COD removal.

**Chapter 3** assesses the impact of long-term salinity exposure on phenol conversion and methanogenic activity. Batch tests were carried out to investigate the effects of the potassium to sodium ratio on COD removal and methane production. The AnMBR membrane filtration performance and the biomass particle size distribution along the experiment were evaluated. The microbial community composition dynamics and diversity were determined to investigate the phenol degraders' adaptation to salinity changes.

**Chapter 4** focuses on the phenol conversion and overall process performance of an AnMBR subjected to increasing high salinity and random large salinity fluctuations. The biomass characteristics and the microbial diversity and dynamics in response to the high salinity fluctuations

were analyzed. Moreover, the membrane resistance to filtration was evaluated with an emphasis on the period with large salinity fluctuations to research the different types of membrane fouling.

**Chapter 5** provides a comparative analysis between an AnMBR and a UASB reactor, treating high saline phenol-containing wastewater. Reactors were operated in parallel, applying a high sodium and phenol concentration to evaluate their response on conversion under these conditions. Both biomass characteristics and microbial composition and diversity were investigated to get insight into the different performance and stability of the two high-rate reactors configurations.

**Chapter 6** provides insight into the temperature susceptibility of an AnMBR as a result of shifting the temperature from mesophilic to thermophilic conditions at high salinity. Phenol conversion capacity, biomass characteristics, microbial community structure, and membrane filtration are evaluated to add knowledge on the impact of temperature shifts on the overall AnMBR system performance.

**Chapter 7** is dedicated to the long-term thermophilic phenol conversion under high salinity conditions. Bioreactor performance and microbial community dynamics were monitored using specific methanogenic activity assays, phenol conversion rate assays, volatile fatty acids permeate characterization and 16S rRNA gene sequencing. The microbial community dynamics were analyzed to elucidate the differences between the acetotrophic and hydrogenotrophic activities observed in the AnMBR. The maximum attainable phenol conversion rate under thermophilic and high salinity conditions was determined.

**Chapter 8** addresses the main results and conclusions obtained in this thesis. Recommendations and future perspectives of AnMBR under extreme conditions are provided in light of the scientific contribution of this thesis.

## References

- Aquastat, F. (2019) Country Fact Sheet Netherlands. [https://storage.googleapis.com/fao-aquastat.appspot.com/countries\\_regions/factsheets/summary\\_statistics/en/NLD-CF.pdf](https://storage.googleapis.com/fao-aquastat.appspot.com/countries_regions/factsheets/summary_statistics/en/NLD-CF.pdf)
- Aslan, S. and Şekerdağ, N. (2016) Salt inhibition on anaerobic treatment of high salinity wastewater by upflow anaerobic sludge blanket (UASB) reactor. *Desalination and Water Treatment* 57(28), 12998-13004.
- Baêta, B.E.L., Luna, H.J., Sanson, A.L., Silva, S.Q. and Aquino, S.F. (2013) Degradation of a model azo dye in submerged anaerobic membrane bioreactor (SAMBR) operated with powdered activated carbon (PAC). *Journal of Environmental Management* 128, 462-470.
- Bhattacharyya, D., Allison, M.J., Webb, J.R., Zanatta, G.M., Singh, K.S. and Grant, S.R. (2013) Treatment of an Industrial Wastewater Containing Acrylic Acid and Formaldehyde in an Anaerobic Membrane Bioreactor. *Journal of Hazardous, Toxic, and Radioactive Waste* 17(1), 74-79.
- Busca, G., Berardinelli, S., Resini, C. and Arrighi, L. (2008) Technologies for the removal of phenol from fluid streams: A short review of recent developments. *Journal of Hazardous Materials* 160(2), 265-288.
- Chen, L., Cheng, P., Ye, L., Chen, H., Xu, X. and Zhu, L. (2020) Biological performance and fouling mitigation in the biochar-amended anaerobic membrane bioreactor (AnMBR) treating pharmaceutical wastewater. *Bioresource Technology* 302.
- Chen, L., Hu, Q., Zhang, X., Chen, Z., Wang, Y. and Liu, S. (2019) Effects of salinity on the biological performance of anaerobic membrane bioreactor. *Journal of Environmental Management* 238, 263-273.
- Chen, Y., Cheng, J.J. and Creamer, K.S. (2008) Inhibition of anaerobic digestion process: A review. *Bioresource Technology* 99(10), 4044-4064.
- Chen, Z., Li, X., Hu, D., Cui, Y., Gu, F., Jia, F., Xiao, T., Su, H., Xu, J., Wang, H., Wu, P., Zhang, Y. and Jiang, N. (2018) Performance and methane fermentation characteristics of a pilot scale anaerobic membrane bioreactor (AnMBR) for treating pharmaceutical wastewater containing m-cresol (MC) and iso-propyl alcohol (IPA). *Chemosphere* 206, 750-758.
- Cornelissen, E., Buggenhout, S., Van Ermen, S., Smedt, M., Van Impe, J. and Koning, J. (2001) Anaerobic treatment of brewery wastewater with an internal membrane bioreactor. *Mededelingen (Rijksuniversiteit te Gent. Fakulteit van de Landbouwkundige en Toegepaste Biologische Wetenschappen)* 66, 135-138.
- De Amorim, E.L.C., Sader, L.T. and Silva, E.L. (2015) Effects of the Organic-Loading Rate on the Performance of an Anaerobic Fluidized-Bed Reactor Treating Synthetic Wastewater Containing Phenol. *Journal of Environmental Engineering (United States)* 141(10).
- De Vrieze, J., Coma, M., Debeuckelaere, M., Van der Meeren, P. and Rabaey, K. (2016a) High salinity in molasses wastewaters shifts anaerobic digestion to carboxylate production. *Water Research* 98, 293-301.
- De Vrieze, J., Regueiro, L., Props, R., Vilchez-Vargas, R., Jáuregui, R., Pieper, D.H., Lema, J.M. and Carballa, M. (2016b) Presence does not imply activity: DNA and RNA patterns differ in response to salt perturbation in anaerobic digestion. *Biotechnology for Biofuels* 9(1), 244.
- Dereli, R.K., Ersahin, M.E., Ozgun, H., Ozturk, I., Jeison, D., van der Zee, F. and van Lier, J.B. (2012) Potentials of anaerobic membrane bioreactors to overcome treatment limitations induced by industrial wastewaters. *Bioresource Technology* 122, 160-170.
- Duncan, J., Bokhary, A., Fatehi, P., Kong, F., Lin, H. and Liao, B. (2017) Thermophilic membrane bioreactors: A review. *Bioresource Technology* 243(Supplement C), 1180-1193.
- Dvořák, L., Gómez, M., Dolina, J. and Černín, A. (2016) Anaerobic membrane bioreactors—a mini review with emphasis on industrial wastewater treatment: applications, limitations and perspectives. *Desalination and Water Treatment* 57(41), 19062-19076.
- Ersahin, M.E., Ozgun, H., Dereli, R.K., Ozturk, I., Roest, K. and van Lier, J.B. (2012) A review on dynamic membrane filtration: Materials, applications and future perspectives. *Bioresource Technology* 122, 196-206.
- Ersahin, M.E., Ozgun, H., Tao, Y. and van Lier, J.B. (2014) Applicability of dynamic membrane technology in anaerobic membrane bioreactors. *Water Research* 48, 420-429.
- Evans and Fuchs, G. (1988) Anaerobic Degradation of Aromatic Compounds. *Annual Review of Microbiology* 42(1), 289-317.
- Fang, H.H.P. and Chan, O.C. (1997) Toxicity of phenol towards anaerobic biogranules. *Water Research* 31(9), 2229-2242.



- Fang, H.H.P., Liang, D.W., Zhang, T. and Liu, Y. (2006) Anaerobic treatment of phenol in wastewater under thermophilic condition. *Water Research* 40(3), 427-434.
- Feijoo, G., Soto, M., Méndez, R. and Lema, J.M. (1995) Sodium inhibition in the anaerobic digestion process: Antagonism and adaptation phenomena. *Enzyme and Microbial Technology* 17(2), 180-188.
- Fermoso, F.G., Bartacek, J., Jansen, S. and Lens, P.N.L. (2009) Metal supplementation to UASB bioreactors: from cell-metal interactions to full-scale application. *Science of the Total Environment* 407(12), 3652-3667.
- Ferrer-Polonio, E., García-Quijano, N.T., Mendoza-Roca, J.A., Iborra-Clar, A. and Pastor-Alcañiz, L. (2016) Effect of alternating anaerobic and aerobic phases on the performance of a SBR treating effluents with high salinity and phenols concentration. *Biochemical Engineering Journal* 113, 57-65.
- Franchi, O., Cabrol, L., Chamy, R. and Rosenkranz, F. (2020) Correlations between microbial population dynamics, bamA gene abundance and performance of anaerobic sequencing batch reactor (ASBR) treating increasing concentrations of phenol. *Journal of Biotechnology* 310, 40-48.
- Fuchs, G. (2008) Anaerobic Metabolism of Aromatic Compounds. *Annals of the New York Academy of Sciences* 1125(1), 82-99.
- Gagliano, M.C., Ismail, S.B., Stams, A.J.M., Plugge, C.M., Temmink, H. and Van Lier, J.B. (2017) Biofilm formation and granule properties in anaerobic digestion at high salinity. *Water Research* 121, 61-71.
- Gao, W.J., Han, M.N., Xu, C., Liao, B.Q., Hong, Y., Cumin, J. and Dagnew, M. (2016) Performance of submerged anaerobic membrane bioreactor for thermomechanical pulping wastewater treatment. *Journal of Water Process Engineering* 13, 70-78.
- Gao, W.J., Leung, K.T., Qin, W.S. and Liao, B.Q. (2011) Effects of temperature and temperature shock on the performance and microbial community structure of a submerged anaerobic membrane bioreactor. *Bioresource Technology* 102(19), 8733-8740.
- Gao, W.J., Lin, H.J., Leung, K.T. and Liao, B.Q. (2010) Influence of elevated pH shocks on the performance of a submerged anaerobic membrane bioreactor. *Process Biochemistry* 45(8), 1279-1287.
- Guerrero, L., Omil, F., Méndez, R. and Lema, J.M. (1997) Treatment of saline wastewaters from fish meal factories in an anaerobic filter under extreme ammonia concentrations. *Bioresource Technology* 61(1), 69-78.
- Hemmelmann, A., Torres, A., Vergara, C., Azocar, L. and Jeison, D. (2013) Application of anaerobic membrane bioreactors for the treatment of protein-containing wastewaters under saline conditions. *Journal of Chemical Technology and Biotechnology* 88(4), 658-663.
- Hou, M., Li, W., Li, H., Li, C., Wu, X. and Liu, Y.-d. (2019) Performance and bacterial characteristics of aerobic granular sludge in response to alternating salinity. *International Biodeterioration & Biodegradation* 142, 211-217.
- Hoyos-Hernandez, C., Hoffmann, M., Guenne, A. and Mazeas, L. (2014) Elucidation of the thermophilic phenol biodegradation pathway via benzoate during the anaerobic digestion of municipal solid waste. *Chemosphere* 97, 115-119.
- Hu, D., Li, X., Chen, Z., Cui, Y., Gu, F., Jia, F., Xiao, T., Su, H., Xu, J., Wang, H., Wu, P. and Zhang, Y. (2018) Performance and extracellular polymers substance analysis of a pilot scale anaerobic membrane bioreactor for treating tetrahydrofuran pharmaceutical wastewater at different HRTs. *Journal of Hazardous Materials* 342, 383-391.
- Huang, B., Wang, H.-C., Cui, D., Zhang, B., Chen, Z.-B. and Wang, A.-J. (2018) Treatment of pharmaceutical wastewater containing  $\beta$ -lactams antibiotics by a pilot-scale anaerobic membrane bioreactor (AnMBR). *Chemical Engineering Journal* 341, 238-247.
- Huang, J., He, H. and Wiegel, J. (1999) Cloning, Characterization, and Expression of a Novel Gene Encoding a Reversible 4-Hydroxybenzoate Decarboxylase from *Clostridium hydroxybenzoicum*. *Journal of Bacteriology* 181(16), 5119-5122.
- Ismail, S.B., de La Parra, C.J., Temmink, H. and van Lier, J.B. (2010) Extracellular polymeric substances (EPS) in upflow anaerobic sludge blanket (UASB) reactors operated under high salinity conditions. *Water Research* 44(6), 1909-1917.
- Ismail, S.B., Gonzalez, P., Jeison, D. and Van Lier, J.B. (2008) Effects of high salinity wastewater on methanogenic sludge bed systems. *Water Science and Technology* 58, 1963-1970.
- Jeison, D., Del Rio, A. and Van Lier, J.B. (2008a) Impact of high saline wastewaters on anaerobic granular sludge functionalities. *Water Science and Technology* 57(6), 815-819.

- Jeison, D., Kremer, B. and van Lier, J.B. (2008b) Application of membrane enhanced biomass retention to the anaerobic treatment of acidified wastewaters under extreme saline conditions. *Separation and Purification Technology* 64(2), 198-205.
- Jeison, D., Plugge, C.M., Pereira, A. and Lier, J.B.v. (2009a) Effects of the acidogenic biomass on the performance of an anaerobic membrane bioreactor for wastewater treatment. *Bioresource Technology* 100(6), 1951-1956.
- Jeison, D., Telkamp, P. and van Lier, J.B. (2009b) Thermophilic sidestream anaerobic membrane bioreactors: the shear rate dilemma. *Water Environ Res* 81(11), 2372-2380.
- Jeison, D. and van Lier, J.B. (2007a) Cake formation and consolidation: Main factors governing the applicable flux in anaerobic submerged membrane bioreactors (AnSMBR) treating acidified wastewaters. *Separation and Purification Technology* 56(1), 71-78.
- Jeison, D. and van Lier, J.B. (2007b) Thermophilic treatment of acidified and partially acidified wastewater using an anaerobic submerged MBR: Factors affecting long-term operational flux. *Water Research* 41(17), 3868-3879.
- Jeison, D. and van Lier, J.B. (2008) Feasibility of thermophilic anaerobic submerged membrane bioreactors (AnSMBR) for wastewater treatment. *Desalination* 231(1), 227-235.
- Kaya, Y., Bacaksiz, A.M., Bayrak, H., Gnder, Z.B., Vergili, I., Hasar, H. and Yilmaz, G. (2017) Treatment of chemical synthesis-based pharmaceutical wastewater in an ozonation-anaerobic membrane bioreactor (AnMBR) system. *Chemical Engineering Journal* 322, 293-301.
- Khan, M.A., Ngo, H.H., Guo, W.S., Liu, Y.W., Zhou, J.L., Zhang, J., Liang, S., Ni, B.J., Zhang, X.B. and Wang, J. (2016) Comparing the value of bioproducts from different stages of anaerobic membrane bioreactors. *Bioresource Technology* 214, 816-825.
- Kleerebezem, R. (1999) Anaerobic treatment of Phthalates: Microbial and Technological aspects, Wageningen University, Wageningen, The Netherlands.
- Kleerebezem, R. and Macarie, H. (2003) Treating industrial wastewater: Anaerobic digestion comes of age. *Chemical Engineering* 110(4), 56-64.
- Kleerebezem, R., Mortier, J., Hulshoff Pol, L.W. and Lettinga, G. (1997) Anaerobic pre-treatment of petrochemical effluents: Terephthalic acid wastewater, pp. 237-248.
- Kong, Z., Li, L., Kurihara, R., Zhang, T. and Li, Y.-Y. (2019a) Anaerobic treatment of N,N-dimethylformamide-containing high-strength wastewater by submerged anaerobic membrane bioreactor with a co-cultured inoculum. *Science of The Total Environment* 663, 696-708.
- Kong, Z., Li, L., Xue, Y., Yang, M. and Li, Y.-Y. (2019b) Challenges and prospects for the anaerobic treatment of chemical-industrial organic wastewater: A review. *Journal of Cleaner Production* 231, 913-927.
- Lay, W.C.L., Liu, Y. and Fane, A.G. (2010) Impacts of salinity on the performance of high retention membrane bioreactors for water reclamation: A review. *Water Research* 44(1), 21-40.
- Le Borgne, S., Paniagua, D. and Vazquez-Duhalt, R. (2008) Biodegradation of Organic Pollutants by Halophilic Bacteria and Archaea. *Journal of Molecular Microbiology and Biotechnology* 15(2-3), 74-92.
- Lefebvre, O. and Moletta, R. (2006) Treatment of organic pollution in industrial saline wastewater: A literature review. *Water Research* 40(20), 3671-3682.
- Lefebvre, O., Quentin, S., Torrijos, M., Godon, J.J., Delgens, J.P. and Moletta, R. (2007) Impact of increasing NaCl concentrations on the performance and community composition of two anaerobic reactors. *Applied Microbiology and Biotechnology* 75(1), 61-69.
- Lettinga, G. (2005) The anaerobic treatment approach towards a more sustainable and robust environmental protection. *Water Science and Technology* 52(1-2), 1-11.
- Lettinga, G. (2014) My anaerobic sustainability story. , LeAF Publisher, Wageningen
- Levn, L., Nyberg, K. and Schnrer, A. (2012) Conversion of phenols during anaerobic digestion of organic solid waste – A review of important microorganisms and impact of temperature. *Journal of Environmental Management* 95, Supplement(0), S99-S103.
- Levn, L. and Schnrer, A. (2005) Effects of temperature on biological degradation of phenols, benzoates and phthalates under methanogenic conditions. *International Biodeterioration & Biodegradation* 55(2), 153-160.
- Li, L., Kong, Z., Xue, Y., Wang, T., Kato, H. and Li, Y.Y. (2020) A comparative long-term operation using up-flow anaerobic sludge blanket (UASB) and anaerobic membrane bioreactor (AnMBR) for the upgrading of

- anaerobic treatment of N, N-dimethylformamide-containing wastewater. *Science of The Total Environment* 699.
- Liao, B.-Q., Kraemer, J.T. and Bagley, D.M. (2006) Anaerobic Membrane Bioreactors: Applications and Research Directions. *Critical Reviews in Environmental Science and Technology* 36(6), 489-530.
- Lin, H., Liao, B.-Q., Chen, J., Gao, W., Wang, L., Wang, F. and Lu, X. (2011) New insights into membrane fouling in a submerged anaerobic membrane bioreactor based on characterization of cake sludge and bulk sludge. *Bioresource Technology* 102(3), 2373-2379.
- Lin, H., Peng, W., Zhang, M., Chen, J., Hong, H. and Zhang, Y. (2013) A review on anaerobic membrane bioreactors: Applications, membrane fouling and future perspectives. *Desalination* 314, 169-188.
- Lutchmiah, K., Verliefe, A.R.D., Roest, K., Rietveld, L.C. and Cornelissen, E.R. (2014) Forward osmosis for application in wastewater treatment: A review. *Water Research* 58, 179-197.
- Maaz, M., Yasin, M., Aslam, M., Kumar, G., Atabani, A.E., Idrees, M., Anjum, F., Jamil, F., Ahmad, R., Khan, A.L., Lesage, G., Heran, M. and Kim, J. (2019) Anaerobic membrane bioreactors for wastewater treatment: Novel configurations, fouling control and energy considerations. *Bioresource Technology* 283, 358-372.
- Madigou, C., Poirier, S., Bureau, C. and Chapleur, O. (2016) Acclimation strategy to increase phenol tolerance of an anaerobic microbiota. *Bioresource Technology* 216, 77-86.
- McCarty, P.L., Bae, J. and Kim, J. (2011) Domestic Wastewater Treatment as a Net Energy Producer—Can This be Achieved? *Environmental Science & Technology* 45(17), 7100-7106.
- Mishra, S., Chowdhary, P. and Bharagava, R.N. (2019) Emerging and Eco-Friendly Approaches for Waste Management. Bharagava, R.N. and Chowdhary, P. (eds), pp. 1-31, Springer Singapore, Singapore.
- Ng, H.Y., Ong, S.L. and Ng, W.J. (2005) Effects of Sodium Chloride on the Performance of a Sequencing Batch Reactor. *Journal of Environmental Engineering* 131(11), 1557-1564.
- Ng, K.K., Shi, X. and Ng, H.Y. (2015) Evaluation of system performance and microbial communities of a bioaugmented anaerobic membrane bioreactor treating pharmaceutical wastewater. *Water Research* 81, 311-324.
- Nguyen, T.-B., Bui, X.T., Vo, T.-D.-H., Cao, N.-D.-T., Dang, B.-T., Tra, V.-T., Tran, H.-T., Tran, L.-L. and Ngo, H.H. (2020) Current Developments in Biotechnology and Bioengineering. Ngo, H.H., Guo, W., Ng, H.Y., Mannina, G. and Pandey, A. (eds), pp. 167-196, Elsevier.
- Osuna, M.B., van Hullebusch, E.D., Zandvoort, M.H., Iza, J. and Lens, P.N. (2004) Effect of cobalt sorption on metal fractionation in anaerobic granular sludge. *J Environ Qual* 33(4), 1256-1270.
- Ozgun, H., Dereli, R.K., Ersahin, M.E., Kinaci, C., Spanjers, H. and van Lier, J.B. (2013) A review of anaerobic membrane bioreactors for municipal wastewater treatment: Integration options, limitations and expectations. *Separation and Purification Technology* 118, 89-104.
- Pevere, A., Guibaud, G., van Hullebusch, E.D., Boughzala, W. and Lens, P.N.L. (2007) Effect of Na<sup>+</sup> and Ca<sup>2+</sup> on the aggregation properties of sieved anaerobic granular sludge. *Colloids and Surfaces A: Physicochemical and Engineering Aspects* 306(1-3 SPEC. ISS.), 142-149.
- Poirier, S., Bize, A., Bureau, C., Bouchez, T. and Chapleur, O. (2016) Community shifts within anaerobic digestion microbiota facing phenol inhibition: Towards early warning microbial indicators? *Water Research* 100(Supplement C), 296-305.
- Praveen, P., Nguyen, D.T.T. and Loh, K.-C. (2015) Biodegradation of phenol from saline wastewater using forward osmotic hollow fiber membrane bioreactor coupled chemostat. *Biochemical Engineering Journal* 94(Supplement C), 125-133.
- Ramakrishnan, A. and Surampalli, R.Y. (2013) Performance and energy economics of mesophilic and thermophilic digestion in anaerobic hybrid reactor treating coal wastewater. *Bioresource Technology* 127, 9-17.
- Razo-Flores, E., Macarie, H. and Morier, F. (2006) Application of biological treatment systems for chemical and petrochemical wastewaters. In: Cervantes FJ, Pavlostathis SP, van Haandel AC (eds) *Advanced biological treatment processes for industrial wastewaters*. IWA publishing, London.
- Rinzema, A., van Lier, J. and Lettinga, G. (1988) Sodium inhibition of acetoclastic methanogens in granular sludge from a UASB reactor. *Enzyme and Microbial Technology* 10(1), 24-32.
- Ritchie, H. and Roser, M. (2017) *Water Use and Stress*. Published online at OurWorldInData.org. Retrieved from: '<https://ourworldindata.org/water-use-stress>' [Online Resource].

- Robles, Á., Ruano, M., Charfi, A., Lesage, G., Heran, M., Harmand, J., Seco, A., Steyer, J.P., Batstone, D., Kim, J. and Ferrer, J. (2018) A review on anaerobic membrane bioreactors (AnMBRs) focused on modelling and control aspects. *Bioresource Technology* 270.
- Rosenkranz, F., Cabrol, L., Carballa, M., Donoso-Bravo, A., Cruz, L., Ruiz-Filippi, G., Chamy, R. and Lema, J.M. (2013) Relationship between phenol degradation efficiency and microbial community structure in an anaerobic SBR. *Water Research* 47(17), 6739-6749.
- Schink, B., Philipp, B. and Müller, J. (2000) Anaerobic Degradation of Phenolic Compounds. *Naturwissenschaften* 87(1), 12-23.
- Schneider, C., Evangelio Oñoro, A., Hélix-Nielsen, C. and Fotidis, I.A. (2021) Forward-osmosis anaerobic-membrane bioreactors for brewery wastewater remediation. *Separation and Purification Technology* 257, 117786.
- Sipma, J., Osuna, M.B., Emanuelsson, M.A.E. and Castro, P.M.L. (2010) Biotreatment of Industrial Wastewaters under Transient-State Conditions: Process Stability with Fluctuations of Organic Load, Substrates, Toxicants, and Environmental Parameters. *Critical Reviews in Environmental Science and Technology* 40(2), 147-197.
- Skouteris, G., Hermosilla, D., López, P., Negro, C. and Blanco, Á. (2012) Anaerobic membrane bioreactors for wastewater treatment: A review. *Chemical Engineering Journal* 198-199, 138-148.
- Smith, A.L., Stadler, L.B., Love, N.G., Skerlos, S.J. and Raskin, L. (2012) Perspectives on anaerobic membrane bioreactor treatment of domestic wastewater: A critical review. *Bioresource Technology* 122, 149-159.
- Song, X., Luo, W., Hai, F.I., Price, W.E., Guo, W., Ngo, H.H. and Nghiem, L.D. (2018) Resource recovery from wastewater by anaerobic membrane bioreactors: Opportunities and challenges. *Bioresource Technology* 270, 669-677.
- Song, X., McDonald, J., Price, W.E., Khan, S.J., Hai, F.I., Ngo, H.H., Guo, W. and Nghiem, L.D. (2016) Effects of salinity build-up on the performance of an anaerobic membrane bioreactor regarding basic water quality parameters and removal of trace organic contaminants. *Bioresource Technology* 216, 399-405.
- Srivastava, A., Parida, V.K., Majumder, A., Gupta, B. and Gupta, A.K. (2021) Treatment of saline wastewater using physicochemical, biological, and hybrid processes: Insights into inhibition mechanisms, treatment efficiencies and performance enhancement. *Journal of Environmental Chemical Engineering*, 105775.
- Stuckey, D.C. (2012) Recent developments in anaerobic membrane reactors. *Bioresource Technology* 122, 137-148.
- Svojitka, J., Dvořák, L., Studer, M., Straub, J.O., Frömelt, H. and Wintgens, T. (2017) Performance of an anaerobic membrane bioreactor for pharmaceutical wastewater treatment. *Bioresource Technology* 229, 180-189.
- Tian, X., Song, Y., Shen, Z., Zhou, Y., Wang, K., Jin, X., Han, Z. and Liu, T. (2020) A comprehensive review on toxic petrochemical wastewater pretreatment and advanced treatment. *Journal of Cleaner Production* 245, 118692.
- Tomei, M.C., Mosca Angelucci, D., Clagnan, E. and Brusetti, L. (2021) Anaerobic biodegradation of phenol in wastewater treatment: achievements and limits. *Applied Microbiology and Biotechnology* 105(6), 2195-2224.
- Tszech, A. and Fuchs, G. (1989) Anaerobic degradation of phenol via carboxylation to 4-hydroxybenzoate: in vitro study of isotope exchange between  $^{14}\text{CO}_2$  and 4-hydroxybenzoate. *Archives of Microbiology* 152(6), 594-599.
- Umaiyakunjaram, R. and Shanmugam, P. (2016) Study on submerged anaerobic membrane bioreactor (SAMBR) treating high suspended solids raw tannery wastewater for biogas production. *Bioresource Technology* 216, 785-792.
- UN (2015) Transforming our world: the 2030 Agenda for Sustainable Development.
- Vallero, M.V.G., Hulshoff Pol, L.W., Lettinga, G. and Lens, P.N.L. (2003a) Effect of NaCl on thermophilic (55°C) methanol degradation in sulfate reducing granular sludge reactors. *Water Research* 37(10), 2269-2280.
- Vallero, M.V.G., Lettinga, G. and Lens, P.N.L. (2003b) Long-term adaptation of methanol-fed thermophilic (55°C) sulfate-reducing reactors to NaCl. *Journal of Industrial Microbiology and Biotechnology* 30(6), 375-382.

- Vallero, M.V.G., Sipma, J., Lettinga, G. and Lens, P.N.L. (2004) High-Rate Sulfate Reduction at High Salinity (up to 90 mS.cm<sup>-1</sup>) in Mesophilic UASB Reactors. *Biotechnology and Bioengineering* 86(2), 226-235.
- van Hullebusch, E.D., Guibaud, G., Simon, S., Lenz, M., Yekta, S.S., Fermoso, F.G., Jain, R., Duester, L., Roussel, J., Guillon, E., Skjellberg, U., Almeida, C.M.R., Pechaud, Y., Garuti, M., Frunzo, L., Esposito, G., Carliell-Marquet, C., Ortner, M. and Collins, G. (2016) Methodological approaches for fractionation and speciation to estimate trace element bioavailability in engineered anaerobic digestion ecosystems: An overview. *Critical Reviews in Environmental Science and Technology* 46(16), 1324-1366.
- van Lier, J.B. (2008) High-rate anaerobic wastewater treatment: diversifying from end-of-the-pipe treatment to resource-oriented conversion techniques. *Water Science and Technology* 57(8), 1137-1148.
- van Lier, J.B., Mahmoud, N. and Zeeman, G. (2020) *Biological Wastewater Treatment, Principles, Modelling and Design*, 2nd Edition, pp. 701-756, IWA Publishing, London, UK.
- van Lier, J.B., Tilche, A., Ahring, B.K., Macarie, H., Moletta, R., Dohanyos, M., Hulshoff Pol, L.W., Lens, P. and Verstraete, W. (2001) New perspectives in anaerobic digestion, pp. 1-18.
- van Lier, J.B., van der Zee, F.P., Frijters, C.T.M.J. and Ersahin, M.E. (2015) Celebrating 40 years anaerobic sludge bed reactors for industrial wastewater treatment. *Reviews in Environmental Science and Bio/Technology* 14(4), 681-702.
- Van Zyl, P.J., Wentzel, M.C., Ekama, G.A. and Riedel, K.J. (2008) Design and start-up of a high rate anaerobic membrane bioreactor for the treatment of a low pH, high strength, dissolved organic waste water. *Water Science and Technology* 57(2), 291-295.
- Vinardell, S., Astals, S., Mata-Alvarez, J. and Dosta, J. (2020) Techno-economic analysis of combining forward osmosis-reverse osmosis and anaerobic membrane bioreactor technologies for municipal wastewater treatment and water production. *Bioresource Technology* 297, 122395.
- Vítězová, M., Kohoutová, A., Vítěz, T., Hanišáková, N. and Kushkevych, I. (2020) Methanogenic Microorganisms in Industrial Wastewater Anaerobic Treatment. *Processes* 8(12), 1546.
- Vyrides, I. (2015) Anaerobic Treatment of Organic Saline Waste/Wastewater: Overcome Salinity Inhibition by Addition of Compatible Solutes. In: Sukla L., Pradhan N., Panda S., Mishra B. (eds) *Environmental Microbial Biotechnology*. Soil Biology, Springer, Cham.
- Vyrides, I., Santos, H., Mingote, A., Ray, M.J. and Stuckey, D.C. (2010) Are Compatible Solutes Compatible with Biological Treatment of Saline Wastewater? Batch and Continuous Studies Using Submerged Anaerobic Membrane Bioreactors (SAMBRs). *Environmental Science & Technology* 44(19), 7437-7442.
- Vyrides, I. and Stuckey, D.C. (2009) Adaptation of anaerobic biomass to saline conditions: Role of compatible solutes and extracellular polysaccharides. *Enzyme and Microbial Technology* 44(1), 46-51.
- Vyrides, I. and Stuckey, D.C. (2011) Fouling cake layer in a submerged anaerobic membrane bioreactor treating saline wastewaters: Curse or a blessing? *Water Science and Technology* 63(12), 2902-2908.
- Vyrides, I. and Stuckey, D.C. (2017) Compatible solute addition to biological systems treating waste/wastewater to counteract osmotic and other environmental stresses: a review. *Critical Reviews in Biotechnology* 37(7), 865-879.
- Wang, J., Wu, B., Muñoz Sierra, J., He, C., Hu, Z. and Wang, W. (2020) Influence of particle size distribution on anaerobic degradation of phenol and analysis of methanogenic microbial community. *Environmental Science and Pollution Research* 27(10), 10391-10403.
- Wang, L., Wijekoon, K.C., Nghiem, L.D. and Khan, S.J. (2014) Removal of polycyclic musks by anaerobic membrane bioreactor: Biodegradation, biosorption, and enantioselectivity. *Chemosphere* 117, 722-729.
- Wang, S., Ma, C., Pang, C., Hu, Z. and Wang, W. (2019) Membrane fouling and performance of anaerobic ceramic membrane bioreactor treating phenol- and quinoline-containing wastewater: granular activated carbon vs polyaluminum chloride. *Environmental Science and Pollution Research* 26(33), 34167-34176.
- Wang, W. and Han, H. (2012) Recovery strategies for tackling the impact of phenolic compounds in a UASB reactor treating coal gasification wastewater. *Bioresource Technology* 103(1), 95-100.
- Wang, W., Han, H., Yuan, M., Li, H., Fang, F. and Wang, K. (2011a) Treatment of coal gasification wastewater by a two-continuous UASB system with step-feed for COD and phenols removal. *Bioresource Technology* 102(9), 5454-5460.
- Wang, W., Ma, W., Han, H., Li, H. and Yuan, M. (2011b) Thermophilic anaerobic digestion of Lurgi coal gasification wastewater in a UASB reactor. *Bioresource Technology* 102(3), 2441-2447.

- Wang, W., Wang, S., Ren, X., Hu, Z. and Yuan, S. (2017a) Rapid establishment of phenol- and quinoline-degrading consortia driven by the scoured cake layer in an anaerobic baffled ceramic membrane bioreactor. *Environmental Science and Pollution Research* 24, 1-11.
- Wang, W., Wu, B., Pan, S., Yang, K., Hu, Z. and Yuan, S. (2017b) Performance robustness of the UASB reactors treating saline phenolic wastewater and analysis of microbial community structure. *Journal of Hazardous Materials* 331, 21-27.
- Wang, W., Yang, K., Muñoz Sierra, J., Zhang, X., Yuan, S. and Hu, Z. (2017c) Potential impact of methyl isobutyl ketone (MIBK) on phenols degradation in an UASB reactor and its degradation properties. *Journal of Hazardous materials* 333, 73-79.
- Wood, J.M. (2015) Bacterial responses to osmotic challenges. *The Journal of General Physiology* 145(5), 381-388.
- Yang, J., Spanjers, H., Jeison, D. and Van Lier, J.B. (2013) Impact of Na<sup>+</sup> on biological wastewater treatment and the potential of anaerobic membrane bioreactors: A review. *Critical Reviews in Environmental Science and Technology* 43(24), 2722-2746.
- Yang, J., Tian, Z., Spanjers, H. and Van Lier, J.B. (2014) Feasibility of using NaCl to reduce membrane fouling in anaerobic membrane bioreactors. *Water Environment Research* 86(4), 340-345.
- Yun, Y.-M., Kim, M., Kim, H., Kim, D.-H., Kwon, E.E. and Kang, S. (2019) Increased biodegradability of low-grade coal wastewater in anaerobic membrane bioreactor by adding yeast wastes. *Journal of Environmental Management* 234, 36-43.
- Yurtsever, A., Basaran, E. and Ucar, D. (2020) Process optimization and filtration performance of an anaerobic dynamic membrane bioreactor treating textile wastewaters. *Journal of Environmental Management* 273, 111114.
- Yurtsever, A., Calimlioglu, B., Görür, M., Çinar, Ö. and Sahinkaya, E. (2016) Effect of NaCl concentration on the performance of sequential anaerobic and aerobic membrane bioreactors treating textile wastewater. *Chemical Engineering Journal* 287, 456-465.
- Yurtsever, A., Calimlioglu, B. and Sahinkaya, E. (2017) Impact of SRT on the efficiency and microbial community of sequential anaerobic and aerobic membrane bioreactors for the treatment of textile industry wastewater. *Chemical Engineering Journal* 314, 378-387.
- Zhang, W., Liu, F., Wang, D. and Jin, Y. (2018) Impact of reactor configuration on treatment performance and microbial diversity in treating high-strength dyeing wastewater: Anaerobic flat-sheet ceramic membrane bioreactor versus upflow anaerobic sludge blanket reactor. *Bioresource Technology* 269, 269-275.
- Zhao, W.T., Huang, X., Lee, D.J., Wang, X.H. and Shen, Y.X. (2009) Use of submerged anaerobic-anoxic-oxic membrane bioreactor to treat highly toxic coke wastewater with complete sludge retention. *Journal of Membrane Science* 330(1-2), 57-64.
- Zhao, W.T., Shen, Y.X., Xiao, K. and Huang, X. (2010) Fouling characteristics in a membrane bioreactor coupled with anaerobic-anoxic-oxic process for coke wastewater treatment. *Bioresource Technology* 101(11), 3876-3883.
- Zhao, Y., Zhuang, X., Ahmad, S., Sung, S. and Ni, S.-Q. (2020) Biotreatment of high-salinity wastewater: current methods and future directions. *World Journal of Microbiology and Biotechnology* 36(3), 37.
- Zhen, G., Pan, Y., Lu, X., Li, Y.-Y., Zhang, Z., Niu, C., Kumar, G., Kobayashi, T., Zhao, Y. and Xu, K. (2019) Anaerobic membrane bioreactor towards biowaste biorefinery and chemical energy harvest: Recent progress, membrane fouling and future perspectives. *Renewable and Sustainable Energy Reviews* 115, 109392.







## Trace metals leaching by sodium in AnMBRs

---

This chapter has been published as “Muñoz Sierra, J.D., Lafita, C., Gabaldón, C., Spanjers, H. and van Lier, J.B. (2017) Trace metals supplementation in anaerobic membrane bioreactors treating highly saline phenolic wastewater. *Bioresource Technology* 234, 106-114.”

<https://doi.org/10.1016/j.biortech.2017.03.032>

## Abstract

Biomass requires trace metals (TM) for maintaining its growth and activity. This study aimed to determine the effect of TM supplementation and partitioning on the specific methanogenic activity (SMA), with a focus on cobalt and tungsten, during the start-up of two lab-scale Anaerobic Membrane Bioreactors (AnMBRs) treating saline phenolic wastewater. The TM partitioning revealed a strong accumulation of sodium in the biomass matrix and a wash-out of the majority of TM in the reactors, which led to an SMA decrease and a low COD removal of about 30%. The SMA exhibits a maximum at about  $6 \text{ gNa}^+\cdot\text{L}^{-1}$  and nearly complete inhibition at  $34 \text{ gNa}^+\cdot\text{L}^{-1}$ . The dose of  $0.5 \text{ mgL}^{-1}$  of tungsten increases the SMA by 17%, but no improvement was observed with the addition of cobalt. The results suggested that TM were not bioavailable at high salinity. Accordingly, an increased COD removal efficiency was achieved by doubling the supply of TM.

## 2.1 Introduction

An increasing number of industries generate wastewaters with high salinity and high concentrations of organic pollutants. Chemical and petrochemical industries have been identified as the major producers of these types of wastewaters. Recently, researchers have shown interest in the impact of salinity on anaerobic wastewater treatment (Ismail et al. 2008, Vyrides and Stuckey 2009, Yang et al. 2013). The presence of high concentrations of sodium chloride has a negative impact on the biological conversion with the major effect attributed to the sodium ions. Sodium is toxic when high intracellular concentrations are reached in microorganisms because of electrochemical and osmotic interactions with proteins and nucleic acids (Valentine 2007). High salinity reduces the effectiveness of anaerobic processes (Lefebvre et al. 2007, Vallero et al. 2003) and induces the disintegration of flocs and granules, leading to a prominent biomass wash-out (Ismail et al. 2010, Pevere et al. 2007). The decrease in granule strength due to high sodium concentration results in a significant reduction in particle size in sludge bed reactor systems (Ismail et al. 2008, Jeison and van Lier 2007).

In addition, saline chemical wastewaters often contain aromatic compounds such as phenolics that are not easily biodegradable (Ferrer-Polonio et al. 2016). Phenolic compounds interfere with the transmembrane electrochemical proton gradient and electron transport involved in energy production, which may lead to an inhibitory effect in the wastewater treatment process (Escher et al. 1996). Nevertheless, anaerobic biomass exhibits tolerance towards phenol (Fang and Chan 1997). Phenol is a key intermediate in the anaerobic degradation of a wide variety of aromatics (Fuchs 2008), and is therefore of particular interest for treating industrial chemical wastewater streams.

In order to optimize the function of microorganisms involved in anaerobic degradation pathways, attention to the trace metals (TM) content, fractionation, and speciation is required (Fermoso et al. 2009, van Hullebusch et al. 2016). Especially under high salinity and the presence of aromatic compounds, the supply of TM can have significant effects on the anaerobic biological treatment. Metals such as nickel, iron, cobalt, zinc, tungsten, or molybdenum are contained in several enzymes, regulating the anaerobic pathways (Zandvoort et al. 2006). This work focused on the essential TM cobalt and tungsten. Cobalt was shown to play a key role in the methanogenic activity of high-rate anaerobic reactors treating phenolic wastewater and methanol (Florescio et al. 1994, Melamane et al. 2007, Sharma and Singh 2001). The polyphenol removal efficiency increased from 65 to 93% with the addition of 50 mg L<sup>-1</sup> of Co<sup>3+</sup> (Melamane et al. 2007). Similarly, tungsten plays an important role in the anaerobic degradation process (Schmidt et al. 2014). Tungsto-enzymes appear in catalytic reactions involving extremely low chemical potential that require anaerobic conditions, which is reported as stimulatory to the growth of many types of prokaryotes, including Archaea (Kletzin and Adams 1996). Tungsten is antagonistic to molybdenum, and under certain conditions, tungsto-enzymes rather than molybdoenzymes catalyze the same degradation reactions (Boll et al. 2005). The concentration of TM that causes the inhibition or the stimulation of methanogenesis depends on their bioavailability (Osuna et al. 2004). Metals fractionation can be used for assessing the potential bioavailability of TM by taking into account the following four (4) operationally defined fractions: 1) exchangeable, 2) carbonates, 3) organic matter and sulfides, and 4) residual fraction.

According to Tessier et al. (1979), these fractions are characterized by metal binding forms with declining solubility and reactivity in the order listed above.

However, only a few studies have focused on the effect on biomass activity of TM concentration, partitioning, and bioavailability (Worms et al. 2006). What is not yet well understood is the role and fate of TM and their partitioning and speciation in anaerobic bioreactors, particularly under high salinity conditions. Indeed, to the best of the author's knowledge, no TM partitioning or bioavailability studies have been reported previously in AnMBR reactors.

AnMBRs have shown to be a promising technology for treating wastewaters under high salinity (Dereli et al. 2012, Jeison et al. 2008b, Vyrides and Stuckey 2011). Therefore, the aim of this study was to determine the effect of TM supplementation and partitioning, on methanogenic biomass activity during the start-up of an AnMBR treating high salinity phenolic wastewater. The impact of sodium on the biomass and potential bioavailability of TM are evaluated by using laboratory-scale batch reactors and continuous flow AnMBRs. The findings of this study will contribute to the successful start-up and operation of AnMBRs, as treatment of hazardous and saline wastewaters is becoming more important.

## 2.2 Materials and methods

### 2.2.1 Batch reactor tests

#### 2.2.1.1 SMA response to sodium concentration

The effect of increasing sodium concentrations on the SMA was assessed using the AnMBR inoculum. A medium with only sodium chloride (NaCl) and one with NaCl and sodium bicarbonate ( $\text{NaHCO}_3$ ) (ratio 1:1  $\text{Na}^+$  w/w), both maintaining the same total sodium concentration. SMA tests were performed in duplicate using an automated methane potential test system (AMPTS, Bioprocess Control, Sweden). The initial pH of all SMA test bottles was adjusted to 7.0 ( $18 \pm 0.4^\circ\text{C}$ ).

#### 2.2.1.2 Phenol:acetate ratio effect on methanogenic activity

SMA tests using different ratios of phenol:acetate as substrate were carried out in triplicate. The ratio was varied from 0 (acetate as a sole substrate) to 1 (50% COD from acetate and 50% COD from phenol), while keeping a total COD concentration of 2 g  $\text{COD}\cdot\text{L}^{-1}$ . The detailed concentrations are presented in Table 2.1.

Table 2.1. Substrate phenol and sodium acetate concentrations in batch assays.

Phenol:acetate COD ratio	Phenol [ $\text{mg}\cdot\text{L}^{-1}$ ]	$\text{CH}_3\text{COONa}\cdot 3\text{H}_2\text{O}$ [ $\text{mg}\cdot\text{L}^{-1}$ ]
0.00	0	4250
0.25	168.1	3400
0.43	252.1	2975
0.67	336.1	2553
1.00	420.2	2127

### 2.2.1.3 Effect of TM on methanogenic activity: tungsten and cobalt

The effect of cobalt, both in the form of  $\text{CoCl}_2$  and vitamin  $\text{B}_{12}$ , and tungsten on the methane production rate was investigated using SMA assays in triplicate. These assays were carried out with a mixture of phenol and sodium acetate in a COD ratio 1:4 and two different medium compositions A and B. In medium A, the sodium concentration was composed of 10 g  $\text{NaCl L}^{-1}$  and 18.3 g  $\text{NaHCO}_3 \text{ L}^{-1}$  and the solution was buffered with 1.05 g  $\text{K}_2\text{HPO}_4 \text{ L}^{-1}$  and 0.5 g  $\text{KH}_2\text{PO}_4 \text{ L}^{-1}$ . The macro and micro nutrients composition in the model wastewater was as follows (in  $\text{mg L}^{-1}$  unless otherwise indicated):  $\text{NH}_4\text{Cl}$ , 1020;  $\text{CaCl}_2 \cdot 2\text{H}_2\text{O}$ , 48;  $\text{MgSO}_4 \cdot 7\text{H}_2\text{O}$ , 54;  $\text{FeCl}_3 \cdot 6\text{H}_2\text{O}$ , 1.2;  $\text{MnCl}_2 \cdot 4\text{H}_2\text{O}$ , 0.3;  $\text{CuCl}_2 \cdot 2\text{H}_2\text{O}$ , 0.02;  $\text{ZnCl}_2$ , 0.03;  $\text{HBO}_3$ , 0.03;  $(\text{NH}_4)_6\text{Mo}_7\text{O}_{24} \cdot 4\text{H}_2\text{O}$ , 0.05;  $\text{Na}_2\text{SeO}_3$ , 0.06;  $\text{NiCl}_2 \cdot 6\text{H}_2\text{O}$ , 0.03; EDTA, 0.6, resazurin, 0.3; yeast extract, 1.2, HCl 35%,  $6 \cdot 10^{-4} \text{ ml L}^{-1}$ . In medium B, the composition of sodium compounds was changed while keeping the same total sodium concentration, i.e., 10 g  $\text{Na}^+ \text{L}^{-1}$ , by using 16.7 g  $\text{NaCl L}^{-1}$  and 9 g  $\text{NaHCO}_3 \text{ L}^{-1}$ . Typical seawater contains about 10.5 g  $\text{Na}^+ \text{L}^{-1}$ . Micronutrients concentration in medium B were doubled from medium A, resulting in the following composition (in  $\text{mg L}^{-1}$  unless otherwise indicated):  $\text{NH}_4\text{Cl}$ , 1020;  $\text{CaCl}_2 \cdot 2\text{H}_2\text{O}$ , 48;  $\text{MgSO}_4 \cdot 7\text{H}_2\text{O}$ , 54;  $\text{FeCl}_3 \cdot 6\text{H}_2\text{O}$ , 2.4;  $\text{MnCl}_2 \cdot 4\text{H}_2\text{O}$ , 0.6;  $\text{CuCl}_2 \cdot 2\text{H}_2\text{O}$ , 0.04;  $\text{ZnCl}_2$ , 0.06;  $\text{HBO}_3$ , 0.06;  $(\text{NH}_4)_6\text{Mo}_7\text{O}_{24} \cdot 4\text{H}_2\text{O}$ , 0.1;  $\text{Na}_2\text{SeO}_3$ , 0.12;  $\text{NiCl}_2 \cdot 6\text{H}_2\text{O}$ , 0.06; EDTA, 1.2, resazurin, 0.6; yeast extract, 2.4; HCl 35%,  $6 \cdot 10^{-4} \text{ ml L}^{-1}$ . SMA assays were performed with different concentrations of cobalt and tungsten as indicated in Table 2.2. In the tungsten assays, the cobalt content was 0.29  $\text{mgCo L}^{-1}$  and 0.58  $\text{mgCo L}^{-1}$  for medium A and B, respectively. In the cobalt assays, no tungsten was added.

Table 2.2. Cobalt, as  $\text{CoCl}_2$  or vitamin  $\text{B}_{12}$ , and tungsten concentrations added to mediums A and B in SMA tests. All tests were carried out in triplicate.

Medium	Cobalt source	Cobalt Concentration [ $\text{mg L}^{-1}$ ]	Tungsten Concentration [ $\text{mg L}^{-1}$ ]
A	$\text{CoCl}_2$	0	-
A	$\text{CoCl}_2$	0.29	-
A	$\text{CoCl}_2$	5	-
A	$\text{CoCl}_2$	10	-
A	$\text{CoCl}_2$	20	-
B	$\text{CoCl}_2$	0.58	-
A	Vitamin $\text{B}_{12}$	0.29	-
A	Vitamin $\text{B}_{12}$	5	-
B	Vitamin $\text{B}_{12}$	0.58	-
A	$\text{CoCl}_2$	0.29	0
A	$\text{CoCl}_2$	0.29	0.5
A	$\text{CoCl}_2$	0.29	1
A	$\text{CoCl}_2$	0.29	3
A	$\text{CoCl}_2$	0.29	5
B	$\text{CoCl}_2$	0.58	0.5

## 2.2.2 AnMBR

### 2.2.2.1 Inoculum

Two reactors were seeded with concentrated anaerobic biomass obtained from a full-scale UASB reactor treating industrial wastewater (Shell, Moerdijk, The Netherlands) mainly containing acetate and benzoate. Three consecutive samplings were conducted before the inoculation to characterize the biomass. Total solids (TS), volatile solids (VS) and volatile suspended solids (VSS) concentrations of the inoculum used were  $96 \text{ g}\cdot\text{L}^{-1}$ ,  $57 \text{ g}\cdot\text{L}^{-1}$ , and  $55 \text{ g}\cdot\text{L}^{-1}$ , respectively. The alkalinity of the inoculum was  $19 \text{ g CaCO}_3\cdot\text{L}^{-1}$ , electrical conductivity was  $22.5 \text{ mS cm}^{-1}$  ( $19.1^\circ\text{C}$ ) and pH was 8.1 ( $19.2^\circ\text{C}$ ).

### 2.2.2.2 Experimental setup

The continuous flow experiments were performed using two laboratory-scale AnMBR reactors with an effective volume of 6.5 L, equipped with an ultra-filtration (UF) side-stream membrane module (. A tubular polyvinylidene fluoride membrane (X-flow, Pentair, The Netherlands) with 5.2 mm inner diameter, 0.64 m length, and 30 nm nominal pore size was used. The reactors were equipped with feed, recycle and effluent pumps with 4-20 mA variable speed (120U/DV, 220Du, Watson-Marlow, The Netherlands), pH, and temperature sensors (Memosens, Endress & Hauser, Germany), and a biogas meter (Milligas Counter MGC-1 PMMA, Ritter, Germany). A biogas recirculation diaphragm pump (KNF) at a rate of  $40 \text{ L}\cdot\text{h}^{-1}$  was used to mix the liquor. The temperature of the jacketed reactor was kept constant at  $35.0 \pm 0.8^\circ\text{C}$  by a thermostatic water bath (Tamson Instruments, The Netherlands). Transmembrane pressure (TMP) was measured by using three pressure sensors (AE Sensors ATM, The Netherlands). The cross-flow velocity was kept constant at  $0.6 \text{ m s}^{-1}$ . A cyclic membrane filtration operation was carried out, consisting of 500 s filtration and 30 s backwash. Backwash was done by reversing the effluent pump flow. The two reactors were operated in parallel under similar conditions. The entire setup was controlled by a programmable logic controller (PLC) connected to a PC with LabVIEW software (version 15.0.1f1, National Instruments, USA).

### 2.2.2.3 Start-up procedure

The reactors were inoculated at a concentration of  $30 \text{ gVSS}\cdot\text{L}^{-1}$ . The model wastewater contained  $10 \text{ g Na}^+\cdot\text{L}^{-1}$  (medium A). The AnMBRs were continuously fed during a start-up period of three months. In the first month, acetate was used as the sole carbon source in the model wastewater. Hereafter, phenol was added, starting at  $10 \text{ mg}\cdot\text{L}^{-1}$  and gradually increased once the start-up period was completed.

## 2.2.3 Particle Size Distribution

PSD analysis was carried out by using a DIPA-2000 Eyeteck particle analyzer (Donner Technologies) with a B100 laser lens (measuring range  $10\text{-}2000 \mu\text{m}$ ) and liquid flow cell DCM-104A ( $10\times 10\text{mm}$ ). Values D10, D50, and D90 from the volume particle size distribution were reported.

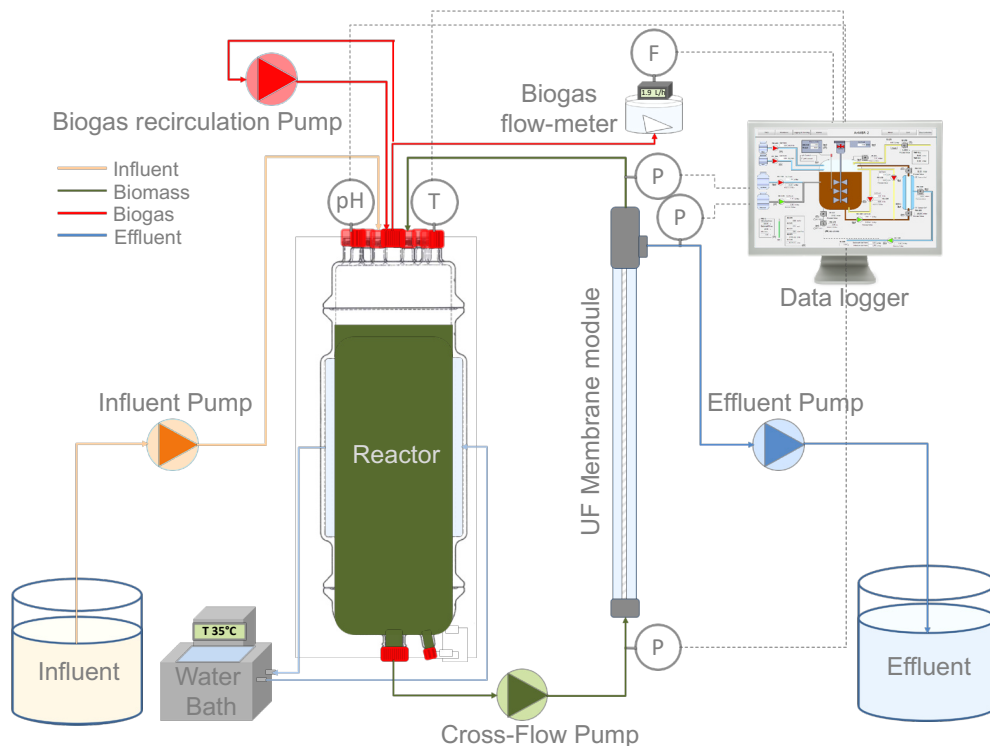


Figure 2.1 Schematic representation of the mesophilic AnMBR.

## 2.2.4 Metals partitioning in biomass matrix

A modified Tessier sequential extraction procedure proposed by Osuna et al. (Osuna et al. 2004) was used to assess the TM partitioning in the exchangeable, the carbonate, the organic matter and sulfides, and the residual operationally defined fractions. For this purpose, 1 g TS of anaerobic biomass was treated as described in Table 2.3. Closed pressurized vessels and a microwave oven (Milestone MLS 1200 Mega) were used to carry out the extraction of the residual fraction. The heating period was 28 minutes at different microwave powers as follows: 2 min at 250W, 2 min at 0W, 5 min at 250W, 5 min at 400W, and 14 min at 650W.

Table 2.3. Operating conditions required in sequential extraction method. Modified from Van Hullebusch et al. 2005.

Fraction	Extracting agent	Extraction conditions	
		Shaking time	Temperature
Exchangeable	10 ml $\text{NH}_4\text{CH}_3\text{COO}$ 1M	1 h	20 °C
Carbonates	10 ml $\text{CH}_3\text{COOH}$ 1M	1 h	20 °C
Organic matter and sulfides	5 ml $\text{H}_2\text{O}_2$ 30% (pH=2)	3 h	35 °C
Residual	10 ml aqua regia ( $\text{HCl}:\text{HNO}_3$ 3:1)		Microwave oven

### 2.2.5 Biomass and supernatant metal content determination

Inductively coupled plasma/optical emission spectrometry (ICP-OES) was used to characterize the main metals present in the biomass after the sequential extraction and in the supernatant. All samples were filtered through polyethersulfone syringe filters (0.45 $\mu$ m, VWR), and two dilutions (1:50 and 1:1000) were made in a solution of nitric acid (HNO<sub>3</sub> 3% v/v) for analysis by the ICP-OES spectrometer (Spectro Arcos).

### 2.2.6 Statistical analysis

Means and standard deviations were calculated from the assays carried out in triplicate. The differences in SMA biomass activities between the test treatments were analyzed by one-way analysis of variance (ANOVA). Post hoc analysis was performed using Tukey's honest significant difference (HSD) test of multiple means comparison at a significance level of  $\alpha=0.05$ . Two-way ANOVA was used for the evaluation of particle size distribution data. A four-parameter logistic function, i.e.,  $f(x, (a, b, c, d)) = d + (a-d)/(1+10^{(c-\log_e)x/b})$ , was used to fit the experimental data from the sodium concentration-SMA response curves. The half-maximal inhibition concentration (IC<sub>50</sub>) was estimated. The analysis was performed using OriginPro 8 (OriginLab Corporation, Northampton, USA).

## 2.3 Results and discussion

### 2.3.1 SMA response to sodium concentration and inoculum characterization

A deterioration of the biomass activity was observed during the start-up period in the AnMBRs 1 and 2. The SMA of the biomass decreased from  $0.68 \pm 0.07$  gCOD-CH<sub>4</sub>gVSS<sup>-1</sup>d<sup>-1</sup> to  $0.31 \pm 0.04$  gCOD-CH<sub>4</sub>gVSS<sup>-1</sup>d<sup>-1</sup> after one month in both reactors. Other studies also observed a decrease in removal performance due to the negative effect of the salinity increase on the bioreactor activity (Song et al. 2016). The SMA of the inoculum was about  $0.80$  gCOD-CH<sub>4</sub>gVSS<sup>-1</sup>d<sup>-1</sup> at a sodium concentration of about  $6$  gNa<sup>+</sup>L<sup>-1</sup> as depicted in Figure 2.2. As shown by Feijoo et al. (1995), a sodium concentration between  $4.4$ – $17.7$  gNa<sup>+</sup>L<sup>-1</sup> may result in 50% inhibition of the methane production rate. According to the results, a sodium concentration of about  $23$  gNa<sup>+</sup>L<sup>-1</sup> decreased the methanogenic activity to half of the maximum value and was regarded as the 50% inhibition concentration (IC<sub>50</sub>). Almost complete inhibition was found at  $34$  gNa<sup>+</sup>L<sup>-1</sup>. This exposure of the biomass to high salinity could result in cell plasmolysis and corresponding loss of activity (Yogalakshmi and Joseph 2010).

The tendency observed in the SMA response to sodium concentration is similar to that found in previous studies (Jeison et al. 2008a). However, in our present study higher specific methanogenic activities were observed with a similar source of inoculum, with values of up to four times higher for sodium concentrations in the range of  $0$ – $12$  gNa<sup>+</sup>L<sup>-1</sup>. For all sodium concentrations tested, the use of only sodium chloride resulted in higher methanogenic activity. Nevertheless, from the inoculum supernatant metals characterization (Table 2.4) the mass ratio Na<sup>+</sup>:Cl<sup>-</sup> ( $4.65$  mg·mg<sup>-1</sup>) was higher than expected ( $0.64$  mg·mg<sup>-1</sup>) given that all sodium would have only originated from sodium



chloride. Furthermore, it is shown in Table 2.4. that the presence of tungsten had a remarkable concentration variation (1.1 – 18.5 mgW<sup>+6</sup>L<sup>-1</sup>). The major variation (>40%) was found in the third sample for the ions Na<sup>+</sup>, Cl<sup>-</sup>, SO<sub>4</sub><sup>2-</sup>, and W<sup>+6</sup>, whereas a less significant variation was observed for Ca<sup>2+</sup>, K<sup>+</sup>, and PO<sub>4</sub><sup>3-</sup>. These variations could be attributed to salinity swing fluctuations due to changes in operation from the production plant (Shell, Moerdijk). Additionally, the K<sup>+</sup>:Na<sup>+</sup> ratio, a key parameter for maintaining biodegradation activity under saline conditions, ranged from 0.14 to 0.045 mg-mg<sup>-1</sup> in the inoculum according to the ICP-OES analysis. The K<sup>+</sup>:Na<sup>+</sup> ratio was kept constant at 0.05 in the model wastewater.

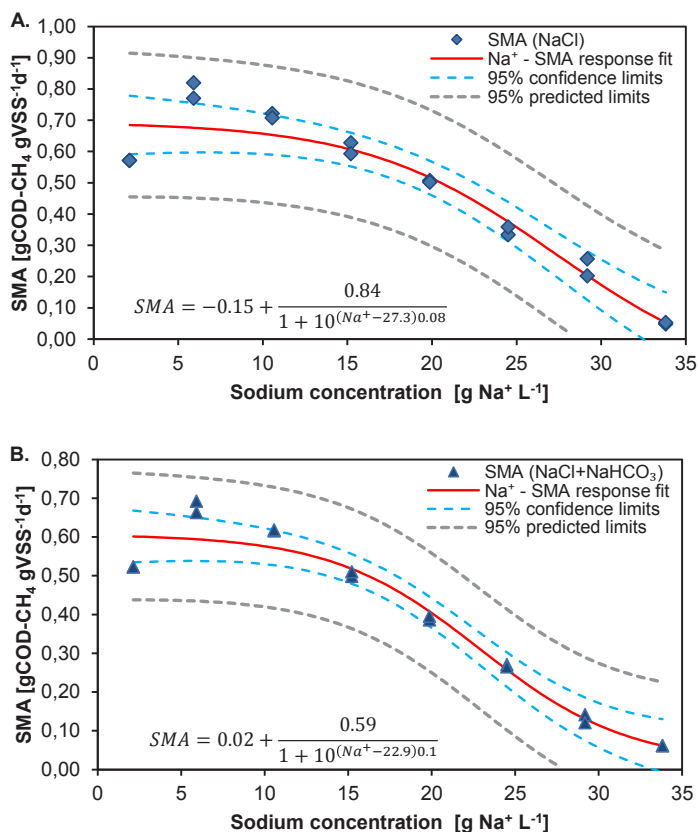


Figure 2.2 A. Specific methanogenic activity response to sodium concentrations. A. Sodium concentration from NaCl with 95% confidence limits of SMA. The logistic model fit the data adequately,  $\chi^2=0.009$ , adj. R<sup>2</sup>=0.965. The four parameters standard errors were SE<sub>a</sub>=0.05, SE<sub>b</sub>=0.03, SE<sub>c</sub>=3.01, SE<sub>d</sub>=0.21. IC<sub>50</sub>predicted=27.30. B. Sodium concentration from NaCl and NaHCO<sub>3</sub> (1:1 Na<sup>+</sup> w/w) with 95% confidence limits of SMA. The logistic model fit the data satisfactorily,  $\chi^2=0.005$ , adj. R<sup>2</sup>=0.976. The four parameters standard errors were SE<sub>a</sub>=0.03, SE<sub>b</sub>=0.02, SE<sub>c</sub>=0.88, SE<sub>d</sub>=0.03. IC<sub>50</sub>predicted=22.88. Both fitted curves significantly explained the SMA R<sup>2</sup> NaCl= 0.97, F NaCl(4,15)=119.08, p< 0.001. R<sup>2</sup> NaCl+NaHCO<sub>3</sub>= 0.98, F NaCl+NaHCO<sub>3</sub>(4,15)=168.51, p< 0.001

Table 2.4 Main ions present in the inoculum supernatant characterized by ICP-OES. Samples 1-3 were taken in three different sampling campaigns. All concentrations in  $\text{mg}\cdot\text{L}^{-1}$ .

Sampling campaign	$\text{Ca}^{2+}$	$\text{K}^+$	$\text{Na}^+$	$\text{Cl}^-$	$\text{PO}_4^{3-}$	$\text{SO}_4^{2-}$	$\text{W}^{+6}$
1	871.7	1264.0	8956.5	1933.0	1859.7	201.1	18.5
2	800.0	1294.0	9632.0	1958.0	1815.0	174.1	6.6
3	833.3	844.0	18430.0	4189.5	1692.7	9.52	1.1

### 2.3.2 Effect of phenol:acetate ratio on methanogenic activity

SMA tests were performed with inoculum biomass under varying phenol:acetate COD ratios in medium A to assess the potential toxicity of phenol on biomass activity in the reactor operation. The results (Figure 2.3) show that the biomass methanogenic activity decreased while increasing the phenol:acetate COD ratio. An SMA of about  $0.25 \pm 0.01 \text{ gCOD}\cdot\text{CH}_4\cdot\text{gVSS}^{-1}\cdot\text{d}^{-1}$  was obtained with a ratio of 1, i.e., adding  $420.2 \text{ mgPh}\cdot\text{L}^{-1}$  to the medium, implying a reduction of about 43% of the SMA compared to the maximum found with no phenol addition ( $0.44 \pm 0.01 \text{ gCOD}\cdot\text{CH}_4\cdot\text{gVSS}^{-1}\cdot\text{d}^{-1}$ ) within these assays. A similar SMA value was found by Razo-Flores et al. (2003) when starting-up a UASB reactor with biomass with acetate medium and subsequent addition of a mixture of phenolic compounds. The observed SMA reduction is in accordance with Fang and Chang (1997) who showed a decrease in SMA with the increase in phenol concentration. The concentration of phenol in these assays is in accordance with average medium-high phenol concentrations (from 120 to  $1200 \text{ mg}\cdot\text{L}^{-1}$ ) that are related to industrial wastewaters such as oil refineries (6 to  $500 \text{ mg}\cdot\text{L}^{-1}$ ), coke (28 to  $3900 \text{ mg}\cdot\text{L}^{-1}$ ), and petrochemical wastewaters (2.8 to  $1220 \text{ mg}\cdot\text{L}^{-1}$ ) (Rosenkranz et al. 2013). However, the SMA obtained with a phenol:acetate COD ratio of 1 at the start of the test is still higher than that reported in previous studies using the same biomass source without any recalcitrant or toxic compound present but under similar salinity conditions (Ismail et al. 2008, Jeison et al. 2008a, Yang et al. 2013).

### 2.3.3 Effect of tungsten on methanogenic activity

Because tungsten stimulates the growth of many types of prokaryotes, including methanogenic Archaea (Kletzin and Adams 1996, Plugge et al. 2009) the role of this trace metal and its dosage were assessed. Medium A was used in SMA tests with increasing concentrations of tungsten. A 17% increase in the methane production rate was achieved with the addition of 0.5 and  $1 \text{ mg}\cdot\text{L}^{-1}$  of tungsten in comparison with the reference test with no tungsten addition (Figure 2.4.A). Feng et al. (2010) observed an increase in methane production efficiency from 7 to 15% for an anaerobic reactor treating food industry waste by adding a tungsten concentration of  $1.8 \text{ mg}\cdot\text{W}\cdot\text{L}^{-1}$ . However, in our current study, the presence of tungsten concentrations higher than  $1 \text{ mg}\cdot\text{W}\cdot\text{L}^{-1}$  caused a decrease in SMA, suggesting partial inhibition under the conditions applied in batch, resulting in about one-third of the maximum SMA with the addition of  $5 \text{ mg}\cdot\text{W}\cdot\text{L}^{-1}$ .

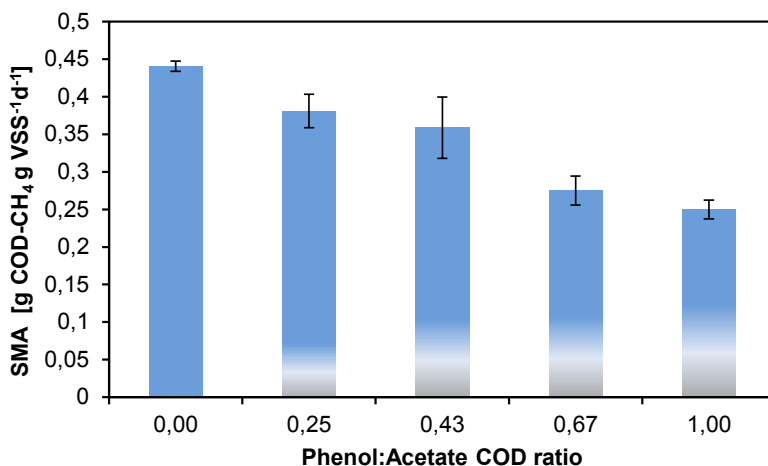


Figure 2.3 Specific methanogenic activity under different phenol:acetate COD ratios. The means of all SMA were significantly different,  $F(4,10) = 33.46$ ,  $p < 0.001$ . Tukey's test for significance specified that at the 0.05 level, the means difference did not significantly differ between the phenol:acetate COD ratios of 0 ( $M=0.44$ ,  $SD=0.01$ ) and 0.25 ( $M=0.38$ ,  $SD=0.02$ ); 0.25 and 0.43 ( $M=0.36$ ,  $SD=0.04$ ); 0.67 ( $M=0.28$ ,  $SD=0.02$ ) and 1.0 ( $M=0.25$ ,  $SD=0.01$ ).

As the assessment of the potential bioavailability of trace metals by sequential extraction is based on the availability of metal-binding forms for microbial uptake, metals associated with the exchangeable fraction are defined as the most available and those associated with the residual fraction as the least available (Tessier et al. 1979). Comparing the SMA results with the distribution of tungsten over the biomass fractions, it is postulated that particularly its presence in the exchangeable fraction, the most available one, caused a decline in SMA, as observed after the addition of  $5 \text{ mgW}\cdot\text{L}^{-1}$  (Figure 2.4.A). The relative increase in tungsten concentration in the organic matter and sulfides fraction indicates its high affinity to this fraction.

The biomass in the presence of  $0.5 \text{ mgW}\cdot\text{L}^{-1}$  doubled the tungsten content in the organic matter and sulfides fraction in comparison with the inoculum, but with concentrations higher than  $1 \text{ mgW}\cdot\text{L}^{-1}$ , the content of tungsten in the organic matter and sulfides fraction was four times higher in comparison with no tungsten addition (Figure 2.4.B). As expected, the increase in the tungsten concentration in the organic matter and sulfides fraction did not result in any improvement in methane production. Furthermore, at  $0.5 \text{ mgW}\cdot\text{L}^{-1}$ , an increase in the tungsten content of 36.4% and 53.4% in the residual fraction and 29.8% and 36% in the carbonate fraction was observed in comparison with the inoculum and biomass exposed to  $1 \text{ mgW}\cdot\text{L}^{-1}$ , respectively. Consequently, the optimum dosage of tungsten was determined to be  $0.5 \text{ mgW}\cdot\text{L}^{-1}$  since it matched the maximum SMA found.

### 2.3.4 Effect of cobalt on methanogenic activity

Similarly, the effect of cobalt addition on the methane production rate was evaluated through SMA assays using inoculum biomass under different concentrations of cobalt as  $\text{CoCl}_2$  and vitamin  $\text{B}_{12}$ . Cobalt-containing carbon monoxide dehydrogenase complex is involved in the acetate and phenol degradation via 4-hydrogenate and the benzoyl-CoA pathway (Levén et al. 2012). Furthermore, cobalt is present in methylcob(III)alamin:coenzyme M methyltransferase which is a key intermediate in methanogenesis (Zandvoort et al. 2006). The results are depicted in Figure 2.4. C and D. Medium A was used as the macro/micronutrients solution. The maximum SMA was measured without cobalt (blank) in the presence of  $0.29 \text{ mg}\cdot\text{L}^{-1}$  of cobalt as vitamin  $\text{B}_{12}$  or  $\text{CoCl}_2$  and  $5 \text{ mg}\cdot\text{L}^{-1}$  of cobalt as  $\text{CoCl}_2$ . The increase from 0 to  $5 \text{ mg}\cdot\text{L}^{-1}$  had no impact on the methane production rate. A decrease by approximately one-third in the SMA in comparison with the maximum SMA was observed with the addition of  $5 \text{ mg}\cdot\text{L}^{-1}$  as vitamin  $\text{B}_{12}$ , whereas  $20 \text{ mg}\cdot\text{L}^{-1}$  as  $\text{CoCl}_2$  was needed to achieve a similar decrease in the SMA.

Results suggest that a likely higher bioavailability of cobalt as vitamin  $\text{B}_{12}$  caused the inhibition of the methane production with lower cobalt concentration compared to the  $\text{CoCl}_2$  test. Bhattacharya et al. (1995) observed an inhibition of methanogenesis of 7 and 17% when  $\text{CoCl}_2$  was added as cobalt source in a concentration of 600 and 800  $\text{mg}\cdot\text{L}^{-1}$ , respectively, demonstrating the importance of determining the optimum cobalt dosage.

Cobalt partitioning was assessed with biomass to which no cobalt was added and with biomass supplemented with  $5 \text{ mg}\cdot\text{L}^{-1}$  as  $\text{CoCl}_2$  or vitamin  $\text{B}_{12}$ . Cobalt was present in all fractions in the reactors operated with no cobalt addition (Figure 2.4.D). Apparently, the inoculum biomass contained the minimum cobalt levels to achieve maximum SMA values. An increase in total cobalt content was observed with the addition of  $\text{CoCl}_2$  or vitamin  $\text{B}_{12}$ , showing the availability of active sites in the biomass to adsorb and accumulate a higher quantity of cobalt. The affinity of cobalt in the form of  $\text{CoCl}_2$  to the carbonate, organic matter, and sulfides, and residual fraction caused higher accumulation of cobalt in the presence of  $5 \text{ mg}\cdot\text{L}^{-1}$  as  $\text{CoCl}_2$  in comparison to those with  $5 \text{ mg}\cdot\text{L}^{-1}$  as vitamin  $\text{B}_{12}$ . In the presence of vitamin  $\text{B}_{12}$ , cobalt concentration in the exchangeable fraction was doubled, corroborating the higher affinity of vitamin  $\text{B}_{12}$  to the exchangeable fraction.

### 2.3.5 Particle size impacted by sodium

The particle size of the biomass significantly decreased during the membrane bioreactor's start-up period. The results of the particle size distribution analysis demonstrated a drastic reduction after three months of operation from an initial median size (D50) of  $424 \pm 73 \mu\text{m}$  to  $112 \pm 4.1 \mu\text{m}$  and  $100 \pm 2.5 \mu\text{m}$  for the AnMBRs 1 and 2, respectively (Figure 2.5). Both the high shear force in the side stream AnMBR and the high sodium concentration may have contributed to the particle size reduction, the latter because of its negative impact on the particle strength (Ismail et al. 2008). This is in agreement with the observations made by Jeison et al. (2008a) who operated reactors at sodium concentrations of about 10, 12, and  $7.5 \text{ g Na}^+\cdot\text{L}^{-1}$  and found a significant reduction in particle size in comparison to the inoculum. The reduction in granule strength was higher in the reactors operated at a higher salinity level.

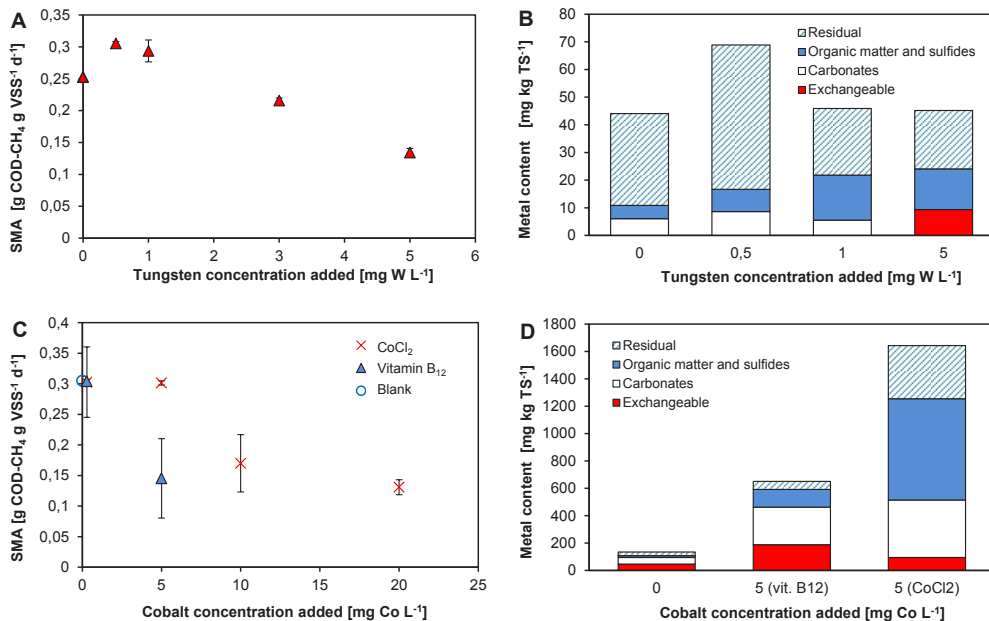


Figure 2.4. A. Specific methanogenic activity of the inoculum using medium A at different concentrations of tungsten added. SMA results were statistically significant,  $F(4,10) = 220.59, p < 0.001$ . Tukey's test revealed that at the 0.05 level, the difference of the means was not significant between 0.5 mgW L<sup>-1</sup> ( $M=0.30, SD=0.00$ ) and 1 mgW L<sup>-1</sup> ( $M=0.29, SD=0.01$ ). B. Partitioning of tungsten (mg kg TS<sup>-1</sup>) in the operationally defined fractions of the biomass from SMA assays. C. Specific methanogenic activity of the inoculum biomass using medium A at different concentrations of cobalt as CoCl<sub>2</sub> and vitamin B12. SMA results were statistically significant,  $F_{CoCl_2}(4,10) = 39.91, p < 0.001$  and,  $F_{vitamin\ B12}(2,6)=17.53, p=0.003$ . Tukey's test inferred that the difference of the means between the blank and 0.29 mgCo L<sup>-1</sup> was not significant at the 0.05 level for both CoCl<sub>2</sub> and vitamin B12. D. Partitioning of cobalt (mg kg TS<sup>-1</sup>) in the operationally defined fractions of the biomass from SMA assays.

Unexpectedly, the reduction of particle size in reactor 2 was 48% less after one month than in reactor 1, indicating a different biomass matrix in the two reactors, but analogous distribution was observed in the third month with similar D10 and D90 values. It should be noted that free cells or smaller biomass particles are subject to reduced mass transfer limitation and thus more sensitive to toxicity.

### 2.3.6 Effect of trace metals composition on AnMBR methanogenic activity

The response of biomass from the AnMBRs 1 and 2 in the presence of medium B was assessed in batch reactors after one and two months of operation. The inoculum biomass was used as the control. The experiments were carried out with the addition of CoCl<sub>2</sub>, vitamin B<sub>12</sub>, or tungsten. Cobalt concentration was double (0.58 mgCoL<sup>-1</sup>) in comparison to the concentration applied to the reactors, but for tungsten, the optimal supply determined in previous SMA assays (0.5 mgW L<sup>-1</sup>) was added. A wash-out of essential TM from the biomass in the AnMBR reactors applying high salinity conditions could have been the cause for the observed lower SMA values after one month

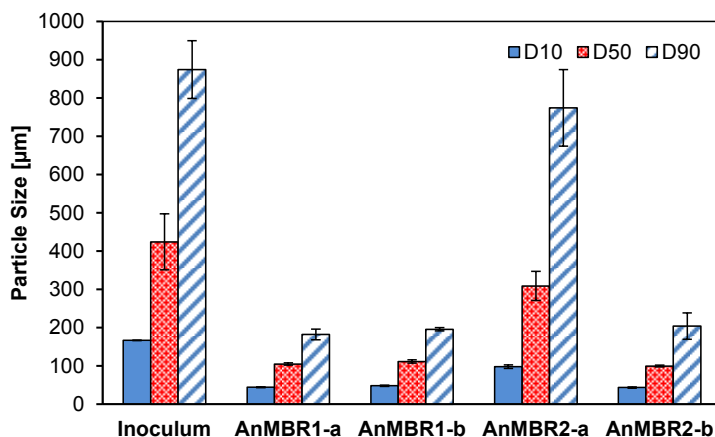


Figure 2.5 Particle size distribution D10, D50, and D90 corresponding to the percentages 10%, 50%, and 90% of particles under the reported particle size. a. One month after inoculation. b. Three months after inoculation. Particle size results were statistically significant,  $p < 0.001$ . Tukey's test specified that the means difference is not significant at the level of 0.05 between the inoculum and AnMBR2 after one month, and between the AnMBR1 and AnMBR2 after three months.

of reactor operation (Table 2.5). A similar effect of high salinity was observed by Ismail et al. (2010) with a 38% decrease in  $\text{Ca}^{2+}$  biomass content after adding  $20 \text{ g Na}^+ \text{ L}^{-1}$  to the influent.

The assays with  $0.5 \text{ mgW} \cdot \text{L}^{-1}$  showed a decrease in SMA compared to SMA with inoculum biomass. The latter indicated that the role of this metal changed during the reactor operation without any addition of tungsten, which could be attributed to changes in the distribution of metals concentration in biomass as observed by Espinosa et al. (1995) in a UASB reactor during different operational periods.

### 2.3.7 Metals partitioning and concentration from AnMBRs

Figure 2.6 shows the partitioning of trace and major elements in the operationally defined fractions and total concentrations in the inoculum and the biomass from the two AnMBRs. The inoculum biomass showed a high content of the TM cobalt and iron (higher than  $3000 \text{ mg} \cdot \text{kgTS}^{-1}$ ) and a relatively high content of molybdenum, manganese, and zinc (about  $300 \text{ mg} \cdot \text{kgTS}^{-1}$ ), which were mainly associated with the residual fraction. The content of tungsten was  $44 \text{ mg} \cdot \text{kgTS}^{-1}$ , and it was bound to the carbonates (13.6%), organic matter and sulfides (10.9%), and residual (75.5%) fractions (Figure 2.6. A). Phosphorus and magnesium were found to be predominantly associated with the residual fraction (96.7 and 48.4% of the total amount, respectively), whereas sodium showed higher affinity to the exchangeable fraction (59.3%) and, calcium to the carbonates (45.9%) and residual (43.2%) fractions (Figure 2.6. B). Even though a portion of about 11% of the total TM content in the inoculum biomass was found in the exchangeable and carbonates fractions (the more soluble ones), the TM amount found in these fractions was reasonable for ensuring bioavailability in the inoculum, except for copper.

Table 2.5. The specific methanogenic activity from inoculum and reactors biomass after one month of operation. Batch test using medium B with the addition of tungsten and cobalt as  $\text{CoCl}_2$  and Vitamin B<sub>12</sub>.

Trace metal added	SMA [ $\text{gCOD-CH}_4\text{gVSS}^{-1}\text{d}^{-1}$ ]		
	Inoculum	AnMBR1	AnMBR2
0.58 mg Co L <sup>-1</sup> as $\text{CoCl}_2$	0.43±0.01	0.10±0.01	0.11±0.01
0.58 mg Co L <sup>-1</sup> as Vitamin B <sub>12</sub>	0.35±0.02	0.09±0.01	0.10±0.01
0.5 mg W L <sup>-1</sup> as $\text{Na}_2\text{WO}_4$	0.36±0.01	0.06±0.02	0.06±0.01

A decrease in the total content of all metals in the biomass of AnMBRs was observed one month after inoculation, except for sodium and selenium. Moreover, higher metal solubilization was observed in reactor 2, resulting in 46% less metal content in reactor 2 compared to reactor 1, whereas a different metal partitioning was found in each reactor. The major reduction in the total metal content was found in the residual fraction, 64% reduction in reactor 1, and 86% in reactor 2. This difference in the biomass metal matrix could also explain the observed discrepancy in particle size reduction in both reactors during this period of operation.

In contrast, an increase in the nickel and iron concentration in the exchangeable fraction was measured in both reactors, while cobalt and molybdenum concentrations only increased in this fraction in reactor 1 and selenium in reactor 2, indicating an increase in the bioavailability of these metals for the biomass during the start-up period (Figure 2.6 C and E). Evidently, the metal composition of the reactor's influent impacted the chemical equilibrium of the initial biomass' metal content, therefore affecting the biomass metal partitioning, as was also observed by Bhatti et al (1995).

In spite of the high solubilization of metals into the reactors, relatively low concentrations of all TM were measured after ultrafiltration through the reactor's membrane after one month of operation (see Figure 2.7), except for tungsten, molybdenum, and selenium. This suggests that the wash-out of the main portion of TM took place during the first month after inoculation. The concentration in the effluent of molybdenum and tungsten in both reactors was higher than in the influent (no addition of tungsten in the influent) showing that the solubilization and wash-out of these TM were slower than for the other metals and were still ongoing after one month of operation. According to Figure 2.6 C and D, solubilization of tungsten mainly occurred in the carbonates fraction, whereas the content in the exchangeable fraction increased from non-detectable to 9.2 and 12.8  $\text{mg}\cdot\text{kgTS}^{-1}$  in reactor 1 and 2, respectively. The content in the organic matter and sulfides fraction increased to nearly three times its original value in both reactors.

The solubilization could have caused a change in the role played by tungsten in the anaerobic conversion of organic matter to methane, as shown by the SMA decrease (Table 2.5). With respect to the solubilization of molybdenum, similar molybdenum content was observed in the carbonates and the organic matter and sulfides fractions in the inoculum and reactors, showing that the major reduction in molybdenum was in the residual fraction. Selenium uptake in biomass was associated

with the organic matter and sulfides fraction as was evidenced by the increase in selenium content in this fraction from 0 mg·kg<sup>-1</sup>TS to 2.4 mg·kg<sup>-1</sup>TS in reactor 1 and 3.5 mg·kg<sup>-1</sup>TS in reactor 2.

Macroelements, except sodium, were also solubilized (Figure 2.6 D and F). The major solubilization of macroelements occurred in the residual fraction (64% reduction in total macroelements content in reactor 1 and 86% in reactor 2), while an increase in total macroelements content was measured in the exchangeable fraction (44% increase in reactor 1 and 30% in reactor 2).

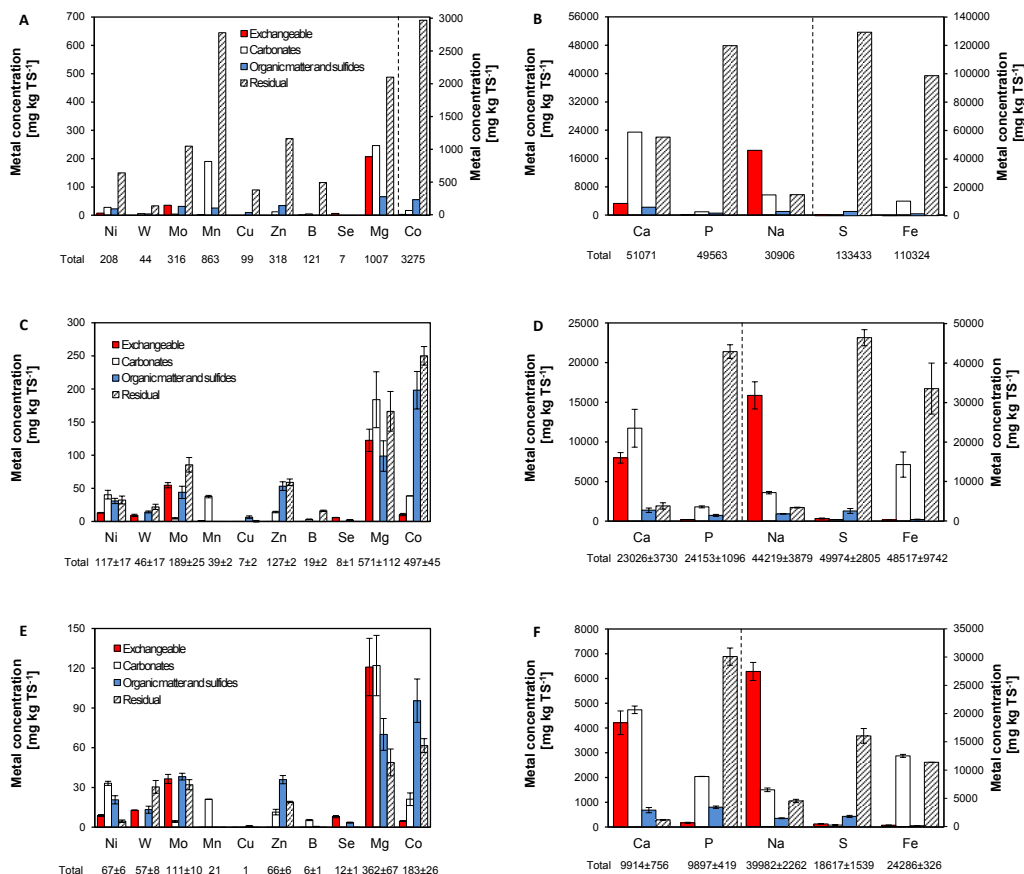


Figure 2.6 Trace and macro elements concentration [mg·kg<sup>-1</sup>TS<sup>-1</sup>], and partitioning in the operationally defined fractions after one month of operation. A, B. Inoculum biomass. C, D. AnMBR1. E, F. AnMBR2. After the dashed line the concentration must be read from the secondary y-axis.



The main increase in the exchangeable fraction was associated with sodium that was mainly bound to the exchangeable and the organic matter and sulfides fractions, with an increase in each fraction of about 40% in reactor 1 and 30% in reactor 2, showing the higher affinity of sodium to these fractions. This accumulation was caused by the elevated concentration of sodium in the model wastewater and the probable displacement of TM from the biomass metal matrix by this cation. Although the supply of TM provided should be sufficient, the metals may not be present in a bioavailable form that can be taken up by the microorganisms. Therefore, it was postulated that an apparently low amount of bioavailable TM due to the high sodium concentration caused the low COD removal observed during the start-up of the AnMBRs. The poorest performance was obtained (about 50% COD removal in reactor 1 and 30% removal in reactor 2) when wash-out of the majority of metals and the accumulation of sodium in the biomass occurred.

Other studies researching anaerobic treatment under highly saline conditions completely relied on the microbial acclimatization process adapting the biomass to halotolerant conditions and gradually recovering the treatment performance (Luo et al. 2016, Qiu and Ting 2013). However, the bioavailability of micronutrients impacted by the high concentration of sodium has never been considered. Affirmatively, after doubling the TM supplementation, an increasing COD removal was measured (90% of COD removal in both reactors on day 60, data not shown). Very likely, an increased TM concentration prevents depletion of bioavailable metals, preventing exhaustive removal of exchangeable compounds, ions substitution, or displacement of other TM by sodium. Similar changes in partitioning and bioavailability have been reported with other cations such as potassium and iron (Mulligan et al. 2010, Shakeri Yekta et al. 2014). It was beyond the scope of this study to examine the complexation reactions that play an important role in the AnMBRs making a particular metal either more or less bioavailable. The TM partitioning in the biomass matrix and determination of effluent metal concentration under high salinity conditions as performed in this study predicts TM leachability. Additional research is required to evaluate the long-term impact of high salinity conditions on reactor performance and TM speciation in the AnMBRs.

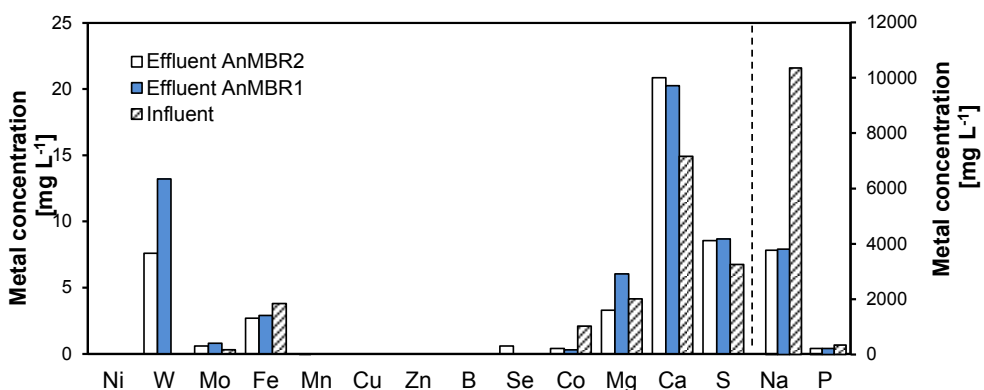


Figure 2.7. Influent and effluent trace and major element concentrations from AnMBRs after one month of operation. [W, Mo, Fe, Se, Co]  $\times 10$ . [Ni, Mn, Cu, Zn, B] below the level of detection [ $5 \mu\text{g}\cdot\text{L}^{-1}$ ]. After the dashed line the concentration must be read from the secondary y-axis.

## 2.4 Conclusions

The following conclusions could be drawn:

- The maximum SMA was obtained at  $6 \text{ gNa}^+\cdot\text{L}^{-1}$ . The high sodium content and reduced bioavailability of TM significantly decreased the SMA.
- The supply of tungsten increased the SMA by 17%, but no improvement was found with the addition of cobalt.
- High sodium concentration, mainly bound to the exchangeable fraction, resulted in different TM partitioning in the biomass matrix, with TM becoming more soluble and prone to wash out. In agreement with this, the particle size and COD removal decreased in the two AnMBRs. Accordingly, by doubling the TM supplementation a higher COD removal was achieved.

## References

- Bhattacharya, S.K., Uberoi, V., Madura, R.L. and Haghghi-Podeh, M.R. (1995) Effect of Cobalt on Methanogenesis. *Environmental Technology* 16(3), 271-278.
- Bhatti, Z.I., Furukawa, K. and Fujita, M. (1995) Comparative composition and characteristics of methanogenic granular sludges treating industrial wastes under different conditions. *Journal of Fermentation and Bioengineering* 79(3), 273-280.
- Boll, M., Schink, B., Messerschmidt, A. and Kroneck Peter, M.H. (2005) Novel bacterial molybdenum and tungsten enzymes: three-dimensional structure, spectroscopy, and reaction mechanism, p. 999.
- Dereli, R.K., Ersahin, M.E., Ozgun, H., Ozturk, I., Jeison, D., van der Zee, F. and van Lier, J.B. (2012) Potentials of anaerobic membrane bioreactors to overcome treatment limitations induced by industrial wastewaters. *Bioresource Technology* 122, 160-170.
- Escher, B.I., Snozzi, M. and Schwarzenbach, R.P. (1996) Uptake, speciation, and uncoupling activity of substituted phenols in energy transducing membranes. *Environmental Science and Technology* 30(10), 3071-3079.
- Espinosa, A., Rosas, L., Ilangovan, K. and Noyola, A. (1995) Effect of trace metals on the anaerobic degradation of volatile fatty acids in molasses stillage, pp. 121-129.
- Fang, H.H.P. and Chan, O.C. (1997) Toxicity of phenol towards anaerobic biogranules. *Water Research* 31(9), 2229-2242.
- Feijoo, G., Soto, M., Méndez, R. and Lema, J.M. (1995) Sodium inhibition in the anaerobic digestion process: Antagonism and adaptation phenomena. *Enzyme and Microbial Technology* 17(2), 180-188.
- Fermoso, F.G., Bartacek, J., Jansen, S. and Lens, P.N.L. (2009) Metal supplementation to UASB bioreactors: from cell-metal interactions to full-scale application. *Science of the Total Environment* 407(12), 3652-3667.
- Ferrer-Polonio, E., García-Quijano, N.T., Mendoza-Roca, J.A., Iborra-Clar, A. and Pastor-Alcañiz, L. (2016) Effect of alternating anaerobic and aerobic phases on the performance of a SBR treating effluents with high salinity and phenols concentration. *Biochemical Engineering Journal* 113, 57-65.
- Florencio, L., Field, J.A. and Lettinga, G. (1994) Importance of cobalt for individual trophic groups in an anaerobic methanol-degrading consortium. *Applied and Environmental Microbiology* 60(1), 227-234.
- Fuchs, G. (2008) Anaerobic Metabolism of Aromatic Compounds. *Annals of the New York Academy of Sciences* 1125(1), 82-99.
- Ismail, S.B., de La Parra, C.J., Temmink, H. and van Lier, J.B. (2010) Extracellular polymeric substances (EPS) in upflow anaerobic sludge blanket (UASB) reactors operated under high salinity conditions. *Water Research* 44(6), 1909-1917.
- Ismail, S.B., Gonzalez, P., Jeison, D. and Van Lier, J.B. (2008) Effects of high salinity wastewater on methanogenic sludge bed systems, pp. 1963-1970.
- Jeison, D., Del Rio, A. and Van Lier, J.B. (2008a) Impact of high saline wastewaters on anaerobic granular sludge functionalities, pp. 815-819.
- Jeison, D., Kremer, B. and van Lier, J.B. (2008b) Application of membrane enhanced biomass retention to the anaerobic treatment of acidified wastewaters under extreme saline conditions. *Separation and Purification Technology* 64(2), 198-205.
- Jeison, D. and van Lier, J.B. (2007) Cake formation and consolidation: Main factors governing the applicable flux in anaerobic submerged membrane bioreactors (AnSMBR) treating acidified wastewaters. *Separation and Purification Technology* 56(1), 71-78.
- Kletzin, A. and Adams, M.W.W. (1996) Tungsten in biological systems. *FEMS Microbiology Reviews* 18(1), 5-63.
- Lefebvre, O., Quentin, S., Torrijos, M., Godon, J.J., Delgenès, J.P. and Moletta, R. (2007) Impact of increasing NaCl concentrations on the performance and community composition of two anaerobic reactors. *Applied Microbiology and Biotechnology* 75(1), 61-69.

- Levén, L., Nyberg, K. and Schnürer, A. (2012) Conversion of phenols during an anaerobic digestion of organic solid waste - A review of important microorganisms and impact of temperature. *Journal of Environmental Management* 95(SUPPL.), S99-S103.
- Luo, W., Phan, H.V., Hai, F.I., Price, W.E., Guo, W., Ngo, H.H., Yamamoto, K. and Nghiem, L.D. (2016) Effects of salinity build-up on the performance and bacterial community structure of a membrane bioreactor. *Bioresource Technology* 200, 305-310.
- Melamane, X.L., Tandlich, R. and Burgess, J.E. (2007) Treatment of wine distillery wastewater by high rate anaerobic digestion, pp. 9-16.
- Mulligan, C.N., Fokue, M. and Sato, Y. (2010) *Sediments contamination and sustainable remediation*, CRC Press, USA.
- Osuna, M.B., van Hullebusch, E.D., Zandvoort, M.H., Iza, J. and Lens, P.N. (2004) Effect of cobalt sorption on metal fractionation in anaerobic granular sludge. *J Environ Qual* 33(4), 1256-1270.
- Pevere, A., Guibaud, G., van Hullebusch, E.D., Boughzala, W. and Lens, P.N.L. (2007) Effect of Na<sup>+</sup> and Ca<sup>2+</sup> on the aggregation properties of sieved anaerobic granular sludge. *Colloids and Surfaces A: Physicochemical and Engineering Aspects* 306(1-3 SPEC. ISS.), 142-149.
- Plugge, C.M., Jiang, B., De Bok, F.A.M., Tsai, C. and Stams, A.J.M. (2009) Effect of tungsten and molybdenum on growth of a syntrophic coculture of Syntrophobacter fumaroxidans and Methanospirillum hungatei. *Archives of Microbiology* 191(1), 55-61.
- Qiu, G. and Ting, Y.-P. (2013) Osmotic membrane bioreactor for wastewater treatment and the effect of salt accumulation on system performance and microbial community dynamics. *Bioresource Technology* 150, 287-297.
- Razo-Flores, E., Iniestra-González, M., Field, J.A., Olguin-Lora, P. and Puig-Grajales, L. (2003) Biodegradation of mixtures of phenolic compounds in an upward-flow anaerobic sludge blanket reactor. *Journal of Environmental Engineering* 129(11), 999-1006.
- Rosenkranz, F., Cabrol, L., Carballa, M., Donoso-Bravo, A., Cruz, L., Ruiz-Filippi, G., Chamy, R. and Lema, J.M. (2013) Relationship between phenol degradation efficiency and microbial community structure in an anaerobic SBR. *Water Research* 47(17), 6739-6749.
- Schmidt, T., Nelles, M., Scholwin, F. and Pröter, J. (2014) Trace element supplementation in the biogas production from wheat stillage – Optimization of metal dosing. *Bioresource Technology* 168, 80-85.
- Shakeri Yekta, S., Lindmark, A., Skyllberg, U., Danielsson, Å. and Svensson, B.H. (2014) Importance of reduced sulfur for the equilibrium chemistry and kinetics of Fe(II), Co(II) and Ni(II) supplemented to semi-continuous stirred tank biogas reactors fed with stillage. *Journal of Hazardous Materials* 269, 83-88.
- Sharma, J. and Singh, R. (2001) Effect of nutrients supplementation on anaerobic sludge development and activity for treating distillery effluent. *Bioresource Technology* 79(2), 203-206.
- Song, X., McDonald, J., Price, W.E., Khan, S.J., Hai, F.I., Ngo, H.H., Guo, W. and Nghiem, L.D. (2016) Effects of salinity build-up on the performance of an anaerobic membrane bioreactor regarding basic water quality parameters and removal of trace organic contaminants. *Bioresource Technology* 216, 399-405.
- Tessier, A., Campbell, P.G.C. and Blsson, M. (1979) Sequential extraction procedure for the speciation of particulate trace metals. *Analytical Chemistry* 51(7), 844-851.
- Valentine, D.L. (2007) Adaptations to energy stress dictate the ecology and evolution of the Archaea. *Nature Reviews Microbiology* 5(4), 316-323.
- Vallero, M.V.G., Hulshoff Pol, L.W., Lettinga, G. and Lens, P.N.L. (2003) Effect of NaCl on thermophilic (55°C) methanol degradation in sulfate reducing granular sludge reactors. *Water Research* 37(10), 2269-2280.
- van Hullebusch, E.D., Guibaud, G., Simon, S., Lenz, M., Yekta, S.S., Feroso, F.G., Jain, R., Duyster, L., Roussel, J., Guillon, E., Skyllberg, U., Almeida, C.M.R., Pechaud, Y., Garuti, M., Frunzo, L., Esposito, G., Carliell-Marquet, C., Ortner, M. and Collins, G. (2016) Methodological approaches for fractionation and

- speciation to estimate trace element bioavailability in engineered anaerobic digestion ecosystems: An overview. *Critical Reviews in Environmental Science and Technology* 46(16), 1324-1366.
- Van Hullebusch, E.D., Peerbolte, A., Zandvoort, M.H. and Lens, P.N.L. (2005) Sorption of cobalt and nickel on anaerobic granular sludges: Isotherms and sequential extraction. *Chemosphere* 58(4), 493-505.
- Vyrides, I. and Stuckey, D.C. (2009) Effect of fluctuations in salinity on anaerobic biomass and production of soluble microbial products (SMPs). *Biodegradation* 20(2), 165-175.
- Vyrides, I. and Stuckey, D.C. (2011) Fouling cake layer in a submerged anaerobic membrane bioreactor treating saline wastewaters: Curse or a blessing? *Water Science and Technology* 63(12), 2902-2908.
- Worms, I., Simon, D.F., Hassler, C.S. and Wilkinson, K.J. (2006) Bioavailability of trace metals to aquatic microorganisms: importance of chemical, biological and physical processes on biouptake. *Biochimie* 88(11), 1721-1731.
- Yang, J., Spanjers, H., Jeison, D. and Van Lier, J.B. (2013) Impact of Na<sup>+</sup> on biological wastewater treatment and the potential of anaerobic membrane bioreactors: A review. *Critical Reviews in Environmental Science and Technology* 43(24), 2722-2746.
- Yogalakshmi, K.N. and Joseph, K. (2010) Effect of transient sodium chloride shock loads on the performance of submerged membrane bioreactor. *Bioresource Technology* 101(18), 7054-7061.
- Zandvoort, M.H., van Hullebusch, E.D., Feroso, F.G. and Lens, P.N.L. (2006) Trace metals in anaerobic granular sludge reactors: Bioavailability and dosing strategies. *Engineering in Life Sciences* 6(3), 293-301.



## Phenol conversion in AnMBR at high salinity

---

This chapter has been published as “Muñoz Sierra, J.D., Oosterkamp, M.J., Wang, W., Spanjers, H., and van Lier, J.B. (2018) Impact of long-term salinity exposure in anaerobic membrane bioreactors treating phenolic wastewater: Performance robustness and endured microbial community. *Water Research*, 141, pp. 172-184.”

<https://doi.org/10.1016/j.watres.2018.05.006>

## Abstract

Industrial wastewaters are becoming increasingly associated with extreme conditions such as the presence of refractory compounds and high salinity that adversely affect biomass retention or reduce biological activity. Hence, this study evaluated the impact of long-term salinity increase to 20 gNa<sup>+</sup>·L<sup>-1</sup> on the bioconversion performance and microbial community composition in anaerobic membrane bioreactors treating phenolic wastewater. Phenol removal efficiency of up to 99.9% was achieved at 14 gNa<sup>+</sup>·L<sup>-1</sup>. Phenol conversion rates of 5.1 mgPh.gVSS<sup>-1</sup>·d<sup>-1</sup>, 4.7 mgPh.gVSS<sup>-1</sup>·d<sup>-1</sup>, and 11.7 mgPh.gVSS<sup>-1</sup>·d<sup>-1</sup> were obtained at 16 gNa<sup>+</sup>·L<sup>-1</sup>, 18 gNa<sup>+</sup>·L<sup>-1</sup> and 20 gNa<sup>+</sup>·L<sup>-1</sup>, respectively. The AnMBR's performance was not affected by short-term step-wise salinity fluctuations of 2 gNa<sup>+</sup>·L<sup>-1</sup> in the last phase of the experiment. It was also demonstrated in batch tests that the COD removal and methane production rate were higher at a K<sup>+</sup>:Na<sup>+</sup> ratio of 0.05, indicating the importance of potassium to maintain the methanogenic activity. The salinity increase adversely affected the transmembrane pressure likely due to a particle size decrease from 185 μm at 14 gNa<sup>+</sup>·L<sup>-1</sup> to 16 μm at 20 gNa<sup>+</sup>·L<sup>-1</sup>. Microbial community was dominated by bacteria belonging to the *Clostridium* genus and archaea by *Methanobacterium* and *Methanosaeta* genus. Syntrophic phenol degraders, such as *Pelotomaculum* genus were found to be increased when the maximum phenol conversion rate was attained at 20 gNa<sup>+</sup>·L<sup>-1</sup>. Overall, the observed robustness of the AnMBR performance indicated an endured microbial community to salinity changes in the range of the sodium concentrations applied.



### 3.1. Introduction

Chemical, food processing, textile, and petroleum industries are considered as the primary producers of saline wastewater (Ng et al. 2005, Yang et al. 2013). About 5% of these industrial effluents have saline or hypersaline characteristics (Lefebvre et al. 2007, Praveen et al. 2015). The degradation of a large variety of aromatic contaminants such as phenols and polyphenols remains a challenge for industrial wastewater treatment, which often needs to be accomplished at high salinity.

Previous research indicated the potentials of adaptation of halotolerant microorganisms in anaerobic treatment processes to saline conditions (Lefebvre et al. 2007, Margesin and Schinner 2001). Due to an osmotic pressure difference across the cell membrane, salt concentrations higher than 1% induce disintegration of cells because of plasmolysis and dehydration (Wood 2015). As a result, a decrease in biodegradation and effluent quality are recognized as the most important consequences (Abou-Elela et al. 2010, Yogalakshmi and Joseph 2010). Osmo-adaptation by producing or adding compatible solutes or accumulation of intracellular potassium could mitigate the loss of biomass activity due to pressure differences across the cell membrane caused by high salinity (Le Borgne et al. 2008, Vyrides and Stuckey 2017).

High salinity, mainly resulting from sodium salts, has an adverse impact on the performance of anaerobic wastewater treatment systems due to an inhibitory effect of sodium and the disintegration of flocs leading to a prominent biomass washout (Ismail et al. 2008, Pevere et al. 2007, Vyrides and Stuckey 2009a). In anaerobic high-rate reactors, retaining biomass such as by sludge granulation is essential for an efficient treatment (van Lier et al. 2015). Sludge granulation could be hampered at high salt concentrations as granule strength is considerably reduced when sodium replaces the calcium ions (Ismail et al. 2010, Jeison et al. 2008a). In contrast, because of the membrane filtration in anaerobic membrane bioreactors (AnMBRs), suspended biomass under highly saline conditions can be retained and enriched. This advantage of AnMBRs provides an opportunity for microorganisms to adapt to a wide range of sodium concentrations. However, several harmful effects of high salinity on the anaerobic biodegradation of waste streams have been reported by previous studies (Muñoz Sierra et al. 2017, Song et al. 2016). Muñoz Sierra et al. (2017) found 50% inhibition of methanogenic activity at about  $23 \text{ gNa}^+\text{L}^{-1}$  and complete inhibition at about  $34 \text{ gNa}^+\text{L}^{-1}$ . Song et al. (2016) showed that a salt concentration above  $10 \text{ gNaCl}\text{L}^{-1}$  reduced biogas production and COD removal in an AnMBR. Furthermore, the adaptation of microbial communities to an extended range of salinity enhances the opportunities for anaerobic biological wastewater treatment applications. Luo et al. (2016) demonstrated that acclimation to high salt concentration could lead to the succession of halotolerant or even halophilic microorganisms, thereby gradually recovering the bioreactor performance. Sudmalis et al. (2018) indicated that increase in salinity results in a shift in the bacterial and hydrogenotrophic methanogens populations. Archaea abundance and the genes involved in methanogenesis decrease significantly when salinity increases from low to high levels; likewise, the gene abundance in the hydrogenotrophic pathway is lower (Wu et al. 2017). Correspondingly, acetoclastic methanogens show a higher resistance to high salinity than hydrogenotrophic methanogens (Wang et al. 2017a).

However, studies that have reported the performance of AnMBRs during long-term continuous operation at high salinity are few and limited; especially there is none for the degradation of phenolic compounds. The studies focused either on the treatment of saline acidified wastewater (6-24 gNa<sup>+</sup>L<sup>-1</sup>) (Jeison et al. 2008b), or protein-containing saline wastewater (25 gNa<sup>+</sup>L<sup>-1</sup>) (Hemmelmann et al. 2013). On the other hand, other studies give attention to municipal wastewater (Vyrides and Stuckey 2009b), the removal of specific trace organic contaminants (0-15 gNaClL<sup>-1</sup>) (Song et al. 2016), and the contribution to membrane fouling when operating an AnMBR under saline conditions (35 gNaClL<sup>-1</sup>) (Vyrides and Stuckey 2011). Also, the use of forward osmosis-AnMBRs with transient salinity build-up has been explored (Chen et al. 2014).

The COD of chemical wastewater dissipates little energy during its breakdown, leading to low biomass yield and thus long or even infinite sludge retention times. The latter is a striking advantage for AnMBRs since there is no sludge wash-out giving the chance to enrich salt-tolerant biomass or even halophilic species able to degrade a model aromatic compound as phenol. Previous research on microbial community structure and dynamics under high salinity conditions have focused specifically on solid-state digesters (De Vrieze et al. 2017) and UASB reactors (Gagliano et al. 2017, Wang et al. 2017c), but there is no insight into the response of the retained biomass in an AnMBR to long-term high salinity exposure with phenolic wastewaters. Therefore, further research is required that will advance the understanding to successful application of AnMBRs for the treatment of chemical wastewaters under extreme conditions such as high salinity conditions. In view of the above, this study aims to evaluate the phenol bioconversion performance and microbial community dynamics in the long-term operation of an AnMBR in response to a stepwise increase in sodium concentration. Six phases of operation were established to investigate whether the changes in sodium concentrations affected the membrane filtration behavior, biomass particle size, methanogenic activity, microbial diversity, and phenol degraders abundance. The effect of K<sup>+</sup>:Na<sup>+</sup> concentration ratio on phenol and COD bioconversion at high salinity was assessed in batch tests.

## 3.2. Materials and Methods

### 3.2.1. Experimental set-up and operation

The experiments were carried out using a laboratory-scale AnMBR reactor with an effective volume of 6.5 L, equipped with an ultra-filtration (UF) side-stream membrane module (Figure 3.1). The average sludge retention time (SRT) was kept at about 400±20 days. A tubular PVDF membrane (Pentair, The Netherlands) with 5.5 mm inner diameter, 30 nm pore size, and 0.64 m length was used. The experimental set-up was equipped with feed, recycle, and effluent pumps (Watson-Marlow 120U/DV, 220Du), temperature and pH sensors (Endress & Hauser, Memosens), and a biogas flowmeter (Ritter, Milligas Counter MGC-1 PMMA, Germany). Transmembrane pressure (TMP) was measured by three pressure sensors (AE Sensors ATM, The Netherlands). The temperature of the reactor was controlled by a thermostatic water bath (Tamson Instruments, The Netherlands). The system was monitored by a computer running LabView software (version

15.0.1f1, National Instruments, USA). The AnMBR was inoculated with mesophilic anaerobic biomass obtained from a full-scale UASB reactor treating industrial wastewater (Shell, Moerdijk, The Netherlands). The initial concentration of volatile suspended solids (VSS) and total suspended solids (TSS) were 20.1 g L<sup>-1</sup> and 50.9 g L<sup>-1</sup>, respectively.

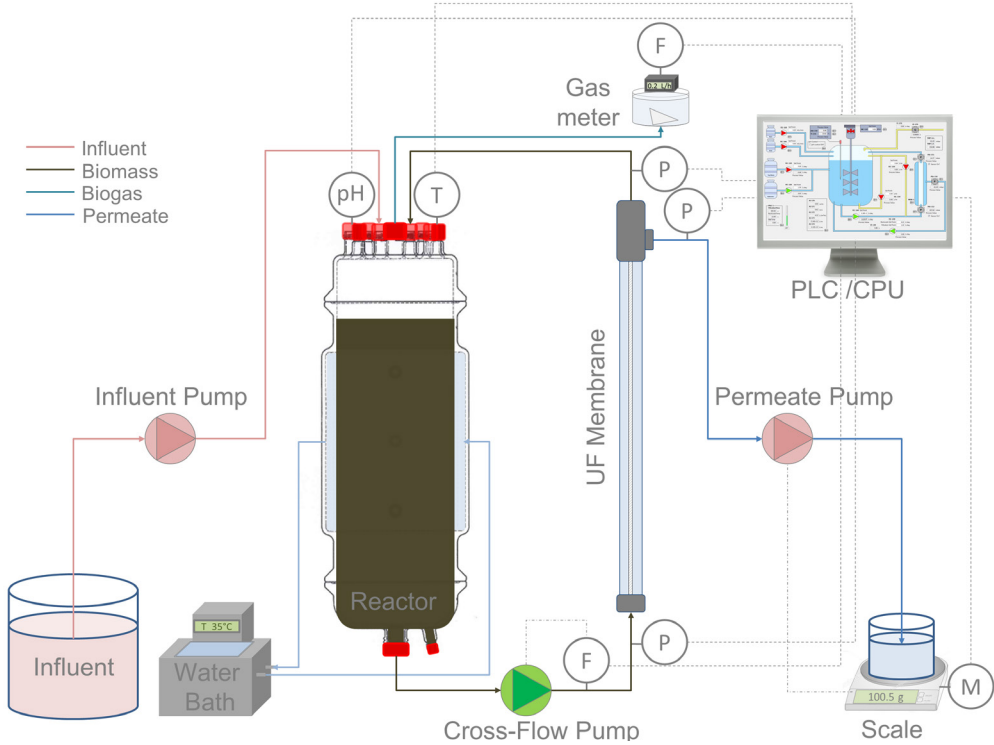


Figure 3.1 Schematic illustration of mesophilic AnMBR setup.

The synthetic wastewater consisted of sodium acetate ( $C_2H_3NaO_2$ ) and phenol ( $C_6H_6O$ ) with varying concentrations depending on reactor operational conditions. The amount of sodium chloride ( $NaCl$ ), and solutions of  $K_2HPO_4$  (34.85 g L<sup>-1</sup>) and  $KH_2PO_4$  (24 g L<sup>-1</sup>) varied according to the sodium concentration applied in the reactor maintaining a fixed  $K^+:Na^+$  ratio of 0.05. Yeast extract (0.5 g L<sup>-1</sup>), macronutrients (9 mL L<sup>-1</sup>), and micronutrients (4.5 mL L<sup>-1</sup>) were supplemented. Macronutrients solution included (in g L<sup>-1</sup>):  $NH_4Cl$  170,  $CaCl_2 \cdot 2H_2O$  8, and  $MgSO_4 \cdot 7H_2O$  9; and micronutrients solution contained (in g L<sup>-1</sup>):  $FeCl_3 \cdot 6H_2O$  2,  $CoCl_2 \cdot 6H_2O$  2,  $MnCl_2 \cdot 4H_2O$  0.5,  $CuCl_2 \cdot 2H_2O$  0.03,  $ZnCl_2$  0.05,  $H_3BO_3$  0.05,  $(NH_4)_6Mo_7O_{24} \cdot 4H_2O$  0.09,  $Na_2SeO_3$  0.1,  $NiCl_2 \cdot 6H_2O$  0.05, EDTA 1,  $Na_2WO_4$  0.08 (Muñoz Sierra et al. 2017). The influent concentration of phenol was gradually increased to 0.5 g L<sup>-1</sup> as indicated in Figure 3.2 A. Moreover, the sodium concentrations in the reactor were increased from 8 to 20 g Na<sup>+</sup> L<sup>-1</sup> by long-term and short-term exposures in six

phases. In phase, I, the salinity rise in the AnMBR occurred starting at 8 gNa<sup>+</sup>L<sup>-1</sup> and then to 10 gNa<sup>+</sup>L<sup>-1</sup> with exposures of about 20 days each. Long-term (phases II-IV) exposure was carried out for 112 days at 14 gNa<sup>+</sup>L<sup>-1</sup>, 24 days at 18 gNa<sup>+</sup>L<sup>-1</sup>, and 133 days at 16 gNa<sup>+</sup>L<sup>-1</sup>. Short-term salinity exposure cycles (phases V and VI) of 40 days were carried out at the end of the long-term operation, first by a step-wise increase from 16 to 19 gNa<sup>+</sup>L<sup>-1</sup> and second by a step-wise increase/decrease from 18 to 20 gNa<sup>+</sup>L<sup>-1</sup>. The AnMBR was operated during 391 days under mesophilic conditions (35.0 ± 1.4 °C). The operational conditions during all phases are shown in Table 3.1. In this study, the term high salinity refers to the high concentration of sodium in the water.

Table 3.1 Operational conditions of the AnMBR

Day	Salinity [gNa <sup>+</sup> L <sup>-1</sup> ]	OLR [gCOD L <sup>-1</sup> d <sup>-1</sup> ]	Phenol loading rate [mgPh L <sup>-1</sup> d <sup>-1</sup> ]	VSS [gVSS L <sup>-1</sup> ]	Phase
0	8	0.15	0.77	30.87	I
30	10	1.54	0.77	14.15	
100	14	3.06	12.85	19.19	II
128	14	3.08	15.38	16.15	
148	14	3.12	30.77	17.75	
157	18	3.12	38.46	17.75	III
178	18	3.12	38.46	8.16	
221	16	5.45	67.23	12.78	IV
280	16	3.12	38.46	9.26	
311	16	3.12	38.46	16.93	
350	19	6.24	113.85	13.50	V
382	20	6.24	113.85	9.70	VI

### 3.2.2. K<sup>+</sup>:Na<sup>+</sup> ratio effect on bioconversion through batch tests

Biomass samples from the AnMBR were taken, and two anaerobic batch tests were conducted at the end of the phase IV and phase VI. 500 mL Schott glass bottles at sodium concentrations of 16, 20, and 24 gNa<sup>+</sup>L<sup>-1</sup> were used to assess the K<sup>+</sup>:Na<sup>+</sup> concentration ratio effect on the bioconversion. Temperature and mixing were controlled in an orbital shaker (New Brunswick™ Biological Shakers Innova® 44/44R, USA) at 35°C and 120 rpm respectively. The first test, at the end of phase IV, was carried out maintaining the K<sup>+</sup>:Na<sup>+</sup> ratio at 0.05 while keeping the above concentrations of sodium. In the second test, the K<sup>+</sup> concentration was kept constant for all sodium concentrations (see Table 3.2). The K<sup>+</sup>:Na<sup>+</sup> ratios tested were 0.05, 0.03, 0.025 and 0.002. Four consecutive feedings of the substrate (acetate and phenol) were applied. Initial COD and phenol concentrations were 3.5 gL<sup>-1</sup> and 50 mgPhL<sup>-1</sup>, respectively. The methane production rate was recorded by an AMPTS device (Bioprocess Control, Sweden).

Table 3.2 K<sup>+</sup>, Na<sup>+</sup> concentrations and K<sup>+</sup>:Na<sup>+</sup> ratios used in batch tests.

	1 <sup>st</sup> Batch			2 <sup>nd</sup> Batch		
gK <sup>+</sup> L <sup>-1</sup>	0.8	1	1.2	0.5	0.5	0.5
gNa <sup>+</sup> L <sup>-1</sup>	16	20	24	16	20	24
K <sup>+</sup> :Na <sup>+</sup>	0.05	0.05	0.05	0.03	0.025	0.02

### 3.2.3. Microbial community and statistical analysis

Biomass samples were taken from the AnMBR in all phases to evaluate the microbial community dynamics. The DNeasy UltraClean Microbial Kit (Qiagen, Hilden, Germany) was used to extract DNA from 0.5 grams of biomass. The quality and quantity of the DNA obtained was checked by agarose gel electrophoresis and Qubit3.0 DNA detection (Qubit® dsDNA HS Assay Kit, Life Technologies, U.S.), respectively. High throughput sequencing was performed by using the MiSeq Illumina platform and primers for bacterial and archaeal (V3-V4) 16S rRNA genes (BaseClear, Leiden, the Netherlands). The QIIME pipeline (version 1.9.0) was used to analyze the sequences (Caporaso et al. 2010). Demultiplexing and quality filtering were performed with parameter values Q=20, r=3, and p=0.75. Chimeric sequences were removed using UCHIME2 (version 9.0) algorithm (Edgar 2016). Sequences were clustered into operational taxonomic units (OTUs) with a 97% similarity as the cutoff, with UCLUST algorithm (Edgar 2010). Singletons were removed, and OTUs with an occurrence less than three times in at least one sample were excluded. The taxonomic assignment was performed using the Silva database (SILVA-128) with UCLUST (McDonald et al. 2012). Alpha diversity was determined after random subsampling using the metrics Chao1, observed OTUs, and Faith's phylogenetic distance in QIIME. For beta diversity, separate non-metric distance scaling (NMDS) and PcoA analysis of the microbial community were made based on the unweighted Unifrac distance measure. Both alpha and beta diversity plots were generated with the phyloseq (McMurdie and Holmes 2013) and ggplot2 packages in the R environment. Sequences have been submitted and assigned the number SRP128989.

### 3.2.4. Analytical techniques

#### 3.2.4.1. Particle size distribution

Measurement of the particle size distribution (PSD) was carried out by using a DIPA-2000 EyeTech™ particle analyzer (Donner Technologies, Or Akiva, Israel) with an A100 and B100 laser lens (measuring range 0.1-300 μm and 1-2000 μm, respectively) and a liquid flow cell DCM-104A (10x10 mm).

#### 3.2.4.2. Flow Cytometry Assay

Flow cytometry (FCM) assay was conducted to determine the quality of the biomass samples after sodium concentration changes between phase II, III, and IV, and significant volatile suspended solids reduction. BD Accuri C6® flow cytometer (BD Accuri cytometers, Belgium) was used, with a

50 mW laser emitting at a fixed wavelength of 488 nm. BD Accuri Cflow® software was used for data processing of cells with intact and compromised membranes. Biomass samples were diluted (to obtain bacterial concentration less than  $2 \times 10^5$  cells mL<sup>-1</sup>), stained (live/dead) and evaluated following the protocol defined by Prest et al. (2013).

#### 3.2.4.3. Specific methanogenic activity (SMA) and biogas content

SMA tests were performed in triplicate using an automated methane potential test system (AMPTS, Bioprocess Control, Sweden) and were carried out at 35°C. The ratio K<sup>+</sup>:Na<sup>+</sup> was kept constant at 0.05 in the media. The initial pH was adjusted to 7.0 ( $20 \pm 0.4^\circ\text{C}$ ). Methane content of the biogas was analyzed using a gas chromatograph 7890A (GC) system (Agilent Technologies, US) equipped with a flame ionization detector. The temperatures of the oven, front inlet, and front detector were 45°C, 200 °C, and 200 °C, respectively.

#### 3.2.4.4. Other analytical methods

Hach Lange kits were used to measure chemical oxygen demand (COD). The COD was measured using a VIS – spectrophotometer (DR3900, Hach Lange, Germany). Phenol concentration was measured by Merck – Spectroquant® Phenol cell kits using a spectrophotometer NOVA60 (Merck, Germany). Phenol concentrations were double-checked using a high-performance liquid chromatography HPLC LC-20AT (Shimadzu, Japan) equipped with a 4.6 mm reversed-phase C18 column (Phenomenex, The Netherlands) and a UV detector at a wavelength of 280 nm. The solvent used was 25% (v/v) acetonitrile as mobile phase at a flow rate of 0.95 mL.min<sup>-1</sup>. The column oven was set at 30°C. Sodium concentrations in the reactor were measured by Ion Chromatography (Metrohm, Switzerland). Dilutions were applied to samples and were prepared in triplicates. Calibration curves were made using standard solution (Sigma-Aldrich) in the range between 0.1 to 50 mg.L<sup>-1</sup>. The final concentrations were calculated by using the MagIC Net 3.2 software.

### 3.3. Results and Discussion

#### 3.3.1. AnMBR process performance

Phenol, COD, and sodium concentrations of the influent were controlled and monitored during the operation of the AnMBR (Figure 3.2 A). During phase I, COD and phenol removal efficiency varied from 83.8% to 98.6% and 0 to 77.0%, respectively (Figure 3.2 B, C). The performance of the reactor was unstable, coinciding with the acclimation of biomass to the operational conditions, when sodium concentration was increased from 8 gNa<sup>+</sup>L<sup>-1</sup> to 14 gNa<sup>+</sup>L<sup>-1</sup> and organic loading rate was increased from 0.2 gCOD.L<sup>-1</sup>.d<sup>-1</sup> to 3.1 gCOD.L<sup>-1</sup>.d<sup>-1</sup>. The influent phenol concentration was increased from 10 to 100 mgPh.L<sup>-1</sup> at the end of this phase. The maximum conversion rates achieved under the aforementioned conditions were 2.9 mgPh.L<sup>-1</sup>.d<sup>-1</sup> (0.2 mgPh.gVSS<sup>-1</sup>.d<sup>-1</sup>) and 3.0 gCOD.L<sup>-1</sup>.d<sup>-1</sup> (0.2 gCOD.gVSS<sup>-1</sup>.d<sup>-1</sup>). Biogas production rate gradually increased by raising the OLR in accordance with the expected methane production (Figure S3.1). In phase II, when influent phenol concentration was increased from 100 to 500 mg.L<sup>-1</sup>, a phenol removal efficiency of up to

99.9% was achieved (Figure 3.2 C). Better stability of the AnMBR and higher phenol conversion rates than in phase I were observed; in phase II the sodium concentration was kept constant at  $14 \text{ gNa}^+\cdot\text{L}^{-1}$ . The phenol conversion rate increased with 88% to  $30.8 \text{ mgPh}\cdot\text{L}^{-1}\cdot\text{d}^{-1}$  ( $1.7 \text{ mgPh}\cdot\text{gVSS}^{-1}\cdot\text{d}^{-1}$ ), indicating that the applied constant salt concentration was beneficial for developing a stable microbial conversion process, enhancing the phenol uptake. Similarly, Wang et al. (2017c) reported that a constant sodium concentration of  $10 \text{ gNa}^+\cdot\text{L}^{-1}$  resulted in stable biomass activities of the phenolics degraders and methanogens at influent total phenols (phenol, catechol, resorcinol, and hydroquinone) concentrations in the range of  $100\text{-}500 \text{ mgL}^{-1}$ . Moreover, Poirier et al. (2016) inferred that the stability of the anaerobic digestion process is reduced by phenol concentrations above concentrations of  $1 \text{ gPh}\cdot\text{L}^{-1}$ , and therefore the impact on phenol biodegradation might be attributed mainly to the salinity changes in this case.

At the beginning of phase III, a one-step salinity increase of  $4 \text{ gNa}^+\cdot\text{L}^{-1}$  (from  $14$  to  $18 \text{ gNa}^+\cdot\text{L}^{-1}$ ) was applied. Phenol and COD removal efficiencies decreased at the end of this phase with COD values in the permeate of about  $1.29 \text{ gCOD}\cdot\text{L}^{-1}$ . The volatile suspended solids (VSS) concentration remarkably decreased by 54% (Table 3.1), and higher biogas production was observed around day 170.

An average phenol conversion rate of  $38.4 \text{ mgPh}\cdot\text{L}^{-1}\cdot\text{d}^{-1}$  was achieved at  $18 \text{ gNa}^+\cdot\text{L}^{-1}$ . However, the phenol conversion rate varied between  $2.2 \text{ mgPh}\cdot\text{gVSS}^{-1}\cdot\text{d}^{-1}$  and  $4.7 \text{ mgPh}\cdot\text{gVSS}^{-1}\cdot\text{d}^{-1}$ . Interestingly, flow cytometry (FCM) results indicated a 21.2% increase in the number of cells with compromised membranes, when salinity increased from  $14$  to  $18 \text{ gNa}^+\cdot\text{L}^{-1}$  (Table 3.3). FCM results inferred that the quality of the biomass was reduced after this one-step increase of  $4 \text{ gNa}^+\cdot\text{L}^{-1}$ . The rise in the number of cells with compromised membranes could be attributed to the fact that microbial cultures are sensitive and exhibit limited adaptation to changes in ionic strength (Woolard and Irvine 1995).

In phase IV, the sodium concentration was reduced to  $16 \text{ gNa}^+\cdot\text{L}^{-1}$  to alleviate the negative effect observed in phase III. An additional 5.3% of cells with compromised membranes was observed with this salinity reduction, compared to the previous phase, reaching a total of 48.5% and 51.5% of cells with compromised and intact membranes, respectively (Table 3.3). Because of the observed increased phenol concentration of about  $67 \text{ mgPh}\cdot\text{L}^{-1}$  in the reactor permeate, the OLR was temporarily reduced to prevent phenol toxicity. Instability of the reactor was observed for about 85 days, and COD permeate concentration increased up to  $1.14 \text{ gCOD}\cdot\text{L}^{-1}$  (Figure 3.2 B). Phenol and COD conversion rates of  $65.1 \text{ mgPh}\cdot\text{L}^{-1}\cdot\text{d}^{-1}$  ( $5.1 \text{ mgPh}\cdot\text{gVSS}^{-1}\cdot\text{d}^{-1}$ ) and  $5.4 \text{ gCOD}\cdot\text{L}^{-1}\cdot\text{d}^{-1}$  ( $0.4 \text{ gCOD}\cdot\text{gVSS}^{-1}\cdot\text{d}^{-1}$ ) were observed, respectively. Praveen et al. (2015) showed that once a microbial community is acclimated to a certain salt concentration, the adaptation can become quickly lost if salinity is changed. However, the AnMBR COD conversion performance was not highly affected by a step-wise increase to  $19 \text{ gNa}^+\cdot\text{L}^{-1}$  in phase V, neither by the salinity step-wise increases and decreases in phase VI. OLR was increased to  $6.2 \text{ gCOD}\cdot\text{L}^{-1}\cdot\text{d}^{-1}$  at the beginning of phase V.

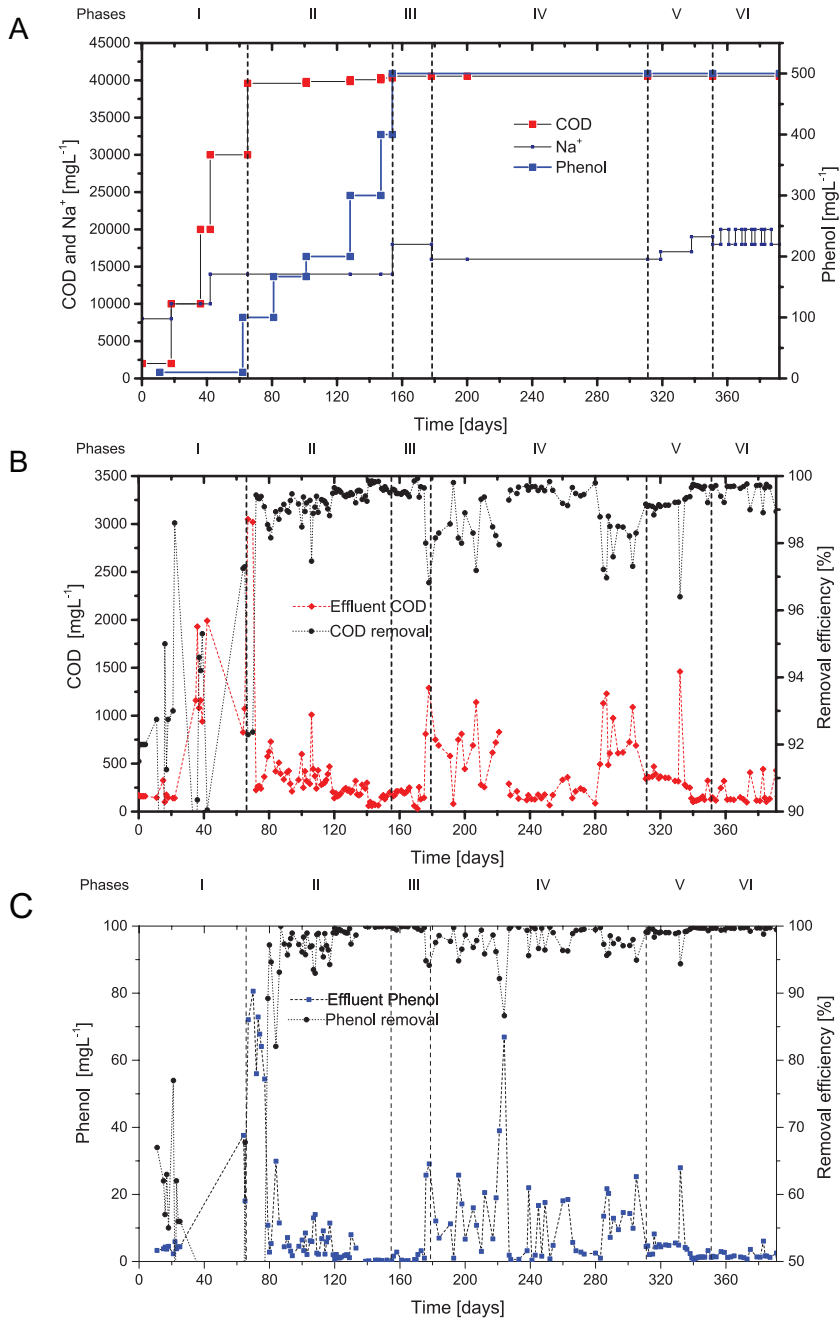


Figure 3.2 A. Influent COD and Phenol, and reactor sodium concentrations. B. Permeate COD concentration and COD removal efficiency. C. Permeate phenol concentration and phenol removal efficiency.



Table 3.3 Cells with compromised and intact membranes after different sodium concentrations exposure.

<b>Na<sup>+</sup> in AnMBR</b> <b>[gNa<sup>+</sup>·L<sup>-1</sup>]</b>	<b>Compromised membranes</b> <b>[%]</b>	<b>Intact membranes</b> <b>[%]</b>
14	22.1	77.9
18	43.3	56.7
16	48.5	51.5

Table 3.4 Specific methanogenic activities at different sodium concentrations in the AnMBR.

<b>Salinity</b> <b>[g Na<sup>+</sup>·L<sup>-1</sup>]</b>	<b>SMA</b> <b>[gCOD-CH<sub>4</sub>gVSS<sup>-1</sup> d<sup>-1</sup>]</b>	<b>Phase</b>
14	0.55±0.00	II
18	0.64±0.03	III
16	0.54±0.02	IV
19	0.43±0.05	V
20	0.42±0.22	VI

In these periods, the average phenol conversion rates were 113.0 mgPh·L<sup>-1</sup>·d<sup>-1</sup> (8.4 mgPh·gVSS<sup>-1</sup>·d<sup>-1</sup>) during phase V and 113.3 mgPh·L<sup>-1</sup>·d<sup>-1</sup> (11.7 mgPh·gVSS<sup>-1</sup>·d<sup>-1</sup>) at VI. The phenol and COD effluent concentration fluctuated to some extent by each sodium concentration change between 18 and 20 gNa<sup>+</sup>·L<sup>-1</sup>. That is in contrast to what was observed by Aslan and Şekerdağ (2016), who indicated that the COD removal significantly decreased at about 20 gNa<sup>+</sup>·L<sup>-1</sup> when treating saline wastewater in a UASB reactor. Our results demonstrated that a short-term continuous fluctuation between 18 and 20 gNa<sup>+</sup>·L<sup>-1</sup> eventually has no impact on the bioconversion anymore after a long-term operation, suggesting a successful gradual adaptation to higher sodium concentrations. As Carballa et al. (2015) inferred, a step-wise adaptation of the microbial community to stressful environmental conditions results in a strengthened microbiome against upcoming disturbances. In our current research, the salinity changes resulted in an endured microbial community increasing the process performance robustness in the range of sodium concentrations applied.

The methane production rate was more prone to variations during these last two phases. The specific methanogenic activities (SMA) obtained along with the long-term operation of the AnMBR at the different sodium concentrations (see Table 3.4) decreased by 24% when salinity was increased from 14 gNa<sup>+</sup>·L<sup>-1</sup> to 20 gNa<sup>+</sup>·L<sup>-1</sup>. Nevertheless, the SMA of 0.55±0.00 gCOD-CH<sub>4</sub>gVSS<sup>-1</sup>·d<sup>-1</sup> at 14 gNa<sup>+</sup>·L<sup>-1</sup> and 0.42±0.22 gCOD-CH<sub>4</sub>gVSS<sup>-1</sup>·d<sup>-1</sup> at 20 gNa<sup>+</sup>·L<sup>-1</sup>, remained relatively high, which confirmed the adaptation of the methanogenic population to the salinity levels applied after long-term operation of the AnMBR. Earlier studies reported SMAs of biomass treating phenolic wastewater in a range from 0.15 to 0.66 gCOD-CH<sub>4</sub>gVSS<sup>-1</sup>·d<sup>-1</sup> (Hussain and Dubey 2014, Wang et al. 2017d). The obtained SMA was higher than in other studies, applying sodium concentrations in

the range of 0-20 gNa<sup>+</sup>L<sup>-1</sup> (Jeison et al. 2008a, Muñoz Sierra et al. 2017), which might be attributed to the long-term acclimation of the biomass.

### 3.3.2. AnMBR membrane filtration performance

Transmembrane pressure (TMP) was lower than 150 mbar during the phases I to III at a flux of 2.0 L·m<sup>-2</sup>·h<sup>-1</sup> (Figure 3.3 A). This relatively low TMP is attributed to operation below the critical flux. However, the TMP was negatively affected by the salt concentration changes in phases III and IV and increased to 350 mbar in phases V and VI at a flux of 4.0 L·m<sup>-2</sup>·h<sup>-1</sup>. During these phases, the membrane filtration resistance increased from about 6.0×10<sup>12</sup> m<sup>-1</sup> to 28.0×10<sup>12</sup> m<sup>-1</sup>. The deterioration of membrane filtration performance was attributed to the observed decrease in biomass particle size when salinity was increased (see Figure 3.3 B.). Likely, the low particle size had a significant influence on the cake layer compaction that increased the operational values of the filtration resistance (Hemmelmann et al. 2013). The median particle size decreased from 185 μm at 14 gNa<sup>+</sup>L<sup>-1</sup> to 91 μm at 18 gNa<sup>+</sup>L<sup>-1</sup> in phase III and to 56 μm at 16 gNa<sup>+</sup>L<sup>-1</sup> in phase IV. The median biomass particle size was 35 μm at 19 gNa<sup>+</sup>L<sup>-1</sup> and 16 μm at 20 gNa<sup>+</sup>L<sup>-1</sup> meaning a ten-fold decrease following the long-term salinity exposure. TMP and membrane filtration resistance fluctuated especially during the salinity changes in phases V and VI. Possibly, in addition to the reduction in particle size, there were more biomass properties affected by salinity that contributed to a fluctuating membrane filtration resistance. For example, Yang et al. (2014) concluded that high sodium concentrations promote a compact gel layer formation. Similarly, Yurtsever et al. (2016) indicated that salinity induced large molecules, to be detected as foulants in gel/cake layer, may originate from biomass loosely bound extracellular polymeric substances.

### 3.3.3. K<sup>+</sup>:Na<sup>+</sup> ratio effect on bioconversion

Since the intracellular ionic concentration of anaerobic microorganisms needs to be balanced with the environment, the K<sup>+</sup>:Na<sup>+</sup> concentration ratio in the medium was assessed to identify its effect on bioconversion at high salinity. Biomass was taken from the AnMBR at the end of phase IV. Observed COD and phenol concentrations at 16, 20 and 24 gNa<sup>+</sup>L<sup>-1</sup> under a fixed ratio K<sup>+</sup>:Na<sup>+</sup> of 0.05 are depicted in Figure 3.4 A, B and C. About 93.6% COD removal and 99.9% phenol removal was found at 16 gNa<sup>+</sup>L<sup>-1</sup>. The lowest total COD concentration was about 207 mgCOD·L<sup>-1</sup> at the end of the 2<sup>nd</sup> feed. At 20 gNa<sup>+</sup>L<sup>-1</sup> and 24 gNa<sup>+</sup>L<sup>-1</sup>, about 91.6% and 89.6% COD removal was achieved within all feedings, respectively, whereas 39% and 25% of phenol removal were observed. At 20 gNa<sup>+</sup>L<sup>-1</sup>, the lowest phenol concentration was about 9 mgPh·L<sup>-1</sup> at the end of the 1<sup>st</sup> feed, and the lowest COD concentration was 248.8 mgCOD·L<sup>-1</sup> in the 4<sup>th</sup> feed. At 24 gNa<sup>+</sup>L<sup>-1</sup> the lowest COD and phenol concentrations were 319 mgCOD·L<sup>-1</sup> and 21 mgPh·L<sup>-1</sup>, respectively. After the 2<sup>nd</sup> feed, a decrease in phenol degradation was detected for all tests, most probably because of phenol accumulation in subsequent feeding meaning a higher initial concentration that possibly leads to inhibition. The maximum methane production rates at 16, 20, and 24 gNa<sup>+</sup>L<sup>-1</sup> were 0.16±0.01, 0.13±0.03, 0.09±0.02 LCH<sub>4</sub>d<sup>-1</sup>, respectively, inferring the negative impact of increasing sodium on methanogenic activity.

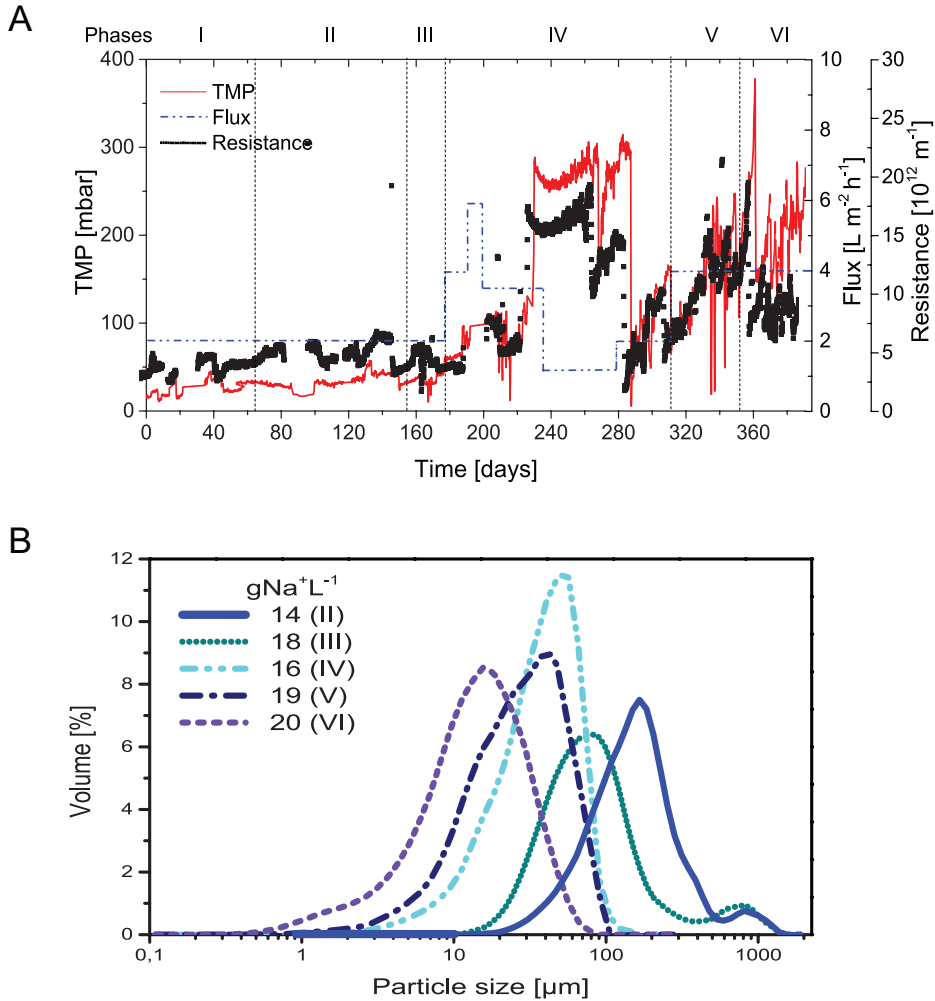


Figure 3.3 A. Membrane Filtration performance. B. Biomass particle size distribution at different sodium concentrations.

At the end of phase VI, batch tests were carried out at  $K^+ : Na^+$  ratios of 0.03, 0.025 and 0.02 corresponding to 16, 20, 24  $gNa^+L^{-1}$ , respectively. The corresponding results are depicted in Figure 3.4 D, E and F. At 16  $gNa^+L^{-1}$ , COD and phenol removals were 96.6% and 96.8%, respectively. Phenol was degraded completely at the end of the feed 1 to 3 at 20 and 24  $gNa^+L^{-1}$ , but the degradation lasted longer than in the previous batch. At 20  $gNa^+L^{-1}$ , 99% phenol removal was observed during the first feed and complete removal in the others. At 24  $gNa^+L^{-1}$ , an average of 82.7% COD removal and 94.4% phenol removal were found. The lowest COD concentrations obtained were 56  $mgL^{-1}$ , 118  $mgL^{-1}$  and 179  $mgL^{-1}$  at 16, 20, and 24  $gNa^+L^{-1}$ , respectively.

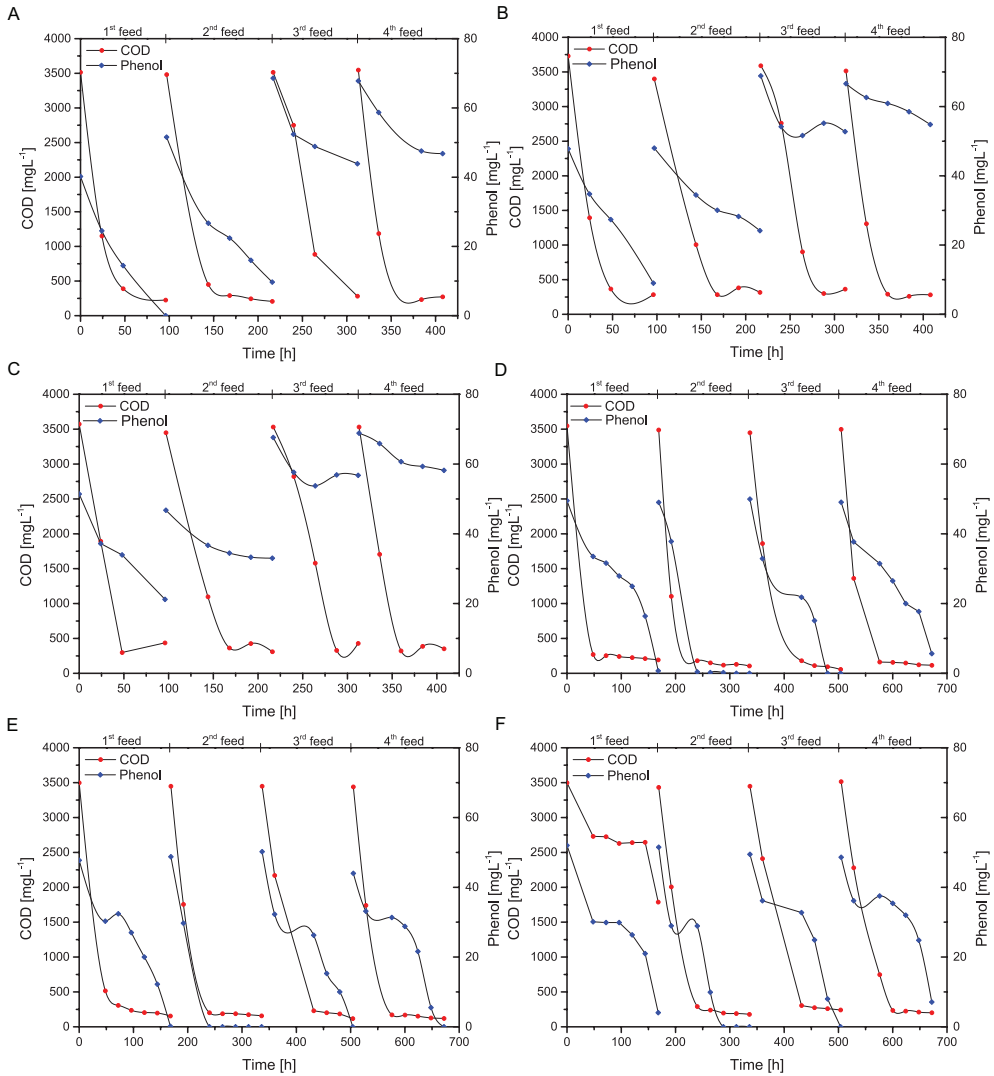


Figure 3.4 Batch test assessment of impact of  $K^+ : Na^+$  ratio on COD and Phenol degradation. Constant  $K^+ : Na^+$  ratio of 0.05 A.  $16 \text{ gNa}^+ \cdot \text{L}^{-1}$  (0.05) B.  $20 \text{ gNa}^+ \cdot \text{L}^{-1}$  (0.05) and C.  $24 \text{ gNa}^+ \cdot \text{L}^{-1}$  (0.05) . Varying  $K^+ : Na^+$  ratio D.  $16 \text{ gNa}^+ \cdot \text{L}^{-1}$  (0.03) . E.  $20 \text{ gNa}^+ \cdot \text{L}^{-1}$  (0.025) and F.  $24 \text{ gNa}^+ \cdot \text{L}^{-1}$  (0.02).

It is inferred that in bacteria  $K^+$  allows the adaptation to environmental and metabolic changes (Kuo et al. 2005).

Thereby, the improvement of phenol degradation might be attributed to the adaptation of biomass after it has been exposed to higher salinities of up to  $20 \text{ gNa}^+ \cdot \text{L}^{-1}$  in phases V and VI. Methane

production rates average values of  $0.13 \pm 0.01$ ,  $0.11 \pm 0.01$ , and  $0.07 \pm 0.02$   $\text{LCH}_4\text{d}^{-1}$  were observed at 16, 20 and 24  $\text{gNa}^+\text{L}^{-1}$ , respectively. Although the biomass could degrade phenol successfully, the COD removal and methane production rates for the 0.03, 0.025, and 0.02  $\text{K}^+:\text{Na}^+$  ratios were found to be lower than for the 0.05  $\text{K}^+:\text{Na}^+$  ratio. The latter seems to agree with the evidence that halophilic archaea use the salt-in strategy accumulating high intracellular concentrations of  $\text{K}^+$  to balance and stabilize enzymes, being apparently more favorable for archaea than for bacteria (Le Borgne et al. 2008). This fact highlights the importance of  $\text{K}^+$  for the archaea to preserve the methanogenic activity under saline conditions. Gagliano et al. (2017) found that a potassium concentration of  $0.7 \text{ gK}^+\text{L}^{-1}$  alleviates the negative effect of  $20 \text{ gNa}^+\text{L}^{-1}$  in a UASB. In both batch tests, the COD and phenol removal efficiency were lower at  $24 \text{ gNa}^+\text{L}^{-1}$  compared to 16 and  $20 \text{ gNa}^+\text{L}^{-1}$ .

Our current results confirmed the adverse impact of high sodium concentration on biomass activity as demonstrated by Muñoz Sierra et al. (2017). However, due to the long-term operation of the AnMBR at high salinity and adaptation of the microbial community to high sodium concentrations, this negative impact could be overcome.

Further research should look at the effects of larger short-term random salinity fluctuations on the AnMBR phenol bioconversion and biomass properties analogous to treating actual industrial chemical wastewaters where such fluctuations can be expected.

### 3.3.4. Microbial community structure and dynamics

Based on the sequences from all biomass samples, 930 OTUs were identified of which 835 belonged to the bacteria and 95 to the archaea domain.

In the start-up phase I, the reactor performance was unstable (Figure 3.2). Alpha diversity increased with a median initially of 390 and finally of 485 for the Chao1 alpha diversity metric of the samples, respectively (Figure 3.5. A). The metrics observed OTUs and Faith's phylogenetic diversity showed a similar trend (Figure S3.2). Dominant microorganisms included bacteria belonging to the *Clostridium* genus and the families Pseudomonadaceae, Thermovirgaceae and uncultured ML1228J-1 (Figure 3.6). *Clostridium* species and members of the Pseudomonadaceae have been found to anaerobically degrade phenol (Lack and Fuchs 1994, Zhang and Wiegel 1994). Bacteria belonging to Thermovirgaceae may be related to the degradation of phenolic compounds (DiPippo et al. 2009). The family of uncultured ML1228J-1 is associated with anoxic and saline conditions (Humayoun et al. 2003). Archaea present in the start-up phase included the dominating hydrogenotrophic methanogens belonging to the Methanobacterium genus and acetoclastic Methanosaeta genus (Figure 3.6).

In phase II, the phenol concentration was increased. Alpha diversity showed further adaptation of the microbial community to phenol with an initial decrease and subsequent increase of the diversity (Figure 3.5 A). The relative abundance of *Clostridium* species increased (to 19%) while the relative abundance of members of Pseudomonadaceae slightly reduced and Mogibacteriaceae became more dominant in phase II. Mogibacteriaceae are anaerobic Gram-positive bacteria that have been found

in anaerobic digestion processes and of which the function in the reactor is unclear (da Silva Martins et al. 2017). Other microorganisms, bacteria belonging to the order BA021, were dominating more prominently at the beginning of phase II but were also present throughout the entire experiment (in relative abundances from 21 to 2%). The order BA021 is part of the OP9 and JS1 lineages (Figure S3.3). These lineages are also referred to as Atribacteria and may be thriving using a syntrophic metabolism (Nobu et al. 2015). Archaeal species dominating in this phase belonged to the *Methanobacterium* and *Methanosaeta* genus (Figure 3.6).

Sodium concentration was increased in phase III, and the alpha diversity of the overall microbial community showed an increase (from a Chao1 median of 421 to 517, see Figure 3.5 A), which may indicate that the microbial community was likely influenced by the increased salinity. Members of the Pseudomonadaceae increased in relative abundance from 1 to 20%, while the ML1228J-1 and Mogibacteriaceae families decreased to an abundance of 1% (Figure 3.6).

A definite decrease in alpha diversity was observed in phase IV when the sodium was changed to  $16 \text{ gNa}^+\cdot\text{L}^{-1}$  (median of the Chao1 metric was 261) (Figure 5. A). In general, Gram-positive bacteria and archaea can better tolerate salinity changes because of the strong cell wall (Yan et al. 2015). Salinity is known to enrich for salt-tolerant and halophilic bacteria in membrane bioreactors and other anaerobic reactors (Luo et al. 2016, Wang et al. 2017b). Decreases in relative abundances were observed for the Gram-negative Pseudomonadaceae, where salt-tolerant Thermovirgaceae and Gram-positive *Clostridium* species were highly abundant (26% and 31%, respectively). Among the archaea, the hydrogenotrophic *Methanobacterium* species became more dominant (Figure 3.6). The dominance of *Methanobacterium* and *Methanosaeta* was described in a UASB reactor operated under high salinity, and although the *Methanosaeta* species were dominant, they do not have a very high salt tolerance (Onodera et al. 2017). Possibly, the presence of *Methanosaeta* is crucial for granule formation in UASB reactors, but in the AnMBR, these species may be less essential, and hydrogenotrophic *Methanobacterium* are also dominant. Madigou et al. (2016) also indicated the importance of hydrogenotrophic methanogenesis at high phenol concentrations. During the temporary lowering of the OLR, the community alpha diversity increased indicating a recovery of the microbial diversity (Chao1 median of 356). *Clostridium* species highly dominated among bacteria (54%). Furthermore, among archaea, the relative abundance of *Methanosaeta* increased (from 1 to 10%) and of *Methanobacterium* decreased (from 20 to 5%, Figure 3.6).

Alpha diversity did not reach similar high values as before phase IV (with Chao1 index medians of 438 and 386 for phase V and VI, respectively). However, the alpha diversities were similar, indicating that the microbial community was more tolerant to fluctuating salinity (Figure 3.5 A).

Accordingly, the community composition in phase V and VI was very similar with *Clostridium*, Thermovirgaceae as well as ML1228J-1 as dominating bacteria and *Methanobacterium* and *Methanosaeta* as main archaea (Figure 3.6).

Beta diversity or between-sample diversity was determined to illustrate the influence of the salinity on the microbial community diversity. In the NMDS plot, samples from the start-up phase I

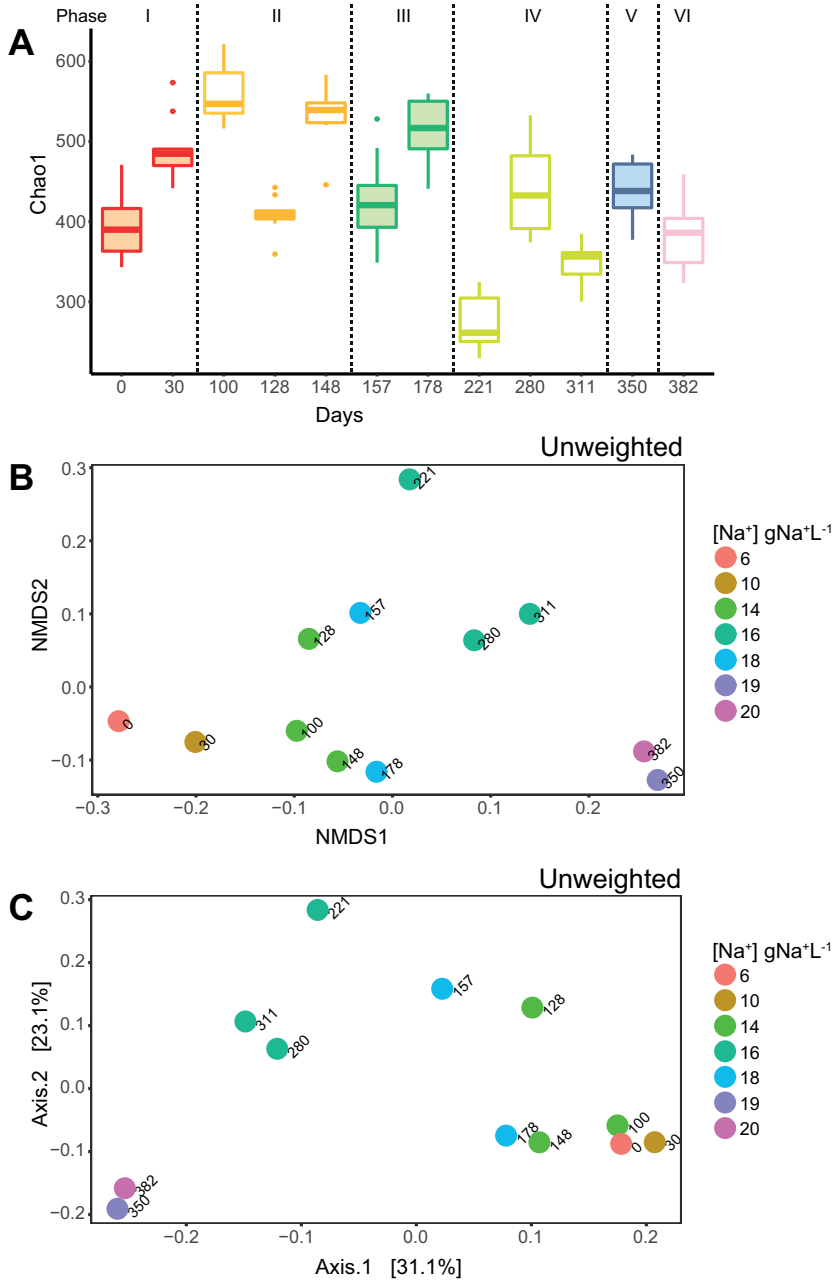


Figure 3.5. Diversity plots for the microbial community in AnMBR. Plots present for different phases of operation the alpha diversity (Chao1 metric) (A), for different sodium concentrations the NMDS beta diversity based on unweighted Unifrac values (B) and the PCoA analysis of unweighted Unifrac values (C).

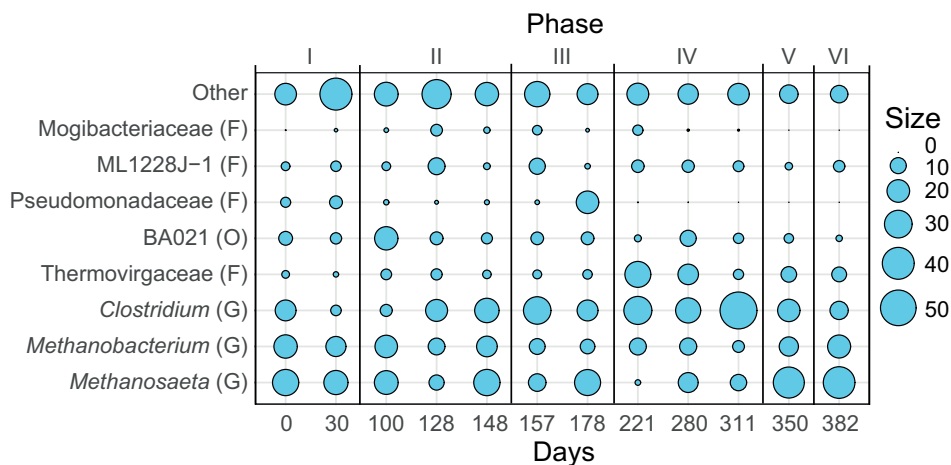


Figure 3.6. Microbial community composition of the AnMBR treating high salinity phenolic wastewater according to the most detailed level of taxonomy that could be inferred from the OTU sequences. Relative abundance cut-off at 5%.

seemed to cluster separately from the phases II to IV in which phenol or sodium concentration was changed (Figure 3.5 B). However, this could not be confirmed by the PCoA analysis (Figure 3.5. C). Together, the beta diversity plots indicated a gradual change in the community diversity although this did not result in differences in the clustering. Samples from the final phases V and VI in which the reactors were operated with short-term salinity changes, were not clustering with any of the samples from phases I to IV (Figure 3.5. B, C). The microbial community could have responded in different ways to disturbances in phenol and sodium concentration from the ecological point-of-view (Shade et al. 2012). Although sodium concentration fluctuated in phase V and VI, the community diversity remained more similar compared to previous phases. Given the similar microbial community diversity and profile as well as efficient bioreactor performance in phase V and VI, a gradual adaptation to environmental conditions increased the resistance of the microbial community to sodium fluctuations, which increased the robustness of the AnMBR system.

#### 3.3.4.1. Phenol-degrading bacteria in the AnMBR

*Clostridium* has been identified as dominating and was possibly related to phenol degradation in the AnMBR. *Clostridium hydroxybenzoicum* can transform phenol to 4-hydroxybenzoate (Zhang and Wiegel 1994), and *Clostridium* strain 6 enhanced phenol degradation when growing in coculture (Letowski et al. 2001). In a UASB reactor treating phenolic wastewater at high salinity, increased phenolics concentrations increased the relative abundance of Clostridia (Wang et al. 2017c).

Additionally, anaerobic phenol degradation could occur via syntrophic conversions. However, the role of syntrophic microorganisms in anaerobic digestion is yet poorly understood, and the



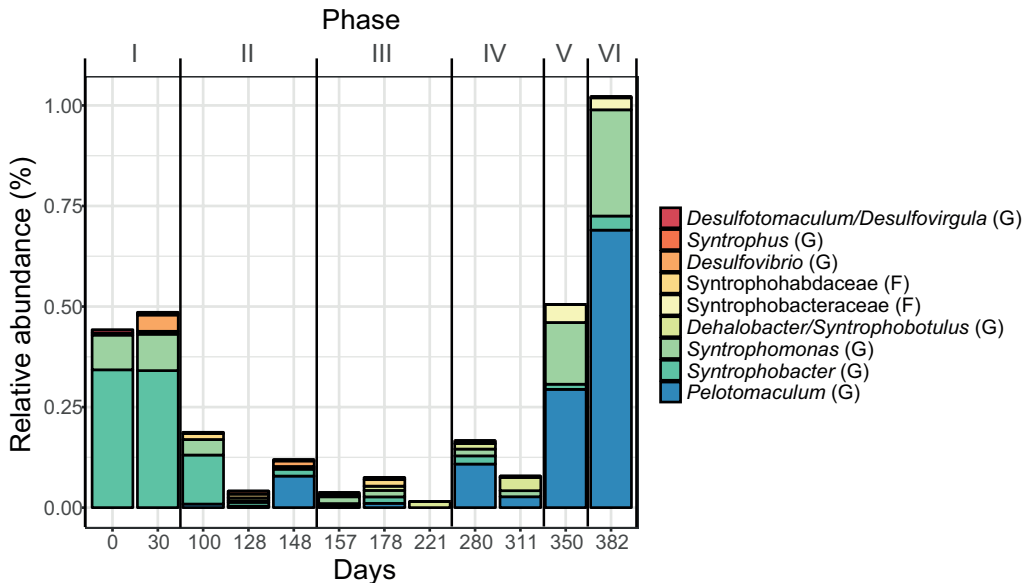


Figure 3.7. Relative abundance of taxa related to syntrophic phenol degradation that are present in the AnMBR.

relationship between the so-called microbial dark matter with syntrophy remains unclear (Narihiro et al. 2015). However, in an attempt to shed some light on possible syntrophic microorganisms, the low abundant taxa (relative abundance below 1%) were studied, and among them, syntrophic phenol degraders could be identified. These included bacteria related to the genera *Desulfotomaculum*, *Syntrophus*, *Desulfovibrio*, *Syntrophorhabdus*, and *Pelotomaculum*, among others (Figure 3.7). *Desulfovibrio* was identified in a phenol-degrading and biogas-producing reactor (Ju and Zhang 2014). *Syntrophorhabdus* was found in a phenolic-degrading UASB reactor at high salinity (Wang et al. 2017c). *Syntrophorhabdus aromaticivorans* strain UI was the first isolated syntrophic phenol degrader (Qiu et al. 2008) via benzoate as intermediate (Nobu et al. 2014). *Pelotomaculum* species were shown to syntrophically degrade aromatic compounds (Qiu et al. 2006). *Desulfotomaculum*, *Syntrophus*, and *Pelotomaculum* were identified in phenol-containing wastewater (Chen et al. 2008). Moreover, *Syntrophus*, *Syntrophorhabdus*, and *Pelotomaculum* were identified in lab- and full-scale reactors treating aromatics containing wastewater (Nobu et al. 2017). In this study, the syntrophic phenol-degraders were observed in the start-up phase I, decreased during the long-term phases II and III and increased in phases IV to VI, likely indicating the establishment of this functional group of phenol degraders (Figure 3.7). *Pelotomaculum* showed an evident increase in relative abundance when the microbial community was adapted to sodium fluctuations and exhibited maximum phenol conversion rates.

### 3.4. Conclusions

The conclusions drawn from the present work can be summarized as follows:

- Salinity was increased from 8 to 20 gNa<sup>+</sup>·L<sup>-1</sup> during long-term operation of the AnMBR reactor. Phenol removal efficiency of 99.9% was achieved at 14 gNa<sup>+</sup>·L<sup>-1</sup>. Phenol conversion rates increased from 5.1 mgPh·gVSS<sup>-1</sup>·d<sup>-1</sup> at 16 gNa<sup>+</sup>·L<sup>-1</sup> to a maximum conversion rate of 11.7 mgPh·gVSS<sup>-1</sup>·d<sup>-1</sup> at 20 gNa<sup>+</sup>·L<sup>-1</sup>. Adaptation of the microbial community to salinity changes promoted a higher removal efficiency of phenol. The specific methanogenic activity decreased by 24% when the Na<sup>+</sup> concentration increased from 14 to 20 gNa<sup>+</sup>·L<sup>-1</sup>.
- A one-step salinity increase from 14 to 18 gNa<sup>+</sup>·L<sup>-1</sup> compromised 21.2% of the cells membranes, reducing the quality, and biological stability of the biomass. However, the AnMBR overall conversion performance was not affected by a short-term step-wise 2 gNa<sup>+</sup>·L<sup>-1</sup> salinity fluctuations inside the reactor. The process exhibited robustness and strengthened microbial community to salinity changes in the range of concentrations applied.
- Membrane filtration was adversely affected by the salinity increase, which was exhibited by an increasing transmembrane pressure to about 350 mbar, and concomitantly the membrane filtration resistance increase was attributed to a ten-fold reduction on biomass particle size from 185 μm at 14 gNa<sup>+</sup>·L<sup>-1</sup> to 16 μm at 20 gNa<sup>+</sup>·L<sup>-1</sup>.
- Batch tests demonstrated that COD removal and methane production rates for the 0.03, 0.025, 0.02 K<sup>+</sup>:Na<sup>+</sup> ratios were found to be lower than for the 0.05 K<sup>+</sup>:Na<sup>+</sup> ratio. However, phenol removal was lower at 24 gNa<sup>+</sup>·L<sup>-1</sup> compared to 16 and 20 gNa<sup>+</sup>·L<sup>-1</sup>.
- Bacteria belonging to the *Clostridium* genus (up to 54% relative abundance) dominated the bacterial community and archaea were dominated by *Methanobacterium* and *Methanosaeta* genus. Syntrophic phenol-degrading bacteria, such as *Pelotomaculum* showed an increased relative abundance after adaptation of the microbial community to salinity changes in combination with higher phenol degradation.

## Supplementary Information

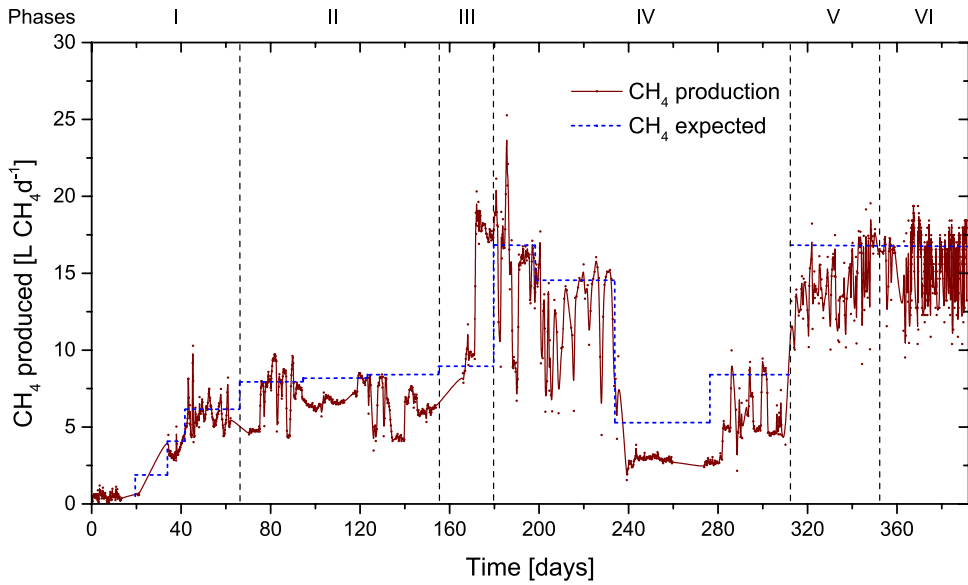


Figure S3.1. Methane flow rate and theoretical methane expected during the long- and short-term salinity exposure.

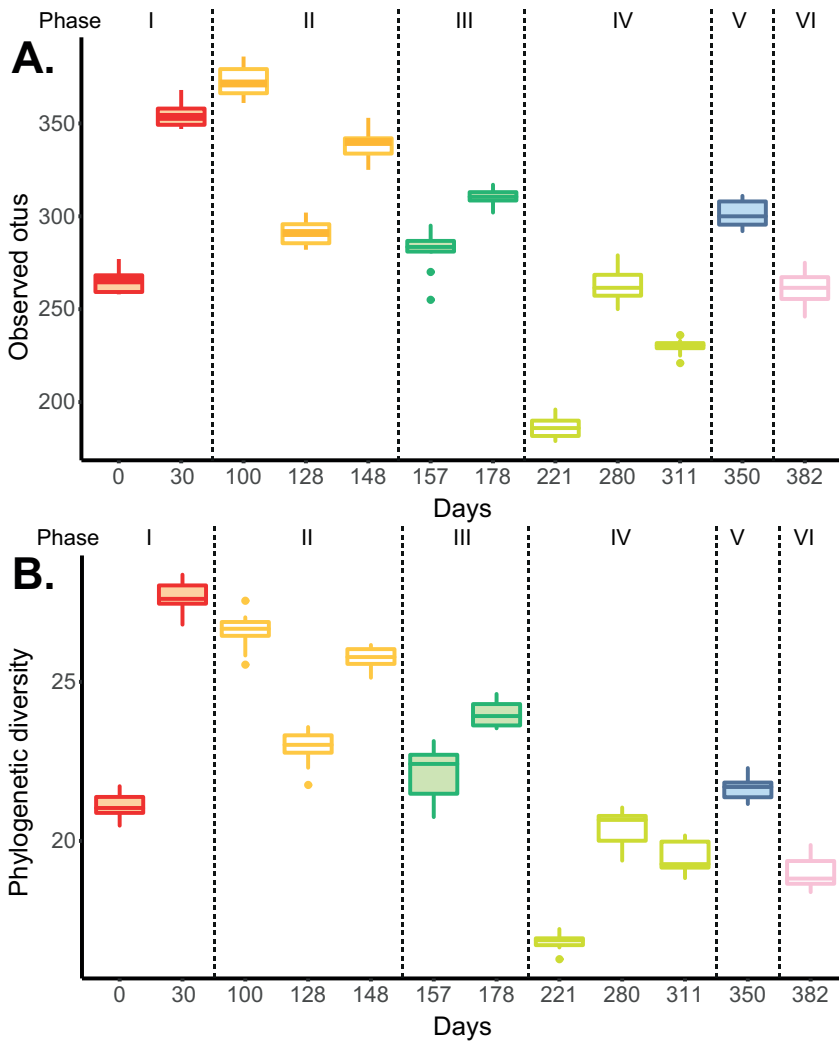


Figure S3.2. Alpha diversity according to the observed OTUs (A) and Faith's phylogenetic diversity (B) for the different phases of operation of an AnMBR treating highly saline phenolic wastewater.

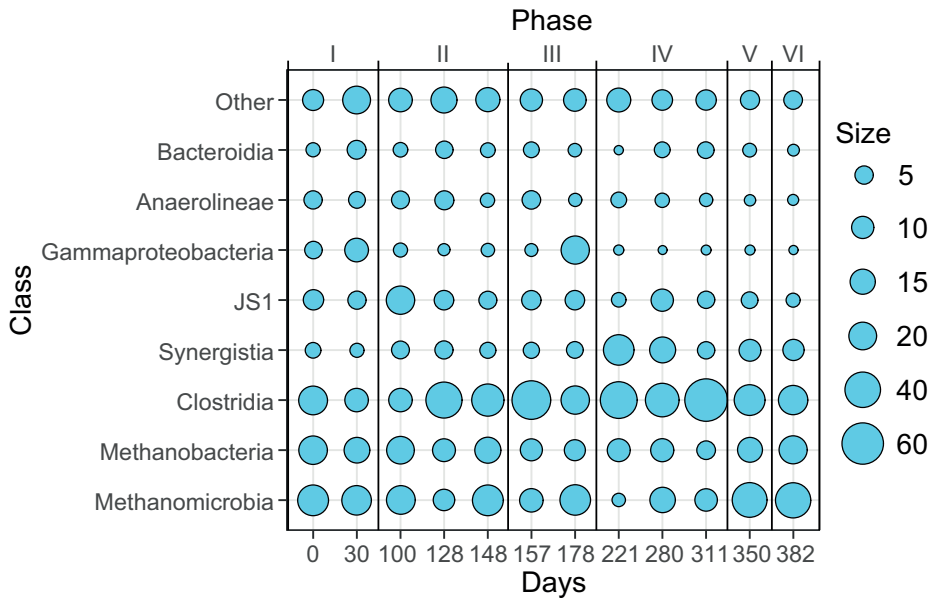


Figure S3.3. Microbial community profile of an AnMBR treating highly saline phenolic wastewater in which taxa are shown at the class level and with a relative abundance cut-off at 5%.

## References

- Abou-Elela, S.I., Kamel, M.M. and Fawzy, M.E. (2010) Biological treatment of saline wastewater using a salt-tolerant microorganism. *Desalination* 250(1), 1-5.
- Aslan, S. and Şekerdag, N. (2016) Salt inhibition on anaerobic treatment of high salinity wastewater by upflow anaerobic sludge blanket (UASB) reactor. *Desalination and Water Treatment* 57(28), 12998-13004.
- Caporaso, J.G., Kuczynski, J., Stombaugh, J., Bittinger, K., Bushman, F.D., Costello, E.K., Fierer, N., Pena, A.G., Goodrich, J.K., Gordon, J.I., Huttley, G.A., Kelley, S.T., Knights, D., Koenig, J.E., Ley, R.E., Lozupone, C.A., McDonald, D., Muegge, B.D., Pirrung, M., Reeder, J., Sevinsky, J.R., Turnbaugh, P.J., Walters, W.A., Widmann, J., Yatsunenko, T., Zaneveld, J. and Knight, R. (2010) QIIME allows analysis of high-throughput community sequencing data. *Nat Meth* 7(5), 335-336.
- Carballa, M., Regueiro, L. and Lema, J.M. (2015) Microbial management of anaerobic digestion: exploiting the microbiome-functionality nexus. *Current Opinion in Biotechnology* 33(Supplement C), 103-111.
- Chen, C.-L., Wu, J.-H. and Liu, W.-T. (2008) Identification of important microbial populations in the mesophilic and thermophilic phenol-degrading methanogenic consortia. *Water Research* 42(8), 1963-1976.
- Chen, L., Gu, Y., Cao, C., Zhang, J., Ng, J.-W. and Tang, C. (2014) Performance of a submerged anaerobic membrane bioreactor with forward osmosis membrane for low-strength wastewater treatment. *Water Research* 50, 114-123.
- da Silva Martins, A., Ornelas Ferreira, B., Ribeiro, N.C., Martins, R., Rabelo Leite, L., Oliveira, G., Colturato, L.F., Chernicharo, C.A. and de Araujo, J.C. (2017) Metagenomic analysis and performance of a mesophilic anaerobic reactor treating food waste at various load rates. *Environmental Technology* 38(17), 2153-2163.
- De Vrieze, J., Christiaens, M.E.R., Walraedt, D., Devooght, A., Ijaz, U.Z. and Boon, N. (2017) Microbial community redundancy in anaerobic digestion drives process recovery after salinity exposure. *Water Research* 111, 109-117.
- DiPippo, J.L., Nesbø, C.L., Dahle, H., Doolittle, W.F., Birkland, N.-K. and Noll, K.M. (2009) *Kosmotoga olearia* gen. nov., sp. nov., a thermophilic, anaerobic heterotroph isolated from an oil production fluid. *International Journal of Systematic and Evolutionary Microbiology* 59(12), 2991-3000.
- Edgar, R. (2016) UCHIME2: improved chimera prediction for amplicon sequencing. [bioRxiv](https://doi.org/10.1101/054749).
- Edgar, R.C. (2010) Search and clustering orders of magnitude faster than BLAST. *Bioinformatics* 26(19), 2460-2461.
- Gagliano, M.C., Ismail, S.B., Stams, A.J.M., Plugge, C.M., Temmink, H. and Van Lier, J.B. (2017) Biofilm formation and granule properties in anaerobic digestion at high salinity. *Water Research* 121, 61-71.
- Hemmelmann, A., Torres, A., Vergara, C., Azocar, L. and Jeison, D. (2013) Application of anaerobic membrane bioreactors for the treatment of protein-containing wastewaters under saline conditions. *Journal of Chemical Technology and Biotechnology* 88(4), 658-663.
- Humayoun, S.B., Bano, N. and Hollibaugh, J.T. (2003) Depth Distribution of Microbial Diversity in Mono Lake, a Meromictic Soda Lake in California. *Applied and Environmental Microbiology* 69(2), 1030-1042.
- Hussain, A. and Dubey, S.K. (2014) Specific methanogenic activity test for anaerobic treatment of phenolic wastewater. *Desalination and Water Treatment* 52(37-39), 7015-7025.
- Ismail, S.B., de La Parra, C.J., Temmink, H. and van Lier, J.B. (2010) Extracellular polymeric substances (EPS) in upflow anaerobic sludge blanket (UASB) reactors operated under high salinity conditions. *Water Research* 44(6), 1909-1917.
- Ismail, S.B., Gonzalez, P., Jeison, D. and Van Lier, J.B. (2008) Effects of high salinity wastewater on methanogenic sludge bed systems, pp. 1963-1970.

- Jeison, D., Del Rio, A. and Van Lier, J.B. (2008a) Impact of high saline wastewaters on anaerobic granular sludge functionalities, pp. 815-819.
- Jeison, D., Kremer, B. and van Lier, J.B. (2008b) Application of membrane enhanced biomass retention to the anaerobic treatment of acidified wastewaters under extreme saline conditions. *Separation and Purification Technology* 64(2), 198-205.
- Ju, F. and Zhang, T. (2014) Novel Microbial Populations in Ambient and Mesophilic Biogas-Producing and Phenol-Degrading Consortia Unraveled by High-Throughput Sequencing. *Microbial Ecology* 68(2), 235-246.
- Kuo, M.M.C., Haynes, W.J., Loukin, S.H., Kung, C. and Saimi, Y. (2005) Prokaryotic K<sup>+</sup> channels: From crystal structures to diversity. *FEMS Microbiology Reviews* 29(5), 961-985.
- Lack, A. and Fuchs, G. (1994) Evidence that phenol phosphorylation to phenylphosphate is the first step in anaerobic phenol metabolism in a denitrifying *Pseudomonas* sp. *Archives of Microbiology* 161(2), 132-139.
- Le Borgne, S., Paniagua, D. and Vazquez-Duhalt, R. (2008) Biodegradation of Organic Pollutants by Halophilic Bacteria and Archaea. *Journal of Molecular Microbiology and Biotechnology* 15(2-3), 74-92.
- Lefebvre, O., Quentin, S., Torrijos, M., Godon, J.J., Delgenès, J.P. and Moletta, R. (2007) Impact of increasing NaCl concentrations on the performance and community composition of two anaerobic reactors. *Applied Microbiology and Biotechnology* 75(1), 61-69.
- Letowski, J., Juteau, P., Villemur, R., Duckett, M.-F., Beaudet, R., Lépine, F. and Bisailon, J.-G. (2001) Separation of a phenol carboxylating organism from a two-member, strict anaerobic co-culture. *Canadian Journal of Microbiology* 47(5), 373-381.
- Luo, W., Phan, H.V., Hai, F.I., Price, W.E., Guo, W., Ngo, H.H., Yamamoto, K. and Nghiem, L.D. (2016) Effects of salinity build-up on the performance and bacterial community structure of a membrane bioreactor. *Bioresource Technology* 200(Supplement C), 305-310.
- Madigou, C., Poirier, S., Bureau, C. and Chapleur, O. (2016) Acclimation strategy to increase phenol tolerance of an anaerobic microbiota. *Bioresource Technology* 216(Supplement C), 77-86.
- Margesin, R. and Schinner, F. (2001) Potential of halotolerant and halophilic microorganisms for biotechnology. *Extremophiles* 5(2), 73-83.
- McDonald, D., Price, M.N., Goodrich, J., Nawrocki, E.P., Desantis, T.Z., Probst, A., Andersen, G.L., Knight, R. and Hugenholtz, P. (2012) An improved Greengenes taxonomy with explicit ranks for ecological and evolutionary analyses of bacteria and archaea. *ISME Journal* 6(3), 610-618.
- McMurdie, P.J. and Holmes, S. (2013) Phyloseq: An R Package for Reproducible Interactive Analysis and Graphics of Microbiome Census Data. *PloS One* 8(4).
- Muñoz Sierra, J.D., Lafita, C., Gabaldón, C., Spanjers, H. and van Lier, J.B. (2017) Trace metals supplementation in anaerobic membrane bioreactors treating highly saline phenolic wastewater. *Bioresource Technology* 234, 106-114.
- Narihiro, T., Nobu, M.K., Kim, N.-K., Kamagata, Y. and Liu, W.-T. (2015) The nexus of syntrophy-associated microbiota in anaerobic digestion revealed by long-term enrichment and community survey. *Environmental Microbiology* 17(5), 1707-1720.
- Ng, H.Y., Ong, S.L. and Ng, W.J. (2005) Effects of Sodium Chloride on the Performance of a Sequencing Batch Reactor. *Journal of Environmental Engineering* 131(11), 1557-1564.
- Nobu, M.K., Dodsworth, J.A., Murugapiran, S.K., Rinke, C., Gies, E.A., Webster, G., Schwientek, P., Kille, P., Parkes, R.J., Sass, H., Jørgensen, B.B., Weightman, A.J., Liu, W.-T., Hallam, S.J., Tsiamis, G., Woyke, T. and Hedlund, B.P. (2015) Phylogeny and physiology of candidate phylum 'Atribacteria' (OP9/JS1) inferred from cultivation-independent genomics. *The ISME Journal* 10, 273.
- Nobu, M.K., Narihiro, T., Liu, M., Kuroda, K., Mei, R. and Liu, W.-T. (2017) Thermodynamically diverse syntrophic aromatic compound catabolism. *Environmental Microbiology* 19(11), 4576-4586.

- Nobu, M.K., Narihiro, T., Tamaki, H., Qiu, Y.-L., Sekiguchi, Y., Woyke, T., Goodwin, L., Davenport, K.W., Kamagata, Y. and Liu, W.-T. (2014) Draft Genome Sequence of *Syntrophorhabdus aromaticivorans* Strain UI, a Mesophilic Aromatic Compound-Degrading Syntroph. *Genome Announcements* 2(1), e01064-01013.
- Onodera, T., Syutsubo, K., Hatamoto, M., Nakahara, N. and Yamaguchi, T. (2017) Evaluation of cation inhibition and adaptation based on microbial activity and community structure in anaerobic wastewater treatment under elevated saline concentration. *Chemical Engineering Journal* 325, 442-448.
- Pevere, A., Guibaud, G., van Hullebusch, E.D., Boughzala, W. and Lens, P.N.L. (2007) Effect of Na<sup>+</sup> and Ca<sup>2+</sup> on the aggregation properties of sieved anaerobic granular sludge. *Colloids and Surfaces A: Physicochemical and Engineering Aspects* 306(1-3 SPEC. ISS.), 142-149.
- Poirier, S., Bize, A., Bureau, C., Bouchez, T. and Chapleur, O. (2016) Community shifts within anaerobic digestion microbiota facing phenol inhibition: Towards early warning microbial indicators? *Water Research* 100(Supplement C), 296-305.
- Praveen, P., Nguyen, D.T.T. and Loh, K.-C. (2015) Biodegradation of phenol from saline wastewater using forward osmotic hollow fiber membrane bioreactor coupled chemostat. *Biochemical Engineering Journal* 94(Supplement C), 125-133.
- Prest, E.I., Hammes, F., Köttsch, S., van Loosdrecht, M.C.M. and Vrouwenvelder, J.S. (2013) Monitoring microbiological changes in drinking water systems using a fast and reproducible flow cytometric method. *Water Research* 47(19), 7131-7142.
- Qiu, Y.-L., Hanada, S., Ohashi, A., Harada, H., Kamagata, Y. and Sekiguchi, Y. (2008) *Syntrophorhabdus aromaticivorans* gen. nov., sp. nov., the First Cultured Anaerobe Capable of Degrading Phenol to Acetate in Obligate Syntrophic Associations with a Hydrogenotrophic Methanogen. *Applied and Environmental Microbiology* 74(7), 2051-2058.
- Qiu, Y.-L., Sekiguchi, Y., Hanada, S., Imachi, H., Tseng, I.-C., Cheng, S.-S., Ohashi, A., Harada, H. and Kamagata, Y. (2006) *Pelotomaculum terephthalicum* sp. nov. and *Pelotomaculum isophthalicum* sp. nov.: two anaerobic bacteria that degrade phthalate isomers in syntrophic association with hydrogenotrophic methanogens. *Archives of Microbiology* 185(3), 172-182.
- Shade, A., Peter, H., Allison, S.D., Baho, D.L., Berga, M., Bürgmann, H., Huber, D.H., Langenheder, S., Lennon, J.T., Martiny, J.B.H., Matulich, K.L., Schmidt, T.M. and Handelsman, J. (2012) Fundamentals of Microbial Community Resistance and Resilience. *Frontiers in Microbiology* 3, 417.
- Song, X., McDonald, J., Price, W.E., Khan, S.J., Hai, F.I., Ngo, H.H., Guo, W. and Nghiem, L.D. (2016) Effects of salinity build-up on the performance of an anaerobic membrane bioreactor regarding basic water quality parameters and removal of trace organic contaminants. *Bioresource Technology* 216(Supplement C), 399-405.
- Sudmalis, D., Gagliano, M.C., Pei, R., Grolle, K., Plugge, C.M., Rijnaarts, H.H.M., Zeeman, G. and Temmink, H. (2018) Fast anaerobic sludge granulation at elevated salinity. *Water Research* 128(Supplement C), 293-303.
- van Lier, J.B., van der Zee, F.P., Frijters, C.T.M.J. and Ersahin, M.E. (2015) Celebrating 40 years anaerobic sludge bed reactors for industrial wastewater treatment. *Reviews in Environmental Science and Biotechnology* 14(4), 681-702.
- Vyrides, I. and Stuckey, D.C. (2009a) Effect of fluctuations in salinity on anaerobic biomass and production of soluble microbial products (SMPs). *Biodegradation* 20(2), 165-175.
- Vyrides, I. and Stuckey, D.C. (2009b) Saline sewage treatment using a submerged anaerobic membrane reactor (SAMBR): Effects of activated carbon addition and biogas-sparging time. *Water Research* 43(4), 933-942.
- Vyrides, I. and Stuckey, D.C. (2011) Fouling cake layer in a submerged anaerobic membrane bioreactor treating saline wastewaters: Curse or a blessing? *Water Science and Technology* 63(12), 2902-2908.



- Vyrides, I. and Stuckey, D.C. (2017) Compatible solute addition to biological systems treating waste/wastewater to counteract osmotic and other environmental stresses: a review. *Critical Reviews in Biotechnology* 37(7), 865-879.
- Wang, S., Hou, X. and Su, H. (2017a) Exploration of the relationship between biogas production and microbial community under high salinity conditions. *Scientific Reports* 7(1).
- Wang, S., Hou, X. and Su, H. (2017b) Exploration of the relationship between biogas production and microbial community under high salinity conditions. *Scientific Reports* 7(1), 1149.
- Wang, W., Wu, B., Pan, S., Yang, K., Hu, Z. and Yuan, S. (2017c) Performance robustness of the UASB reactors treating saline phenolic wastewater and analysis of microbial community structure. *Journal of Hazardous Materials* 331(Supplement C), 21-27.
- Wang, W., Yang, K., Muñoz Sierra, J., Zhang, X., Yuan, S. and Hu, Z. (2017d) Potential impact of methyl isobutyl ketone (MIBK) on phenols degradation in an UASB reactor and its degradation properties. *Journal of Hazardous Materials* 333(Supplement C), 73-79.
- Wood, J.M. (2015) Bacterial responses to osmotic challenges. *The Journal of General Physiology* 145(5), 381-388.
- Woolard, C.R. and Irvine, R.L. (1995) Treatment of hypersaline wastewater in the sequencing batch reactor. *Water Research* 29(4), 1159-1168.
- Wu, Y., Wang, X., Tay, M.Q.X., Oh, S., Yang, L., Tang, C. and Cao, B. (2017) Metagenomic insights into the influence of salinity and cytostatic drugs on the composition and functional genes of microbial community in forward osmosis anaerobic membrane bioreactors. *Chemical Engineering Journal* 326, 462-469.
- Yan, N., Marschner, P., Cao, W., Zuo, C. and Qin, W. (2015) Influence of salinity and water content on soil microorganisms. *International Soil and Water Conservation Research* 3(4), 316-323.
- Yang, J., Spanjers, H., Jeison, D. and Van Lier, J.B. (2013) Impact of Na<sup>+</sup> on biological wastewater treatment and the potential of anaerobic membrane bioreactors: A review. *Critical Reviews in Environmental Science and Technology* 43(24), 2722-2746.
- Yang, J., Tian, Z., Spanjers, H. and Van Lier, J.B. (2014) Feasibility of using NaCl to reduce membrane fouling in anaerobic membrane bioreactors. *Water Environment Research* 86(4), 340-345.
- Yogalakshmi, K.N. and Joseph, K. (2010) Effect of transient sodium chloride shock loads on the performance of submerged membrane bioreactor. *Bioresource Technology* 101(18), 7054-7061.
- Yurtsever, A., Calimlioglu, B., Görür, M., Çınar, Ö. and Sahinkaya, E. (2016) Effect of NaCl concentration on the performance of sequential anaerobic and aerobic membrane bioreactors treating textile wastewater. *Chemical Engineering Journal* 287, 456-465.
- Zhang, X. and Wiegel, J. (1994) Reversible Conversion of 4-Hydroxybenzoate and Phenol by *Clostridium hydroxybenzoicum*. *Applied and Environmental Microbiology* 60(11), 4182-4185.



# Effects of large salinity fluctuations on phenol conversion in AnMBR

---

This chapter has been published as “Muñoz Sierra, J.D., Oosterkamp, M.J., Spanjers, H. and van Lier, J.B. (2021) Effects of large salinity fluctuations on an anaerobic membrane bioreactor treating phenolic wastewater. *Chemical Engineering Journal* 417, art. no. 129263.”

<https://doi.org/10.1016/j.ccej.2021.129263>

## Abstract

High salinity is becoming more common in industrial process water and final effluents, particularly when striving to close water loops. There is limited knowledge on the anaerobic treatment of chemical wastewaters characterized by distinct salinity fluctuations. This study investigates the high and fluctuating salinity effects on the conversion capacity and membrane filtration performance of an anaerobic membrane bioreactor (AnMBR) in treating phenol-containing wastewater. The AnMBR operated for 180 days with sodium concentrations between 8 and 37 gNa<sup>+</sup>·L<sup>-1</sup>. At ≤26 gNa<sup>+</sup>·L<sup>-1</sup>, approximately 99% COD and phenol removal efficiencies were achieved. At 37 gNa<sup>+</sup>·L<sup>-1</sup>, phenol and COD removal efficiencies decreased to 86 and 82%, respectively, while the biomass specific methanogenic activity was 0.12±0.05 gCOD-CH<sub>4</sub>·gVSS<sup>-1</sup>·d<sup>-1</sup>. Due to large salinity fluctuations, phenol and COD removal efficiencies reduced to ≤45% but recovered to ≥88%. Compared to phenol conversion, methanogenesis was more severely affected. Calculations showed a maximum in-situ phenol conversion rate of 25.5 mgPh·gVSS<sup>-1</sup>·d<sup>-1</sup>. Concomitantly, biomass integrity was compromised, and the median particle size severely dropped from 65.6 to 4.3 μm, resulting in a transmembrane pressure increase above 400 mbar. Cake layer resistance to filtration contributed to 85% of the total resistance. Nonetheless, all biomass was effectively retained in the AnMBR. A change in salinity ≥14 gNa<sup>+</sup>·L<sup>-1</sup> substantially reduced the microbial richness and diversity. The microbial community was dominated by Bacteria belonging to Clostridiales and Archaea of the orders Methanosarcinales and Methanobacteriales. Our findings demonstrate AnMBRs as suitable techniques for treating chemical process water, with possible subsequent reclamation, characterized by high phenols concentrations and largely fluctuating salinity levels.

## 4.1 Introduction

Worldwide, the introduction of cleaner industrial production processes has promoted closing water cycles, particularly in water-intensive industries, such as the chemical industry (Kong et al. 2019). Consequently, industrial residual waters are becoming increasingly associated with extreme conditions, such as high salinity and the presence of high concentrations of toxic aromatic compounds that can adversely reduce biological activity (Muñoz Sierra et al. 2017). Inorganic salts in wastewaters are mainly present as sodium chloride (NaCl). Moreover, hypersaline wastewater streams represent 5% of the world's total industrial effluents (Lefebvre et al. 2004). High sodium concentrations may reduce the effectiveness of anaerobic treatment and could induce the disintegration of flocs or granules, leading to operational challenges (Dereli et al. 2012), although anaerobic consortia may adapt to high salinity levels (Gagliano et al. 2018).

Previous studies have reported the effect of increasing sodium concentrations on high-rate anaerobic reactors for both granular sludge bed and membrane-based systems. Vyrides and Stuckey (2009) reported that anaerobic biomass could acclimate to sodium concentrations from 4 to 12  $\text{gNa}^+\cdot\text{L}^{-1}$ . Ismail et al. (2010) suggested that by increasing sodium concentration from 5 to 20  $\text{gNa}^+\cdot\text{L}^{-1}$  in a UASB, sludge granulation was hampered following a considerable reduction in granule strength by the exchange of calcium with sodium ions. However, when adding calcium to the influent to compensate exchange losses, Sudmalis et al. (2018a) noted stable granule formation at both 5 and 20  $\text{gNa}^+\cdot\text{L}^{-1}$  concentration in a UASB reactor, although the COD removal efficiency was reduced at 20  $\text{gNa}^+\cdot\text{L}^{-1}$ . Song et al. (2016) concluded that in an AnMBR, a step-wise increase in the sodium concentration beyond 4  $\text{gNa}^+\cdot\text{L}^{-1}$  reduced the COD removal efficiency to values lower than 80%. Similarly, Chen et al. (2019) demonstrated a decrease in the COD removal efficiency from 96% to 78% by sequentially increasing the sodium concentration from 0 to 2, 4, 8, and 16  $\text{gNa}^+\cdot\text{L}^{-1}$ . In contrast, in our previous study, we achieved COD removal efficiencies exceeding 90% in an AnMBR treating phenol-containing wastewater, after a step-wise increase in the sodium concentration from 8 to 18  $\text{gNa}^+\cdot\text{L}^{-1}$  (Muñoz Sierra et al. 2018). It should be realized that large amounts of industrial effluents containing priority organic pollutants, such as phenol, exhibit very high salt concentrations. Sodium chloride in phenolic wastewaters from chemical processes and agro-food industries ranged from 2 to 100  $\text{gNaCl}\cdot\text{L}^{-1}$  (Rincón-Llorente et al. 2018, Tan et al. 2019) which is equivalent to approximately 0.8 to 39  $\text{gNa}^+\cdot\text{L}^{-1}$ .

Regarding the microbial community composition, Lu et al. (2019) showed that a salinity increase from 0 to 9.2  $\text{gNa}^+\cdot\text{L}^{-1}$  only enriched specific lineages, but no drastic changes in the composition were observed. In contrast, Chen et al. (2019) indicated that a step-wise salinity increase to about 16  $\text{gNa}^+\cdot\text{L}^{-1}$  in an AnMBR affected the diversity of the microbial community. Further research is required to better understand the effect of changes in the sodium concentration on both anaerobic reactor performance and microbial composition. To the best of our knowledge, all previous studies only investigated a gradual increase in salinity. However, in practice, more drastic salinity fluctuations may occur owing to process operation dynamics, device cleaning, and/or water recycling (Vyrides 2015). Presently, there is very little research on salinity fluctuations in anaerobic reactors, including AnMBRs.

Based on the above considerations, this study aimed to assess the effects of large fluctuations in sodium concentration on the anaerobic conversion capacity and membrane filtration performance in an AnMBR used for treating phenol-containing chemical wastewater. Four operation phases were applied to examine whether salinity variations deteriorate the phenol conversion rate, methanogenic activity, and biomass characteristics, such as particle size, extracellular polymeric substances, and filterability. Moreover, we investigated the effect of salinity fluctuations on microbial community diversity.

## 4.2 Material and Methods

### 4.2.1 Experimental reactor set-up and operation

The experiments were carried out by using laboratory-scale AnMBR reactor with 6.5 L effective volume, equipped with an ultra-filtration side-stream membrane module (Figure 4.1). A tubular polyvinylidene fluoride (PVDF) membrane was used (Pentair, The Netherlands) with dimensions of 5.5 mm inner diameter, 0.64 m length, and 30 nm nominal pore size. The system was equipped with feed, recycle and effluent pumps (120U/DV, 520Du, Watson Marlow, The Netherlands), pH and temperature sensors (Memosens, Endress & Hauser, Germany), biomass recirculation flow meter (Mag-view MVM-030-PN, Bronkhorst, The Netherlands), a permeate scale (EW 2200-2NM, Kern-Sohn, Germany), and a biogas flowmeter (Milligas Counter MGC-1 PMMA, Ritter, Germany). Transmembrane pressure (TMP) was measured using three pressure sensors (AE Sensors ATM, The Netherlands). Warm water was recirculated by a thermostatic water bath (Tamson Instruments, The Netherlands) through the reactor's water jacket, and the temperature was controlled at  $35.0 \pm 0.8^\circ\text{C}$ . The AnMBR was controlled by a computer running LabView software (version 15.0.1f1, National Instruments, USA).

The AnMBR operated as a continuously mixed reactor during 180 days in phases of 40 (phase I-III) and 60 (phase IV) days. The biomass was continuously recirculated at a cross-flow velocity of  $0.6 \text{ m}\cdot\text{s}^{-1}$  with a reactor turnover of about 190 times per day. The sludge of the AnMBR was acclimated to sodium concentrations in the range of 8 -  $22 \text{ gNa}^+\cdot\text{L}^{-1}$ . The sodium concentration in the AnMBR was varied in each of the four phases of operation as shown in Fig. 2.A. Different modes, simulating high salinity variations, were applied, i.e., increasing/decreasing between 18 and  $23 \text{ gNa}^+\cdot\text{L}^{-1}$ , stepwise increase from 20 to  $37 \text{ gNa}^+\cdot\text{L}^{-1}$ , decrease from 37 to  $26 \text{ gNa}^+\cdot\text{L}^{-1}$ , and random fluctuations between 8 and  $35 \text{ gNa}^+\cdot\text{L}^{-1}$  with different variation frequencies between 2 and 7 days. In phase III, the sodium concentration was kept constant once it reached  $26 \text{ gNa}^+\cdot\text{L}^{-1}$ . In phase IV, the random salinity fluctuations followed a random data set generated with Minitab statistical software (Minitab 17, Minitab LLC). A completely mixed reactor mass balance model was used to determine the sodium feed solution composition in order to reach the desired in-reactor sodium concentrations with a control bulk-liquid volume of 6.5 L.

Sodium mass balance:

$$\frac{dC}{dt} = \frac{Q}{V}C_{in} - \frac{Q}{V}C \quad (\text{Eq.1})$$

with

$$\frac{Q}{V} = \tau \quad \text{and} \quad \frac{dC}{dt} = C'(t)$$

Rearranging the equation as a function of time:

$$C'(t) = \tau C_{in} - \tau C(t) \quad (\text{Eq. 2})$$

Integrating to solve the Eq. 2 then:

$$C(t) = C_{in} + c e^{-\tau t} \quad (\text{Eq. 3})$$

with  $c$  as the integration constant:

$$c = C(0) - C_{in} \quad (\text{Eq. 4})$$

Therefore, by knowing the actual sodium concentration ( $C(0)$ ) and the final concentration ( $C(t)$ ) that is determined to be reached in the fluctuation within a time ( $t$ ), the corresponding sodium concentration of the AnMBR feed solution ( $C_{in}$ ) and the constant value ( $c$ ) were calculated.

Table 4.1 summarizes the operational conditions of the AnMBR continuous flow experiment. The average SRT of the AnMBR was maintained at about  $517 \pm 180$  days (Table 4.1).

Table 4.1. Operational conditions of the AnMBR.

Parameter	Value	Units
Influent phenol	0.50	gPh.L <sup>-1</sup>
OLR	$8.07 \pm 0.1$	gCOD.L <sup>-1</sup> .d <sup>-1</sup>
Flow rate	$1.48 \pm 0.2$	L.d <sup>-1</sup>
SRT	$517 \pm 180$	d
Flux	$5.9 \pm 0.8$	L.m <sup>-2</sup> .h <sup>-1</sup>
Cross flow velocity	0.60	m.s <sup>-1</sup>
TMP	80-250 (I-III)	mbar
	>250 (IV)	mbar
Temperature	$35.0 \pm 0.8$	°C
pH	$8.1 \pm 0.2$	pH

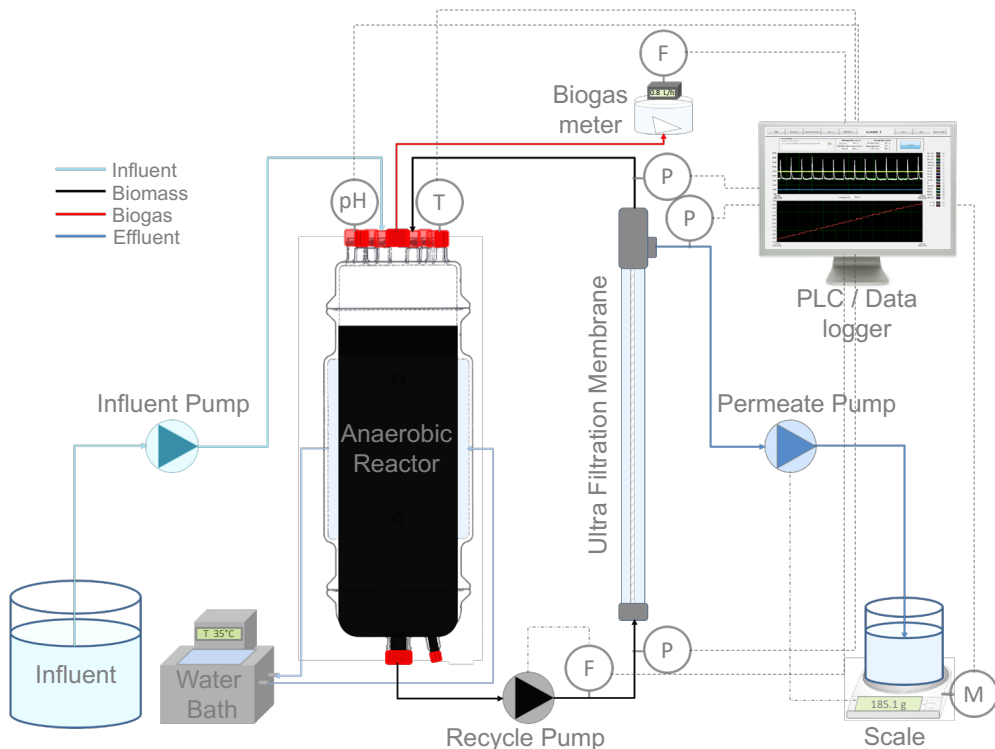


Figure 4.1 Schematic representation of the AnMBR.

The reactor was fed with synthetic wastewater containing sodium acetate trihydrated ( $70.8 \text{ g.L}^{-1}$ ) and phenol ( $0.5 \text{ gPh.L}^{-1}$ ). The sodium chloride ( $\text{NaCl}$ ),  $\text{K}_2\text{HPO}_4$  ( $34.85 \text{ g.L}^{-1}$ ) and  $\text{KH}_2\text{PO}_4$  ( $24 \text{ g.L}^{-1}$ ) varied depending on the sodium concentration applied in the reactor maintaining a fixed  $\text{K}^+:\text{Na}^+$  ratio of 0.05. Macronutrients ( $9 \text{ mL.L}^{-1}$ ), micronutrients ( $4.5 \text{ mL.L}^{-1}$ ) and yeast extract ( $2.0 \text{ g.L}^{-1}$ ) were supplemented. Macronutrients solution included (in  $\text{g.L}^{-1}$ ):  $\text{NH}_4\text{Cl}$  170,  $\text{CaCl}_2 \cdot 2\text{H}_2\text{O}$  8, and  $\text{MgSO}_4 \cdot 7\text{H}_2\text{O}$  9; and micronutrients solution contained (in  $\text{g.L}^{-1}$ ):  $\text{FeCl}_3 \cdot 6\text{H}_2\text{O}$  2,  $\text{CoCl}_2 \cdot 6\text{H}_2\text{O}$  2,  $\text{MnCl}_2 \cdot 4\text{H}_2\text{O}$  0.5,  $\text{CuCl}_2 \cdot 2\text{H}_2\text{O}$  0.03,  $\text{ZnCl}_2$  0.05,  $\text{H}_3\text{BO}_3$  0.05,  $(\text{NH}_4)_6\text{Mo}_7\text{O}_{24} \cdot 4\text{H}_2\text{O}$  0.09,  $\text{Na}_2\text{SeO}_3$  0.1,  $\text{NiCl}_2 \cdot 6\text{H}_2\text{O}$  0.05, EDTA 1,  $\text{Na}_2\text{WO}_4$  0.08.

#### 4.2.2 Specific methanogenic activity (SMA)

SMA tests were performed in triplicate using an automated methane potential test system (AMPTS, Bioprocess Control, Sweden) and were carried out at  $35 \text{ }^\circ\text{C}$  following the method described by Spanjers and Vanrolleghem (2016). The ratio  $\text{K}^+:\text{Na}^+$  was kept constant at 0.05 in the media. The initial pH was adjusted to 7.0 ( $20 \pm 0.4 \text{ }^\circ\text{C}$ ).



### 4.2.3 Flow cytometry assay

Flow cytometry assay was conducted with biomass samples at different sodium concentrations. BD Accuri C6® flow cytometer (BD Accuri cytometers, Belgium) was used, with a 50 mW laser emitting at a fixed wavelength of 488 nm. BD Accuri CFlow® software was used for data analysis to distinguish between intact cells and cells with compromised membranes. Biomass samples were diluted to obtain bacteria concentrations less than  $2 \times 10^5$  cells mL<sup>-1</sup>. Samples were stained and evaluated following the protocol defined by Prest et al. (2013).

### 4.2.4 Biomass characteristics stress index (BSI)

ATP was measured by QG21Waste™ test kits from biomass samples following the manufacturer's method (Luminultra®). Total ATP (tATP) and dissolved ATP (dATP) were determined to observe the impact of sodium concentration on biomass integrity. The tATP is the sum of intracellular and extracellular ATP and the dATP is the ATP present outside living cells and rejected by dead microorganisms. Analyses were conducted in duplicates. After dilution and extraction steps, samples were read immediately by a luminometer. The biomass stress index (BSI %), which indicates the stress level or mortality of the biomass, was calculated with the equation:  $BSI [\%] = 100 (dATP / tATP)$  (Luján-Facundo et al. 2018).

### 4.2.5 Biomass characteristics

#### 4.2.5.1 Extracellular polymeric substances (EPS) and soluble microbial products (SMP)

EPS and SMP were characterized based on proteins and polysaccharides methods (Dubois et al. 1956, Frølund et al. 1996). Biomass samples were centrifuged at 4 °C and 12,000 rpm for 15 min. The supernatant was filtered (0.45 µm) and directly used to measure the SMP. EPS extraction was carried out by the cation exchange resin method. DOWEX Marathon C (20–50 µm mesh, sodium form, Fluka 91973) was used as a cation exchange resin. Extraction was carried out at 4 °C, 800 rpm, during 4 h. EPS was normalized against the volatile suspended solids (VSS) concentration of the biomass in the reactor. The VSS and total suspended solids (TSS) concentrations were determined following standard methods using the lowest possible sample volume (American Public Health et al. 2005).

#### 4.2.5.2 Relative Hydrophobicity

Biomass relative hydrophobicity (RH) was determined by bacterial adhesion to hydrocarbons method with dodecane as the hydrocarbon phase (Rosenberg et al. 1980). Analyses and sampling were conducted in triplicates. 1 g/L TSS of biomass samples was obtained by dilution with permeate. 4 mL dodecane was added to each sample (4 mL) and the resulting suspension was mixed for 1 min. The water phase was taken with a pipette after 10 min gravitational phase separation, and the corresponding absorbance (Absf) was determined at 600 nm by a UV spectrophotometer (DR3900, Hach Lange, Germany). The AnMBR permeate was used as the blank and the diluted

biomass sample was measured as the initial absorbance (Abs<sub>i</sub>). All measurements were carried out in triplicates, and RH was calculated as  $RH[\%] = 100 (1 - Abs_f / Abs_i)$ .

#### 4.2.5.3 Biomass filterability: capillary suction time (CST)

CST of the biomass was measured by a Capillary Suction Timer device (Model 304M, Triton Electronics, Essex, England, UK). A CST paper (7 × 9 cm) was used for each sample (6.4 mL). Samples were measured in triplicate. The results were normalized by dividing the CST by total suspended solids concentration (Jamal Khan et al. 2008).

#### 4.2.5.4 Particle size distribution (PSD)

PSD measurements were carried out employing a DIPA-2000 EyeTech™ particle analyzer (Donner Technologies, Or Akiva, Israel) with an A100 and B100 laser lens (0.1–300 μm and 1–2000 μm, respectively) and a liquid flow cell DCM-104A (10 × 10 mm). The median particle size of the PSD is expressed as D50.

### 4.2.6 Permeate characterization

#### 4.2.6.1 Sodium concentration

Sodium concentrations in the reactor permeate were measured by Ion Chromatography (Metrohm, Switzerland). Dilutions were applied to samples and were prepared in triplicates. Calibration curves were made using standard solutions (Sigma-Aldrich) in the range between 0.1 and 50 mgL<sup>-1</sup>. The final concentrations were calculated by using the MagIC Net 3.2 software.

#### 4.2.6.2 Phenol and COD analysis

Phenol concentrations were measured by high-performance liquid chromatography HPLC LC-20AT (Shimadzu, Japan) equipped with a 4.6 mm reversed-phase C18 column (Phenomenex, The Netherlands) and a UV detector at a wavelength of 280 nm. The mobile phase was 25% (v/v) acetonitrile solution at a flow rate of 0.95 mL·min<sup>-1</sup>. The column oven was set at 30 °C. Quick phenol concentration measurements were carried out by Merck – Spectroquant® Phenol cell kits using a spectrophotometer NOVA60 (Merck, Germany). Hach Lange kits were used to measure chemical oxygen demand (COD). Proper dilutions were made to avoid interference by high chloride concentrations, without compromising the accuracy of the measurement. The COD was measured using a VIS - spectrophotometer (DR3900, Hach Lange, Germany).

### 4.2.7 Membrane cleaning

At the end of the experiment, the membrane of the AnMBR was cleaned, first physically and then chemically, to determine the different fouling resistances. The physical membrane cleaning was performed by flushing the membrane with water to remove the cake layer. The chemical cleaning was carried out by soaking the membrane in 500 mgL<sup>-1</sup> NaClO and 2000 mgL<sup>-1</sup> citric acid solution sequentially for 2 hours each. After each step, the membrane resistance to water filtration was measured. The total resistance to filtration is formulated as the sum or the intrinsic, removable,

irreversible and irrecoverable resistance,  $R_{total} = \Delta P_T \cdot \eta \cdot J = R_{intrinsic} + R_{removable} + R_{irreversible} + R_{irrecoverable}$ ; where  $R_{total}$  is the total filtration resistance ( $m^{-1}$ ),  $R_{intrinsic}$  the intrinsic membrane resistance ( $m^{-1}$ ),  $R_{removable}$  the cake layer resistance that is physically removed by flushing with water ( $m^{-1}$ ),  $R_{irreversible}$  the resistance caused by inorganic and organic foulants which is removed by chemical cleaning ( $m^{-1}$ ),  $R_{irrecoverable}$  the resistance caused by foulants that are not removed by physical and chemical cleaning ( $m^{-1}$ ), and  $J$ ,  $\Delta P_T$  and  $\eta$  refer to the flux ( $m^3 \cdot m^{-2} \cdot s^{-1}$ ), transmembrane pressure (TMP) (Pa) and the dynamic viscosity of water (Pa·s), respectively.

#### 4.2.8 Microbial community analysis

Samples were taken within the four operational phases with intervals  $\geq 20$  days. The DNA extraction was carried out from AnMBR's biomass samples by using the DNeasy UltraClean Microbial Kit (Qiagen, Hilden, Germany) to evaluate the microbial community dynamics. DNA obtained was checked by agarose gel electrophoresis (quality) and Qubit3.0 DNA detection (Qubit® dsDNA HS Assay Kit, Life Technologies, U.S.) (quantity). 16S rRNA gene amplicon sequencing was carried out by the MiSeq Illumina platform and using the primers 341F (5'-CCTACGGGNGGCWGCAG-3') 785R (5'-GACTACHVGGGTATCTAATCC-3') for bacteria/archaea in the V3-V4 region (BaseClear, Leiden, the Netherlands). The QIIME pipeline (version 1.9.0) was used to analyze the sequences (Caporaso et al. 2010). Demultiplexing and quality filtering were performed with parameter values  $Q = 20$ ,  $r = 3$ , and  $p = 0.75$ . Chimeric sequences were removed with UCHIME2 (version 9.0) algorithm (Edgar 2016). Sequences were clustered into operational taxonomic units (OTUs) with a 97% similarity as the cutoff, with UCLUST algorithm (Edgar 2010). Singletons were removed, and OTUs with an occurrence less than three times in at least one sample were excluded. The taxonomic assignment was performed using the Silva database (SILVA-128) with UCLUST (McDonald et al. 2012). Alpha diversity was determined after random subsampling using the metrics Chao1, observed OTUs, Shannon, and Simpson indices in QIIME. The sequences reported in this paper have been deposited at ENA under the study accession number PRJEB38420.

### 4.3 Results and Discussion

#### 4.3.1 AnMBR process performance

The AnMBR treating phenol-containing wastewater was subjected to sodium concentration fluctuations (Figure 4.2. A). Phenol removal efficiencies of 99% were achieved at 18-23  $gNa^+ \cdot L^{-1}$  after 20 days of operation (Phase I, Figure 4.2. B). The lowest and highest volumetric phenol conversion rates achieved were 78  $mgPh \cdot L^{-1} \cdot d^{-1}$  (7.5  $mgPh \cdot gVSS^{-1} \cdot d^{-1}$ ) and 114  $mgPh \cdot L^{-1} \cdot d^{-1}$  (15.0  $mgPh \cdot gVSS^{-1} \cdot d^{-1}$ ), respectively (Table 4.2). Concomitantly, COD removal efficiencies between 96-99% were achieved (Phase I, Figure 4.2. C). The SMA decreased by 21% at the end of phase I from the initial value of 0.39  $gCOD \cdot CH_4 \cdot gVSS^{-1} \cdot d^{-1}$  (Table 4.2).

In phase II, after the sodium concentration reached  $37 \text{ gNa}^+\cdot\text{L}^{-1}$  on days 62-79, the phenol removal efficiency decreased from 98% to 86%. The in-situ phenol conversion rate on day 80 was  $101 \text{ mgPh}\cdot\text{L}^{-1}\cdot\text{d}^{-1}$  ( $13 \text{ mgPh}\cdot\text{gVSS}^{-1}\cdot\text{d}^{-1}$ ). The COD removal efficiency was maintained above 99% at sodium concentrations of up to  $26 \text{ gNa}^+\cdot\text{L}^{-1}$ . However, at the end of phase II, the COD removal efficiency reduced to 84%, corresponding to a COD effluent concentration of  $5,445 \text{ mgCOD}\cdot\text{L}^{-1}$  (Phase II, Figure 4.2. C). The SMA was  $0.12\pm 0.05 \text{ gCOD-CH}_4\cdot\text{gVSS}^{-1}\cdot\text{d}^{-1}$  before COD removal deteriorated at  $36.3 \text{ gNa}^+\cdot\text{L}^{-1}$ . This SMA value was ten-fold higher than that expected based on our previously reported sodium response curve (Muñoz Sierra et al. 2017), suggesting that the AnMBR biomass was well adapted to high sodium concentrations. Wang et al. (2017b) also showed a significant decrease in methanogenic activity of 59% by increasing the sodium concentration from 10 to  $20 \text{ gNa}^+\cdot\text{L}^{-1}$  in a UASB reactor treating phenolic wastewater.

In phase III, sodium concentration was reduced to  $26 \text{ gNa}^+\cdot\text{L}^{-1}$ , and was maintained at a constant level to recover the biomass from reactor perturbation caused by the high salinity built up in phase II. We observed a notably fast recovery in the phenol removal efficiency of 93 – 97% in the remainder of phase III (Phase III, Figure 4.2. B). In contrast, the COD removal efficiency only slowly recovered with a concomitant increase in SMA to  $0.56\pm 0.02 \text{ gCOD-CH}_4\cdot\text{gVSS}^{-1}\cdot\text{d}^{-1}$ . On day 119, a COD removal efficiency of 73% was observed (Phase III, Figure 4.2. C). The results indicated that compared to phenol conversion, methanogenesis was more severely affected by increasing sodium concentrations. Wu et al. (2017) concluded that when increasing the salinity from low ( $3.3 \text{ mS}\cdot\text{cm}^{-1}$ ) to high ( $21.0 \text{ mS}\cdot\text{cm}^{-1}$ ), the abundance of hydrogenotrophic and acetoclastic methanogens decreased significantly, which resulted in a reduced COD conversion to methane.

In phase IV, when the salinity decreased from 26 to  $18.9 \text{ gNa}^+\cdot\text{L}^{-1}$  on day 123, the lowest phenol removal efficiency was 43%, and the SMA was  $0.05\pm 0.03 \text{ gCOD-CH}_4\cdot\text{gVSS}^{-1}\cdot\text{d}^{-1}$ . On day 140, the sodium concentration decreased to  $13 \text{ gNa}^+\cdot\text{L}^{-1}$ , causing an increase in the phenol removal efficiency to 97%, whereas an increase to  $29 \text{ gNa}^+\cdot\text{L}^{-1}$  on day 142 decreased the efficiency to 84% (Phase IV, Figure 4.2. B). A subsequent decrease to  $8 \text{ gNa}^+\cdot\text{L}^{-1}$  resulted in an increase in the phenol removal efficiency increase to 87%. Vyrides et al. (2010) also suggested an improved process performance after a step-wise decrease from  $13.8 \text{ gNa}^+\cdot\text{L}^{-1}$  to  $0.08 \text{ gNa}^+\cdot\text{L}^{-1}$  in a submerged AnMBR. We noted that the consecutive large fluctuations to 27, 13, 28 and  $13 \text{ gNa}^+\cdot\text{L}^{-1}$  (Phase IV, Figure 4.2. A) did not have a negative effect on the phenol removal efficiency that increased from 83% to 95% at the end of phase IV. The phenol conversion rate increased from 50 ( $6.9 \text{ mgPh}\cdot\text{gVSS}^{-1}\cdot\text{d}^{-1}$ ) to  $109 \text{ mgPh}\cdot\text{L}^{-1}\cdot\text{d}^{-1}$  ( $25.5 \text{ mgPh}\cdot\text{gVSS}^{-1}\cdot\text{d}^{-1}$ ) during phase IV. Fluctuating the sodium concentrations between 13 and  $35 \text{ gNa}^+\cdot\text{L}^{-1}$ , revealed a decreasing trend in the COD removal efficiency with the minimum value reaching 28% on day 142. However, further fluctuations up to day 180 did not negatively affect the COD removal efficiency. In contrast, a gradual recovery of up to 88% was observed (Phase IV, Figure 4.2. C). Concurrently, the SMA increased to  $0.39\pm 0.05$  at a sodium concentration of  $16.0 \text{ gNa}^+\cdot\text{L}^{-1}$  (Table 4.2). Previous studies on AnMBRs at high salinity suggested that step-wise increases in sodium concentration of up to  $16 \text{ gNa}^+\cdot\text{L}^{-1}$  reduced the COD removal efficiency to values lower than 80% (Chen et al. 2019, Song et al. 2016). Moreover, small salinity fluctuations of  $2 \text{ gNa}^+\cdot\text{L}^{-1}$  between 18 and  $20 \text{ gNa}^+\cdot\text{L}^{-1}$  were

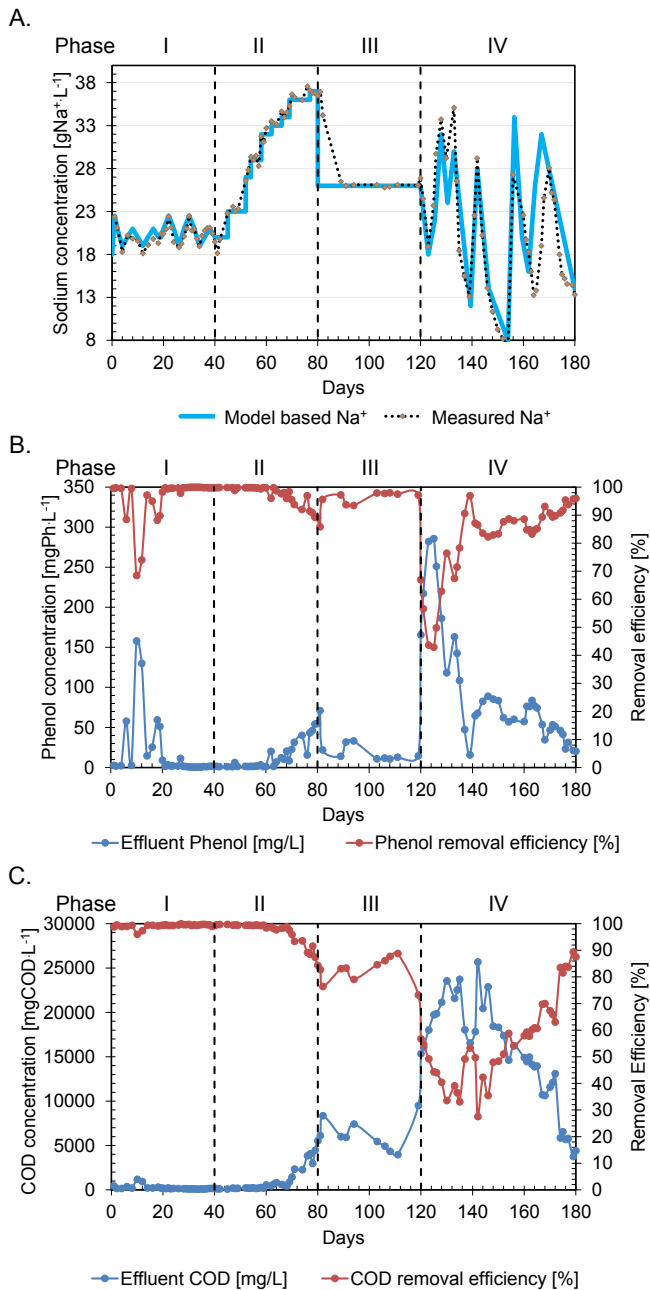


Figure 4.2 Anaerobic membrane bioreactors performance. A. Applied sodium concentrations. B. Effluent phenol concentration and removal efficiency. C. Effluent COD concentration and removal efficiency.

previously assessed, which did not affect the overall AnMBR conversion performance (Muñoz Sierra et al. 2018). In contrast, despite the application of high salinities (8–37 gNa<sup>+</sup>L<sup>-1</sup>), the results suggested that the microbial community became more resilient to disturbances caused by large fluctuations in salinity. As a result, the AnMBR phenol and COD conversion capacities were sustained and recovered, respectively, to values higher than 88%.

The flow cytometry results showed that most cells (84%) with compromised membranes were observed after the salinity increased from 20 to 37 gNa<sup>+</sup>L<sup>-1</sup> at the beginning of phase III (Figure 4.3 A). Moreover, during the large fluctuations in the range of 8–37 gNa<sup>+</sup>L<sup>-1</sup> (phase IV), 67% of cells had compromised membranes on day 146. On the contrary, the number of cells with compromised membranes was only 15% in phase I and approximately 20% at the end of phase IV, corresponding to the highest phenol and COD removal efficiencies in the AnMBR. By measuring the dissolved ATP over total ATP, the biomass stress index (BSI) was determined, which reflects the microbial stress level of the biomass and indicates the deterioration of the biological process (Luján-Facundo et al. 2018) (Figure 4.3 B). Biomass samples from phase I showed a relatively low BSI with an average of 38%. During phase II, an increasing trend from 39% to 99% was observed with a step-wise increase in salinity to 37 gNa<sup>+</sup>L<sup>-1</sup>. A decrease to a BSI of 50% was attained when no salinity fluctuations were imposed on the reactor in phase III, which can be considered indicative of microbial adaptation and cell recovery (John et al. 2017). In addition, osmoprotectants present in the yeast extract and protein (PN)-like substances may have played a role in alleviating the osmotic stress of the anaerobic biomass (Sudmalis et al. 2018b). In phase IV, the BSI index was unstable and increased up to 99%, following biomass exposure to fluctuations in sodium concentrations exceeding 14 gNa<sup>+</sup>L<sup>-1</sup>. Hereafter, the BSI decreased to 49% at sodium concentrations in the range of 8–28 gNa<sup>+</sup>L<sup>-1</sup>.

### 4.3.2 Effect of salinity fluctuations on biomass characteristics

#### 4.3.2.1 Extracellular polymeric substances (EPS) and soluble microbial products (SMP)

Proteins (PN) and polysaccharides (PS) were determined as the main compounds in EPS and SMP in the AnMBR. EPS-PN accounted for 82% of the total EPS, with their content being 5 mg·gVSS<sup>-1</sup> at the initial sodium concentration of 22.4 gNa<sup>+</sup>L<sup>-1</sup> (Table 4.3). Salinity fluctuations in phase I (18–23 gNa<sup>+</sup>L<sup>-1</sup>) increased the EPS-PN content from 5.0 to 35.2 mg·gVSS<sup>-1</sup>. However, the EPS-PS content did not significantly increase in both phase II and III. Similarly, Ismail et al. (2010) reported that the PN fraction of EPS in a UASB operated at 20 gNa<sup>+</sup>L<sup>-1</sup> was much higher, i.e., 87–94%, than the PS fraction. The exposure to increased salinity in the AnMBR biomass in phase II increased the PN content of EPS to 42.5 mg·gVSS<sup>-1</sup>; however, it decreased to 22.8 mg·gVSS<sup>-1</sup> when the sodium concentration in the reactor reached 36.9 gNa<sup>+</sup>L<sup>-1</sup> on day 80. Concomitantly, the SMP-PN content increased from 14 mg·gVSS<sup>-1</sup> at 19.5 gNa<sup>+</sup>L<sup>-1</sup> to 136.6 mg·gVSS<sup>-1</sup> at the end of phase II, suggesting protein solubilization due to high salinity exposure (Yogalakshmi and Joseph 2010). During random fluctuations in phase IV, the highest amount of EPS-PN of 118.6 mg·gVSS<sup>-1</sup> was observed under the fluctuation from 14 to 8 gNa<sup>+</sup>L<sup>-1</sup>. For SMP-PN, the highest PN concentration

was  $163.7 \text{ mg} \cdot \text{gVSS}^{-1}$  on day 163, after the variation from 27 to  $16 \text{ gNa}^+ \cdot \text{L}^{-1}$ . We noted foaming in the AnMBR within this phase. Foaming might be attributed to the increase in proteins at the gas/liquid interface owing to their surface-active properties (Ganidi et al. 2009).

Table 4.2. Specific methanogenic activity, as well as volumetric and specific phenol conversion rate at different sodium concentrations in the four operational phases of the AnMBR.

Phase	Day	Sodium concentration [ $\text{gNa}^+ \cdot \text{L}^{-1}$ ]	SMA [ $\text{gCOD} \cdot \text{CH}_4 \cdot \text{gVSS}^{-1} \cdot \text{d}^{-1}$ ]	Phenol conversion rate [ $\text{mgPh} \cdot \text{L}^{-1} \cdot \text{d}^{-1}$ ]	Min. and Max. phenol conversion rates [ $\text{mgPh} \cdot \text{L}^{-1} \cdot \text{d}^{-1}$ ]	Specific phenol conversion rate [ $\text{mgPh} \cdot \text{gVSS}^{-1} \cdot \text{d}^{-1}$ ]
I	1	22.3	$0.39 \pm 0.00$	113	78 <sup>Min</sup>	10.7
	30	22.5	$0.31 \pm 0.03$	114	114 <sup>Max</sup>	15.0
II	70	36.3	$0.12 \pm 0.05$	109	101 <sup>Min</sup>	14.3
					114 <sup>Max</sup>	
III	101	26.1	$0.56 \pm 0.02$	111	98 <sup>Min</sup>	15.1
					111 <sup>Max</sup>	
IV	123	18.9	$0.50 \pm 0.10$	50		6.9
	137	15.5	$0.05 \pm 0.03$	103	49 <sup>Min</sup>	18.6
	163	16.0	$0.39 \pm 0.05$	95	110 <sup>Max</sup>	12.6
	180	13.3	$0.28 \pm 0.04$	109		25.5

#### 4.3.2.2 Relative hydrophobicity (RH)

The RH of the AnMBR biomass during phases I, II, III, and IV was, on average,  $37 \pm 15\%$ ,  $44 \pm 5\%$ ,  $35 \pm 19\%$ , and  $11 \pm 5\%$ , respectively (Figure 4.4). The biomass was highly hydrophobic at the start of phase I as well as after being exposed to a high sodium concentration ( $36.9 \text{ gNa}^+ \cdot \text{L}^{-1}$ ) at the end of phase II. High content of EPS-PN is generally responsible for high biomass hydrophobicity. In contrast, large salinity fluctuations in phase IV decreased AnMBR biomass hydrophobicity to 8%, even though extracellular PN-like substances were higher than PS. The low hydrophobicity of the AnMBR biomass in phase IV, likely resulted in increased cake/gel layer accumulation on the hydrophilic membranes and therefore to a higher transmembrane pressure. Reversely, Van den Broeck et al. (2011) reported that an increase in biomass hydrophobicity resulted in decreased

membrane fouling, which can be attributed to a reduced interaction between hydrophobic biomass and usually hydrophilic membranes.

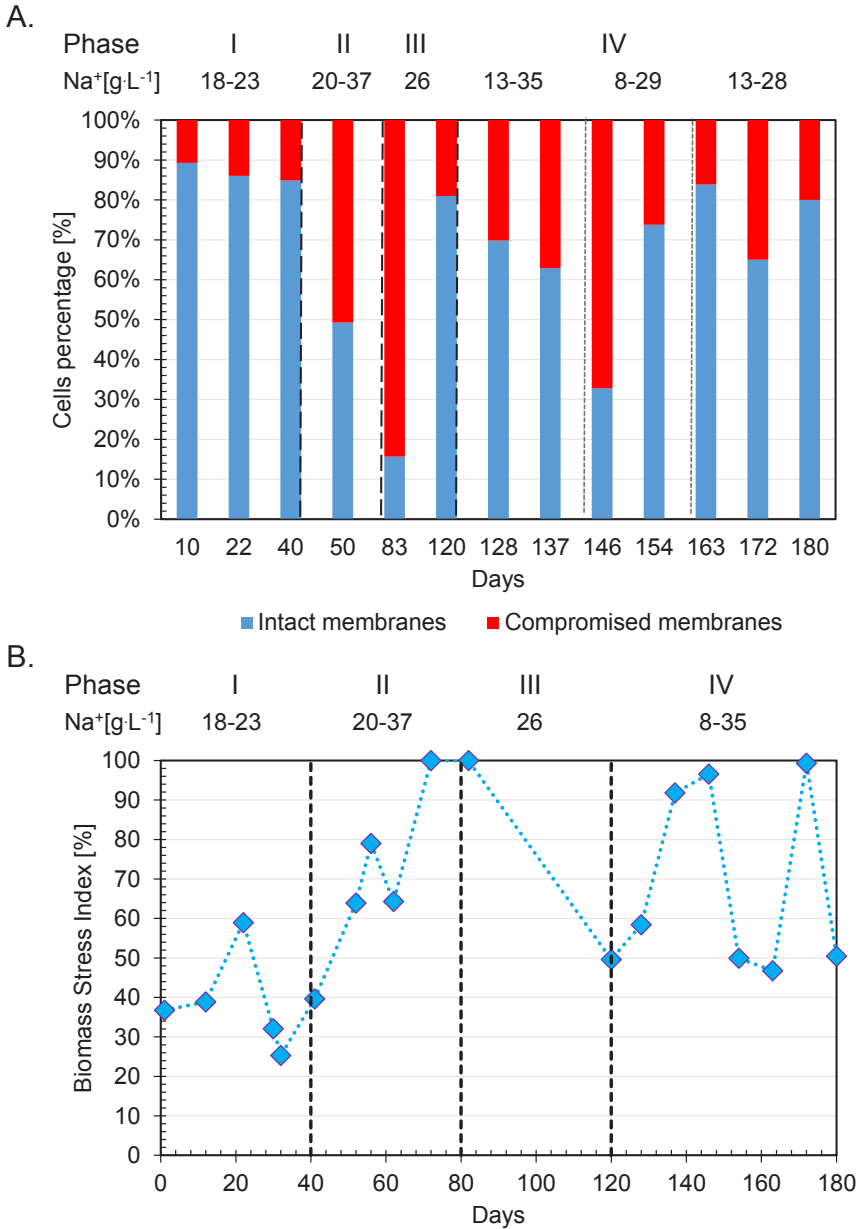


Figure 4.3 A. Cells percentage with intact and compromised membranes. B. Biomass stress index (BSI).



Table 4.3. EPS and SMP concentrations resulting from salinity fluctuations. PN: Proteins, PS: Polysaccharides.

Phase	Day	Sodium concentration [gNa <sup>+</sup> L <sup>-1</sup> ]	EPS		SMP	
			[mggVSS <sup>-1</sup> ]		[mggVSS <sup>-1</sup> ]	
			PS	PN	PS	PN
I	0	22.4	1.1	5.0	0.7	24.2
	14	19.1	0.4	32.3	0.1	127.8
	28	20.1	0.2	26.1	0.3	51.0
	40	19.5	2.1	35.2	0.0	14.0
II	54	29.4	1.9	30.3	1.7	62.9
	68	34.6	2.4	42.5	1.6	72.5
III	80	36.9	0.9	22.8	2.3	136.6
IV	120	26.9	2.6	65.6	5.1	154.3
	137	15.5	5.6	62.6	2.5	112.3
	146	14.1	6.3	75.6	2.3	128.9
	154	8.0	8.0	118.6	3.1	128.7
	163	16.0	10.0	113.2	2.9	163.7
	172	24.4	5.2	68.9	2.8	87.8
	180	13.3	7.0	91.2	1.2	64.5

#### 4.3.2.3 Biomass particle size and capillary suction time (CST)

The median biomass particle size (D50) decreased by approximately 45% from 21.0  $\mu\text{m}$  at the start of phase I (22.4 gNa<sup>+</sup>L<sup>-1</sup>) to 11.5  $\mu\text{m}$  at the end of phase I (Figure 4.4). In phase II, along with the step-wise increase in salinity to 37 gNa<sup>+</sup>L<sup>-1</sup>, D50 increased to 19.4  $\mu\text{m}$  on day 80. Ismail et al. (2010) and Gagliano et al. (2017), assessed granular sludge in UASB reactors, and observed that granules formed at 20 gNa<sup>+</sup>L<sup>-1</sup> were bigger than those formed at 10 gNa<sup>+</sup>L<sup>-1</sup>. The high concentration of sodium might weaken the binding of EPS and induce enlarged flocs, resulting in a likely weaker structure.

In phase III, the median particle size increased to 65.6  $\mu\text{m}$ , under a constant sodium concentration of 26 gNa<sup>+</sup>L<sup>-1</sup>. However, a total reduction of 93.4% in the D50 to 4.3  $\mu\text{m}$  from the beginning to the end of phase IV notably indicated a substantial negative effect on the biomass particle size due

to the large salinity fluctuations. Moreover, Liu and Fang (2003) concluded that a reduction in the biomass particle size could also result from a decreasing sludge hydrophobicity, as was observed in phase IV. Although a decrease in biomass particle size under increasing salinity conditions is observed by other studies (De Vrieze et al. 2016), our present results clearly show the detrimental effects of large salinity fluctuations on biomass morphology.

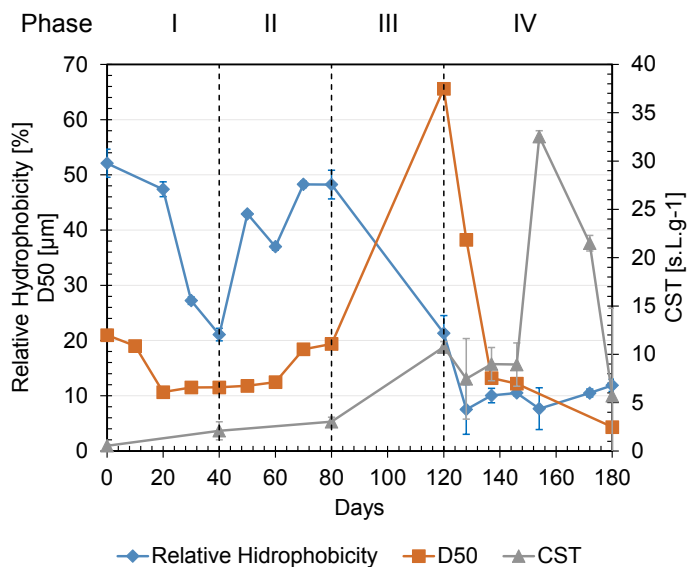


Figure 4.4 Left y-axis: Relative hydrophobicity [%] and median biomass particle size D50 [μm]. Right y-axis: Normalized capillary suction time [s.L.g<sup>-1</sup>]

CST ranged from 0.5 s.L.gTSS<sup>-1</sup> in phase I to 32.5 s.L.gTSS<sup>-1</sup> in phase IV. These results corroborated with those described above of D50. When the biomass was exposed to 8 gNa<sup>+</sup>.L<sup>-1</sup> on day 154, the measured CST (32.5 s.L.gTSS<sup>-1</sup>) was three times higher than the initially observed 10.8 s.L.gTSS<sup>-1</sup> on day 120, which corresponded the major decrease in particle size in phase IV. This increased in CST indicated that the biomass had the worst filterability characteristics after being exposed to large salinity fluctuations in phase IV, which contributed to an increasing resistance to filtration.

### 4.3.3 Membrane filtration performance

The AnMBR exhibited a non-disturbed filtration performance in phases I, II, and III, when the reactor was operated under a transmembrane pressure (TMP) of 80 to 250 mbar and an average flux of 5.9 L.m<sup>-2</sup>.h<sup>-1</sup>. A TMP of 250 mbar was reached in phase II, while operating the AnMBR at 37 gNa<sup>+</sup>.L<sup>-1</sup>. However, in phase IV, when sodium concentrations between 29 and 35 gNa<sup>+</sup>.L<sup>-1</sup> were

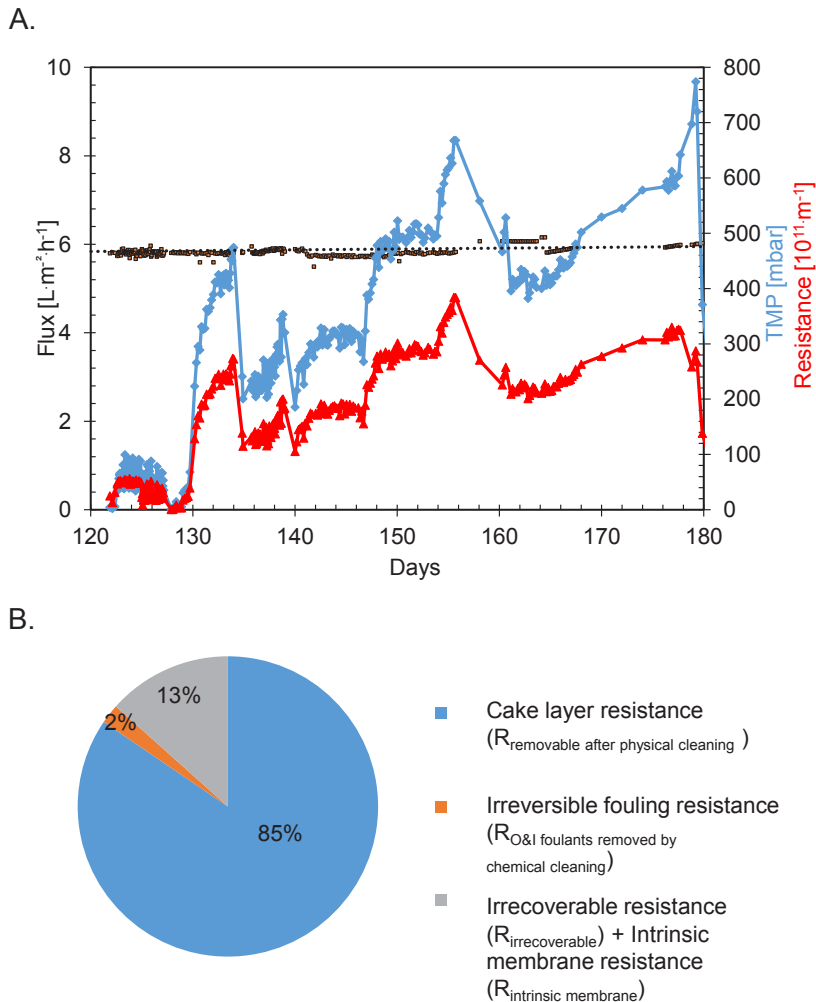


Figure 4.5 A. Membrane filtration performance during large salinity fluctuations in phase IV. B. Relative contribution of the different types of fouling to the total filtration resistance at the end of the experiment.

applied (days 120–137), the TMP rapidly increased to 452 mbar (day 133), concomitantly with a membrane filtration resistance increase to  $26.1 \times 10^{12} \text{ m}^{-1}$  (Figure 4.5. A). The deterioration of the membrane filtration performance was attributed to the decrease in biomass particle size from 65.6 to 13.2  $\mu\text{m}$  (Figure 4.4.). The TMP and membrane filtration resistance increased gradually, reaching peaks on days 138, 148, and 156. The change from 8 to 27.3  $\text{gNa}^+\cdot\text{L}^{-1}$  apparently led to an increase in the TMP and membrane resistance to filtration reaching 667 mbar and  $38 \times 10^{12} \text{ m}^{-1}$ , respectively on day 156. After day 163, TMP gradually increased further up to 774 mbar at the end of AnMBR operation, with a particle size reduction from 12.2 to 4.3  $\mu\text{m}$ . Zhou et al. (2019) indicated that

particles in the range 0.45-10  $\mu\text{m}$  are the main foulants in AnMBRs, and especially particles in the size-fraction from 5-10  $\mu\text{m}$  led to higher cake resistances. Hence, the low biomass particle size at the end of our experiment most likely contributed to cake layer compaction and, thereby, to a higher resistance to filtration.

Figure 4.5. B shows the relative contributions of the different types of fouling to the total resistance to filtration in AnMBR at the end of the experiment. Cake layer resistance compromised the largest portion of total filtration resistance, i.e., 85%, which confirmed that the primary fouling mechanism in the AnMBR was cake layer formation. Sequential chemical cleaning conducted using NaClO and citric acid resulted in an increase in the membrane permeability of only 2%. Complete restoration of the membrane permeability was not possible, and 13% of the permeability loss was attributed to both intrinsic and irrecoverable fouling. Both the role of osmotic pressure changes on filtration resistance (Chen et al. 2012) and gel layer formation mechanisms due to high SMP accumulation (Yurtsever et al. 2016), resulting from salinity fluctuations, should be investigated further.

#### 4.3.4 Microbial community diversity and dynamics

The microbial community dynamics of the reactor biomass was determined in the four phases of the AnMBR operation. Alpha diversity indices (Lemos et al. 2011) were used to compare the evenness and richness of the microbial population in the reactor (Figure 4.6.). The alpha diversity metrics from the Chao1 index slightly decreased at the end of phase I on day 40 from 611 to 586. An increasing trend to 649 and 666 in phases II and III, respectively, and up to 707 in phase IV on day 142 was observed. The observed OTUs showed a similar trend (Figure 4.6.A). The Chao1 (498) and observed OTUs (383) scores showed that at the end of AnMBR operation, the number of OTUs was lower than the initial and maximum values observed on days 0 and 142, respectively. This, indicated that larger salinity fluctuations had a considerable effect on the microbial population diversity. However, both scores were high compared with those noted in our previous study (Muñoz Sierra et al. 2018), where a maximum sodium concentration of 20  $\text{gNa}^+\cdot\text{L}^{-1}$  was applied. Both the Shannon's and Simpson's index scores, consider the richness and evenness of the microbial population. The highest values were observed in phase IV on day 163 when a sodium concentration of 16  $\text{gNa}^+\cdot\text{L}^{-1}$  was applied (Figure 4.6. B, C). The decrease in the bacterial diversity (Simpson's = 0.85; Shannon's = 4.33) at the end of the operation indicated a high stress level, which was attributed to the sodium concentration fluctuations exceeding 14  $\text{gNa}^+\cdot\text{L}^{-1}$  within four days.

A lower evenness of the microbial community at high stress levels could be caused by the dominance of a few halophilic/salt-tolerant microorganisms. Disturbances, e.g., large salinity fluctuations, could promote higher diversity but could also lead to variable microbial community function. However, we cannot assume that a more diverse community yields a community with better functionality (Santillan et al. 2019).

Under the disturbances caused by different frequencies and concentrations of sodium in the AnMBR in phase IV, a higher alpha diversity did not suggest a healthier system, but on the contrary, the COD conversion gradually increased, whereas there was a decrease in the microbial community diversity in the reactor.

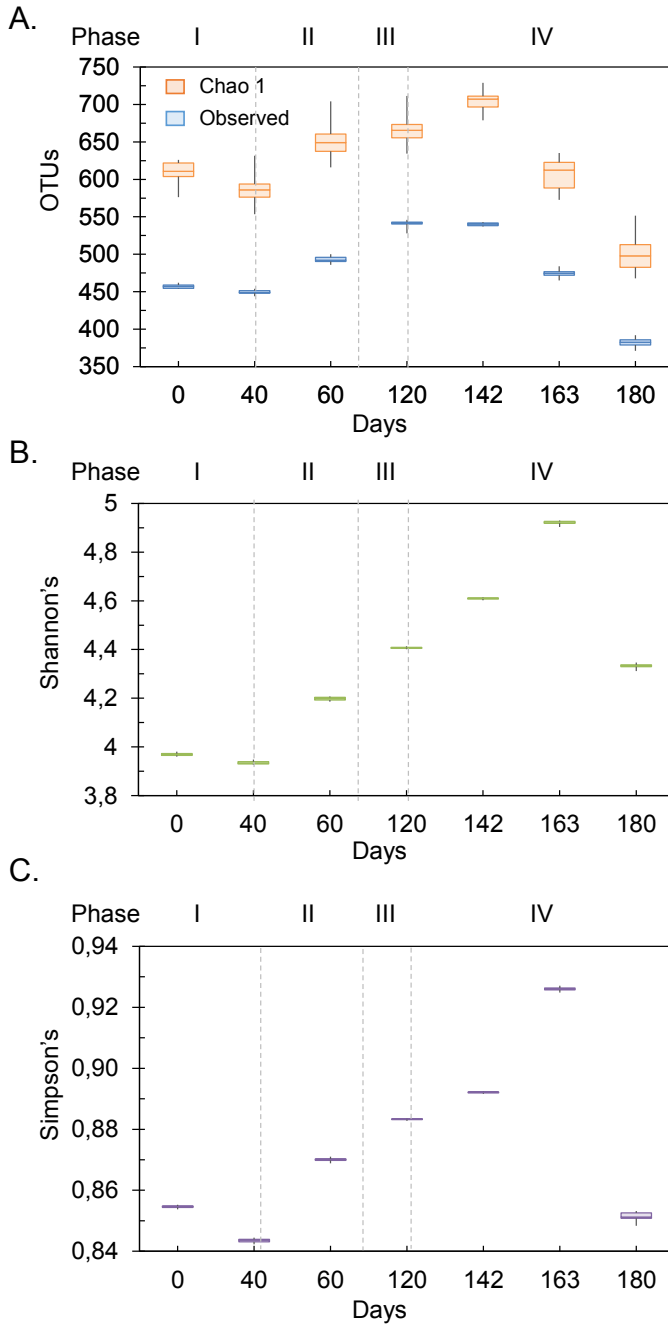


Figure 4.6 Alpha diversity plots for the microbial community in AnMBR at different phases of operation. A. Chao1 index and Observed OTU numbers B. Simpson's index C. Shannon's index

The most dominant bacteria in the AnMBR during the entire operation belonged to class Clostridia (25.2%), Synergistia (16.9%), and Bacteroidia (7.9%), while the dominant archaea were Methanomicrobia (27.9%) and Methanobacteria (11.8%) (Figure 4.7 A). Na et al. (2016) also reported that most detected bacteria in a UASB reactor treating phenols belonged to class Clostridia.

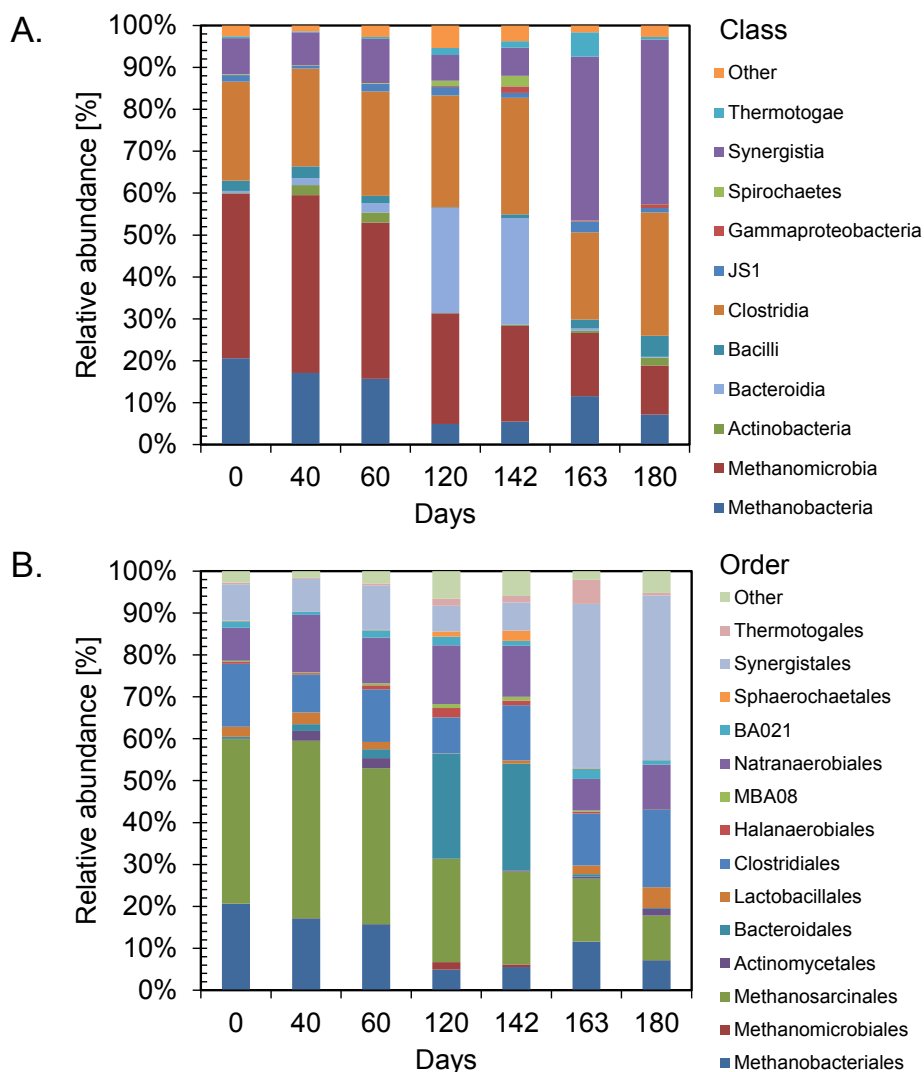


Figure 4.7 Microbial community dynamics in AnMBR at the A. Class, B. Order level.

Two major population changes were observed following salinity fluctuations in AnMBR. Bacteria belonging to Bacteroidia remarkably increased from 1.8% to 25.1% relative abundance during phase II to III, respectively, and thereafter decreased to 2.1% in phase IV, whereas Synergistia increased from 6.7% to 39.3% during phase IV. At the order level, Methanobacteriales and Methanosarcinales decreased from 20.6% and 39.3%, respectively, on day 0 to 15.7% and 37.2%, respectively, under  $33 \text{ gNa}^+\cdot\text{L}^{-1}$  in phase II (Figure 4.7 B). In phases III and IV, Methanobacteriales further decreased to 12.6% and 10.6%, and Methanosarcinales decreased to 10.8% and 7.1, respectively. The highest relative abundance of Methanomicrobiales on day 120 was 1.8%. Along with the large salinity fluctuations in phase IV, Clostridiales increased from 8.6% to 18.6%, while Natranaerobiales decreased from 14.0% to 10.6%. All Synergistales were from the genus *Thermovirgaceae*, whose abundance notably increased from 6.1% to 38.7% in phase IV (see Supplementary information Figure. S4.1). *Thermovirgaceae* members have a high tolerance to high salinity (Wang et al. 2017a) and a preference for PN/amino acid degradation corresponding to the highest soluble PN (SMP-PN) content observed in phase IV. Similarly, all Bacteroidales were from genus *ML635J-40*, which decreased from 25.0% at the beginning of phase IV to 0.2% at the end. The abundance of *Clostridium*, belonging to Clostridiales, varied between 2.3% and 8.9% during phase IV. The maximum relative abundance of *Pelotomaculum* at 0.9% was observed on day 142 under  $29 \text{ gNa}^+\cdot\text{L}^{-1}$  in phase IV. In our previous study (Muñoz Sierra et al. 2018), we related the improvement in the phenol conversion rate to *Pelotomaculum* relative abundance, which, in this study, corresponded with the highest phenol removal observed in phase IV.

#### 4.3.5 Implications and future research

The large salinity fluctuations affected the conversion capacity of the AnMBR but resulted in increasing resilience to more frequent and larger concentration fluctuations. Although sodium concentrations higher than  $26 \text{ gNa}^+\cdot\text{L}^{-1}$  and large fluctuations between 8 and  $35 \text{ gNa}^+\cdot\text{L}^{-1}$  transiently reduced the biomass activity, the reactor preserved a high conversion and recovery capacity. Notably, and to the best of our knowledge, no other anaerobic reactor system, including AnMBRs, have been subjected to sodium concentrations higher than three times the typical seawater sodium concentration ( $10.5 \text{ gNa}^+\cdot\text{L}^{-1}$ ), with continuous concentration fluctuations exceeding  $14 \text{ gNa}^+\cdot\text{L}^{-1}$ .

Overall, the exhibited robustness of the AnMBR to the large sodium concentration fluctuations would imply a forward step in pushing the limits of high-rate anaerobic bioconversion of industrial chemical wastewaters under highly variable saline conditions, as well as supporting research developments on anaerobic treatment, e.g., of concentrated streams resulting from applying forward osmosis or brines with high organic content. Further research should examine the impact of more frequent salinity fluctuations at a lower hydraulic retention time. Similarly, online control strategies to optimize membrane filtration performance and mitigate the reduction of the biomass particle size due to salinity fluctuations; e.g., applying flux enhancers, should be investigated to guarantee sustainable fluxes at full-scale applications.

## 4.4 Conclusions

The AnMBR revealed high robustness against large salinity fluctuations, maintaining phenol conversion rates between 6.9 and 25.5 mgPh-gVSS<sup>-1</sup>·d<sup>-1</sup>. Sodium concentrations exceeding 26 gNa<sup>+</sup>·L<sup>-1</sup> and large sodium fluctuations between 8 and 35 gNa<sup>+</sup>·L<sup>-1</sup> resulted in biomass stress and reduced the biomass methanogenic activity and cell membrane integrity. A reduction in median biomass particle size from 21 to 4.3 μm compromised membrane filtration performance and induced transmembrane pressures above 400 mbar. Cake layer resistance contributed to 85% of the total filtration resistance while only 2% irreversible fouling was determined. Microbial population richness and diversity were substantially reduced by salinity fluctuations larger than 14 gNa<sup>+</sup>·L<sup>-1</sup>. Furthermore, the dominant Bacteria belonging to the orders Clostridiales and Synergistales were enriched, whereas Archaea classified under the orders Methanosarcinales and Methanobacteriales decreased in relative abundance. Nonetheless, there was a gradual increase in COD conversion to 88%. This study revealed the potential of AnMBRs to endure extreme salinity fluctuations, advancing high-rate anaerobic treatment of industrial chemical wastewaters under these conditions.



## Supplementary Information

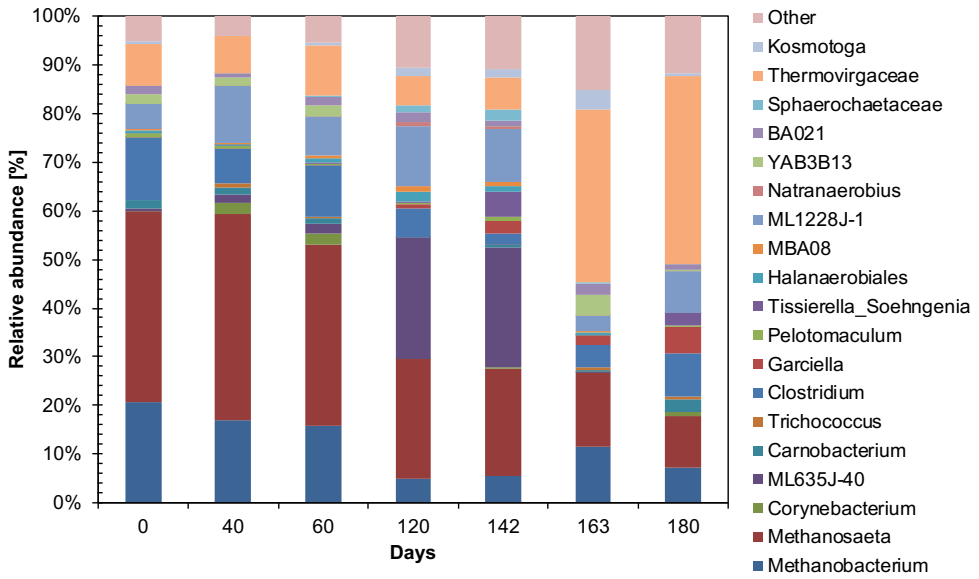


Figure S.4.1. Microbial community dynamics in AnMBR at the Genus level.

## References

- American Public Health, A., Eaton, A.D., American Water Works, A. and Water Environment, F. (2005) Standard methods for the examination of water and wastewater, APHA-AWWA-WEF, Washington, D.C.
- Caporaso, J.G., Kuczynski, J., Stombaugh, J., Bittinger, K., Bushman, F.D., Costello, E.K., Fierer, N., Pena, A.G., Goodrich, J.K., Gordon, J.I., Huttley, G.A., Kelley, S.T., Knights, D., Koenig, J.E., Ley, R.E., Lozupone, C.A., McDonald, D., Muegge, B.D., Pirrung, M., Reeder, J., Sevinsky, J.R., Turnbaugh, P.J., Walters, W.A., Widmann, J., Yatsunenko, T., Zaneveld, J. and Knight, R. (2010) QIIME allows analysis of high-throughput community sequencing data. *Nat Meth* 7(5), 335-336.
- Chen, J., Zhang, M., Wang, A., Lin, H., Hong, H. and Lu, X. (2012) Osmotic pressure effect on membrane fouling in a submerged anaerobic membrane bioreactor and its experimental verification. *Bioresource Technology* 125, 97-101.
- Chen, L., Hu, Q., Zhang, X., Chen, Z., Wang, Y. and Liu, S. (2019) Effects of salinity on the biological performance of anaerobic membrane bioreactor. *Journal of Environmental Management* 238, 263-273.
- De Vrieze, J., Coma, M., Debeuckelaere, M., Van der Meeren, P. and Rabaey, K. (2016) High salinity in molasses wastewaters shifts anaerobic digestion to carboxylate production. *Water Research* 98, 293-301.
- Dereli, R.K., Ersahin, M.E., Ozgun, H., Ozturk, I., Jeison, D., van der Zee, F. and van Lier, J.B. (2012) Potentials of anaerobic membrane bioreactors to overcome treatment limitations induced by industrial wastewaters. *Bioresource Technology* 122, 160-170.
- Dubois, M., Gilles, K.A., Hamilton, J.K., Rebers, P.A. and Smith, F. (1956) Colorimetric method for determination of sugars and related substances. *Analytical Chemistry* 28(3), 350-356.
- Edgar, R. (2016) UCHIME2: improved chimera prediction for amplicon sequencing. *bioRxiv*.
- Edgar, R.C. (2010) Search and clustering orders of magnitude faster than BLAST. *Bioinformatics* 26(19), 2460-2461.
- Frolund, B., Palmgren, R., Keiding, K. and Nielsen, P.H. (1996) Extraction of extracellular polymers from activated sludge using a cation exchange resin. *Water Research* 30(8), 1749-1758.
- Gagliano, M.C., Ismail, S.B., Stams, A.J.M., Plugge, C.M., Temmink, H. and Van Lier, J.B. (2017) Biofilm formation and granule properties in anaerobic digestion at high salinity. *Water Research* 121, 61-71.
- Gagliano, M.C., Neu, T.R., Kuhlicke, U., Sudmalis, D., Temmink, H. and Plugge, C.M. (2018) EPS Glycoconjugate Profiles Shift as Adaptive Response in Anaerobic Microbial Granulation at High Salinity. *Frontiers in Microbiology* 9(1423).
- Ganidi, N., Tyrrel, S. and Cartmell, E. (2009) Anaerobic digestion foaming causes – A review. *Bioresource Technology* 100(23), 5546-5554.
- Ismail, S.B., de La Parra, C.J., Temmink, H. and van Lier, J.B. (2010) Extracellular polymeric substances (EPS) in upflow anaerobic sludge blanket (UASB) reactors operated under high salinity conditions. *Water Research* 44(6), 1909-1917.

- Jamal Khan, S., Visvanathan, C., Jegatheesan, V. and BenAim, R. (2008) Influence of Mechanical Mixing on Sludge Characteristics and Membrane Fouling in MBRs. *Separation Science and Technology* 1826-1838.
- John, M., Trzcinski, A.P., Zhou, Y. and Ng, W.J. (2017) Microbial stress mediated intercellular nanotube-mediated anaerobic microbial consortium digesting cellulose. *Scientific reports* 7(1), 18006-18006.
- Kong, Z., Li, L., Xue, Y., Yang, M. and Li, Y.-Y. (2019) Challenges and prospects for the anaerobic treatment of chemical-industrial organic wastewater: A review. *Journal of Cleaner Production* 231, 913-927.
- Lefebvre, O., Habouzit, F., Bru, V., Delgenes, J.P., Godon, J.J. and Moletta, R. (2004) Treatment of Hypersaline Industrial Wastewater by a Microbial Consortium in a Sequencing Batch Reactor. *Environmental Technology* 25(5), 543-553.
- Lemos, L.N., Fulthorpe, R.R., Triplett, E.W. and Roesch, L.F.W. (2011) Rethinking microbial diversity in the high throughput sequencing era. *Journal of Microbiological Methods* 86(1), 42-51.
- Liu, Y. and Fang, H.H.P. (2003) Influences of Extracellular Polymeric Substances (EPS) on Flocculation, Settling, and Dewatering of Activated Sludge. *Critical Reviews in Environmental Science and Technology* 33(3), 237-273.
- Lu, Q., Yu, Z., Yu, S., Liang, Z., Li, H., Sun, L. and Wang, S. (2019) Organic matter rather than salinity is the predominant feature changes performance and microbiome in methanogenic sludge digesters. *Journal of Hazardous Materials* 377, 349-356.
- Luján-Facundo, M.J., Fernández-Navarro, J., Alonso-Molina, J.L., Amorós-Muñoz, I., Moreno, Y., Roca, J.A. and Pastor-Alcañiz, L. (2018) The role of salinity on the changes of the biomass characteristics and on the performance of an OMBR treating tannery wastewater. *Water Research* 142, 129-137.
- McDonald, D., Price, M.N., Goodrich, J., Nawrocki, E.P., Desantis, T.Z., Probst, A., Andersen, G.L., Hugenholtz, P. (2012) An improved Greengenes taxonomy with explicit ranks for ecological and evolutionary analyses of bacteria and archaea. *ISME Journal* 6(3), 610-618.
- Muñoz Sierra, J.D., Lafita, C., Gabaldón, C., Spanjers, H. and van Lier, J.B. (2017) Trace element supplementation in anaerobic membrane bioreactors treating highly saline phenolic wastewater. *Bioresource Technology* 234, 106-114.
- Muñoz Sierra, J.D., Oosterkamp, M.J., Wang, W., Spanjers, H. and van Lier, J.B. (2018) Impact of salinity exposure in anaerobic membrane bioreactors treating phenolic wastewater: Performance and microbial community. *Water Research* 141, 172-184.
- Na, J.-G., Lee, M.-K., Yun, Y.-M., Moon, C., Kim, M.-S. and Kim, D.-H. (2016) Microbial community structure of anaerobic granules in phenol-degrading UASB by next generation sequencing. *Biochemical Engineering Journal* 112, 241-248.
- Prest, E.I., Hammes, F., Köttsch, S., van Loosdrecht, M.C.M. and Vrouwenvelder, J.S. (2013) Microbiological changes in drinking water systems using a fast and reproducible flow cytometric method. *Water Research* 47(19), 7131-7142.
- Rincón-Llorente, B., De la Lama-Calvente, D., Fernández-Rodríguez, M.J. and Borja-Padilla, R. (2019) Olive Wastewater: Problem, Treatments and Future Strategy. A Review. *Frontiers in Microbiology*

- Rosenberg, M., Gutnick, D. and Rosenberg, E. (1980) Adherence of bacteria to hydrocarbons: A simple method for measuring cell-surface hydrophobicity. *FEMS Microbiology Letters* 9(1), 29-33.
- Santillan, E., Seshan, H., Constancias, F., Drautz-Moses, D.I. and Wuertz, S. (2019) Frequency of disturbance alters diversity, function, and underlying assembly mechanisms of complex bacterial communities. *npj Biofilms and Microbiomes* 5(1), 8.
- Song, X., McDonald, J., Price, W.E., Khan, S.J., Hai, F.I., Ngo, H.H., Guo, W. and Nghiem, L.D. (2016) Effects of salinity build-up on the performance of an anaerobic membrane bioreactor regarding basic water quality parameters and removal of trace organic contaminants. *Bioresource Technology* 216, 399-405.
- Spanjers, H. and Vanrolleghem, P. (2016) In: van Loosdrecht et al. *Experimental methods in wastewater treatment*  
Online, W.I. (ed), p. 360, Water Intell. Online.
- Sudmalis, D., Gagliano, M.C., Pei, R., Grolle, K., Plugge, C.M., Rijnaarts, H.H.M., Zeeman, G. and Temmink, H. (2018a) Fast anaerobic sludge granulation at elevated salinity. *Water Research* 128, 293-303.
- Sudmalis, D., Millah, S.K., Gagliano, M.C., Butré, C.I., Plugge, C.M., Rijnaarts, H.H.M., Zeeman, G. and Temmink, H. (2018b) The potential of osmolytes and their precursors to alleviate osmotic stress of anaerobic granular sludge. *Water Research* 147, 142-151.
- Tan, X., Acquah, I., Liu, H., Li, W. and Tan, S. (2019) A critical review on saline wastewater treatment by membrane bioreactor (MBR) from a microbial perspective. *Chemosphere* 220, 1150-1162.
- Van den Broeck, R., Krzeminski, P., Van Dierdonck, J., Gins, G., Lousada-Ferreira, M., Van Impe, J.F.M., van der Graaf, J.H.J.M., Smets, I.Y. and van Lier, J.B. (2011) Activated sludge characteristics affecting sludge filterability in municipal and industrial MBRs: Unraveling correlations using multi-component regression analysis. *Journal of Membrane Science* 378(1), 330-338.
- Vyrides, I. (2015) Anaerobic Treatment of Organic Saline Waste/Wastewater: Overcome Salinity Inhibition by Addition of Compatible Solutes. In: Sukla L., Pradhan N., Panda S., Mishra B. (eds) *Environmental Microbial Biotechnology*. Soil Biology, Springer, Cham.
- Vyrides, I., Santos, H., Mingote, A., Ray, M.J. and Stuckey, D.C. (2010) Are Compatible Solutes Compatible with Biological Treatment of Saline Wastewater? Batch and Continuous Studies Using Submerged Anaerobic Membrane Bioreactors (SAMBRs). *Environmental Science & Technology* 44(19), 7437-7442.
- Vyrides, I. and Stuckey, D.C. (2009) Effect of fluctuations in salinity on anaerobic biomass and production of soluble microbial products (SMPs). *Biodegradation* 20(2), 165-175.
- Wang, S., Hou, X. and Su, H. (2017a) Exploration of the relationship between biogas production and microbial community under high salinity conditions. *Scientific Reports* 7(1), 1149.
- Wang, W., Wu, B., Pan, S., Yang, K., Hu, Z. and Yuan, S. (2017b) Performance robustness of the UASB reactors treating saline phenolic wastewater and analysis of microbial community structure. *Journal of Hazardous Materials* 331, 21-27.
- Wu, Y., Wang, X., Tay, M.Q.X., Oh, S., Yang, L., Tang, C. and Cao, B. (2017) Metagenomic insights into the influence of salinity and cytostatic drugs on the composition and functional genes of microbial community in forward osmosis anaerobic membrane bioreactors. *Chemical Engineering Journal* 326, 462-469.

- Yogalakshmi, K.N. and Joseph, K. (2010) Effect of transient sodium chloride shock loads on the performance of submerged membrane bioreactor. *Bioresource Technology* 101(18), 7054-7061.
- Yurtsever, A., Calimlioglu, B., Görür, M., Çınar, Ö. and Sahinkaya, E. (2016) Effect of NaCl concentration on the performance of sequential anaerobic and aerobic membrane bioreactors treating textile wastewater. *Chemical Engineering Journal* 287, 456-465.
- Zhou, Z., Tao, Y., Zhang, S., Xiao, Y., Meng, F. and Stuckey, D.C. (2019) Size-dependent microbial diversity of sub-visible particles in a submerged anaerobic membrane bioreactor (SAnMBR): Implications for membrane fouling. *Water Research* 159, 20-29.



# 5

5

## Comparative performance of UASB and AnMBR treating phenolic wastewater at high salinity

---

This chapter has been published as: “Muñoz Sierra, J.D., Oosterkamp, M.J., Wang W., Spanjers, H., and van Lier, J.B. (2019) Comparative performance of upflow anaerobic sludge blanket reactor and anaerobic membrane bioreactor treating phenolic wastewater: Overcoming high salinity. *Chemical Engineering Journal*, 366, pp. 480-490.”

<https://doi.org/10.1016/j.cej.2019.02.097>

## Abstract

Anaerobic membrane bioreactors (AnMBRs) offer an attractive option for treating industrial wastewaters under extreme conditions that might hamper granulation, biomass retention and reduce biological activity. This study assesses the long-term performance of an upflow anaerobic sludge blanket reactor (UASB) and an AnMBR treating highly saline phenolic wastewater. Analysis of bioreactor conversion, biomass characteristics and microbial community dynamics under increasing sodium and phenol concentrations is presented. The results demonstrated that compared to the UASB, the AnMBR process exhibited higher stability, likely due to its enhanced biomass retention. The AnMBR retained specialized microorganisms under increasing influent concentrations of phenol up to  $5 \text{ gPh}\cdot\text{L}^{-1}$  and salinity up to  $26 \text{ gNa}^+\cdot\text{L}^{-1}$ . In contrast, when the UASB reached this high influent phenol and high sodium concentration, deflocculation of biomass, apparently due to calcium leaching, was observed leading to a severe conversion capacity loss. Microbial community dynamics showed higher species evenness in the AnMBR compared to the UASB, leading to a higher methanogenic ability to respond to disturbances such as high phenol and sodium concentration increases. These findings highlighted the promising features of AnMBR technology, in widening the application potentials of high-rate anaerobic wastewater treatment and overcoming specific challenges in the treatment of chemical wastewater streams under extreme environmental conditions such as high salinity.



## 5.1 Introduction

The current challenges of industrial wastewater treatment include degradation of a large variety of contaminants such as phenols and other aromatic compounds under high salt concentrations typical of olive oil mills, oil refineries, textile, coal gasification, and petrochemical industries (Rosenkranz et al. 2013, Yurtsever et al. 2016). Research on both aerobic (Jiang et al. 2016, Su et al. 2019) and anaerobic (Muñoz Sierra et al. 2018b, Wang et al. 2017b) treatment technologies are dealing with these types of wastewaters with emphasis on the limitations associated with high salinity or phenol toxicity. From the two alternatives, high-rate anaerobic treatment receives major interest owing to its positive energy footprint and other advantages associated with it. Sludge bed based technologies such as the upflow anaerobic sludge blanket (UASB) reactor, are thus far considered the most cost-effective at industrial scale for chemical wastewaters (van Lier et al. 2015). In order to apply high organic loading rates and improved hydraulic mixing e.g. by effluent recycling, a proper sludge granulation process is of eminent importance in sludge bed reactors treating these wastewaters. Moreover, as a result of mass transfer limitation phenomena, the granule structure will protect functional microorganisms at the core of the granule from inhibitory and toxic pollutants (Li et al. 2014). Sludge granulation is difficult to accomplish at high salinity because salinity reduces microbial growth and induces the disintegration of flocs and granules leading to a prominent biomass wash-out and induces the disintegration of flocs and granules leading to a prominent biomass wash-out (Jeison et al. 2008, Yang et al. 2013). However, thanks to the presence of an absolute barrier, the achievable treatment efficiencies in anaerobic membrane bioreactors (AnMBRs) are independent of sludge settling properties or sludge granulation. The solids retention time (SRT) in AnMBRs is fully governed by the sludge discharge, giving ample possibilities for enrichment with specialized microbial consortia (Dreli et al. 2012). AnMBRs are generally equipped with Ultrafiltration (UF) membranes, which additionally offer high-quality effluents free of solids, facilitating downstream water recovery (Stuckey 2012). Therefore, regardless their increased costs, AnMBRs may offer an attractive option for treating industrial wastewaters under extreme environmental conditions that hamper granulation, effective biomass retention and reduced biological activity (van Lier et al. 2015), such as high salinity and the presence of toxic compounds (Muñoz Sierra et al. 2017).

To the best of our knowledge, only two studies have attempted to treat highly saline phenolic wastewater using high-rate anaerobic technologies (Muñoz Sierra et al. 2018a, Wang et al. 2017a). Wang et al. (Wang et al. 2017a) used UASB reactors treating wastewater containing 10 and 20 gNa<sup>+</sup>L<sup>-1</sup> in a range of total phenol concentrations (TPh) between 0.1 and 2.0 gTPhL<sup>-1</sup>. At 10 gNa<sup>+</sup>L<sup>-1</sup> and 1.0 gTPhL<sup>-1</sup> the phenol conversion and specific methanogenic activity (SMA) decreased about 57% and 37%, respectively, compared to a non-saline UASB control reactor, whereas either at 20 gNa<sup>+</sup>L<sup>-1</sup> or 2.0 gTPhL<sup>-1</sup> the SMA was reduced by about 75% and 79%, respectively, and a severe inhibition of phenol degradation was observed. On the other hand, Muñoz Sierra et al. (Muñoz Sierra et al. 2018a) evaluated the impact of long-term salinity increase to 20 gNa<sup>+</sup>L<sup>-1</sup> on the bioconversion of phenol in an AnMBR treating an influent with concentrations up to 0.5 gPhL<sup>-1</sup>. The treatment performance of the researched AnMBR remained stable

irrespective the salinity changes, resulting in an endured microbial community and 56% higher phenol conversion rates when salinity increased from  $16 \text{ gNa}^+\cdot\text{L}^{-1}$  to  $20 \text{ gNa}^+\cdot\text{L}^{-1}$ .

In order to determine which type of reactor system, UASB or AnMBR, would be more suitable for treating chemical wastewaters under extreme conditions, a comparative study was performed in which both reactor systems were exposed to the same extreme sodium and phenol loadings conditions. It is hypothesized that by increasing both the sodium and phenol influent concentrations the capacity limits of either system will be reached. A UASB reactor is fully dependent on active well-settling or granular biomass, whereas the suspended biomass in the AnMBR system might become more susceptible for increasing phenol concentrations in the bulk of the reactor broth. However, since all biomass is retained in an AnMBR, the latter could be overcome by in-situ bioaugmentation of the proper phenol degrading consortia. A phenomenon that is likely less apparent in a UASB where the biomass is prone to wash-out. In the present comparative study, the treatment performance of both a UASB and a completely mixed AnMBR under increasing sodium and phenol influent concentrations is assessed. In addition, a comprehensive analysis of the properties of the two types of biomass coming from both reactors, i.e., granular and suspended, was performed, whereas the microbial community dynamics and diversity were analyzed.

## 5.2 Material and Methods

### 5.2.1 Reactors configuration and operation

The experiments were performed using laboratory scale AnMBR and UASB reactors, both with an effective volume of 7 L. A schematic diagram of the reactor configurations is depicted in Figure 5.1. The completely mixed AnMBR was equipped with a side-stream ultrafiltration (UF) membrane module. A tubular PVDF membrane (Pentair X-Flow, The Netherlands) with 5.2 mm inner diameter and 0.64 m length was used. Transmembrane pressure (TMP) was monitored using three pressure sensors (AE Sensors ATM, The Netherlands). The AnMBR was equipped with feed, recycle and effluent pumps (Watson-Marlow 120U/DV, 220Du) and the UASB with feed and effluent recirculation pump (Watson-Marlow 120U/DV). The AnMBR was completely mixed due to a turnover of 170 with a cross-flow velocity of  $0.65 \text{ ms}^{-1}$ . A flux of about  $4 \text{ L}\cdot\text{m}^{-2}\cdot\text{h}^{-1}$  was maintained. The UASB reactor was operated with an up-flow velocity of  $0.6 \text{ m}\cdot\text{h}^{-1}$ . The biogas was collected by means of a three-phase separator installed at the top of the UASB reactor. The reactors were equipped with pH and temperature sensors (Endress & Hauser, Memosens), and biogas flow-rate meters (Ritter, Milligas Counter MGC-1 PMMA, Germany). The temperature of the jacketed reactors was controlled by thermostatic water baths (Tamson Instruments, The Netherlands). The setups were controlled by a computer running LabView software (version 15.0.1f1, National Instruments, USA).

The sodium concentration in the reactors was increased from  $12 \text{ gNa}^+\cdot\text{L}^{-1}$  to  $16 \text{ gNa}^+\cdot\text{L}^{-1}$  for a period of 155 days before the comparison study started, with a further increase to  $26 \text{ gNa}^+\cdot\text{L}^{-1}$  until

day 388 in four phases. Influent phenol concentrations from 0.2 gPhL<sup>-1</sup> up to 5 gPhL<sup>-1</sup> were applied. During the operation of the reactors, the biomass concentration in the UASB decreased mainly due to wash-out from 19.3 gVSS·L<sup>-1</sup> at 8 gNa<sup>+</sup>·L<sup>-1</sup> to a stable concentration of 5.9 gVSS·L<sup>-1</sup> at 16 gNa<sup>+</sup>·L<sup>-1</sup> on day 155 (initial day of this study). In the case of the AnMBR, at day 155 and the same salinity, the biomass concentration was about 15.2 gVSS·L<sup>-1</sup>. The temperature and pH were maintained at 35±0.8 °C and 8.0±2.0 in both reactors. HRT was kept about 7 d in both reactors. The main operational conditions along the experiment are summarized in Table 5.1.

Table 5.1 Reactors operational conditions.

Day	Sodium [gNa <sup>+</sup> · L <sup>-1</sup> ]	OLR [gCOD· L <sup>-1</sup> ·d <sup>-1</sup> ]	PhLR [gPh· L <sup>-1</sup> ·d <sup>-1</sup> ]	Biomass UASB [gVSS·L <sup>-1</sup> ]	Biomass AnMBR [gVSS·L <sup>-1</sup> ]	Phase (Period)
155	16	5.50	0.11	5.9	15.2	I (Day 155-261)
187	16	5.50	0.11	6.1	11.2	I (Day 155-261)
280	18	5.70	0.33	8.6	12.7	II (Day 262-332)
322	18	7.64	1.11	10.9	12.7	II (Day 262-332)
357	24	6.57	0.67	6.4	13.5	III (Day 333-371)
379	26	6.57	0.67	7.9	16.7	IV (Day 372-388)

## 5.2.2 Permeate characterization

### 5.2.2.1 Phenol and COD analysis

Phenol concentrations were measured using high-pressure liquid chromatography HPLC LC-20AT (Shimadzu, Japan) equipped with a 4.6 mm reversed phase C18 column (Phenomenex, The Netherlands) and a UV detector at a wavelength of 280 nm. The mobile phase used was 25% (v/v) acetonitrile at a flow rate of 0.95 mL·min<sup>-1</sup>. The column oven was set at 30 °C. Quick phenol measurements were done by Merck – Spectroquant® Phenol cell kits using a spectrophotometer NOVA60 (Merck, Germany). Hach Lange kits were used to measure chemical oxygen demand (COD). Corresponding dilutions were made to avoid measurements interference by high salinity. The COD was measured using a VIS - spectrophotometer (DR3900, Hach Lange, Germany).

### 5.2.3 Inoculum source and synthetic wastewater composition

The two reactors were inoculated with mesophilic anaerobic biomass obtained from a full-scale UASB reactor (Shell, Moerdijk, The Netherlands). The synthetic wastewater consisted of sodium acetate (C<sub>2</sub>H<sub>3</sub>NaO<sub>2</sub>), and phenol (C<sub>6</sub>H<sub>6</sub>O) with varying concentrations according to the applied phenol loading rates (PhLR). The amount of sodium chloride (NaCl), solution of K<sub>2</sub>HPO<sub>4</sub> (34.85 g·L<sup>-1</sup>) and solution of NaH<sub>2</sub>PO<sub>4</sub> (24 g·L<sup>-1</sup>) varied according to the sodium concentration applied in the reactor in each phase, maintaining a K<sup>+</sup>:Na<sup>+</sup> ratio of 0.05 (Muñoz Sierra et al. 2018a). Yeast extract (2.0 g·L<sup>-1</sup>), macronutrients (9 mL·L<sup>-1</sup>), and micronutrients (4.5 mL·L<sup>-1</sup>) solutions were added (Table 5.2). The chemical reagents were of analytical grade.



solutions (Sigma-Aldrich) in the range between 0.1 and 50 mg.L<sup>-1</sup>. The final concentrations were calculated by using the MagIC Net software.

Biomass samples of 1 gTSS were destructed with Agua regia (mixture of 2.5 mL 65% HNO<sub>3</sub> and 7.5 mL 37 % HCl) in a microwave reaction system (MultiwavePRO, Anton Paar GmbH, Austria) following the procedure described by Ismail et al. (Ismail et al. 2010). After the digestion, liquid samples were analyzed by Inductively Coupled Plasma Optical Emission Spectroscopy (Optima 5300DV, Perkin Elmer Instruments, USA) to determine calcium concentrations.

## **5.2.4 Biomass characteristics**

### **5.2.4.1 Soluble microbial products (SMP) and extracellular polymeric substances (EPS)**

SMP and EPS were characterized based on proteins and polysaccharides. EPS extraction was carried out by cation exchange resin method. The functional groups of EPS extracted at different phases were identified with a Fourier Transform Infrared (FT-IR) Spectrometer (Spectrum 100 Series Perkin-Elmer, UK) as explained by Muñoz Sierra et al. (2018b). EPS was normalized against the biomass VSS concentration in the reactor.

### **5.2.4.2 Particle size distribution (PSD)**

PSD measurements were carried out by using a DIPA-2000 EyeTech™ particle analyzer (Donner Technologies, Or Akiva, Israel) with an A100 and B100 laser lens (measuring range 0.1-300 μm and 1-2000 μm, respectively) and a liquid flow cell DCM-104A (10x10 mm). Furthermore, deflocculation was further studied using a digital microscope (Keyence VHX-5000) with VH-Z20UR lens set and 100x magnification.

### **5.2.4.3 Specific methanogenic activity (SMA) tests**

SMA tests were performed in triplicate using an automated methane potential test system (AMPTS, Bioprocess Control, Sweden). All the SMA tests were carried out at 35 °C following the method described by Loosdrecht et al. (2016).

## **5.2.5 Microbial community and statistical analysis**

### **5.2.5.1 DNA extraction and sequencing**

DNA extraction was performed from both reactors' biomass samples by using the DNeasy UltraClean Microbial kit (Qiagen, Hilden, Germany). Qubit3.0 DNA detection (Qubit® dsDNA HS Assay Kit, Life Technologies, U.S.) and agarose gel electrophoresis were used to check the quantity and quality of the DNA extracted. 16S rRNA gene amplicon sequencing was carried out

by the MiSeq Illumina platform and using the primers 341F (5'-CCTACGGGNGGCWGCAG-3') 785R (5'-GACTACHVGGGTATCTAATCC-3') for bacteria/archaea in the V3-V4 region (BaseClear, Leiden, the Netherlands). The sequences were analyzed using the QIIME pipeline (version 1.9.0). Demultiplexing and quality filtering were performed with Q=20, r=3, and p=0.75

parameters. Chimeric sequences were removed with the UCHIME2 (version 9.0) (Edgar 2016). Sequences were clustered into operational taxonomic units (OTUs) with a 97% similarity as the cutoff, with UCLUST algorithm (Edgar 2010). Singletons were removed and OTUs with an occurrence less than three times in at least one sample were excluded. Taxonomic assignment was performed using the Silva database (SILVA-128) with UCLUST. For beta diversity, separate non-metric distance scaling (NMDS) analysis of the microbial community was made based on the unweighted Unifrac distance measure. Alpha diversity was analyzed following the guidelines of Hill (1973). Beta diversity plots were generated with the phyloseq and ggplot2 packages in the R environment. The sequences reported in this paper have been deposited in the NCBI SRA under the accession number SRP149410.

### 5.2.5.2 Fluorescent in situ hybridization (FISH)

Biomass samples taken from the AnMBR and UASB reactors were treated as cell suspensions and fixed on paraformaldehyde according to a procedure described previously and followed by DAPI staining (Winkler et al. 2011). Archaea were Cy3-stained using the Arc 915 Cy3 FISH oligonucleotide probe. Hybridized biomass samples were examined with a Zeiss Axioplan-2 epifluorescence microscope and Axiovision (release 4.8.2) software (Zeiss, Germany).

### 5.2.5.3 Statistical analysis

Statistical differences between the two reactors and among the reactor samples under different conditions were evaluated using ANOSIM and ADONIS analysis in the QIIME pipeline. Two comparing data sets were considered statistically different when a *p-value*  $\leq 0.05$  was determined. A t-test was done to determine statistical differences between the Alpha diversity measures.

## 5.3 Results and Discussion

### 5.3.1 UASB and AnMBR reactors performance and conversion rates

UASB and AnMBR reactors treating phenolic wastewater were subjected to increasing sodium concentrations. Phenol removal efficiencies fluctuated between 84.4%–99.8% in the UASB and a more stable removal of 98.1%–99.9% was observed in the AnMBR at  $16 \text{ gNa}^+\cdot\text{L}^{-1}$  and influent phenol concentration of  $0.5 \text{ gPh}\cdot\text{L}^{-1}$  (Phase I, Figure 5.2. A). The corresponding phenol loading rate (PhLR) was  $0.11 \text{ gPh}\cdot\text{L}^{-1}\cdot\text{d}^{-1}$  (Table 5.1). Thereby, the AnMBR showed a lower total COD effluent concentration than the UASB reactor when operated at  $16 \text{ gNa}^+\cdot\text{L}^{-1}$  (Figure 5.2. B) and an OLR of  $5.50 \text{ gCOD}\cdot\text{L}^{-1}\cdot\text{d}^{-1}$ . However, the UASB reactor showed gradual improvement within days 155 and 228 showing lower effluent phenol concentrations, dropping from  $68 \text{ mgPh}\cdot\text{L}^{-1}$  to  $1.2 \text{ mgPh}\cdot\text{L}^{-1}$  respectively, indicating biomass adaptation to this sodium concentration (Figure 5.2. A).

Both AnMBR and UASB reactors coped well with an increase in influent phenol concentrations from 0.5 to 1.0 and  $1.2 \text{ gPh}\cdot\text{L}^{-1}$  (Phase II, Figure 5.2. C). The AnMBR showed higher stability most likely due to its higher biomass concentration at a PhLR of  $0.27 \text{ gPh}\cdot\text{L}^{-1}\cdot\text{d}^{-1}$  on day 260. At 18

$\text{gNa}^+\cdot\text{L}^{-1}$  (Phase II) and  $1.5 \text{ gPhL}^{-1}$ , both reactors exhibited a very stable phenol degradation performance (Figure 5.2. C), which is attributed to the long-term adaptation process of the microbial community. The latter suggested that the reactors could manage a higher phenol loading rate and thereby their phenol bioconversion could be maximized. The UASB phenol degradation rate was about  $38.6 \text{ mgPh}\cdot\text{gVSS}^{-1}\cdot\text{d}^{-1}$  and for the AnMBR this was about  $26.1 \text{ mgPh}\cdot\text{gVSS}^{-1}\cdot\text{d}^{-1}$  under the above mentioned conditions. The AnMBR effluent reached lower phenol concentrations of about  $0.88 \text{ mgPh}\cdot\text{L}^{-1}$  compared to the UASB ( $13.5 \text{ mgPh}\cdot\text{L}^{-1}$ ). At phenol influent concentration of  $3.0 \text{ gPh}\cdot\text{L}^{-1}$  and a PhLR of  $0.67 \text{ gPh}\cdot\text{L}^{-1}\cdot\text{d}^{-1}$  the removal efficiency of the UASB reactor decreased to 83.4% with a phenol conversion rate of  $76 \text{ mgPh}\cdot\text{gVSS}^{-1}\cdot\text{d}^{-1}$  (Phase II, Figure 5.2. C). This is in agreement with Wang et al. (Wang et al. 2017a) who found that a UASB reactor performs well under an influent concentration of total phenols lower than  $1.0 \text{ g}\cdot\text{L}^{-1}$  and  $10 \text{ gNa}^+\cdot\text{L}^{-1}$ , but shows severe removal limitations (about 40% efficiency) when  $2.0 \text{ gPh}\cdot\text{L}^{-1}$  and  $20 \text{ gNa}^+\cdot\text{L}^{-1}$  are applied. The AnMBR phenol degradation rate was lower, i.e.  $53 \text{ mgPh}\cdot\text{gVSS}^{-1}\cdot\text{d}^{-1}$  but with a 16% higher removal efficiency than the UASB. When the influent phenol concentration was increased to  $5 \text{ gPh}\cdot\text{L}^{-1}$ , both reactors had a similar reduction in COD removal efficiency to about 70% (Phase II, Figure 5.2. D) at an OLR of  $7.64 \text{ gCOD}\cdot\text{L}^{-1}\cdot\text{d}^{-1}$ . However, phenol concentration increased to  $600 \text{ mgPh}\cdot\text{L}^{-1}$  in the UASB effluent, whereas the AnMBR kept a low phenol concentration of  $25 \text{ mgPh}\cdot\text{L}^{-1}$  (Figure 5.2. C). The phenol conversion rates were  $87.4 \text{ mgPh}\cdot\text{gVSS}^{-1}\cdot\text{d}^{-1}$  and  $97.7 \text{ mgPh}\cdot\text{gVSS}^{-1}\cdot\text{d}^{-1}$  for the AnMBR and the UASB reactor, respectively (Table 5.3).

Table 5.3 SMA phenol conversion and COD removal rates at different salinity levels

Phase	Salinity [ $\text{gNa}^+\cdot\text{L}^{-1}$ ]	Day	SMA		Phenol conversion rate		COD removal rate	
			[ $\text{gCOD}\cdot\text{CH}_4$ $\cdot\text{gVSS}^{-1}\cdot\text{d}^{-1}$ ]		[ $\text{mgPh}\cdot$ $\text{gVSS}^{-1}\cdot\text{d}^{-1}$ ]		[ $\text{gCOD}\cdot$ $\text{gVSS}^{-1}\cdot\text{d}^{-1}$ ]	
			UASB	AnMBR	UASB	AnMBR*	UASB	AnMBR*
I	16	155	$0.50\pm 0.05$	$0.42\pm 0.04$	15.7	7.4	1.22	0.50
	16	187	$0.76\pm 0.06$	$0.87\pm 0.01$	17.6	9.9	0.89	0.49
II	18	280	$0.44\pm 0.10$	$0.65\pm 0.02$	38.6	26.1	0.65	0.44
	18	322	$0.39\pm 0.08$	$0.64\pm 0.01$	97.7	87.4	0.60	0.49
III	24	357	$0.29\pm\text{N.D}^{**}$	$0.31\pm 0.04$	103.2	49.4	0.98	0.43
IV	26	379	$0.16\pm\text{N.D}^{**}$	$0.25\pm 0.05$	32.9	40.1	0.40	0.39

\*AnMBR biomass concentration was higher than the UASB, indicating that the reactor was under loaded.

\*\*Replicates were not available for these samples.

The observed phenol degradation rates were higher than reported in previous studies using AnMBR or UASB under high phenol and high sodium concentrations (Muñoz Sierra et al. 2018a, Wang et al. 2017a). Under an increasing salinity from  $18 \text{ gNa}^+\cdot\text{L}^{-1}$  to  $24 \text{ gNa}^+\cdot\text{L}^{-1}$  (Phase III) and a reduced influent phenol concentration of  $3.0 \text{ gPh}\cdot\text{L}^{-1}$  (PhLR of  $0.67 \text{ gPh}\cdot\text{L}^{-1}\cdot\text{d}^{-1}$ ) the reactors recovered their COD removal efficiencies to values exceeding 90% (Phase III, Figure 2. D). Under this level of salinity, De Vrieze et al. (2016b) reported a COD removal of only  $4.9 \pm 0.8\%$  at  $20 \text{ gNa}^+\cdot\text{L}^{-1}$  and

severe inhibition of methanogenesis in CSTR reactors. The abrupt salinity increase initially did not appear to have a negative effect on the phenol conversion rate in the UASB reactor, contrasting the results obtained in the AnMBR in which a reduction from 87.4 to 49.4 mgPhgVSS<sup>-1</sup>d<sup>-1</sup> was found. However, the effluent concentration of the UASB increased gradually to 113 mgPhL<sup>-1</sup> on day 370. Conversely, the COD removal efficiency of the UASB started to decrease at the end of phase III. These observations are in agreement with Muñoz Sierra et al. (2018a) who observed that a one-step salinity increase of 4 gNa<sup>+</sup>L<sup>-1</sup> already reduces the quality and biological stability of the biomass.

In Phase IV, the UASB phenol effluent concentration increased to about 830 mgPhL<sup>-1</sup>, and the phenol conversion rate decreased remarkably from 103.2 to 32.90 mgPhgVSS<sup>-1</sup>d<sup>-1</sup> at day 379 (Phase IV, Figure 5.2. C). A very poor bioreactor performance was observed compared to the AnMBR at a sodium concentration of 26 gNa<sup>+</sup>L<sup>-1</sup>. A COD removal efficiency of 47% was observed before the biomass started to wash-out. Aslan and Şekerdağ (2016) reported a significant decrease in COD removal efficiency at a sodium concentration of about 20 gNa<sup>+</sup>L<sup>-1</sup> in a UASB treating highly saline glucose-containing wastewater. A severe deflocculation phenomenon was observed in the UASB, as further explained, leading to reactor failure. Jeison et al. (2008) observed that high salinity conditions (20 gNa<sup>+</sup>L<sup>-1</sup>) in a UASB results in sodium inhibition. In contrast, this level of salinity made the AnMBR performance unstable but it continued performing with phenol and COD removal efficiencies of 96% and 80%, respectively, demonstrating that a membrane enhanced biomass retention was needed to overcome biomass losses resulting from high sodium concentration.

The specific methanogenic activities (SMAs) of the biomasses in both reactors are shown in Table 5.3. SMAs were similar in phases I and II before the phenol loading rate was increased to 1.11 gPhL<sup>-1</sup>d<sup>-1</sup>. On day 322, at the end of phase II, the SMA of the UASB biomass decreased to 0.39±0.08 gCOD-CH<sub>4</sub>gVSS<sup>-1</sup>d<sup>-1</sup> compared to 0.64±0.01 gCOD-CH<sub>4</sub>gVSS<sup>-1</sup>d<sup>-1</sup> of the AnMBR. Chapleur et al. (2016) observed that the anaerobic cellulose digestion was progressively affected as phenol concentration increased and that methanogenesis was the most sensitive step with SMA half-inhibition concentration of 1.40 gPhL<sup>-1</sup>. Furthermore, in this study the increase in influent sodium concentrations by a step of 6 gNa<sup>+</sup>L<sup>-1</sup> in phase III affected the SMA in the AnMBR resulting in values lower than half of the SMA observed at 18 gNa<sup>+</sup>L<sup>-1</sup>, suggesting that the half-inhibition sodium concentration (IC<sub>50</sub>) was already reached as described by Muñoz Sierra et al. (2017). In such a condition, the addition of osmoprotectants might promote recovery of methanogenic activity (Zhang et al. 2016). In phase IV on day 379, the SMA in the UASB was 0.16 gCOD-CH<sub>4</sub>gVSS<sup>-1</sup>d<sup>-1</sup> before the effluent phenol concentration increased in the UASB and deflocculating phenomenon occurred. It is also important to note that the rate-limiting step in phenol degradation to methane is the conversion to benzoate. The impact of high sodium and phenol concentrations could also have affected the phenol conversion step to benzoate, causing phenol accumulation in the reactor and subsequent failure of the methanogenesis (Wang et al. 2017a). The transmembrane pressure (TMP) and membrane resistance to filtration of the AnMBR indicated a stable filtration performance during the long-term operation with values of about 145 mbar and 6.8 x 10<sup>12</sup> m<sup>-1</sup>, respectively.



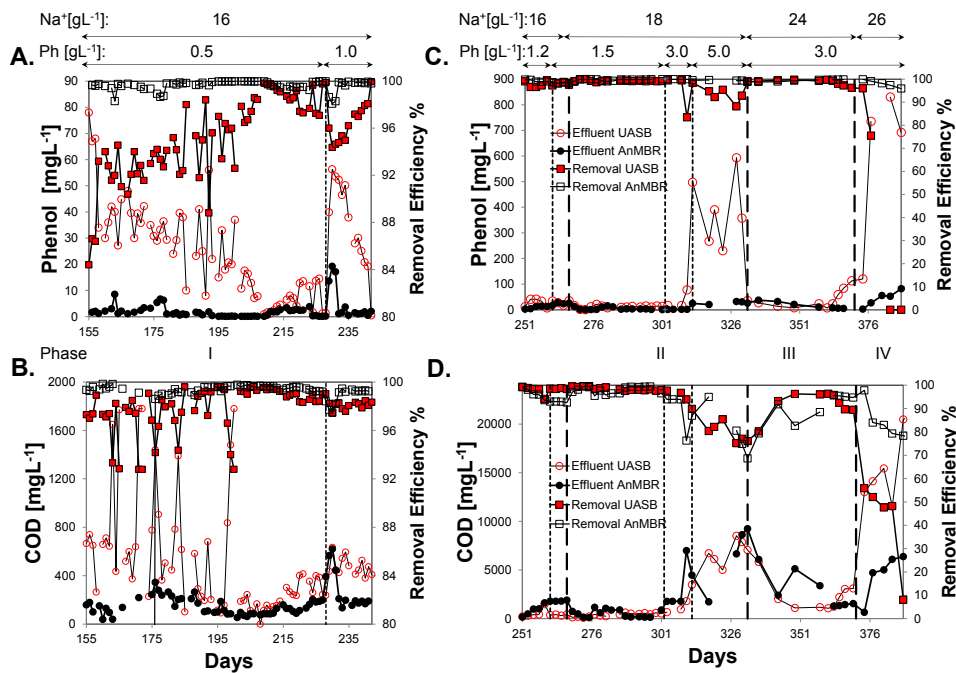


Figure 5.2 Reactors performance. Effluent phenol concentration and removal efficiency A. Phase I , C. Phases II-IV. Effluent COD concentration and removal efficiency B. Phase I, D. Phases II-IV.

### 5.3.2 Impact of high salinity on biomass characteristics

#### 5.3.2.1 Particle size distribution (PSD)

The PSD of the biomass from both reactors expressed as volume fraction % is shown in Figure 5.3. After 283 days of operation and at 18 gNa<sup>+</sup>L<sup>-1</sup> the biomass particle size of the UASB decreased with 57% compared to the inoculum. Thus, the UASB biomass presented a median particle size median size (D50) of about 146 μm, while the AnMBR D50 was about 56 μm. At 24 gNa<sup>+</sup>L<sup>-1</sup> a greater reduction of 38% in particle size was observed in the UASB than in the AnMBR (27%). At 26 gNa<sup>+</sup>L<sup>-1</sup> the particle size decreased further. The observed D50 was about 41 μm in the UASB reactor and 16 μm in the AnMBR on day 372. Previous studies have also indicated the reduction of biomass particle size under increasing salinity (De Vrieze et al. 2016a, Ismail et al. 2010). As a consequence, the UASB biomass started to wash-out, and the sludge bed collapsed at about 26 μm on day 384 as will be discussed in section 5.3.2.3. The effect of long-term calcium leaching on particle size due to high sodium concentration exposure as pictured in Figure 5.4 became apparent with the noticeable particle size reduction in both reactors.

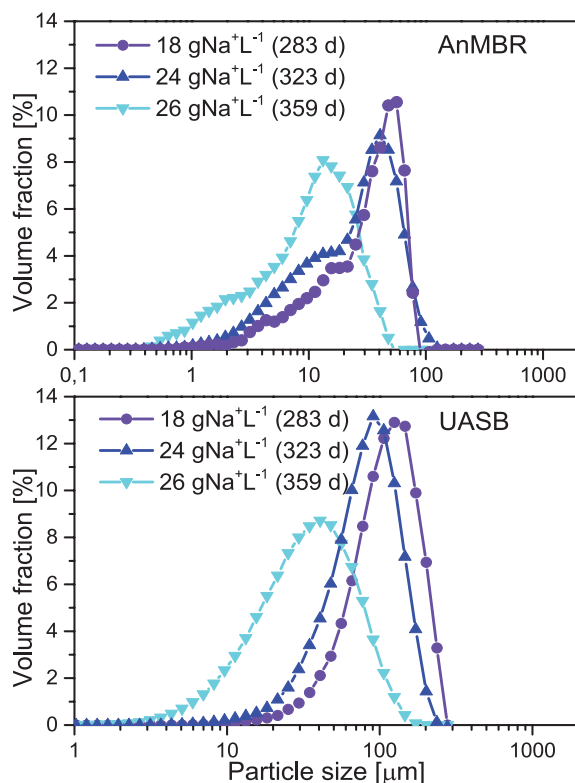


Figure 5.3 Particle size distribution of biomass from AnMBR and UASB under increasing sodium concentrations.

### 5.3.2.2 Extracellular polymeric substances (EPS) and soluble microbial products (SMP)

Proteins (PN) and polysaccharides (PS) were characterized as main constituents from the EPS and SMP in the biomass from both reactors at the end of each phase (Table 5.4). The EPS concentration was 94% PN with a content of about  $66.1 \pm 2.2 \text{ mg gVSS}^{-1}$  at  $16 \text{ gNa}^+\text{L}^{-1}$  in the AnMBR and about  $30.2 \text{ mg gVSS}^{-1}$  in the UASB. A significant increase was observed from  $72.9 \pm 0.0 \text{ mg gVSS}^{-1}$  at  $18 \text{ gNa}^+\text{L}^{-1}$  to  $107.9 \pm 3.1 \text{ mg gVSS}^{-1}$  at  $24 \text{ gNa}^+\text{L}^{-1}$  in the AnMBR, whereas the EPS-PN in the UASB increased from  $13.3 \text{ mg gVSS}^{-1}$  to  $62.9 \pm 0.1 \text{ mg gVSS}^{-1}$  at  $24 \text{ gNa}^+\text{L}^{-1}$ . In the case of EPS-PS, a similar increasing trend was observed in the AnMBR with the highest value at  $26 \text{ gNa}^+\text{L}^{-1}$ . In contrast, in the UASB the EPS-PS concentration was found to be less variable than in the AnMBR.

These results do not agree with Ismail et al. (2010) who observed no differences in EPS content at 10 and 20  $\text{gNa}^+\text{L}^{-1}$ , most likely because of the different feed used that contained acetate, gelatine, and starch. In fact, EPS plays an important role in self-flocculating bacteria, which has been recently presented by Huang et al. (2018) as a strategy to improve saline wastewater treatment. Furthermore,

the FT-IR fingerprint spectra of the EPS extracted presented in Figure S5.1 showed a broad region of adsorption between 3500 and 3000  $\text{cm}^{-1}$ , which is attributed to the O-H bond and the aromatic C-H bond in phenol (Wang et al. 2009). A clear peak around 3450  $\text{cm}^{-1}$  is attributed to the O-H stretching from polysaccharides (Dereli et al. 2015). The two peaks at 1634  $\text{cm}^{-1}$  and 1440  $\text{cm}^{-1}$  are due to N-H, C-N and C=O vibration and stretching from secondary protein structures. The latter peak increased its intensity notably for the UASB at 24  $\text{gNa}^+\cdot\text{L}^{-1}$ . Additionally, the SMP PN:PS ratio was overall higher in the UASB compared to the AnMBR, with the highest value observed after the increase from 18 to 24  $\text{gNa}^+\cdot\text{L}^{-1}$  was applied, indicating a high amount of proteins solubilization. Biomass lysis products caused by the impact of an increase of 6  $\text{gNa}^+\cdot\text{L}^{-1}$  of sodium concentration might have been the reason for the higher amount of PN compared to PS. Higher production of SMP compared to EPS was observed in the UASB at a salinity exceeding 20  $\text{gNa}^+\cdot\text{L}^{-1}$  in line to what was found by Corsino et al. (2017).

Table 5.4 EPS and SMP in the reactors under different sodium concentrations. PN: Proteins. PS: Polysaccharides.

Sodium [ $\text{gNa}^+\cdot\text{L}^{-1}$ ]	Reactor	EPS-PN [ $\text{mg}\cdot\text{gVSS}^{-1}$ ]	EPS-PS [ $\text{mg}\cdot\text{gVSS}^{-1}$ ]	EPS PN:PS ratio	SMP-PN [ $\text{mg}\cdot\text{gVSS}^{-1}$ ]	SMP-PS [ $\text{mg}\cdot\text{gVSS}^{-1}$ ]	SMP PN:PS ratio
16	AnMBR	66.1 $\pm$ 2.2	3.5 $\pm$ 0.1	19	6.4 $\pm$ 0.0	2.2 $\pm$ 1.1	8.7
	UASB	30.2 $\pm$ 2.7	1.7 $\pm$ 0.1	18	9.0 $\pm$ 0.0	1.1 $\pm$ 0.1	8
18	AnMBR	72.9 $\pm$ 0.0	6.4 $\pm$ 0.9	11	27.8 $\pm$ 2.3	1.2 $\pm$ 0.2	22
	UASB	13.3 $\pm$ 0.7	0.8 $\pm$ 0.2	17	54.7 $\pm$ 1.5	0.8 $\pm$ 0.4	68
24	AnMBR	107.9 $\pm$ 3.1	3.5 $\pm$ 0.1	30	88.4 $\pm$ 64.3	2.5 $\pm$ 0.0	36
	UASB	62.9 $\pm$ 0.1	3.8 $\pm$ 0.0	17	87.3 $\pm$ 66.4	0.2 $\pm$ 0.2	386
26	AnMBR	104.3 $\pm$ 5.3	10.7 $\pm$ 0.4	10	61.7 $\pm$ 26.5	3.4 $\pm$ 0.5	18
	UASB	42.5 $\pm$ 0.0	3.0 $\pm$ 0.3	14	53.0 $\pm$ 9.2	2.6 $\pm$ 0.8	20

### 5.3.2.3 Deflocculation phenomenon: biomass calcium leaching

Calcium washed out from the UASB biomass down to 2.7  $\text{mgCa}^{2+}\cdot\text{gTSS}^{-1}$  and to 0.4  $\text{mgCa}^{2+}\cdot\text{gTSS}^{-1}$  at 24 and 26  $\text{gNa}^+\cdot\text{L}^{-1}$ , respectively, compared to 59.3  $\text{mgCa}^{2+}\cdot\text{gTSS}^{-1}$  at 16  $\text{gNa}^+\cdot\text{L}^{-1}$  (Figure 4). Apparently, calcium was leached with the high sodium concentration exposure between days 155 and 386, but increased at 26  $\text{gNa}^+\cdot\text{L}^{-1}$ . Concomitantly, the effluent calcium concentration increased from 9.0  $\text{mgCa}^{2+}\cdot\text{L}^{-1}$  at 16  $\text{gNa}^+\cdot\text{L}^{-1}$  to 15.3  $\text{mgCa}^{2+}\cdot\text{L}^{-1}$  at 18  $\text{gNa}^+\cdot\text{L}^{-1}$  in a period of 140 days. At 26  $\text{gNa}^+\cdot\text{L}^{-1}$  the UASB effluent calcium concentration increased from 15.3  $\text{mgCa}^{2+}\cdot\text{L}^{-1}$  to a maximum of 21.7  $\text{mgCa}^{2+}\cdot\text{L}^{-1}$ . The permeate calcium concentration remained in a range between 0.3 – 3.1  $\text{mgCa}^{2+}\cdot\text{L}^{-1}$  in the AnMBR. At high salinity, the concentration increased from 0.4  $\text{mgCa}^{2+}\cdot\text{L}^{-1}$  at 24  $\text{gNa}^+\cdot\text{L}^{-1}$  to 11.5  $\text{mgCa}^{2+}\cdot\text{L}^{-1}$  at 26  $\text{gNa}^+\cdot\text{L}^{-1}$ , indicating also a severe calcium washed out at this level of sodium concentration. Previous findings were reported by Ismail et al. (2010) who observed a five-times increase in calcium concentration in the bulk liquid with an exposure of only 30 days at 20  $\text{gNa}^+\cdot\text{L}^{-1}$ , concomitant with a reduction from 84 to 52  $\text{mgCa}^{2+}\cdot\text{gTSS}^{-1}$  in the biomass matrix.

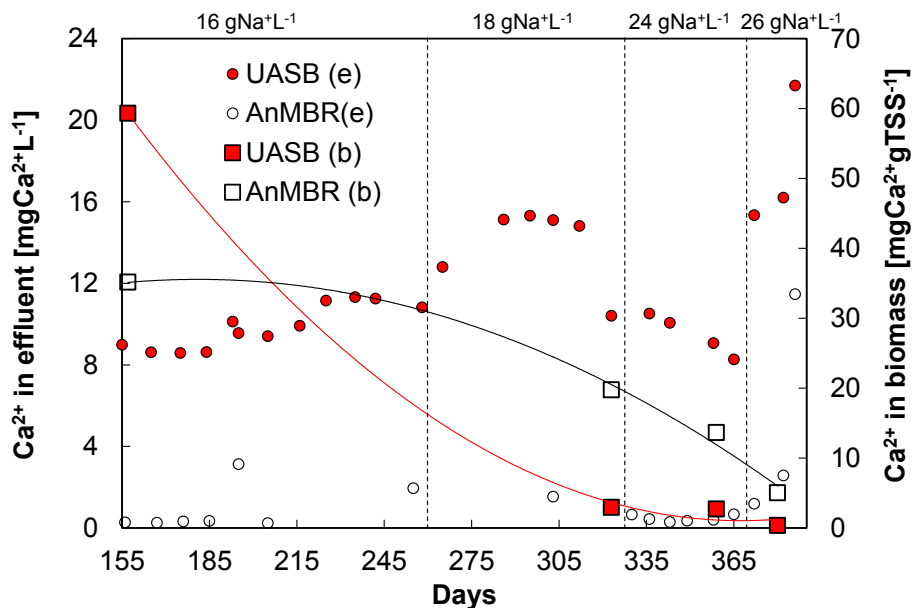


Figure 5.4 Calcium concentration in the effluent (e) (left y-axis) and content in the biomass matrix (b) (right y-axis) from AnMBR and UASB reactors.

Correspondingly, severe UASB biomass deflocculation was observed (Figure 5.5. A, C). UASB median particle size decreased from  $117 \pm 82 \mu\text{m}$  at  $24 \text{ gNa}^+\cdot\text{L}^{-1}$  to  $26 \pm 22 \mu\text{m}$  at  $26 \text{ gNa}^+\cdot\text{L}^{-1}$  (Figure 5.5. B, D), indicating a clear disruption of the sludge bed due to high salinity. This supports the hypothesis that high sodium concentration reduces sludge strength by replacing calcium from the biomass matrix, thereby producing a weak dispersed sludge (Jeison et al. 2008).

In our study, the conductivity was also measured and values over a range from  $43 \text{ mS}\cdot\text{cm}^{-1}$  to  $58 \text{ mS}\cdot\text{cm}^{-1}$  were observed. De Vrieze et al. (2016a) suggested that with high salinity an increase in conductivity up to  $45 \text{ mS}\cdot\text{cm}^{-1}$  caused granular sludge disintegration and biomass washout. A substantial reduction in particle size from about  $1290$  to  $54 \mu\text{m}$  was also associated with exposure to high salinity. In contrast to the observed deflocculation in our study, Li et al. (2014) observed that granule size increased with higher sodium concentrations in a UASB up to  $11.2 \text{ gNa}^+\cdot\text{L}^{-1}$  treating saline sulfate wastewater. Similarly, Sudmalis et al. (2018) managed to obtain larger granules at  $20 \text{ gNa}^+\cdot\text{L}^{-1}$  than at  $5 \text{ gNa}^+\cdot\text{L}^{-1}$  with comparable granule strength, implying that in this case strength was not affected by high sodium concentrations.

This UASB reactor was fed with  $13 \text{ mgCa}^{2+}\cdot\text{L}^{-1}$  during the initial 90 days of operation from a total of 217 days. In our study, the feed contained 100 times lower calcium concentration ( $0.14 \text{ mgCa}^{2+}\cdot\text{L}^{-1}$ ) and a longer-term of operation was applied.

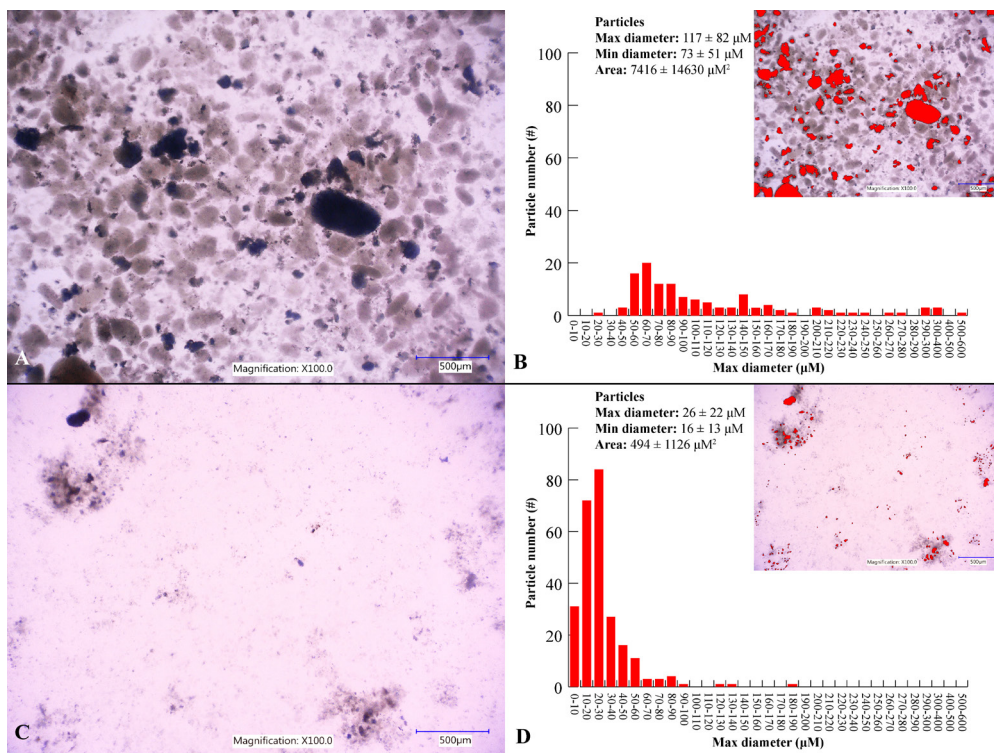


Figure 5.5 Deflocculation phenomenon. A. Observation of biomass under microscope before UASB deflocculated. B. Particle size before UASB deflocculated. C. Observation of biomass under microscope after UASB deflocculated. D. Particle size after UASB deflocculated.

Calcium leaching occurred apparently faster in the AnMBR with a reduction in the calcium content in the biomass matrix and an increase in calcium content in the permeate at high salinity, implying that calcium leaching is rather related to biomass properties rather than to reactor configuration. However, despite the fact that calcium can support granulation by forming cationic bridges with extracellular polymeric substances (EPS) (Shi et al. 2017), other studies have shown that concentrations higher than  $1 \text{ gCa}^{2+}\cdot\text{L}^{-1}$  (Gagliano et al. 2017) have no positive effects on granulation and even detrimental effects on microbial activity. Kobayashi et al. (2018) indicated that calcium addition ( $0.32\text{-}0.64 \text{ gCa}^{2+}\cdot\text{L}^{-1}$ ) accelerated biofilm formation but this positive effect is strongly counteracted by sodium concentrations as low as  $3.45 \text{ gNa}^{+}\cdot\text{L}^{-1}$  due to competition for limited cation binding sites. The different results suggest that cationic bridges formation at high sodium concentrations for cell aggregation are still not well understood. Antagonistic or synergistic effects with other cations like potassium (Muñoz Sierra et al. 2018a, Onodera et al. 2017) also cannot be overlooked.

### 5.3.3 Microbial community comparison

#### 5.3.3.1 Microbial community structure and dynamics

Microbial community analysis resulted in  $48841 \pm 21479$  reads and 958 OTUs in the UASB, while  $56951 \pm 5381$  reads and 944 OTUs were obtained in the AnMBR. Microbial community structure of the reactor biomass was analyzed by next-generation sequencing targeting the 16S rRNA gene along the different operational phases. At the order level (Figure 5.6. A), the most dominant bacteria in the reactors (UASB, AnMBR) were Clostridiales (16.66%, 15.61%), Natranaerobiales (9.83%, 6.89%), Synergistales (3.78%, 3.95%), BA021 (3.52%, 5.42%), Thermotogales (1.25%, 5.36%) and Bacteroidales (8.21%) in the UASB. Methanosarcinales (46.86%) was the dominant Archaea in the UASB and Methanobacteriales (26.22%) and Methanosarcinales (23.99%) in the AnMBR.

Further in phase I, at 0.11 PhLR and after longer exposure to  $16 \text{ gNa}^+\text{L}^{-1}$ , the Methanosarcinales and Natranaerobiales increased to 53.76% and 11.84% in the UASB, and to 37.34%, and 8.50% in the AnMBR, respectively. The decrease in relative abundance was observed mainly in Bacteroidales (5.22%), BA021 (1.18%) and Synergistales (2.71%) in the UASB, whereas in the AnMBR BA021 and Thermotogales decreased to 4.42% and 3.63%, respectively. In phase II, at  $18 \text{ gNa}^+\text{L}^{-1}$ , *Methanosaeata*, belonging to Methanosarcinales order increased from 47.04% to 59.30% as the PhLR increased from 0.33 to  $1.11 \text{ gPhL}^{-1}\text{d}^{-1}$  in the UASB, while in the case of the AnMBR both the *Methanobacterium* and *Methanosaeata* decreased from 9.23%, and 45.72% to 8.33% and 35.63%, respectively (Figure 5.6. B). *Marinobacter* (5.35%), *Halomonas* (8.12%) and *Marinobacterium* (2.81%) all belonging to Gammaproteobacteria class (see Figure S5.2) and involved in aromatics degradation, together with the genus *Paruococcus* (6.86%, Alphaproteobacteria), increased significantly in the UASB at  $0.33 \text{ gPhL}^{-1}\text{d}^{-1}$  on day 280 in phase II. In contrast, all previous Proteobacteria were present in the AnMBR with a relative abundance lower than 0.5%. However, at a higher PhLR and higher salinity in further phases, all Proteobacteria decreased more than five-fold their relative abundance in the UASB most likely due to sensitivity to high sodium. Wang et al. (2017a) related a decrease in relative abundance of Proteobacteria with a reduction in phenol conversion under high salinity. The AnMBR exhibited an increase in the Bacteroidales (ML635J-40), and the genus *Clostridium* and *Pelotomaculum* of about 22%, 25% and 17% due to the increase in PhLR, indicating their involvement in the phenol degradation. Proteobacteria, Firmicutes (*Clostridium*, Natranaerobiales, *Pelotomaculum*), and Bacteroidetes (Bacteroidales) have been reported as the main phyla in anaerobic reactors treating phenolic wastewater (Madigou et al. 2016, Wang et al. 2017a). In phase III, at  $24 \text{ gNa}^+\text{L}^{-1}$  and  $0.67 \text{ gPhL}^{-1}\text{d}^{-1}$ , *Methanobacterium* (16.14%), *Methanosaeata* (39.33%), *Clostridium* (7.01%), Natranaerobiales (7.10% ML1228J-1; 3.56% YAB3B13) and Synergistales (17.06%, Thermovirgaceae) dominated in the AnMBR. This could potentially suggest a shift induced by high salinity from acetoclastic methanogenesis to syntrophic acetate oxidation coupled with hydrogenotrophic methanogenesis, as reported earlier for Clostridiales (Müller et al. 2016). Thermovirgaceae increased about two-fold within phase I and III when the highest soluble protein (SMP-PN) content was observed in the AnMBR corresponding with its protein/amino acid degradation nature. Conversely, the UASB presented a higher variability than the AnMBR in the

bacterial relative abundance. SBR1031 (1.31%, SHA-31), *Enterococcus* (1.51%), *Clostridium* (6.77%), *Pelotomaculum* (1.16%), *Tissierella Soehngenia* (1.60%), Natranaerobiales (1.57%, Anaerobrancaceae; 5.69%, ML1228J-1; 7.98%, YAB3B13) and Synergistales (2.27%, Thermovirgaceae) were the most abundant microorganisms. *Methanosaeta* (54.35%) dominated as Archaea (Figure 5.6. B). FISH (Figure 5.7. A) confirmed the dominance of archaeal filamentous cells in the UASB, positive to the ARC915 probe (in red) after 371 days of operation. There was a clear difference in the morphology of the biomass cells. In the UASB robust and long filaments in conglomerates were observed (Figure 5.7. B). In the AnMBR (Figure 5.7. C) the cells mainly had a single filament morphology without the presence of clusters.

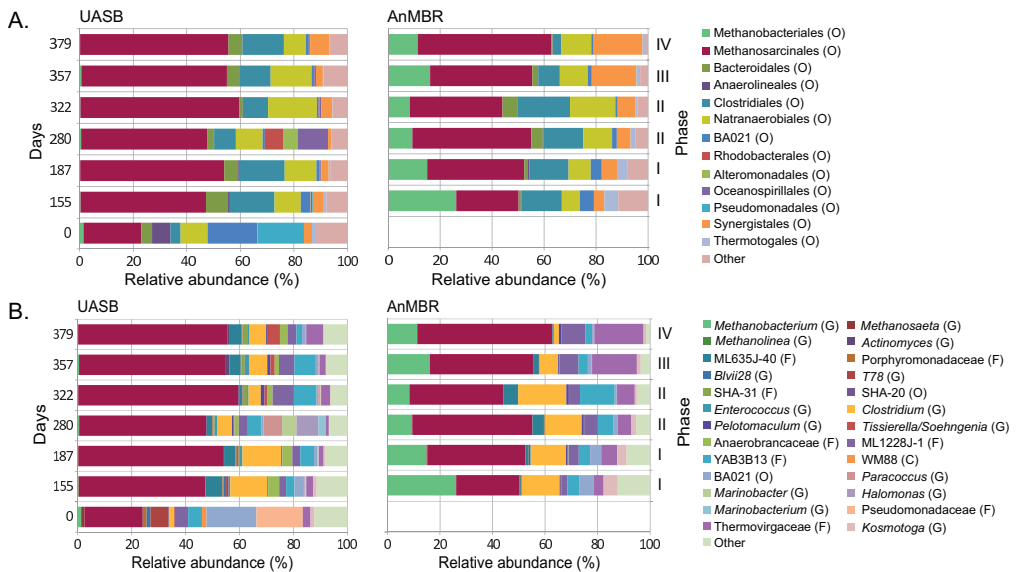


Figure 5.6 Microbial community composition of the UASB and AnMBR treating phenolic wastewater at increasing salinity. A. Order level B. up to Genus level. Relative abundance cutoff at 1%.

In phase IV, at 26 gNa<sup>+</sup>L<sup>-1</sup> and the same PhLR as in phase III, *Methanosaeta* remarkably increased to 51.46% in the AnMBR, while *Methanobacterium* decreased its relative abundance to 11.37%. High sodium concentrations apparently resulted in a strong increase in abundance of *Methanosaeta*, which was not the case for the other methanogens, confirming that at high salinity, salt-tolerant methane-producing archaea can be enriched (Wu et al. 2017). However, as also observed by De Vrieze et al. (2016b), this high abundance does not automatically reflect a high activity, which could explain the lower SMA at 24 and 26 gNa<sup>+</sup>L<sup>-1</sup>. Only in the AnMBR, hydrogenotrophic methanogens were present in relatively high abundance. *Pelotomaculum*, a syntrophic aromatic compound degrader,

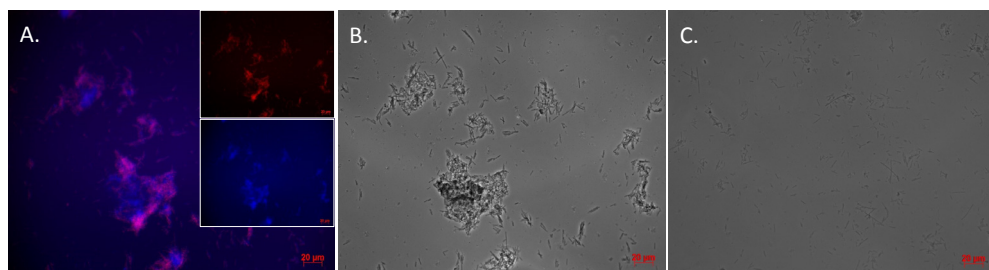


Figure 5.7 A. FISH from UASB reactor. B. Sludge morphology in UASB , C. Sludge morphology in AnMBR after 371 days of operation. The samples were hybridized with the probe specific for archaea (ARC915, red) and were stained with DAPI (blue). Scale bar = 20  $\mu\text{m}$ .

presented the highest abundance in this phase whereas Clostridiales decreased to 3.2% (Figure 5.6. A). In the UASB, an increase of 3.70% in relative abundance from Clostridiales, 4.56% of Synergistales (Thermovirgaceae), and the decrease of Natranaerobiales from 15.31% to 8.27% were observed.

The changes in community structure over time, and with respect to the different salinity and phenol loading rates applied was analyzed by non-metric distance scaling (NMDS) (Figure S5.3). The NMDS analysis indicated that the microbial community in the AnMBR and UASB reactor shifted due to the increase in salinity conditions and phenol loading rate and were dissimilar even though they were exposed to similar operational conditions. Three distinct clusters could be identified, containing the inoculum, UASB and AnMBR reactors samples. The analysis of similarity (ANOSIM) statistical test demonstrated significant differences ( $p=0.04$ ) of the microbial community composition and a high separation ( $R=0.68$ ) for both reactors. Furthermore, ADONIS statistical test revealed that in the UASB the microbial composition at  $16\text{gNa}^+\cdot\text{L}^{-1}$  was significantly different ( $p=0.01$ ,  $R^2=0.42$ ) compared to the samples exposed to higher salinity, whereas in the AnMBR the microbial population at  $26\text{gNa}^+\cdot\text{L}^{-1}$  showed significant differences ( $p=0.01$ ,  $R^2=0.32$ ), compared to the phases under lower sodium concentrations.

### 5.3.3.2 Microbial community diversity analysis

The change in microbial community structure in response to a disturbance such as an increase in salinity was evaluated via alpha diversity analysis using the Hill diversity order numbers approach (Hill 1973). Differences were observed among the three Hill diversity orders for the microbial community of the UASB and AnMBR. A higher richness ( $H_0$ ) was observed in the UASB compared to the AnMBR in Phase I and Phase IV (Figure 5.8. A), while this was not the case for Phases II and III. The diversity in AnMBR ( $H_1$ ), i.e., the abundance of all species and evenness ratio, was comparable to the UASB under the applied conditions (Figure 5.8. B) without significant differences along the phases ( $p=0.11$ ). The  $H_2$  diversity in the AnMBR was higher than for the UASB in phase I (57%), phase II (48%) and phase III (36%), demonstrating that there were more dominant species in the AnMBR (Figure 5.8. C). High species richness and diversity are related to



increased resilience, as a larger pool of microorganisms augments the probability to maintain functionality to respond to disturbances such as high salinity (Werner et al. 2011). Furthermore, the species evenness (Figure 5.8. D) of the AnMBR was significantly higher than that of the UASB in all phases ( $p=0.047$ ), representing a more stable community composition. This is in line with the observation that microbial communities with greater evenness exhibit higher methanogenic robustness. A more even community has a higher potential to use redundant functional pathways under perturbations, leading to a more stable anaerobic digestion process (Wittebolle et al. 2009).

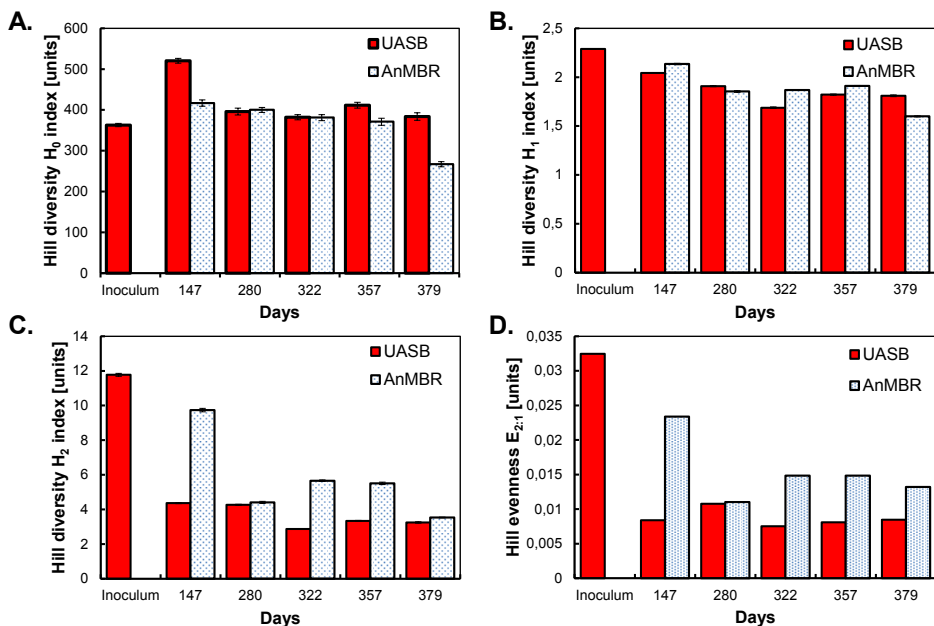


Figure 5.8 Alpha diversity of UASB and AnMBR. A. H<sub>0</sub> (richness, number of OTUs). B. H<sub>1</sub> (exponential value of the Shannon index). C. H<sub>2</sub> (inverse Simpson index). D. E<sub>z:1</sub> (species evenness) were calculated both for bacteria and archaea.

Overall, the AnMBR exhibited better stability and more efficient treatment under long-term high sodium concentrations than the UASB. The question that remains under discussion is whether under random sodium concentration fluctuations a membrane enhanced retention system can permanently maintain microbial stability and robust performance. Further research could, for example, evaluate whether an online calcium supply control strategy can minimize the impact of high sodium concentration on biomass properties when calcium leaching takes place independently of the reactor configuration. The findings of this study highlight the potentials for the AnMBR technology application for chemical wastewater streams under extreme conditions that are more difficult to be overcome by conventional high rate anaerobic technologies such as a UASB.

## 5.4 Conclusions

This study focused on the comparative assessment of a UASB reactor and an AnMBR with respect to phenol degradation under high salinity conditions. The AnMBR process exhibited better stability and performance than the UASB for the treatment of the phenolic wastewater over a range of 16–26 gNa<sup>+</sup>L<sup>-1</sup>. Under the highest sodium concentration, the UASB phenol conversion rate decreased from 103.2 to 32.9 mgPh.gVSS<sup>-1</sup>d<sup>-1</sup>, and a COD removal of 47% was observed before biomass washout occurred. The AnMBR exhibited a phenol and COD removal of 96% and 80%, respectively, demonstrating that a membrane enhanced biomass retention was able to overcome the impact of high salinity. An increase of 6 gNa<sup>+</sup>L<sup>-1</sup> produced high solubilization of protein-like substances in both reactors and a decrease in median particle size of 38% and 27% in the UASB and AnMBR, respectively. Moreover, at 26 gNa<sup>+</sup>L<sup>-1</sup> and phenol concentration of 3 gPh.L<sup>-1</sup>, the UASB biomass deflocculated due to a long-term calcium wash-out from 59.3 mgCa<sup>+</sup>gTSS<sup>-1</sup> at 16 gNa<sup>+</sup>L<sup>-1</sup> to 0.4 mgCa<sup>2+</sup>gTSS<sup>-1</sup>, leading to reactor failure. Concomitantly, a median particle size reduction in both reactors to about 26 μm in the UASB and 16 μm in the AnMBR revealed a clear impact of the increase in sodium concentration on biomass aggregation. Additionally, high salinity promoted a higher variability in microbial community composition on the genus level in the UASB compared to the AnMBR, which reflects the susceptibility of certain microorganisms in biofilms to high salinity. Hence, the AnMBR showed significantly higher species evenness than the UASB, exhibiting higher methanogenic activity due to its greater probability to maintain functionality and to respond to disturbances such as high phenol and sodium concentration increases.

Overall, this study demonstrated that two high-rate anaerobic reactor configurations with different biomass retention systems (biofilm-granule in UASB and membrane in AnMBR) resulted in a diverse performance and stability when treating phenolic wastewater under high salinity.

## Supplementary Information

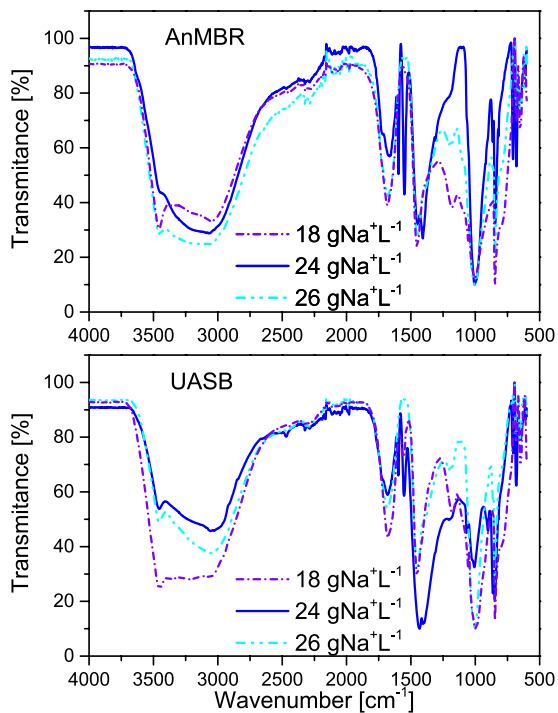


Figure S5.1. FT-IR spectrum of EPS samples from AnMBR and UASB under increasing sodium concentrations.

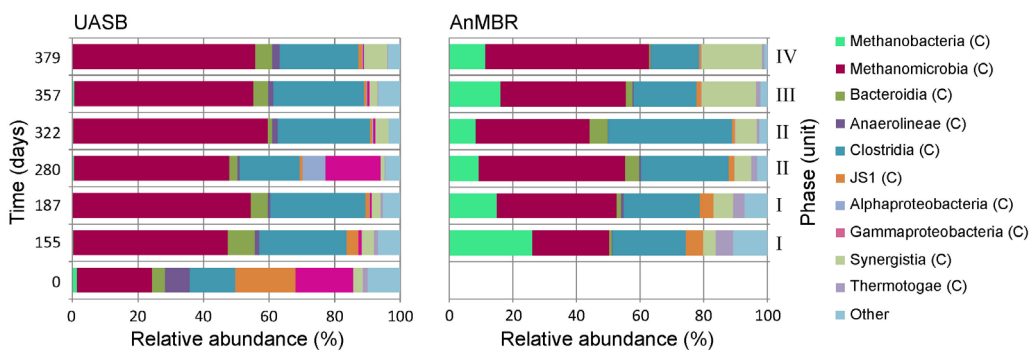


Figure S5.2. Microbial community composition at taxa class level of the UASB and AnMBR treating phenolic wastewater at increasing salinity. Relative abundance cut-off at 1%.

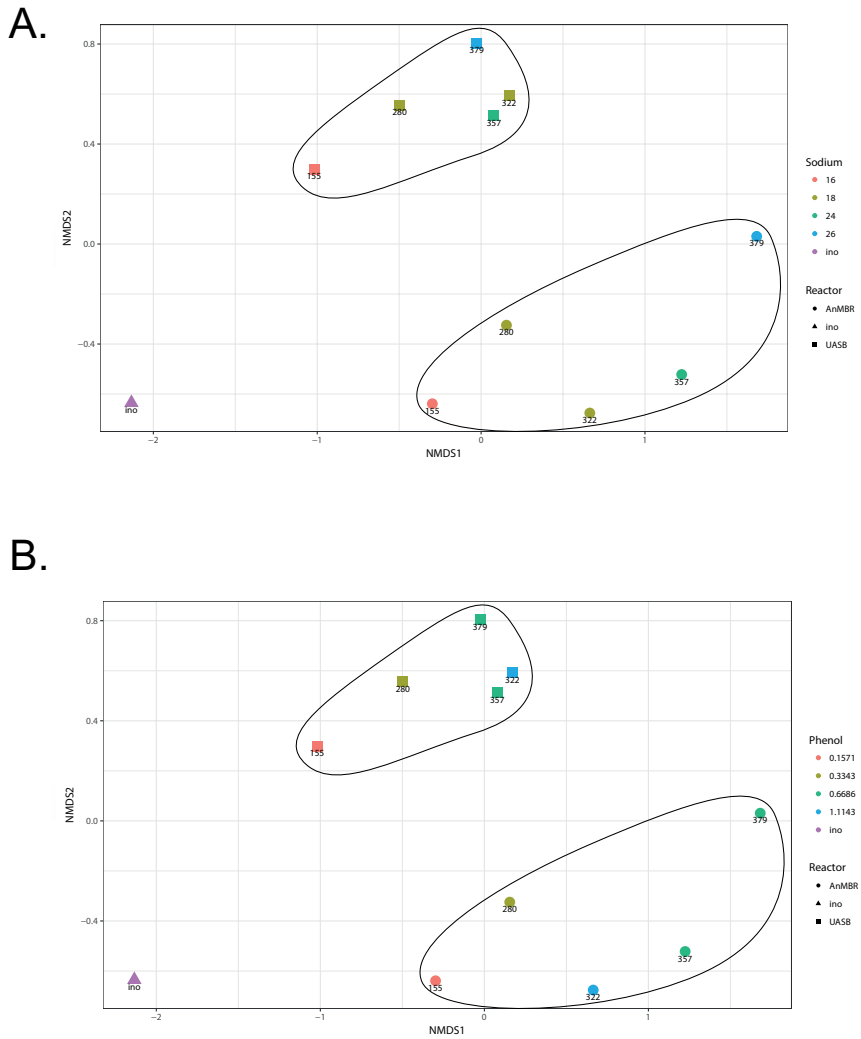


Figure S5.3. Microbial community structure dynamic by non-metric distance scaling (NMDS) with respect to A. increasing sodium concentration [ $\text{Na}^+\cdot\text{L}^{-1}$ ] and B. phenol loading rates applied [ $\text{gPh}\cdot\text{L}^{-1}\cdot\text{d}^{-1}$ ].

## References

- Aslan, S. and Şekerdag, N. (2016) Salt inhibition on anaerobic treatment of high salinity wastewater by upflow anaerobic sludge blanket (UASB) reactor. *Desalination and Water Treatment* 57(28), 12998-13004.
- Chapleur, O., Madigou, C., Civade, R., Rodolphe, Y., Mazéas, L. and Bouchez, T. (2016) Increasing concentrations of phenol progressively affect anaerobic digestion of cellulose and associated microbial communities. *Biodegradation* 27(1), 15-27.
- Corsino, S.F., Capodici, M., Torregrossa, M. and Viviani, G. (2017) Physical properties and Extracellular Polymeric Substances pattern of aerobic granular sludge treating hypersaline wastewater. *Bioresource Technology* 229, 152-159.
- De Vrieze, J., Coma, M., Debeuckelaere, M., Van der Meeren, P. and Rabaey, K. (2016a) High salinity in molasses wastewaters shifts anaerobic digestion to carboxylate production. *Water Research* 98, 293-301.
- De Vrieze, J., Regueiro, L., Props, R., Vilchez-Vargas, R., Jáuregui, R., Pieper, D.H., Lema, J.M. and Carballa, M. (2016b) Presence does not imply activity: DNA and RNA patterns differ in response to salt perturbation in anaerobic digestion. *Biotechnology for Biofuels* 9(1), 244.
- Dereli, R.K., Ersahin, M.E., Ozgun, H., Ozturk, I., Jeison, D., van der Zee, F. and van Lier, J.B. (2012) Potentials of anaerobic membrane bioreactors to overcome treatment limitations induced by industrial wastewaters. *Bioresource Technology* 122, 160-170.
- Dereli, R.K., Heffernan, B., Grelot, A., van der Zee, F.P. and van Lier, J.B. (2015) Influence of high lipid containing wastewater on filtration performance and fouling in AnMBRs operated at different solids retention times. *Separation and Purification Technology* 139, 43-52.
- Edgar, R. (2016) UCHIME2: improved chimera prediction for amplicon sequencing. *bioRxiv*.
- Edgar, R.C. (2010) Search and clustering orders of magnitude faster than BLAST. *Bioinformatics* 26(19), 2460-2461.
- Gagliano, M.C., Ismail, S.B., Stams, A.J.M., Plugge, C.M., Temmink, H. and Van Lier, J.B. (2017) Biofilm formation and granule properties in anaerobic digestion at high salinity. *Water Research* 121, 61-71.
- Hill, M.O. (1973) Diversity and Evenness: A Unifying Notation and Its Consequences. *Ecology* 54(2), 427-432.
- Huang, Z., Wang, Y., Jiang, L., Xu, B., Wang, Y., Zhao, H. and Zhou, W. (2018) Mechanism and performance of a self-flocculating marine bacterium in saline wastewater treatment. *Chemical Engineering Journal* 334, 732-740.
- Ismail, S.B., de La Parra, C.J., Temmink, H. and van Lier, J.B. (2010) Extracellular polymeric substances (EPS) in upflow anaerobic sludge blanket (UASB) reactors operated under high salinity conditions. *Water Research* 44(6), 1909-1917.
- Jeison, D., Del Rio, A. and Van Lier, J.B. (2008) Impact of high saline wastewaters on anaerobic granular sludge functionalities. *Water Science and Technology* 57(6), 815-819.
- Jiang, Y., Wei, L., Zhang, H., Yang, K. and Wang, H. (2016) Removal performance and microbial communities in a sequencing batch reactor treating hypersaline phenol-laden wastewater. *Bioresource Technology* 218, 146-152.
- Kobayashi, T., Hu, Y. and Xu, K.-Q. (2018) Impact of cationic substances on biofilm formation from sieved fine particles of anaerobic granular sludge at high salinity. *Bioresource Technology* 257, 69-75.
- Lí, J., Yu, L., Yu, D., Wang, D., Zhang, P. and Ji, Z. (2014) Performance and granulation in an upflow anaerobic sludge blanket (UASB) reactor treating saline sulfate wastewater. *Biodegradation* 25(1), 127-136.
- Loosdrecht, M.C.V., Nielsen, P.H., Lopez-Vazquez, C.M. and Brdjanovic, D. (2016) Experimental methods in wastewater treatment, *Water Intell.* Online.
- Madigou, C., Poirier, S., Bureau, C. and Chapleur, O. (2016) Acclimation strategy to increase phenol tolerance of an anaerobic microbiota. *Bioresource Technology* 216, 77-86.

- Müller, B., Sun, L., Westerholm, M. and Schnürer, A. (2016) Bacterial community composition and fhs profiles of low- and high-ammonia biogas digesters reveal novel syntrophic acetate-oxidising bacteria. *Biotechnology for Biofuels* 9(1), 48.
- Muñoz Sierra, J.D., Lafita, C., Gabaldón, C., Spanjers, H. and van Lier, J.B. (2017) Trace metals supplementation in anaerobic membrane bioreactors treating highly saline phenolic wastewater. *Bioresource Technology* 234, 106-114.
- Muñoz Sierra, J.D., Oosterkamp, M.J., Wang, W., Spanjers, H. and van Lier, J.B. (2018a) Impact of long-term salinity exposure in anaerobic membrane bioreactors treating phenolic wastewater: Performance robustness and endured microbial community. *Water Research* 141, 172-184.
- Muñoz Sierra, J.D., Wang, W., Cerqueda-García, D., Oosterkamp, M.J., Spanjers, H. and van Lier, J.B. (2018b) Temperature susceptibility of a mesophilic anaerobic membrane bioreactor treating saline phenol-containing wastewater. *Chemosphere* 213, 92-102.
- Onodera, T., Syutsubo, K., Hatamoto, M., Nakahara, N. and Yamaguchi, T. (2017) Evaluation of cation inhibition and adaptation based on microbial activity and community structure in anaerobic wastewater treatment under elevated saline concentration. *Chemical Engineering Journal* 325, 442-448.
- Rosenkranz, F., Cabrol, L., Carballa, M., Donoso-Bravo, A., Cruz, L., Ruiz-Filippi, G., Chamy, R. and Lema, J.M. (2013) Relationship between phenol degradation efficiency and microbial community structure in an anaerobic SBR. *Water Research* 47(17), 6739-6749.
- Shi, Y., Huang, J., Zeng, G., Gu, Y., Chen, Y., Hu, Y., Tang, B., Zhou, J., Yang, Y. and Shi, L. (2017) Exploiting extracellular polymeric substances (EPS) controlling strategies for performance enhancement of biological wastewater treatments: An overview. *Chemosphere* 180, 396-411.
- Stuckey, D.C. (2012) Recent developments in anaerobic membrane reactors. *Bioresource Technology* 122, 137-148.
- Su, X., Wang, Y., Xue, B., Hashmi, M.Z., Lin, H., Chen, J., Wang, Z., Mei, R. and Sun, F. (2019) Impact of resuscitation promoting factor (Rpf) in membrane bioreactor treating high-saline phenolic wastewater: Performance robustness and Rpf-responsive bacterial populations. *Chemical Engineering Journal* 357, 715-723.
- Sudmalis, D., Gagliano, M.C., Pei, R., Grolle, K., Plugge, C.M., Rijnaarts, H.H.M., Zeeman, G. and Temmink, H. (2018) Fast anaerobic sludge granulation at elevated salinity. *Water Research* 128, 293-303.
- van Lier, J.B., van der Zee, F.P., Frijters, C.T.M.J. and Ersahin, M.E. (2015) Celebrating 40 years anaerobic sludge bed reactors for industrial wastewater treatment. *Reviews in Environmental Science and Biotechnology* 14(4), 681-702.
- Wang, W., Wu, B., Pan, S., Yang, K., Hu, Z. and Yuan, S. (2017a) Performance robustness of the UASB reactors treating saline phenolic wastewater and analysis of microbial community structure. *Journal of Hazardous Materials* 331, 21-27.
- Wang, W., Yang, K., Muñoz Sierra, J., Zhang, X., Yuan, S. and Hu, Z. (2017b) Potential impact of methyl isobutyl ketone (MIBK) on phenols degradation in an UASB reactor and its degradation properties. *Journal of Hazardous materials* 333, 73-79.
- Wang, Z., Wu, Z. and Tang, S. (2009) Extracellular polymeric substances (EPS) properties and their effects on membrane fouling in a submerged membrane bioreactor. *Water Research* 43(9), 2504-2512.
- Werner, J.J., Knights, D., Garcia, M.L., Scalfone, N.B., Smith, S., Yarasheski, K., Cummings, T.A., Beers, A.R., Knight, R. and Angenent, L.T. (2011) Bacterial community structures are unique and resilient in full-scale bioenergy systems. *Proceedings of the National Academy of Sciences* 108(10), 4158-4163.
- Winkler, M.K.H., Bassin, J.P., Kleerebezem, R., de Bruin, L.M.M., van den Brand, T.P.H. and van Loosdrecht, M.C.M. (2011) Selective sludge removal in a segregated aerobic granular biomass system as a strategy to control PAO-GAO competition at high temperatures. *Water Research* 45(11), 3291-3299.

- Wittebolle, L., Marzorati, M., Clement, L., Balloi, A., Daffonchio, D., Heylen, K., De Vos, P., Verstraete, W. and Boon, N. (2009) Initial community evenness favours functionality under selective stress. *Nature* 458, 623.
- Wu, Y., Wang, X., Tay, M.Q.X., Oh, S., Yang, L., Tang, C. and Cao, B. (2017) Metagenomic insights into the influence of salinity and cytostatic drugs on the composition and functional genes of microbial community in forward osmosis anaerobic membrane bioreactors. *Chemical Engineering Journal* 326, 462-469.
- Yang, J., Spanjers, H., Jeison, D. and Van Lier, J.B. (2013) Impact of Na<sup>+</sup> on biological wastewater treatment and the potential of anaerobic membrane bioreactors: A review. *Critical Reviews in Environmental Science and Technology* 43(24), 2722-2746.
- Yurtsever, A., Calimlioglu, B., Görür, M., Çınar, Ö. and Sahinkaya, E. (2016) Effect of NaCl concentration on the performance of sequential anaerobic and aerobic membrane bioreactors treating textile wastewater. *Chemical Engineering Journal* 287, 456-465.
- Zhang, L., Zhu, K. and Li, A. (2016) Differentiated effects of osmoprotectants on anaerobic syntrophic microbial populations at saline conditions and its engineering aspects. *Chemical Engineering Journal* 288, 116-125.





# 6

## Upward temperature shifts in mesophilic AnMBR treating saline phenolic wastewater

6

---

This chapter has been published as: “Muñoz Sierra, J.D., Wang, W., Cerqueda-Garcia, D., Oosterkamp, M.J., Spanjers, H., and van Lier, J.B. (2018) Temperature susceptibility of a mesophilic anaerobic membrane bioreactor treating saline phenol-containing wastewater. *Chemosphere*, 213, pp. 92-102.”

<https://doi.org/10.1016/j.chemosphere.2018.09.023>

## Abstract

This study examined the temperature susceptibility of a continuous-flow lab-scale anaerobic membrane bioreactor (AnMBR) to temperature shifts from 35°C to 55°C and its bioconversion robustness treating synthetic phenolic wastewater at 16 gNa<sup>+</sup>L<sup>-1</sup>. During the experiment, the mesophilic reactor was subjected to stepwise temperature increases by 5 °C. The phenol conversion rates of the AnMBR decreased from 3.16 at 35°C to 2.10 mgPhgVSS<sup>-1</sup>d<sup>-1</sup> at 45°C, and further decreased to 1.63 mgPhgVSS<sup>-1</sup>d<sup>-1</sup> at 50°C. At 55 °C, phenol conversion rate stabilized at 1.53 mgPhgVSS<sup>-1</sup>d<sup>-1</sup> whereas COD removal efficiency was 38% compared to 95.5% at 45°C and 99.8% at 35°C. Interestingly, it was found that the phenol degradation process was less susceptible for the upward temperature shifts than the methanogenic process. The temperature increase implied twenty-one operational taxonomic units from the reactor's microbial community with significant differential abundance between mesophilic and thermophilic operation, and eleven of them are known to be involved in aromatic compounds degradation. Reaching the upper-temperature limits for mesophilic operation was associated with the decrease in microbial abundance of the phyla Firmicutes and Proteobacteria, which are linked to syntrophic phenol degradation. It was also found that the particle size decreased from 89.4 μm at 35°C to 21.0 μm at 55°C. The accumulation of small particles and higher content of soluble microbial protein-like substances led to increased transmembrane pressure which negatively affected the filtration performance. Our findings indicated that at high salinity a mesophilic AnMBR can tolerate a temperature up to 45 °C without being limited in the phenol conversion capacity.

## 6.1 Introduction

Phenolic compounds are toxic organics widely present in industrial wastewater streams such as those coming from coal gasification, coke, pulp-paper manufacturing, and oil-refining (Wang et al. 2017a, Wang et al. 2017c). Anaerobic processes are considered a more sustainable and economically attractive technology for the treatment and mineralization of these compounds (Ramakrishnan and Gupta 2006). In the past decade, different anaerobic technologies such as the up-flow anaerobic sludge blanket (UASB), anaerobic sequencing batch reactor (AnSBR), anaerobic fluidized bed reactor (AFBR), anaerobic hybrid reactors (AHR) and recently anaerobic membrane bioreactors (AnMBR) were applied to treat wastewaters containing phenolic compounds under mesophilic conditions (De Amorim et al. 2015, Muñoz Sierra et al. 2018, Ramakrishnan and Surampalli 2013, Rosenkranz et al. 2013, Wang et al. 2011a). Wang et al. (2011a) evaluated a two continuous UASB system for treating coal gasification wastewater at 37°C obtaining maximum COD and total phenols removal of 55–60% and 58–63% respectively. Rosenkranz et al. (2013) obtained high phenol conversion rate up to 0.8 gPh.L<sup>-1</sup> in the synthetic phenol-containing wastewater by a mesophilic AnSBR system. Similarly, De Amorim et al. (2015) evaluated a AFBR system and achieved phenol and COD removal efficiencies higher than 91%. Muñoz Sierra et al. (2018) presented the performance robustness of a mesophilic AnMBR under long-term high salinity exposure achieving phenol conversion rates up to 11.7 mgPh.gVSS<sup>-1</sup>.d<sup>-1</sup>. Interestingly, Ramakrishnan and Surampalli (2013) indicated that with AHR systems the mesophilic anaerobic digestion treating coal wastewater exhibited lower phenolic and COD degradation than thermophilic. Although anaerobic systems exhibited high removal of phenol during stable operation, the fluctuations in phenol concentration and moving to a higher operational temperature were identified as the major obstacles for achieving performance robustness (Levén et al. 2012, Wang and Han 2012). Earlier research indicated that thermophilic anaerobic digestion in continuous flow reactors could improve the biodegradation rates of phenolic compounds, methane yields, and the aerobic post-treatment when compared to mesophilic (Ramakrishnan and Surampalli 2013, Wang et al. 2011b). In contrast, Fang et al. (2006) showed that phenol degradation rate at 55°C was substantially lower than under mesophilic conditions in a UASB reactor with an organic loading rate (OLR) of 0.9 gCOD.L<sup>-1</sup>.d<sup>-1</sup> and an influent phenol concentration of 0.63 gPh.L<sup>-1</sup>. Thus far, only a few studies have been done on continuous flow reactors comparing thermophilic and mesophilic phenol degradation even though most of the chemical waste streams appear to have high temperatures. Moreover, due to the need of closing water loops in industry, these wastewaters are becoming more prone to be saline, adding another harsh condition for the anaerobic degradation of the organics (Muñoz Sierra et al. 2017).

Proper (auto-)immobilization of anaerobic biomass is the main challenge in treating industrial wastewater at both high temperatures and high salinity. Poor settling characteristics and dispersed biomass make it challenging to accomplish immobilization in comparison with mesophilic conditions (Dereli et al. 2012). AnMBRs under thermophilic conditions have been recently shown to be a promising technology with different wastewaters (Duncan et al. 2017). Simultaneous occurrence of toxicity, high salinity, and thermophilic conditions increase the need to combine

membrane separation with anaerobic treatment to prevent biomass washout, achieve a high-quality effluent, and potentially better performance robustness (Lin et al. 2013). Therefore, AnMBRs are considered an appealing alternative for phenolic wastewater treatment under high temperatures and saline conditions, but there are still difficulties to overcome (Jeison and van Lier 2007, van Lier et al. 2015). Assessment of the bioprocess temperature susceptibility is of particular importance for those reactors that treat wastewaters, which are generated at high temperatures in a wide range, and which require cooling to mesophilic conditions. Boušková et al. (2005) proposed a stepwise shift from 35°C to 55°C as a strategy to determine the performance robustness with increasing temperature of a mesophilic anaerobic continuous stirred tank (CSTR) reactor treating sewage sludge. In AnMBR systems, the low concentrated suspended methanogenic sludge is likely more susceptible to such temperature changes, owing to the fact that the biomass activity is less determined by mass transfer limitation. To our knowledge, the application of AnMBRs for saline phenolic chemical wastewater have not been reported, neither the temperature susceptibility of the phenol degradation process linked to microbial community structure analysis. Therefore, the present study aimed to evaluate the temperature susceptibility of a mesophilic AnMBR treating phenol-containing wastewater under high salinity (16 gNa<sup>+</sup>·L<sup>-1</sup>) conditions over the temperature range of 35-55°C, with focus on process performance as well as microbial community dynamics. To provide better insight into high-temperature exposure, a long-term thermophilic operation was also carried out. The effects of stepwise temperature shifts of 5°C on biomass properties such as particle size, filterability, and membrane filtration performance were analyzed. Correspondingly, the phenol conversion rates, methanogenic activities and microbial community structure at the different short- and long-term temperature exposure were compared. Particular attention was given to the phenol degrading related operational taxonomic units (OTUs) and their main changes induced by the temperature shift from mesophilic to thermophilic conditions.

## 6.2 Material and Methods

### 6.2.1 Reactor configuration and operation

The experiments were performed using a laboratory scale AnMBR reactor with an effective volume of 6.5 L, equipped with an ultra-filtration (UF) side-stream membrane module. A tubular PVDF membrane (Pentair, The Netherlands) with 5.2 mm inner diameter, 30 nm pore size, and 0.64 m length was used. The system was equipped with feed, recycle and effluent pumps (Watson-Marlow 120U/DV, 220Du), pH and temperature sensors (Endress & Hauser, Memosens), and a biogas meter (Ritter, Milligas Counter MGC-1 PMMA, Germany). Transmembrane pressure (TMP) was measured using three pressure sensors (AE Sensors ATM, The Netherlands). The temperature of the jacketed reactor was controlled by a thermostatic water bath (Tamson Instruments, The Netherlands). The experimental set-up was controlled by a computer running LabView software (version 15.0.1f1, National Instruments, USA).

The reactor was initially operated under mesophilic conditions (35.0 ± 0.8 °C) for 152 days. During this time, the influent phenol concentration was gradually increased from 100 to 500 mgPh·L<sup>-1</sup>.

Hereafter, the temperature shift was carried out by a stepwise increases of 5°C up to 55°C from days 152 to 193. Subsequently, the reactor was operated until day 270 under thermophilic (55.0 ± 0.8°C) conditions (see Figure 6.1). The reactor was fed (0.7 L·d<sup>-1</sup>) with synthetic phenol-containing wastewater with phenol and sodium concentration of 500 mgPh·L<sup>-1</sup> and 16 gNa<sup>+</sup>·L<sup>-1</sup>, respectively. The organic loading rate (OLR) applied was initially 4.35 gCOD·L<sup>-1</sup>·d<sup>-1</sup>, however, due to deteriorating process performance, it was decreased to 1.86 gCOD·L<sup>-1</sup>·d<sup>-1</sup> on day 218. An average sludge retention time (SRT) of 43 days was maintained, resulting from biomass growth and biomass sampling.

### 6.2.2 Inoculum and model wastewater composition

The reactor was inoculated with mesophilic anaerobic biomass obtained from a full-scale UASB reactor (Shell, Moerdijk, The Netherlands) to be subjected to higher temperatures.. The initial concentration of volatile suspended solids (VSS) and total suspended solids (TSS) were 20.1 g·L<sup>-1</sup> and 50.9 g·L<sup>-1</sup>, respectively. The model synthetic wastewater consisted of C<sub>6</sub>H<sub>6</sub>O (0.5 g·L<sup>-1</sup>), C<sub>2</sub>H<sub>3</sub>NaO<sub>2</sub> (18.2 g·L<sup>-1</sup>), NaCl (32 g·L<sup>-1</sup>), yeast extract (0.5 g·L<sup>-1</sup>), K<sub>2</sub>HPO<sub>4</sub> (1.81 g·L<sup>-1</sup>), KH<sub>2</sub>PO<sub>4</sub> (0.48 g·L<sup>-1</sup>). Macronutrients (9 mL·L<sup>-1</sup>), and micronutrients (4.5 mL·L<sup>-1</sup>) solutions were added. Macronutrients solution included (in g·L<sup>-1</sup>): NH<sub>4</sub>Cl (170), CaCl<sub>2</sub>·2H<sub>2</sub>O (8), and MgSO<sub>4</sub>·7H<sub>2</sub>O (9); micronutrients solution contained (in g L<sup>-1</sup>): FeCl<sub>3</sub>·6H<sub>2</sub>O (2), CoCl<sub>2</sub>·6H<sub>2</sub>O (2), MnCl<sub>2</sub>·4H<sub>2</sub>O (0.5), CuCl<sub>2</sub>·2H<sub>2</sub>O (0.03), ZnCl<sub>2</sub> (0.05), H<sub>3</sub>BO<sub>3</sub> (0.05), (NH<sub>4</sub>)<sub>6</sub>Mo<sub>7</sub>O<sub>24</sub>·4H<sub>2</sub>O (0.09), Na<sub>2</sub>SeO<sub>3</sub> (0.1), NiCl<sub>2</sub>·6H<sub>2</sub>O (0.05), EDTA (1), Na<sub>2</sub>WO<sub>4</sub> (0.08). The chemical reagents were of analytical grade. The feed solution pH was adjusted to 7.0-7.5 by using HCl (35%).

### 6.2.3 Biomass properties

#### 6.2.3.1 Extracellular polymeric substances (EPS) and soluble microbial products (SMP)

EPS and SMP were characterized based on proteins and polysaccharides and its Fourier spectrum. Biomass samples were centrifuged at 4°C and 12000rpm for 15 minutes. The supernatant was filtered (0.45 µm) and directly used to measure the SMP as proteins and polysaccharides. EPS extraction was carried out by cation exchange resin method as proposed by Frølund et al. (1996). DOWEX Marathon C (20–50 µm mesh, sodium form, Fluka 91973) was used as cation exchange resin. Extraction was carried out at 4°C, 800 rpm during 4 hours. For the analysis of proteins, the modified Lowry method of Frølund et al. (1996) was applied. Polysaccharides were analyzed following the phenol-sulfuric acid method (Dubois et al. 1956). EPS was normalized against the VSS concentration of the biomass in the reactor.

The functional groups of EPS extracted at different temperatures were characterized with a Fourier Transform Infrared (FT-IR) Spectrometer (Spectrum 100 Series Perkin–Elmer, UK) equipped with a universal Attenuated Total Reflection (ATR) unit. The spectra were recorded in the range of 4000–550 cm<sup>-1</sup> with 2 cm<sup>-1</sup> resolution. The FT-IR was first calibrated for background signal scanning, and then the experimental sample scanning was conducted in triplicate.

### 6.2.3.2 Particle size distribution (PSD)

Measurement of PSD was carried out by using a DIPA-2000 EyeTech™ particle analyzer (Donner Technologies, Or Akiva, Israel) with an A100 and B100 laser lens (measuring range 0.1-300  $\mu\text{m}$  and 1-2000  $\mu\text{m}$ , respectively) and a liquid flow cell DCM-104A (10x10 mm).

### 6.2.3.3 Biomass filterability: capillary suction time (CST) and specific resistance to filtration (SRF)

CST of the biomass was measured by a Capillary Suction Timer device (Model 304M, Triton Electronics, Essex, England, UK). A CST paper (7x9 cm) was used for each sample of 6.4 mL of biomass. Samples were measured in triplicate. The results were normalized by TSS concentration. Biomass SRF was measured in a dead-end filtration cell under a 1 bar constant pressure. Permeate production was measured by an electronic balance for data acquisition. SRF was assessed by plotting filtration time/filtrate volume ( $t/V$ ) versus the filtrate volume ( $V$ ) and using  $SRF = \frac{2\Delta P A^2 b}{\mu C}$ , where  $\Delta P$ : Pressure (Pa),  $A$ : Effective filtration area ( $\text{m}^2$ ),  $b$ : Slope of  $t/V$ - $V$  plot ( $\text{s L}^{-2}$ ),  $\mu$ : Viscosity ( $\text{Pa s}$ ),  $C$ : TSS concentration ( $\text{kg m}^{-3}$ ) (Dereli et al. 2015b).

### 6.2.4 Specific methanogenic activity (SMA) and biogas content

SMA tests were performed in triplicate using an automated methane potential test system (AMPTS, Bioprocess Control, Sweden). All the SMA tests were carried out at 35°C following the manufacturer's procedure. The pH of all bottles was adjusted to 7.0 ( $20 \pm 0.4^\circ\text{C}$ ). Methane content of the biogas was analyzed using a gas chromatograph 7890A (GC) system (Agilent Technologies, US) equipped with a flame ionization detector.

### 6.2.5 Permeate characterization

Hach Lange kits were used to measure chemical oxygen demand (COD). The COD was measured using a VIS - spectrophotometer (DR3900, Hach Lange, Germany) making proper dilutions preventing a negative impact of high chloride concentrations, without compromising the accuracy of the measurement. Phenol was measured by Merck – Spectroquant® Phenol cell kits using a spectrophotometer NOVA60 (Merck, Germany). Phenol concentrations were double-checked using high-performance liquid chromatography HPLC LC-20AT (Shimadzu, Japan) equipped with a 4.6 mm reversed phase C18 column (Phenomenex, The Netherlands) and a UV detector at a wavelength of 280 nm. The mobile phase used was 25% (v/v) acetonitrile at a flow rate of  $0.95 \text{ mL min}^{-1}$ . The column oven was set at 30°C.

### 6.2.6 Microbial community structure analysis

Biomass samples were taken every time before the temperature was raised. DNA extraction was performed by using the DNeasy UltraClean Microbial kit (Qiagen, Hilden, Germany). Agarose gel electrophoresis and Qubit3.0 DNA detection (Qubit® dsDNA HS Assay Kit, Life Technologies, U.S.) were used to check the quality and quantity of the DNA after extraction. The amplification of the 16S rRNA gene (V3-V4 region) was performed and followed by high throughput sequencing

using the MiSeq Illumina platform (BaseClear, Leiden, the Netherlands). The primers used were 341F (5'-CCTACGGGNGGCWGCAG-3') and

785R (5'-GACTACHVGGGTATCTAATCC-3'). The analysis of the sequencing data was made by using the QIIME pipeline (version 1.9.0) (Caporaso et al. 2010), the demultiplexing and quality filtering was performed with  $Q=20$ ,  $r=3$ , and  $p=0.75$  parameters. Chimeric sequences were removed using the UCHIME2 (version 9.0) algorithm (Edgar 2016). Sequences were clustered into operational taxonomic units (OTUs) with a 97% similarity as a cutoff, with UCLUST algorithm (Edgar 2010). Singletons were removed and OTUs with an occurrence less than three times in at least one sample were excluded. Taxonomic assignation was performed using the green genes database (gg\_13\_8) (McDonald et al. 2012) with UCLUST. Beta diversity workflows were used to generate microbial community composition and PCoA plots with the phyloseq and ggplot2 packages in the R environment. The statistical significance was tested with the ADONIS test. The differential abundances of OTUs among the mesophilic and thermophilic conditions was tested with the edgeR package (Robinson et al. 2010) with an adjusted p-value (FDR) cutoff of 0.001; the result is shown in a log to fold change plot. OTUs with significant differential abundances towards the thermophilic condition were analyzed with BLAST against the refseq\_rna database to identify the closest related species. The four best hits were determined to build a phylogenetic tree. The sequences alignment was built with MUSCLE software (Edgar 2004), and the alignment was trimmed with Gblocks (Castresana 2000) in the Seaview alignment viewer (Gouy et al. 2010). The phylogenetic analysis was performed with the PhyML 3.0 software (Guindon et al. 2010), using the GTR+G+I+F substitution model with 200 bootstraps, the tree was drawn in FigTree (<http://tree.bio.ed.ac.uk/software/figtree/>). Raw sequences' data have been deposited in the NCBI SRA under accession number SRP110336.

## 6.3 Results and Discussion

### 6.3.1 Effect of temperature shifts on AnMBR performance

High COD and phenol removal efficiencies were achieved up to 45°C after two consecutive temperature shifts of the mesophilic AnMBR (Figure 6.1 A). Under stable reactor operation during days 120-178 and at an OLR of 4.35 gCODL<sup>-1</sup>d<sup>-1</sup>, the effluent COD was in the range of 0.1-2.54 gCODL<sup>-1</sup> and the COD removal efficiencies were about 99.8%-93.7%. The increase in temperature from mesophilic (35°C) to hypermesophilic (45°C) conditions induced a decrease in the COD removal rate of the AnMBR from 0.26±0.02 to 0.19±0.01 gCODgVSS<sup>-1</sup>d<sup>-1</sup>. A similar deterioration trend for phenol degradation was observed (Figure 6.1.B). The phenol conversion rate was about 3.16±0.08 mgPhgVSS<sup>-1</sup>d<sup>-1</sup> at 35 °C and 3.06 mgPhgVSS<sup>-1</sup>d<sup>-1</sup> at 40 °C, decreasing to 2.10±0.49 mgPhgVSS<sup>-1</sup>d<sup>-1</sup> at 45 °C. The COD removal and phenol conversion rates (Table 6.1.) further decreased at 50°C to 0.15±0.02 gCODgVSS<sup>-1</sup>d<sup>-1</sup> and 1.63±0.20 mgPhgVSS<sup>-1</sup>d<sup>-1</sup>, respectively. The phenol removal efficiency was in the range of 61.3-72.7%. After the temperature was shifted to 55°C, the phenol conversion rate remained at about 1.42±0.77 mgPhgVSS<sup>-1</sup>d<sup>-1</sup>, and a COD removal rate of 0.05±0.02 gCODgVSS<sup>-1</sup>d<sup>-1</sup> was observed in the reactor. In contrast to COD to

methane conversion, a more stable phenol conversion along the temperature shifts indicated a lower temperature susceptibility of the phenol degrading process compared to methanogenesis. Apparently, the biomass conversion capacity was disrupted by the temperature shift to thermophilic conditions (50°C -55°C) in combination with the high sodium concentration exposure (16 gNa<sup>+</sup>·L<sup>-1</sup>). Thus, OLR was decreased to 1.86 gCOD·L<sup>-1</sup>·d<sup>-1</sup> to avoid system overloading. Hereafter, on days 227-240 the phenol removal efficiency improved to 76%, while the phenol conversion rate increased to 1.69 mgPh·gVSS<sup>-1</sup>·d<sup>-1</sup>. Phenol conversion rates at 55°C were lower than observed at 35°C, and a phenol removal efficiency of about 50% was achieved at the end of the experiment. Similarly, batch studies performed by Levén and Schnürer (2005, 2010) showed higher phenol conversion rates under mesophilic conditions compared to thermophilic conditions. This possibly can be ascribed to the enzymes involved in the degradation of phenol to benzoate, which are temperature sensitive above 48°C, disturbing the phenol degradation at higher temperatures (Levén and Schnürer 2005). The latter corresponds to the reduction in phenol conversion rates once the temperature was raised above hypermesophilic condition to 50°C (Table 6.1). Another possible explanation is the low microbial diversity of both Archaea and bacteria under thermophilic conditions (Levén et al. 2007).

Table 6.1 Phenol conversion and COD removal rates at 16 gNa<sup>+</sup>·L<sup>-1</sup> after the temperature shifts.

Temperature	Phenol conversion rate [mg Ph · gVSS <sup>-1</sup> · d <sup>-1</sup> ]	COD removal rate [g COD · gVSS <sup>-1</sup> · d <sup>-1</sup> ]
35 °C	3.16 ± 0.08	0.26 ± 0.02
40 °C	3.06 ± 0.10	0.25 ± 0.00
45 °C	2.10 ± 0.49	0.19 ± 0.00
50 °C	1.63 ± 0.20	0.15 ± 0.02
55 °C*	1.42 ± 0.77	0.05 ± 0.03

\*Under thermophilic condition phenol conversion rate increased to 1.69 mgPh·gVSS<sup>-1</sup>·d<sup>-1</sup>.

The SMA increased about 23% at a temperature of 40 °C in comparison with 35°C (0.26±0.02 gCOD-CH<sub>4</sub>·gVSS<sup>-1</sup>·d<sup>-1</sup>) (Table 6.2.). At 45 °C, a lower value than at 35 °C was found in agreement with the observed decrease in COD removal efficiency in the reactor. A minimum value of 0.04±0.01 gCOD-CH<sub>4</sub>·gVSS<sup>-1</sup>·d<sup>-1</sup> was observed at 55°C which is in line with the poor COD removal observed in the AnMBR right after the shift to this temperature. Furthermore, a similar decrease was observed by Fang et al. (2006) who reported SMA values in UASB reactors treating phenolic wastewater of about 0.24 gCOD-CH<sub>4</sub>·gVSS<sup>-1</sup>·d<sup>-1</sup> and 0.09 gCOD-CH<sub>4</sub>·gVSS<sup>-1</sup>·d<sup>-1</sup> at 37°C and 55 °C, respectively. The overall reactor biogas production decreased when temperature increased from 35 °C to 55 °C, as shown in Figure S6.1. However, the methane production rate did not recover after 50 days of operation at 55°C in accordance with a low COD removal efficiency of 38%. Likewise,



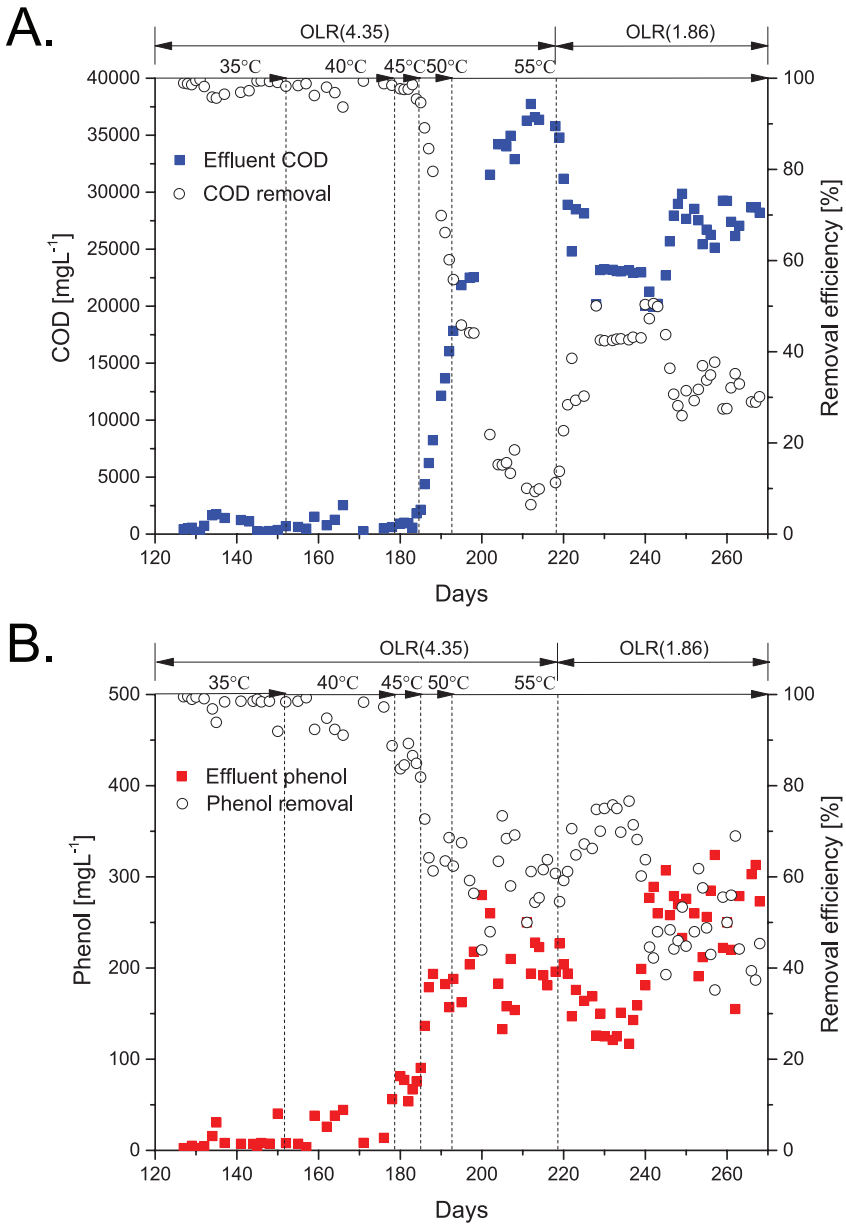


Figure 6.1 AnMBR performance under mesophilic, hyper-mesophilic and thermophilic conditions at 16 gNa<sup>+</sup>.L<sup>-1</sup>.  
 1. A. COD removal efficiency. B. Phenol removal efficiency.

Kim and Lee (2016) pointed out that a temperature change between 45 °C and 50 °C had a critical impact on the methanogenic activity due to a severe restructuring of the reactor's microbial community, particularly of methanogens. A complete shift in the methanogenic subpopulations was also found in previous research, shifting a mesophilic UASB reactor to hyper-mesophilic and thermophilic conditions (Macario et al. 1991, van Lier et al. 1992, van Lier et al. 1993).

Furthermore, the biomass concentration of the AnMBR reactor rapidly dropped to 8.98 gVSS·L<sup>-1</sup> and 13.6 gTSS·L<sup>-1</sup> when 55 °C was reached. The VSS:TSS ratio decreased from 0.77 at 35 °C to 0.59 once the operation at 55 °C was stable at day 268 (see Table 6.2).

Table 6.2 SMA during the temperatures shifts from mesophilic to thermophilic conditions.

Temperature	Days	SMA [gCOD-CH <sub>4</sub> gVSS <sup>-1</sup> d <sup>-1</sup> ]	VSS [g·L <sup>-1</sup> ]	VSS:TSS ratio
35 °C	131	0.26±0.02	16.63 ± 0.07	0.77
35 °C	151	0.29±0.22	16.87± 1.18	0.78
40 °C	179	0.32±0.00	22.10 ± 0.56	0.77
45 °C	184	0.17±0.01	22.72 ± 0.49	0.64
50 °C	191	0.27±0.00	27.76 ± 1.37	0.63
55 °C	214	0.04±0.01	9.65 ± 5.30	0.60
55 °C	241	N.D	8.98 ± 0.21	0.66

\* At 268 days the VSS concentration was 9.5 g L<sup>-1</sup> and the VSS:TSS ratio was 0.59.

## 6.3.2 Biomass properties affected by temperature shifts

### 6.3.2.1 Extracellular polymeric substances (EPS) and soluble microbial products (SMP)

Polysaccharides (PS) and proteins (PN) are accepted as primary constituents of SMP and EPS (Lin et al. 2014). The total SMP concentration was about 16.1 mg.gVSS<sup>-1</sup> at a temperature of 35 °C. A notable increase was observed from 50.5±0.5 mg.gVSS<sup>-1</sup> at 45°C to a maximum of 135.1±2.0 mg.gVSS<sup>-1</sup> with a soluble PN content of 113.0±1.7 mg.gVSS<sup>-1</sup> at 55°C (Table 6.3).

The aforementioned results suggest that if an AnMBR reactor is operated under mesophilic conditions and becomes suddenly exposed to hyper-mesophilic or thermophilic conditions, the observed overall methane production rate is also an indicative for the preserved phenol

bioconversion capacity. The temperature shifts caused disturbances to the overall mesophilic AnMBR performance due to its impact on the biomass properties, filtration performance and microbial population structure as explained in the following sections.

Table 6.3 SMP and EPS during the temperatures shifts from mesophilic to thermophilic conditions. PN: Proteins, PS: Polysaccharides

T °C (Day)	SMP-PN [mg· gVSS <sup>-1</sup> ]	SMP-PS [mg· gVSS <sup>-1</sup> ]	SMP PN:PS ratio	Total SMP [mg· gVSS <sup>-1</sup> ]	EPS-PN [mg· gVSS <sup>-1</sup> ]	EPS-PS [mg· gVSS <sup>-1</sup> ]	EPS PN:PS ratio	Total EPS [mg· gVSS <sup>-1</sup> ]
35 (134)	5.3±0.1	10.7±0.7	0.5	16.0±0.6	67.1±0.3	13.6±1.1	5.0	80.7±0.8
35 (152)	5.3±0.0	10.8±1.1	0.5	16.1±1.1	49.3±0.1	8.4±0.1	5.8	57.8±0.3
40 (178)	35.6±0.1	11.6±0.0	3.1	47.2±0.1	34.3±2.4	8.2±0.9	4.0	42.5±3.3
45 (185)	40.7±0.0	9.8±0.5	4.2	50.5±0.5	68.7±9.3	10.5±1.3	7.4	77.9±10.5
50 (192)	34.6±0.1	10.9±0.8	3.2	45.4±0.8	75.1±2.4	14.0±0.8	5.4	89.1±1.6
55 (215)	102.9±0.2	18.6±1.6	5.5	121.6±1.3	92.2±0.7	12.9±0.4	7.3	104.9±1.1
55 (241)	113.0±1.7	22.1±0.3	5.1	135.1±2.0	35.8±5.3	17.3±1.6	2.1	53.1±6.9

The observed increase is in agreement with Visvanathan et al. (2007) who found that thermophilic condition induces higher SMP production. It is noteworthy that the soluble PN to PS ratio increased about ten times from mesophilic to thermophilic conditions. Exoenzymes in the biomass and cell lysis products that were likely caused by the temperature change might be responsible for the higher amount of PN compared to PS (Neyens et al. 2004). However, overall the EPS concentration from both the PN and PS increased, but not gradually towards thermophilic condition in contrast to what other studies have shown (Al-Amri et al. 2010, Lin et al. 2009). The latter can be attributed to the fact that the exposure time of biomass to each of the imposed temperatures was different. At 55 °C a maximum total EPS was found of about 104.9±1.1 mg.gVSS<sup>-1</sup> whereas it was 57.8±0.3 mg.gVSS<sup>-1</sup> at 35°C.

Likewise, the variation of the EPS fingerprint can be observed in the FT-IR spectra in Figure S2. The peak around 3220 cm<sup>-1</sup> is attributed to the O-H stretching of the alcohols from PS and phenol (Dereli et al. 2015a, Wang et al. 2009). The two peaks at 1640 cm<sup>-1</sup> and 840 cm<sup>-1</sup> are due to N-H, C-N, and C=O vibration and stretching, and N-H wagging which are characteristic of secondary PN structures (Gupta and Thakur 2015). The presence of a peak at 1000 cm<sup>-1</sup> is evident in all the spectra and is due to the =C-H bending and C-O stretching of the alkanes from the carbohydrates or carbohydrates like substances (Sajjad and Kim 2015). The peaks at 1400 cm<sup>-1</sup> and 1570 cm<sup>-1</sup> are

due to C-H bending of the alkanes and alkenes from PS. At higher temperatures, the intensity of the peaks increased, especially the region around  $1500\text{ cm}^{-1}$  typical of PN. The latter is also in agreement with the observed higher EPS concentrations because at more elevated temperatures their production might also be stimulated as a mechanism of protection for microorganisms. Overall, more content of microbial substances, especially PN, was observed at higher temperatures in the AnMBR.

### 6.3.2.2 Particle size distribution

The median biomass particle size D50 was  $89.4\text{ }\mu\text{m}$  at  $35^\circ\text{C}$  on day 134 (Figure 6.2). Along with the temperature increase to  $40^\circ\text{C}$  and  $50^\circ\text{C}$ , the median particle size decreased to  $75.7\text{ }\mu\text{m}$  and  $74.6\text{ }\mu\text{m}$ , on days 178 and 192, respectively. The gradual but fast increase from  $45^\circ\text{C}$  to  $55^\circ\text{C}$  caused biomass decay and floc breakage resulting in smaller particle size in the AnMBR as reported before by Gao et al. (2011). At thermophilic conditions, the median particle size D50 decreased to  $22.4\text{ }\mu\text{m}$  and  $21.0\text{ }\mu\text{m}$  on days 220 and 239, respectively. The mean particle size did not drop further until the end of the study. The observed decrease in biomass particle size of about 77% very likely contributed to the accumulation of fine particles leading to higher cake compactness. Increased cake layer compaction resulted in an increased transmembrane pressure (TMP) and membrane resistance at  $55^\circ\text{C}$ .

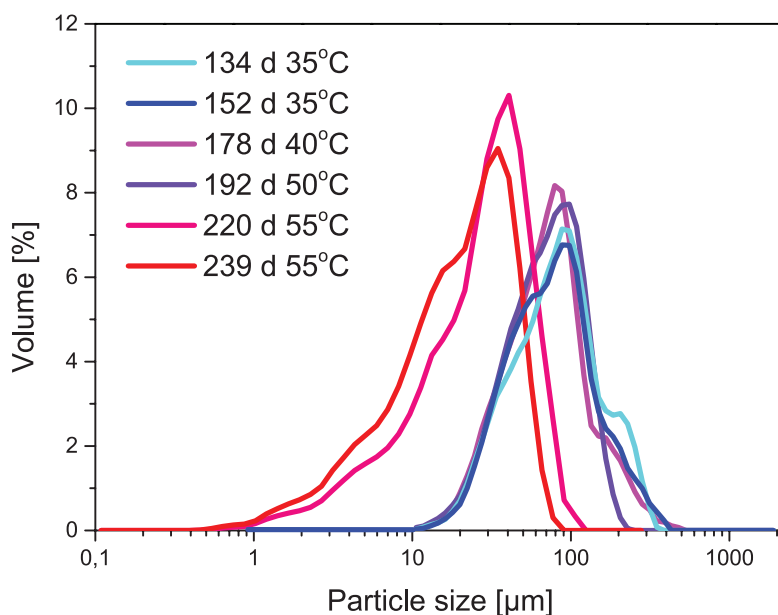


Figure 6.2 Biomass particle size distribution at temperatures  $35^\circ\text{C}$ ,  $40^\circ\text{C}$ ,  $50^\circ\text{C}$  and  $55^\circ\text{C}$ .

### 6.3.3 Effect of temperature shifts on membrane filtration performance and biomass filterability

The mesophilic AnMBR exhibited a satisfactory filtration performance with TMP lower than 250 mbar between mesophilic and hypermesophilic conditions (Figure 6.3 A.). The stable filtration performance was attributed to the operation far below the critical flux which was determined to be 26.0 L.m<sup>2</sup>.h<sup>-1</sup> following the methods explained by Jeison and van Lier (2007). However, the TMP was negatively affected by the temperature shift to 55°C and increased between 200 and 240 days to a maximum of 785 mbar. During this period, the membrane resistance was as high as  $5.18 \times 10^{13} \text{ m}^{-1}$ . The appearance of small biomass particles and high protein concentration seemed to have a remarkable influence on the cake layer compaction that affected the filtration performance. The critical flux measured after reaching 55 °C was about 6.8 L.m<sup>2</sup>.h<sup>-1</sup> indicating that the increased temperature resulted in a 74% decrease in the critical flux. Due to the fact the operational flux was close to the critical flux impacting the filtration performance negatively, a flux reduction was applied on day 218 resulting in a decrease in TMP and membrane resistance. The latter confirms that cake consolidation and compaction was the main explanation for the TMP and overall membrane resistance increase. Similarly, Jeison and van Lier (2008) showed that thermophilic operation (55 °C) causes a significant decrease in the biomass particle size in a submerged AnMBR and consequently a fast reduction in critical flux from 20 to 6–7 L.m<sup>2</sup>.h<sup>-1</sup>.

As cake layer formation is the most significant fouling mechanism in the AnMBR, the specific resistance to filtration (SRF) may also refer to the quality of the cake accumulated on the membrane surface and therefore was also determined as an indication (Dereli et al. 2014). The SRF decreased from  $151.7 \pm 2.2 \cdot 10^{13} \text{ m.kg}^{-1}$  at 35°C to  $39.8 \pm 0.4 \cdot 10^{13} \text{ m.kg}^{-1}$  at 45°C and  $23.6 \pm 0.3 \cdot 10^{13} \text{ m.kg}^{-1}$  at 50°C (Figure 6.3 B).

This decrease is attributed to the disruption of biomass flocs between 35°C and 50°C leading to smaller particle sizes, a less porous, more compact cake layer, and consequently lower SRF values. A decrease of SRF is in agreement with the observed biomass particle size reduction and soluble protein concentration increase (Lin et al. 2011). Correspondingly, the normalized capillary suction time (CST) values followed a similar trend than SRF. The CST ranged from  $72.3 \pm 10.5 \text{ s.L.gTSS}^{-1}$  at 35°C to  $44.4 \pm 6.5 \text{ s.L.gTSS}^{-1}$  at 45°C. At thermophilic conditions, the SRF increased to  $187.8 \pm 12.7 \cdot 10^{13} \text{ m.kg}^{-1}$ , concomitantly the CST increased to  $68.0 \pm 2.0 \text{ s.L.gTSS}^{-1}$  on day 241.

The increased SRF values indicated a cake layer with less compactness once the microbial decay products, SMP, and solids concentrations were steadied at 55°C. It can be concluded from these results that the shifts above hypermesophilic conditions (45°C) deteriorated the biomass filterability and could increase the fouling potential causing the observed detriment of membrane filtration performance.

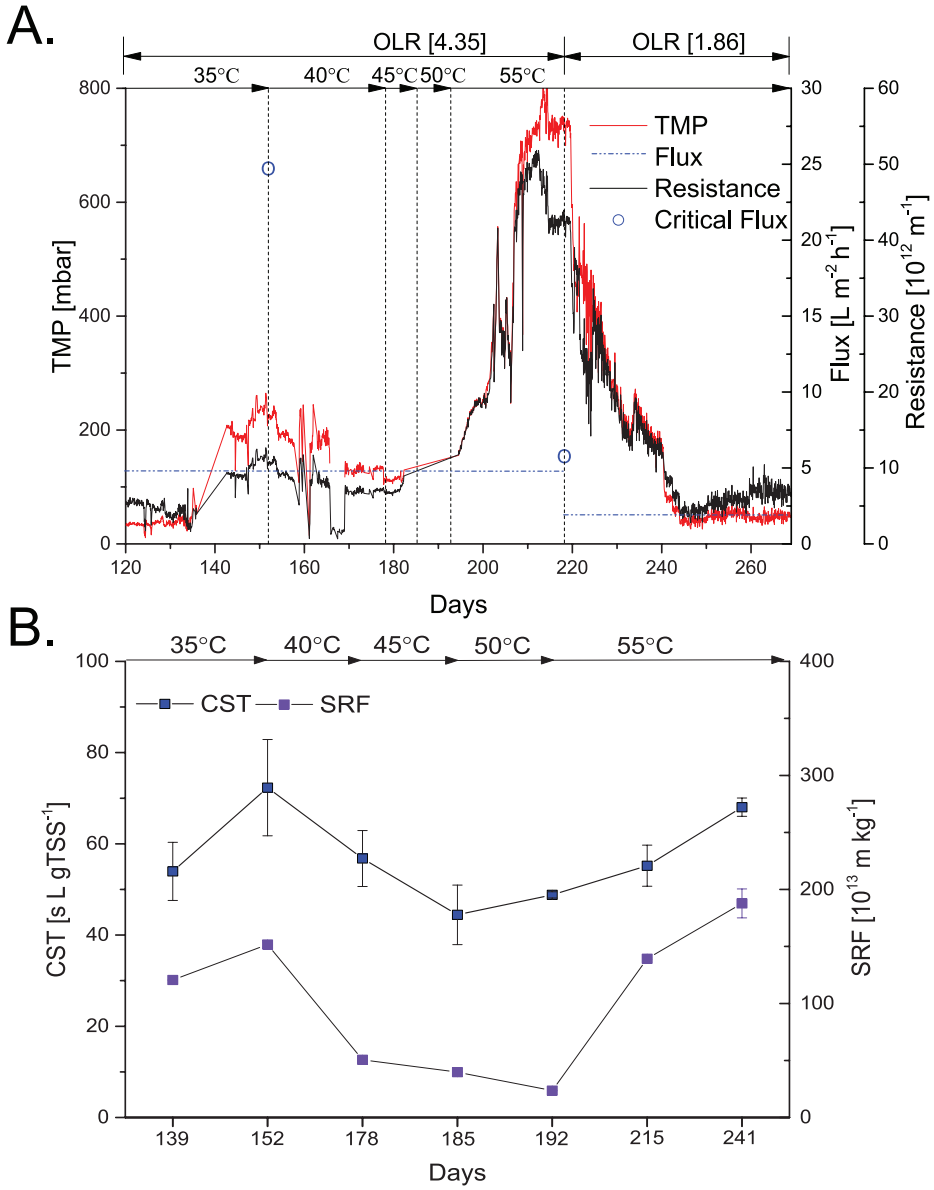


Figure 6.3 A. TMP, membrane filtration resistance, and flux in the AnMBR. B. Biomass filterability: SRF, and CST at different operational temperatures.

### 6.3.4 Microbial community structure dynamics

Microbial community structure dynamics as a response to the temperature changes of the reactor biomass was analyzed by next-generation sequencing targeting the 16S rRNA gene. The principal coordinates' analysis indicated that the microbial community in the AnMBR experienced significant changes due to the consecutive shifts from mesophilic to hypermesophilic, and thermophilic conditions (Figure S6.3.A). Furthermore, ADONIS statistical test (Table 6.4) demonstrated significant differences ( $p < 0.005$ ) of the microbial community along the temperature change ( $R^2 = 0.31$ ).

Table 6.4 Statistical significance for temperature by ADONIS analysis (using unweighted unifracs distance) in the QIIME pipeline.

Factor	R <sup>2</sup>	Pr(>F)
Temperature [°C]	0.31	0.0019
Phenol specific loading rate [mgPh·gVSS <sup>-1</sup> ·d <sup>-1</sup> ]	0.21	0.009
COD specific loading rate [gCOD·gVSS <sup>-1</sup> ·d <sup>-1</sup> ]	0.14	0.1249

At the phylum level (Figure 6.4 A), Firmicutes (41.08%), Euryarchaeota (32.00%), OP9 (6.50%), Chloroflexi (4.66%), Proteobacteria (4.42%) and Synergistetes (3.09%) were the dominant microorganisms after the long-term operation at 35°C. Firmicutes, Proteobacteria and Chloroflexi, were recently reported as main phyla in anaerobic reactors treating phenolic wastewater (Na et al. 2016, Wang et al. 2017b). In this study, all Firmicutes fell within the Clostridia class (Figure 6.4 B), the majority of these Clostridia belonged to the *Clostridium* genus (26.83%) (Figure 6.4 C). Putative phenol degraders under low phenol concentrations in AnSBRs are Clostridia-like (Rosenkranz et al. 2013). Chloroflexi were classified into the Anaerolineae class. Rosenkranz et al. (2013) also indicated that Anaerolineae has the highest proportion in mesophilic AnSBRs treating phenol. Methanomicrobia were mostly all assigned to the *Methanosaeta* genus (20.15%), and Methanobacteria (11.54%) were all assigned to the *Methanobacterium* genus. At 40°C, the Proteobacteria phylum decreased significantly, and both Gammaproteobacteria and Deltaproteobacteria were affected. Interestingly, Wang et al. (2017b) indicated that the decrease in relative abundance of Proteobacteria, and Chloroflexi was observed with a reduction in mesophilic phenol conversion. At 45°C, the predominant phyla were shifted.

The abundance of Methanomicrobia (*Methanosaeta* 28.89%) increased, and Firmicutes (28.27%) decreased significantly. At this temperature, a higher variation in the relative abundance in the AnMBR from the main phyla was observed concomitantly with the decrease in phenol conversion rate of the reactor. Once the temperature rose to 50°C, the increase in relative abundance of the genus *Kosmotoga* was remarkable, which is known to grow over a wide high-temperature range and tolerate highly saline conditions. At 55°C the predominant phyla were similar as at 35°C except for Thermotogae that increased significantly from 0.45% at 35°C to 6.36% at 55°C. Overall, the relative abundance of methanogens was stable, and in the case of OP9, Synergistetes and Thermotogae increased. Recently, Synergistetes was suggested by Poinier et al. (2016) as an early warning indicator

of phenol inhibition towards anaerobic microbiota. On the contrary, the abundance of Firmicutes and Proteobacteria decreased. Specifically, microorganisms from these two phyla have been reported to have the capacity of syntrophically degrading aromatic compounds including phenol, such as the genera *Syntrophorhabdus* and *Pelotomaculum* (Chen et al. 2008b, Nobu et al. 2015). A syntrophic association between phenol carboxylating, benzoate degrading and hydrogenotrophic methane-producing microorganisms is required for the complete phenol degradation to methane. There was no evidence of having *Syntrophorhabdus* in the biomass, as was recently observed at high salinity under mesophilic conditions (Wang et al. 2017b), but there were OTUs with high similarity to *Pelotomaculum* at thermophilic conditions. Moreover, a decrease in abundance of *Methanobacterium* was observed while the reactor performance decreased, indicating the importance of an  $H_2$ -scavenging methanogen partner in syntrophic association with phenol degraders (Qiu et al. 2008).

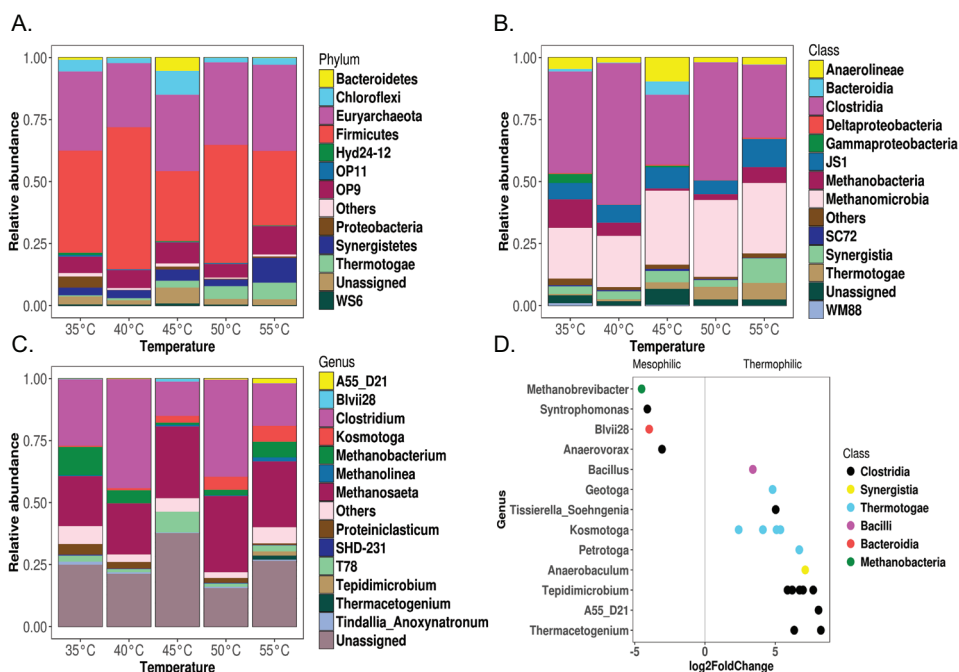


Figure 6.4 Analysis of microbial community structure dynamics due to operational temperature. A. OTUs relative abundance at the phylum level. B. OTUs relative abundance at the class level. C. OTUs relative abundance at the genus level. D. Log<sub>2</sub>fold change plot for the differential abundance of the OTUs among the mesophilic and thermophilic conditions at (p-value < 0.001).

The differential abundances of the OTUs between mesophilic and thermophilic conditions were calculated and described in a log<sub>2</sub> fold change plot at class and genus level (Figure 6.4 D). 21 OTUs that have differential abundance were identified. The genera *Methanobrevibacter*, *Syntrophomonas*, *Blvii28*, and *Anerovorax*; were up to 9 times higher in abundance at mesophilic than compared to



thermophilic conditions. Conversely, the genera *Thermoacetogenium*, *A55\_D21*, *Tepidimicrobium*, *Anaerobaculum*, and *Petrotoga* increased in a range from 12 to 16 times under thermophilic conditions. The abundance of these OTUs is shown in Figure S6.3 B. From these OTUs, a phylogenetic tree was built with the four best hits of each (Figure 6.5). The analysis grouped 11 OTUs within clades with species that have been reported in phenolic wastewater treatment reactors, oil production sites, terephthalic acid, and coking wastewater treatment processes (see Table S6.1).

The phylogenetic distribution of the microbial community and functionality was affected by the temperature increase in the AnMBR. However, it is still unclear whether operating the reactor under hypermesophilic (40°C to 45°C) or thermophilic conditions would maximize the phenol conversion rate and corresponding microbial syntrophic associations. This is the first time that an AnMBR has been used to explore the degradation of phenol at high temperature and high salinity. Further research is needed to account the long-term effects of thermophilic operation on the phenol bioconversion rate to identify whether it increases to the same or higher levels than under mesophilic conditions. Also, long-term adaptation at 55°C could further reveal the differences in microbial population structure with similar functionality in comparison to the operation at 35°C. Based on the overall effects of the shifts from mesophilic to hyper-mesophilic and subsequent thermophilic operation, this study suggests that highly saline phenolic wastewaters are attainable to be treated in a mesophilic AnMBR within the hyper-mesophilic temperature range without the need of long-term acclimation. Although the exact temperature span of the species involved are not known and net growth yields will drop to a minimum reaching the limits of the growth temperature, operation at hypermesophilic conditions e.g. 42-45°C will bring operational energy benefits when treating high temperature wastewaters, especially when opting for process water reuse.

## 6.4 Conclusions

This study was undertaken to evaluate the temperature susceptibility of the phenol bioconversion capacity over a range of 35°C to 55 °C in an AnMBR at high salinity conditions. Due to the temperature shifts over a range of 35°C to 55 °C in an AnMBR operated at 16 gNa<sup>+</sup>·L<sup>-1</sup>, the COD removal and phenol conversion rates decreased from 0.26 gCOD·gVSS<sup>-1</sup>·d<sup>-1</sup> to 0.075 gCOD·gVSS<sup>-1</sup>·d<sup>-1</sup>, and 3.16 mgPh·gVSS<sup>-1</sup>·d<sup>-1</sup> to 1.69 mgPh·gVSS<sup>-1</sup>·d<sup>-1</sup>, respectively. Results clearly showed that the phenol degradation process was less susceptible for the temperature shifts than methanogenesis. The membrane filtration performance was negatively affected by the temperature increases coinciding with a 77% particle size decrease and a higher content of microbial protein-like substances. Microbial community abundance of known phyla for syntrophic phenol degradation decreased as the temperature was shifted. Twenty-one OTUs were identified with differential abundance between mesophilic and thermophilic operation, and eleven of them were similar to species reported in aromatic degradation processes. These findings suggest that under mesophilic and hyper-mesophilic conditions, the phenol degradation capacity of the AnMBR at high salinity was more stable compared to thermophilic conditions. Therefore, by controlling the temperature at the lower limit of the hyper-mesophilic range, operation at e.g. 42-45°C will bring operational

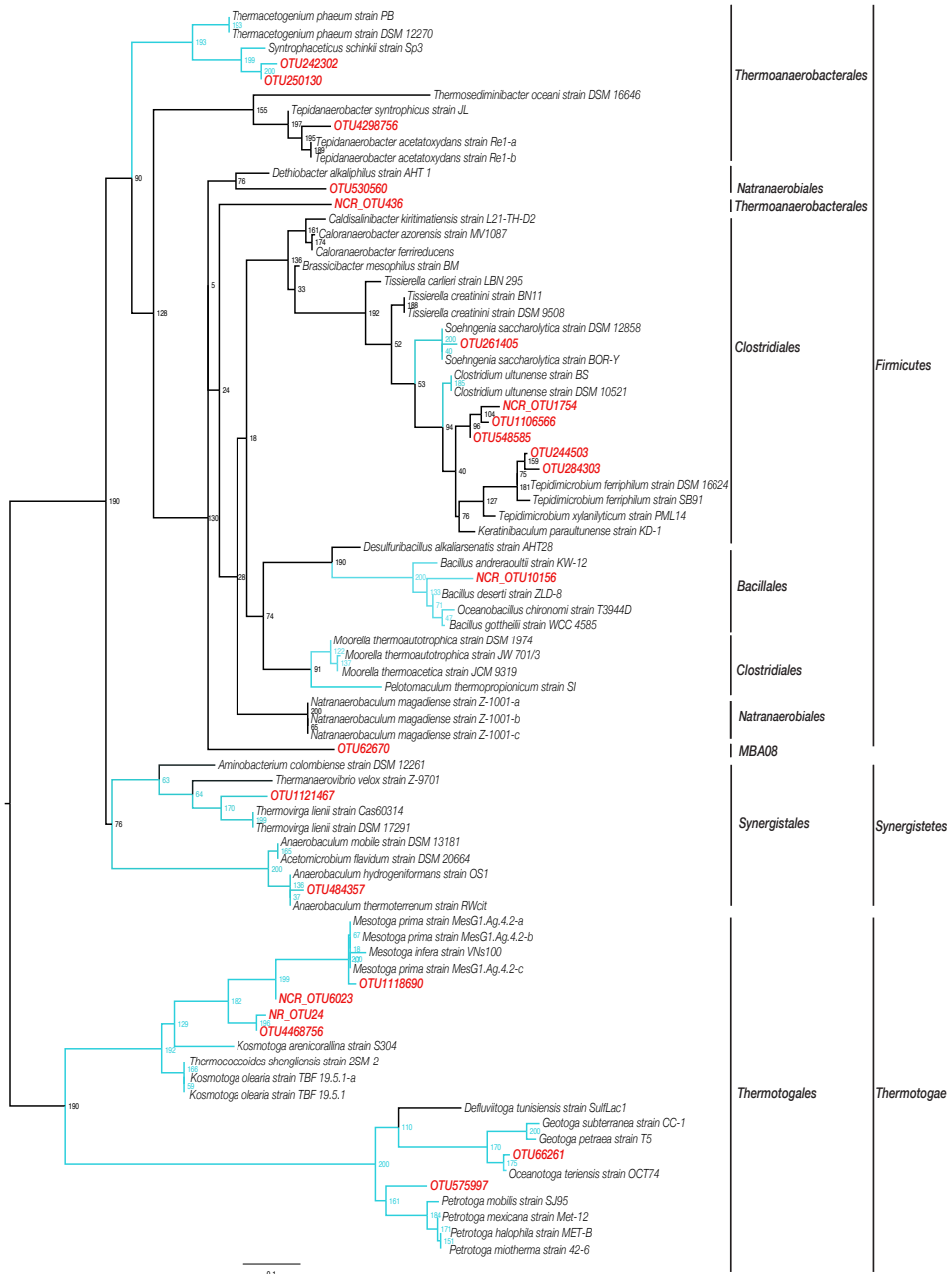


Figure 6.5 Phylogenetic tree of OTUs with significant differential abundances towards thermophilic (55°C) phenol degradation. 0.1 horizontal scale shows the length of branch that represents a genetic change of 0.1. In red: 21 identified OTUs. In light blue: clades with 11 OTUs close to species reported in the process of phenol and similar aromatic compounds degradation.

energy benefits when treating high temperature wastewaters opting for water reuse. Therefore, and considering that the phenol conversion capacity is preserved, it is certainly worthwhile to further explore the treatment potentials at the hyper-mesophilic temperature range.

### Supplementary Information

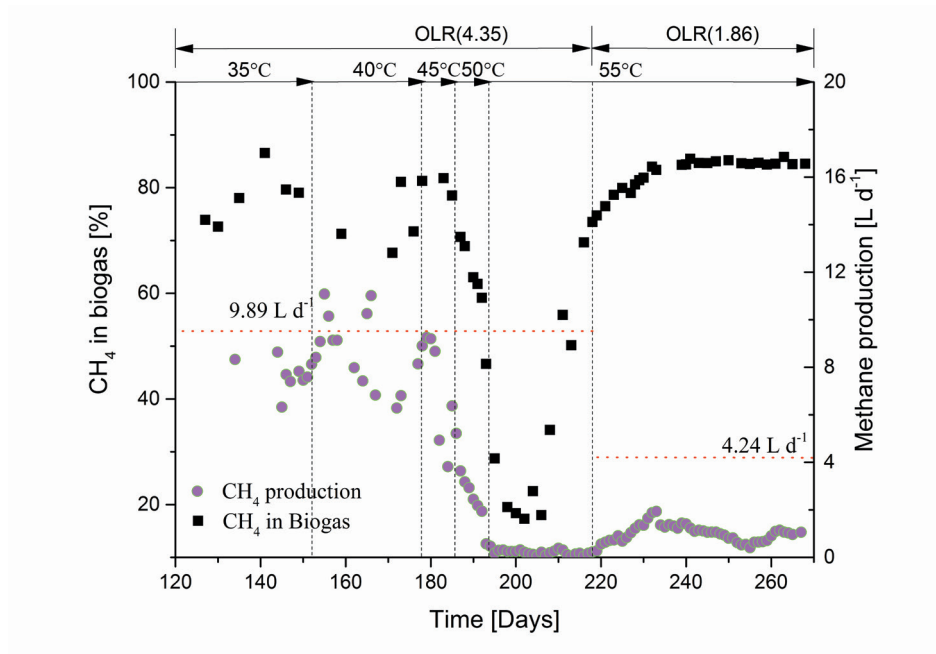


Figure S6.1. Biogas composition and methane production.

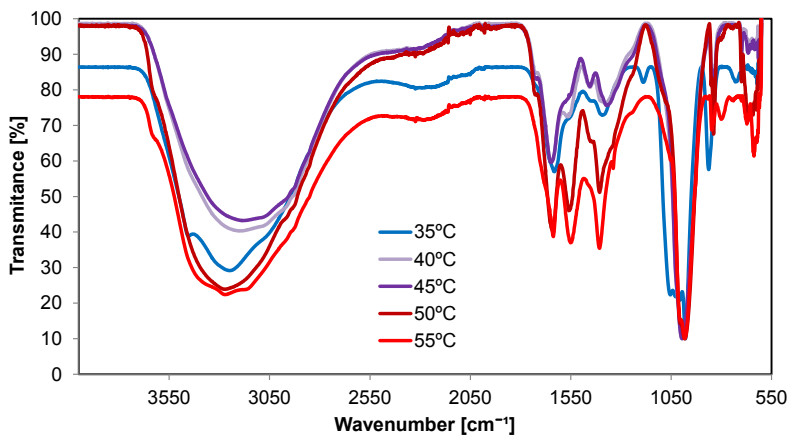


Figure S6.2. FT-IR spectra of the EPS extracted from the AnMBR.

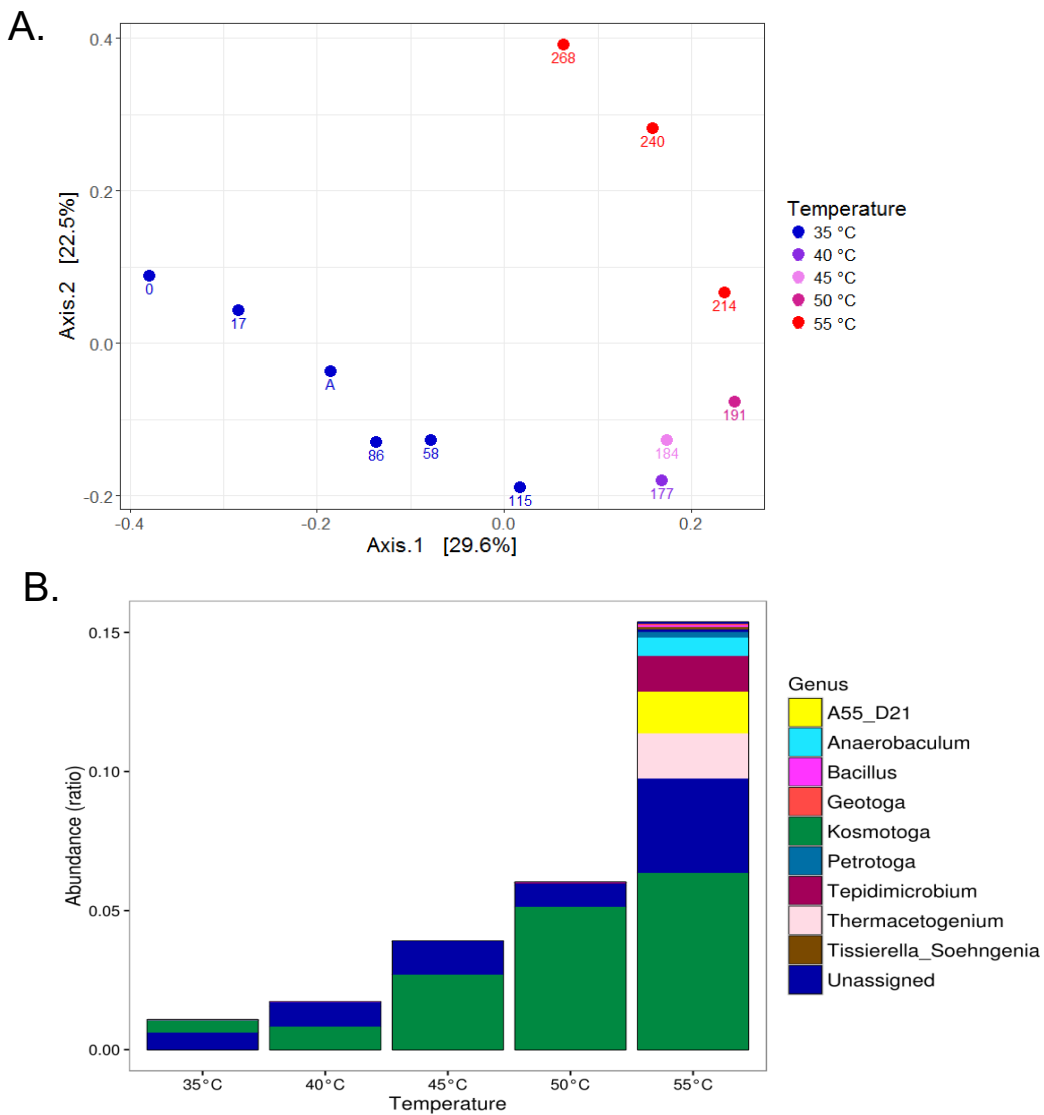


Figure S6.3. Analysis of microbial community structure dynamics due to operational temperature. A. Principal coordinates analysis (PCoA) between samples diversity at different temperature of operation determined via unweighted unifrac. Sample A belongs to the acclimation period to high salinity before starting this study. B. OTUs at genus level increasing its relative abundance with temperature.

Table S6.1. OTUs with four best sequence hits based on similarity. Species in the AnMBR involved in phenol degradation related studies are referenced.

OTU ID	Best Sequence hit ID	Specie	Similarity	Reference
OTU1106566	NR_117379.1	<i>Clostridium sulturnense</i> strain DSM 10521	96.14	(Chen et al. 2009)
	NR_026531.1	<i>Clostridium sulturnense</i> strain BS	96.14	(Chen et al. 2009)
	NR_118544.1	<i>Keratibaculum paraultunense</i> strain KD-1	95.23	
	NR_133054.1	<i>Tissierella carlberi</i> strain LBN 295	94.31	
OTU1118690	NR_102952.1	<i>Mesotoga prima</i> strain MesG1_Ag4.2	99.14	
	NR_117755.1	<i>Mesotoga prima</i> strain MesG1_Ag4.2	98.93	
	NR_117754.1	<i>Mesotoga prima</i> strain MesG1_Ag4.2	98.93	
	NR_117646.2	<i>Mesotoga infera</i> strain VNs100	97.86	(Mei et al. 2016)
OTU1121467	NR_074606.1	<i>Thermoirga lieni</i> strain DSM 17291	93.45	(Dahle and Birkeland 2006)
	NR_043522.1	<i>Thermoirga lieni</i> strain Cas60314	93.45	(Dahle and Birkeland 2006)
	NR_074624.1	<i>Aminobacterium colombiense</i> strain DSM 12261	90.11	
	NR_104765.1	<i>Thermanaerobrio velox</i> strain Z-9701	89.24	
OTU244503	NR_117380.1	<i>Tepidimicrobium ferrophilum</i> strain DSM 16624	99.32	
	NR_043077.1	<i>Tepidimicrobium ferrophilum</i> strain SB91	98.41	
	NR_116042.1	<i>Tepidimicrobium sylvaniticum</i> strain PML14	95.44	
	NR_118544.1	<i>Keratibaculum paraultunense</i> strain KD-1	94.31	
OTU242302	NR_116297.1	<i>Syntrophoaceticus schinkii</i> strain Sp3	95.71	
	NR_074723.1	<i>Thermacetogenium placuum</i> strain DSM 12270	92.10	(Narihira et al. 2015)
	NR_024688.1	<i>Thermacetogenium placuum</i> strain PB	92.10	(Narihira et al. 2015)
OTU250130	NR_074685.1	<i>Pelotomaculum thermopropionicum</i> strain SI	86.97	(Abu Laban et al. 2009, Chen et al. 2008a, Kleinsteuber et al. 2008)
	NR_116297.1	<i>Syntrophoaceticus schinkii</i> strain Sp3	96.61	

NR_074723.1	<i>Thermacetogenium phaeum</i> strain DSM 12270	93.00	(Narihiro et al. 2015)
NR_024688.1	<i>Thermacetogenium phaeum</i> strain PB	93.00	(Narihiro et al. 2015) (Abu Laban et al. 2009, Chen et al. 2008a, Kleinsteuber et al. 2008)
NR_074685.1	<i>Pelotomaculum thermopropionicum</i> strain SJ	87.87	(Cheng et al. 2014, Joshi et al. 2016)
OTU261405	<i>Saehngenia saccharolytica</i> strain DSM 12858	98.86	(Cheng et al. 2014, Joshi et al. 2016)
NR_025761.1	<i>Saehngenia saccharolytica</i> strain BOR-Y	98.86	(Cheng et al. 2014, Joshi et al. 2016)
NR_117155.1	<i>Tissierella creatinini</i> strain DSM 9508	94.08	
NR_104805.1	<i>Tissierella creatinini</i> strain BN11	94.08	
OTU284303	<i>Tepidimicrobium ferriphilum</i> strain DSM 16624	98.63	
NR_043077.1	<i>Tepidimicrobium ferriphilum</i> strain SB91	97.72	
NR_116042.1	<i>Tepidimicrobium sylvaniticum</i> strain PML14	94.76	
NR_118544.1	<i>Keratibaculum parvulturnense</i> strain KD-1	93.62	
OTU4298756	<i>Tepidanaerobacter acetatoydans</i> strain Re1	97.05	
NR_116298.1	<i>Tepidanaerobacter acetatoydans</i> strain Re1	96.82	
NR_040966.1	<i>Tepidanaerobacter syntrophicus</i> strain JL	96.59	
NR_074461.1	<i>Thermosedimentibacter oceanii</i> strain DSM 16646	86.49	
OTU484357	<i>Anaerobaculum hydrogeniformans</i> strain OS1	99.10	(Gieg et al. 2010)
NR_036784.1	<i>Anaerobaculum thermoterrenum</i> strain RWit	98.87	(Meehichi et al. 1999)
NR_102954.1	<i>Anaerobaculum mobile</i> strain DSM 13181	96.84	(Leven and Schnürer 2010)
NR_104752.1	<i>Acetomicrobium flavidum</i> strain DSM 20664	96.84	
OTU4468756	<i>Kosmologa olearia</i> strain TBF 19.5.1	90.41	(Dippio et al. 2009)
NR_044583.1	<i>Kosmologa olearia</i> strain TBF 19.5.1	90.41	(Dippio et al. 2009)
NR_116264.1	<i>Thermococoides shengliensis</i> strain 2SM-2	90.41	
NR_113012.1	<i>Kosmologa arenivorallina</i> strain S304	89.74	(Pattananuwat et al. 2013)

OTU530560	NR_044205.1	<i>Dethiobacter alkalthophilus</i> strain AHT1	90.05
	NR_135713.1	<i>Natranaerobaculum magadiense</i> strain Z-1001	89.62
	NR_135712.1	<i>Natranaerobaculum magadiense</i> strain Z-1001	89.62
	NR_135711.1	<i>Natranaerobaculum magadiense</i> strain Z-1001	89.62
OTU548585	NR_117379.1	<i>Clostridium ulunense</i> strain DSM 10521	96.82
	NR_026531.1	<i>Clostridium ulunense</i> strain BS	96.82
	NR_118544.1	<i>Keratinibaculum parvultunense</i> strain KD-1	95.90
	NR_116042.1	<i>Tepidimicrobium sylvaniticum</i> strain PML14	94.76
OTU575997	NR_043201.1	<i>Petrologa halophila</i> strain MET-B	93.04
	NR_074401.1	<i>Petrologa mobilis</i> strain SJ95	92.83
	NR_104764.1	<i>Petrologa mintherma</i> strain 42-6	92.83
	NR_029058.1	<i>Petrologa mexicana</i> strain Met-12	92.83
OTU62670	NR_136424.1	<i>Caldivalvibacter keritmatiensis</i> strain L21-TT-D2	89.17
	NR_108841.1	<i>Brassicibacter mesophilus</i> strain BM	89.17
	NR_135860.1	<i>Caloranaerobacter ferrireducens</i>	88.94
	NR_028919.1	<i>Caloranaerobacter azorensis</i> strain MV1087	88.71
OTU66261	NR_116378.1	<i>Oceanologa teriensis</i> strain OCT74	98.91
	NR_029145.2	<i>Geotoga subterranea</i> strain CC-1	91.72
	NR_104910.1	<i>Geotoga petraea</i> strain T5	91.74
	NR_122085.1	<i>Defluviitoga tunisiensis</i> strain Sulflac1	86.80
NR_OTU24	NR_074712.1	<i>Kosmotoga olearia</i> strain TBF 19.5.1	90.19
	NR_044583.1	<i>Kosmotoga olearia</i> strain TBF 19.5.1	90.19
	NR_116264.1	<i>Thermococoides sbongliensis</i> strain 2SM-2	90.19
	NR_113012.1	<i>Kosmotoga areniconallina</i> strain S304	89.72



NCR_OTU10156	NR_043700.1	<i>Oceanobacillus chironomi</i> strain T3944D	94.62	(Banerjee and Ghoshal 2017)
	NR_108491.1	<i>Bacillus gothelii</i> strain WCC 4585	94.21	(Banerjee and Ghoshal 2017)
	NR_144713.1	<i>Bacillus andreaeaultii</i> strain KW-12	94.19	(Banerjee and Ghoshal 2017)
	NR_117383.1	<i>Bacillus deserti</i> strain ZLD-8	94.21	(Banerjee and Ghoshal 2017)
NCR_OTU1754	NR_117379.1	<i>Clostridium ulunense</i> strain DSM 10521	96.14	(Chen et al. 2009)
	NR_026531.1	<i>Clostridium ulunense</i> strain BS	96.14	(Chen et al. 2009)
	NR_118544.1	<i>Keratinibaculum parvultunense</i> strain KD-1	95.23	
	NR_133054.1	<i>Tissierella caribei</i> strain LBN 295	93.85	
NCR_OTU436	NR_119088.1	<i>Moorella thermoautotrophica</i> strain DSM 1974	86.75	(Letowski et al. 2001)
	NR_113196.1	<i>Moorella thermoacetica</i> strain JCM 9319	86.54	
	NR_126221.1	<i>Desulfuribacillus alkaliarsenatis</i> strain AHT28	86.24	
	NR_029144.1	<i>Moorella thermoautotrophica</i> strain JW 701/3	86.33	(Letowski et al. 2001)
NCR_OTU6023	NR_117755.1	<i>Mesotoga prima</i> strain MesG1.Ag4.2	92.74	
	NR_117754.1	<i>Mesotoga prima</i> strain MesG1.Ag4.2	92.74	
	NR_102952.1	<i>Mesotoga prima</i> strain MesG1.Ag4.2	92.74	
	NR_117646.2	<i>Mesotoga infera</i> strain VNs100	92.11	(Mei et al. 2016)

## References

- Abu Laban, N., Selesi, D., Jobelius, C. and Meckenstock, R.U. (2009) Anaerobic benzene degradation by Gram-positive sulfate-reducing bacteria. *FEMS Microbiology Ecology* 68(3), 300-311.
- Al-Amri, A., Salim, M.R. and Aris, A. (2010) The effect of different temperatures and fluxes on the performance of membrane bioreactor treating synthetic-municipal wastewater. *Desalination* 259(1-3), 111-119.
- Banerjee, A. and Ghoshal, A.K. (2017) Bioremediation of petroleum wastewater by hyper-phenol tolerant *Bacillus cereus*: Preliminary studies with laboratory-scale batch process. *Bioengineered* 8(5), 446-450.
- Boušková, A., Dohányos, M., Schmidt, J.E. and Angelidaki, I. (2005) Strategies for changing temperature from mesophilic to thermophilic conditions in anaerobic CSTR reactors treating sewage sludge. *Water Research* 39(8), 1481-1488.
- Caporaso, J.G., Kuczynski, J., Stombaugh, J., Bittinger, K., Bushman, F.D., Costello, E.K., Fierer, N., Pena, A.G., Goodrich, J.K., Gordon, J.I., Huttley, G.A., Kelley, S.T., Knights, D., Koenig, J.E., Ley, R.E., Lozupone, C.A., McDonald, D., Muegge, B.D., Pirrung, M., Reeder, J., Sevinsky, J.R., Turnbaugh, P.J., Walters, W.A., Widmann, J., Yatsunenko, T., Zaneveld, J. and Knight, R. (2010) QIIME allows analysis of high-throughput community sequencing data. *Nat Meth* 7(5), 335-336.
- Castresana, J. (2000) Selection of conserved blocks from multiple alignments for their use in phylogenetic analysis. *Molecular Biology and Evolution* 17(4), 540-552.
- Chen, C.-L., Wu, J.-H. and Liu, W.-T. (2008a) Identification of important microbial populations in the mesophilic and thermophilic phenol-degrading methanogenic consortia. *Water Research* 42(8), 1963-1976.
- Chen, C.-L., Wu, J.-H., Tseng, I.C., Liang, T.-M. and Liu, W.-T. (2009) Characterization of Active Microbes in a Full-Scale Anaerobic Fluidized Bed Reactor Treating Phenolic Wastewater. *Microbes and Environments* 24(2), 144-153.
- Chen, C.L., Wu, J.H. and Liu, W.T. (2008b) Identification of important microbial populations in the mesophilic and thermophilic phenol-degrading methanogenic consortia. *Water Research* 42(8-9), 1963-1976.
- Cheng, L., Shi, S., Li, Q., Chen, J., Zhang, H. and Lu, Y. (2014) Progressive degradation of crude oil n-alkanes coupled to methane production under mesophilic and thermophilic conditions. *PLoS One* 9(11), e113253.
- Dahle, H. and Birkeland, N.K. (2006) *Thermovirga lienii* gen. nov., sp. nov., a novel moderately thermophilic, anaerobic, amino-acid-degrading bacterium isolated from a North Sea oil well. *Int J Syst Evol Microbiol* 56(Pt 7), 1539-1545.
- De Amorim, E.L.C., Sader, L.T. and Silva, E.L. (2015) Effects of the Organic-Loading Rate on the Performance of an Anaerobic Fluidized-Bed Reactor Treating Synthetic Wastewater Containing Phenol. *Journal of Environmental Engineering (United States)* 141(10).
- Dereli, R.K., Ersahin, M.E., Ozgun, H., Ozturk, I., Jeison, D., van der Zee, F. and van Lier, J.B. (2012) Potentials of anaerobic membrane bioreactors to overcome treatment limitations induced by industrial wastewaters. *Bioresource Technology* 122, 160-170.

- Dereli, R.K., Grelot, A., Heffernan, B., van der Zee, F.P. and van Lier, J.B. (2014) Implications of changes in solids retention time on long term evolution of sludge filterability in anaerobic membrane bioreactors treating high strength industrial wastewater. *Water Research* 59, 11-22.
- Dereli, R.K., Heffernan, B., Grelot, A., Van Der Zee, F.P. and Van Lier, J.B. (2015a) Influence of high lipid containing wastewater on filtration performance and fouling in AnMBRs operated at different solids retention times. *Separation and Purification Technology* 139, 43-52.
- Dereli, R.K., Loverdou, L., van der Zee, F.P. and van Lier, J.B. (2015b) A systematic study on the effect of substrate acidification degree and acidogenic biomass on sludge filterability. *Water Research* 82, 94-103.
- Dipippo, J.L., Nesbo, C.L., Dahle, H., Doolittle, W.F., Birkland, N.K. and Noll, K.M. (2009) *Kosmotoga olearia* gen. nov., sp. nov., a thermophilic, anaerobic heterotroph isolated from an oil production fluid. *Int J Syst Evol Microbiol* 59(Pt 12), 2991-3000.
- Dubois, M., Gilles, K.A., Hamilton, J.K., Rebers, P.A. and Smith, F. (1956) Colorimetric method for determination of sugars and related substances. *Analytical Chemistry* 28(3), 350-356.
- Duncan, J., Bokhary, A., Fatehi, P., Kong, F., Lin, H. and Liao, B. (2017) Thermophilic membrane bioreactors: A review. *Bioresource Technology* 243(Supplement C), 1180-1193.
- Edgar, R. (2016) UCHIME2: improved chimera prediction for amplicon sequencing. *bioRxiv*.
- Edgar, R.C. (2004) MUSCLE: A multiple sequence alignment method with reduced time and space complexity. *BMC Bioinformatics* 5.
- Edgar, R.C. (2010) Search and clustering orders of magnitude faster than BLAST. *Bioinformatics* 26(19), 2460-2461.
- Fang, H.H.P., Liang, D.W., Zhang, T. and Liu, Y. (2006) Anaerobic treatment of phenol in wastewater under thermophilic condition. *Water Research* 40(3), 427-434.
- Frolund, B., Palmgren, R., Keiding, K. and Nielsen, P.H. (1996) Extraction of extracellular polymers from activated sludge using a cation exchange resin. *Water Research* 30(8), 1749-1758.
- Gao, W.J., Leung, K.T., Qin, W.S. and Liao, B.Q. (2011) Effects of temperature and temperature shock on the performance and microbial community structure of a submerged anaerobic membrane bioreactor. *Bioresource Technology* 102(19), 8733-8740.
- Gieg, L.M., Davidova, I.A., Duncan, K.E. and Suflita, J.M. (2010) Methanogenesis, sulfate reduction and crude oil biodegradation in hot Alaskan oilfields. *Environmental Microbiology* 12(11), 3074-3086.
- Gouy, M., Guindon, S. and Gascuel, O. (2010) Sea view version 4: A multiplatform graphical user interface for sequence alignment and phylogenetic tree building. *Molecular Biology and Evolution* 27(2), 221-224.
- Grabowski, A., Nercessian, O., Fayolle, F., Blanchet, D. and Jeanthon, C. (2005) Microbial diversity in production waters of a low-temperature biodegraded oil reservoir. *FEMS Microbiology Ecology* 54(3), 427-443.
- Guindon, S., Dufayard, J.F., Lefort, V., Anisimova, M., Hordijk, W. and Gascuel, O. (2010) New algorithms and methods to estimate maximum-likelihood phylogenies: Assessing the performance of PhyML 3.0. *Systematic Biology* 59(3), 307-321.

- Gupta, A. and Thakur, I.S. (2015) Study of optimization of wastewater contaminant removal along with extracellular polymeric substances (EPS) production by a thermotolerant *Bacillus* sp. ISTVK1 isolated from heat shocked sewage sludge. *Bioresource Technology* 213, 21-30.
- Holoman, T.R., Elberson, M.A., Cutter, L.A., May, H.D. and Sowers, K.R. (1998) Characterization of a defined 2,3,5, 6-tetrachlorobiphenyl-ortho-dechlorinating microbial community by comparative sequence analysis of genes coding for 16S rRNA. *Applied and Environmental Microbiology* 64(9), 3359-3367.
- Jeison, D. and van Lier, J.B. (2007) Thermophilic treatment of acidified and partially acidified wastewater using an anaerobic submerged MBR: Factors affecting long-term operational flux. *Water Research* 41(17), 3868-3879.
- Jeison, D. and van Lier, J.B. (2008) Feasibility of thermophilic anaerobic submerged membrane bioreactors (AnSMBR) for wastewater treatment. *Desalination* 231(1-3), 227-235.
- Joshi, D.R., Zhang, Y., Tian, Z., Gao, Y. and Yang, M. (2016) Performance and microbial community composition in a long-term sequential anaerobic-aerobic bioreactor operation treating coking wastewater. *Applied Microbiology and Biotechnology* 100(18), 8191-8202.
- Kaster, K.M., Hiorth, A., Kjeilen-Eilertsen, G., Boccadoro, K., Lohne, A., Berland, H., Stavland, A. and Brakstad, O.G. (2012) Mechanisms Involved in Microbially Enhanced Oil Recovery. *Transport in Porous Media* 91(1), 59-79.
- Kim, J. and Lee, C. (2016) Response of a continuous anaerobic digester to temperature transitions: A critical range for restructuring the microbial community structure and function. *Water Research* 89, 241-251.
- Kleinstaub, S., Schleinitz, K.M., Breitedfeld, J., Harms, H., Richnow, H.H. and Vogt, C. (2008) Molecular characterization of bacterial communities mineralizing benzene under sulfate-reducing conditions. *FEMS Microbiology Ecology* 66(1), 143-157.
- Knight, V.K., Kerkhof, L.J. and Hågblom, M.M. (1999) Community analyses of sulfidogenic 2-bromophenol-dehalogenating and phenol-degrading microbial consortia. *FEMS Microbiology Ecology* 29(2), 137-147.
- Letowski, J., Juteau, P., Villemur, R., Duckett, M.F., Beaudet, R., Lépine, F. and Bisailon, J.G. (2001) Separation of a phenol carboxylating organism from a two-member, strict anaerobic co-culture. *Canadian Journal of Microbiology* 47(5), 373-381.
- Levén, L., Eriksson, A.R.B. and Schnürer, A. (2007) Effect of process temperature on bacterial and archaeal communities in two methanogenic bioreactors treating organic household waste. *FEMS Microbiology Ecology* 59(3), 683-693.
- Levén, L., Nyberg, K. and Schnürer, A. (2012) Conversion of phenols during anaerobic digestion of organic solid waste – A review of important microorganisms and impact of temperature. *Journal of Environmental Management* 95, Supplement(0), S99-S103.
- Levén, L. and Schnürer, A. (2005) Effects of temperature on biological degradation of phenols, benzoates and phthalates under methanogenic conditions. *International Biodeterioration and Biodegradation* 55(2), 153-160.
- Levén, L. and Schnürer, A. (2010) Molecular characterisation of two anaerobic phenol-degrading enrichment cultures. *International Biodeterioration and Biodegradation* 64(6), 427-433.

- Lin, H., Liao, B.-Q., Chen, J., Gao, W., Wang, L., Wang, F. and Lu, X. (2011) New insights into membrane fouling in a submerged anaerobic membrane bioreactor based on characterization of cake sludge and bulk sludge. *Bioresource Technology* 102(3), 2373-2379.
- Lin, H., Peng, W., Zhang, M., Chen, J., Hong, H. and Zhang, Y. (2013) A review on anaerobic membrane bioreactors: Applications, membrane fouling and future perspectives. *Desalination* 314(0), 169-188.
- Lin, H., Zhang, M., Wang, F., Meng, F., Liao, B.Q., Hong, H., Chen, J. and Gao, W. (2014) A critical review of extracellular polymeric substances (EPSs) in membrane bioreactors: Characteristics, roles in membrane fouling and control strategies. *Journal of Membrane Science* 460, 110-125.
- Lin, H.J., Xie, K., Mahendran, B., Bagley, D.M., Leung, K.T., Liss, S.N. and Liao, B.Q. (2009) Sludge properties and their effects on membrane fouling in submerged anaerobic membrane bioreactors (SAnMBRs). *Water Research* 43(15), 3827-3837.
- Macario, A.J.L., Visser, F.A., Van Lier, J.B. and De Macario, E.C. (1991) Topography of methanogenic subpopulations in a microbial consortium adapting to thermophilic conditions. *Journal of General Microbiology* 137(9), 2179-2189.
- McDonald, D., Price, M.N., Goodrich, J., Nawrocki, E.P., Desantis, T.Z., Probst, A., Andersen, G.L., Knight, R. and Hugenholtz, P. (2012) An improved Greengenes taxonomy with explicit ranks for ecological and evolutionary analyses of bacteria and archaea. *ISME Journal* 6(3), 610-618.
- Mechichi, T., Labat, M., Patel, B.K., Woo, T.H., Thomas, P. and Garcia, J.L. (1999) *Clostridium methoxybenzovorans* sp. nov., a new aromatic o-demethylating homoacetogen from an olive mill wastewater treatment digester. *Int J Syst Bacteriol* 49 Pt 3, 1201-1209.
- Mei, R., Narihiro, T., Nobu, M.K. and Liu, W.T. (2016) Effects of heat shocks on microbial community structure and microbial activity of a methanogenic enrichment degrading benzoate. *Letters in Applied Microbiology* 63(5), 356-362.
- Muñoz Sierra, J.D., Lafita, C., Gabaldón, C., Spanjers, H. and van Lier, J.B. (2017) Trace metals supplementation in anaerobic membrane bioreactors treating highly saline phenolic wastewater. *Bioresource Technology* 234, 106-114.
- Muñoz Sierra, J.D., Oosterkamp, M.J., Wang, W., Spanjers, H. and van Lier, J.B. (2018) Impact of long-term salinity exposure in anaerobic membrane bioreactors treating phenolic wastewater: Performance robustness and endured microbial community. *Water Research* 141, 172-184.
- Na, J.G., Lee, M.K., Yun, Y.M., Moon, C., Kim, M.S. and Kim, D.H. (2016) Microbial community analysis of anaerobic granules in phenol-degrading UASB by next generation sequencing. *Biochemical Engineering Journal* 112, 241-248.
- Narihiro, T., Nobu, M.K., Mei, R. and Liu, W.-T. (2015) *Anaerobic Biotechnology: Environmental Protection and Resource Recovery*. Imperial College Press, London, 31-48., pp. 31-48.
- Neyens, E., Baeyens, J., Dewil, R. and De Heyder, B. (2004) Advanced sludge treatment affects extracellular polymeric substances to improve activated sludge dewatering. *Journal of Hazardous materials* 106(2-3), 83-92.
- Nobu, M.K., Narihiro, T., Hideyuki, T., Qiu, Y.-L., Sekiguchi, Y., Woyke, T., Goodwin, L., Davenport, K.W., Kamagata, Y. and Liu, W.-T. (2015) The genome of *Syntrophorhabdus aromaticivorans* strain UI provides

- new insights for syntrophic aromatic compound metabolism and electron flow. *Environmental Microbiology* 17(12), 4861-4872.
- Pattananuwat, N., Aoki, M., Hatamoto, M., Nakamura, A., Yamazaki, S., Syutsubo, K., Araki, N., Takahashi, M., Harada, H. and Yamaguchi, T. (2013) Performance and Microbial Community Analysis of a full-scale Hybrid Anaerobic–Aerobic Membrane System for Treating Molasses-Based Bioethanol Wastewater. *International Journal of Environmental Research* 7(4), 979-988.
- Poirier, S., Bize, A., Bureau, C., Bouchez, T. and Chapleur, O. (2016) Community shifts within anaerobic digestion microbiota facing phenol inhibition: Towards early warning microbial indicators? *Water Research* 100, 296-305.
- Qiu, Y.L., Hanada, S., Ohashi, A., Harada, H., Kamagata, Y. and Sekiguchi, Y. (2008) *Syntrophorhabdus aromaticivorans* gen. nov., sp. nov., the first cultured anaerobe capable of degrading phenol to acetate in obligate syntrophic associations with a hydrogenotrophic methanogen. *Applied and Environmental Microbiology* 74(7), 2051-2058.
- Ramakrishnan, A. and Gupta, S.K. (2006) Anaerobic biogranulation in a hybrid reactor treating phenolic waste. *Journal of Hazardous materials* 137(3), 1488-1495.
- Ramakrishnan, A. and Surampalli, R.Y. (2013) Performance and energy economics of mesophilic and thermophilic digestion in anaerobic hybrid reactor treating coal wastewater. *Bioresource Technology* 127, 9-17.
- Robinson, M.D., McCarthy, D.J. and Smyth, G.K. (2010) edgeR: a Bioconductor package for differential expression analysis of digital gene expression data. *Bioinformatics (Oxford, England)* 26(1), 139-140.
- Rosenkranz, F., Cabrol, L., Carballa, M., Donoso-Bravo, A., Cruz, L., Ruiz-Filippi, G., Chamy, R. and Lema, J.M. (2013) Relationship between phenol degradation efficiency and microbial community structure in an anaerobic SBR. *Water Research* 47(17), 6739-6749.
- Sajjad, M. and Kim, K.S. (2015) Studies on the interactions of Ca<sup>2+</sup> and Mg<sup>2+</sup> with EPS and their role in determining the physicochemical characteristics of granular sludges in SBR system. *Process Biochemistry* 50(6), 966-972.
- van Lier, J.B., Grolle, K.C.F., Stams, A.J.M., de Macario, E.C. and Lettinga, G. (1992) Start-up of a thermophilic upflow anaerobic sludge bed (UASB) reactor with mesophilic granular sludge. *Applied Microbiology and Biotechnology* 37(1), 130-135.
- van Lier, J.B., Hulsbeek, J., Stams, A.J.M. and Lettinga, G. (1993) Temperature susceptibility of thermophilic methanogenic sludge: Implications for reactor start-up and operation. *Bioresource Technology* 43(3), 227-235.
- van Lier, J.B., van der Zee, F.P., Frieters, C.T.M.J. and Ersahin, M.E. (2015) Celebrating 40 years anaerobic sludge bed reactors for industrial wastewater treatment. *Reviews in Environmental Science and Bio/Technology* 14(4), 681-702.
- Vasconcellos, S.P.d., Angolini, C.F.F., García, I.N.S., Martins Dellagnezze, B., Silva, C.C.d., Marsaioli, A.J., Neto, E.V.d.s. and de Oliveira, V.M. (2010) Reprint of: Screening for hydrocarbon biodegraders in a metagenomic clone library derived from Brazilian petroleum reservoirs. *Organic Geochemistry* 41(9), 1067-1073.

- Visvanathan, C., Choudhary, M.K., Montalbo, M.T. and Jegatheesan, V. (2007) Landfill leachate treatment using thermophilic membrane bioreactor. *Desalination* 204(1-3 SPEC. ISS.), 8-16.
- Wang, W. and Han, H. (2012) Recovery strategies for tackling the impact of phenolic compounds in a UASB reactor treating coal gasification wastewater. *Bioresource Technology* 103(1), 95-100.
- Wang, W., Han, H., Yuan, M., Li, H., Fang, F. and Wang, K. (2011a) Treatment of coal gasification wastewater by a two-continuous UASB system with step-feed for COD and phenols removal. *Bioresource Technology* 102(9), 5454-5460.
- Wang, W., Ma, W., Han, H., Li, H. and Yuan, M. (2011b) Thermophilic anaerobic digestion of Lurgi coal gasification wastewater in a UASB reactor. *Bioresource Technology* 102(3), 2441-2447.
- Wang, W., Wang, S., Ren, X., Hu, Z. and Yuan, S. (2017a) Rapid establishment of phenol- and quinoline-degrading consortia driven by the scoured cake layer in an anaerobic baffled ceramic membrane bioreactor. *Environmental Science and Pollution Research* 24(33), 26125-26135.
- Wang, W., Wu, B., Pan, S., Yang, K., Hu, Z. and Yuan, S. (2017b) Performance robustness of the UASB reactors treating saline phenolic wastewater and analysis of microbial community structure. *Journal of Hazardous materials* 331, 21-27.
- Wang, W., Yang, K., Muñoz Sierra, J., Zhang, X., Yuan, S. and Hu, Z. (2017c) Potential impact of methyl isobutyl ketone (MIBK) on phenols degradation in an UASB reactor and its degradation properties. *Journal of Hazardous materials* 333, 73-79.
- Wang, Z., Wu, Z. and Tang, S. (2009) Extracellular polymeric substances (EPS) properties and their effects on membrane fouling in a submerged membrane bioreactor. *Water Research* 43(9), 2504-2512.





# 7

## Feasibility of thermophilic phenol conversion in AnMBR at high salinity

7

---

This chapter has been published as: “Muñoz Sierra, J.D., García Rea, V.S., Cerqueda-García, D., Spanjers, H., and van Lier, J.B. (2020) Anaerobic Conversion of Saline Phenol-Containing Wastewater Under Thermophilic Conditions in a Membrane Bioreactor. *Frontiers in Bioengineering and Biotechnology*, 8, art. no. 565311 <https://doi.org/10.3389/fbioe.2020.565311>

## Abstract

Closing water loops in chemical industries result in hot and highly saline residual streams, often characterized by high strength and the presence of refractory or toxic compounds. These streams are attractive for anaerobic technologies, provided the chemical compounds are biodegradable. However, under such harsh conditions, effective biomass immobilization is difficult, limiting the use of the commonly applied sludge bed reactors. In this study, we assessed the long-term phenol conversion capacity of a lab-scale anaerobic membrane bioreactor (AnMBR) operated at 55°C, and high salinity (18 gNa<sup>+</sup>L<sup>-1</sup>). Over 388 days, bioreactor performance and microbial community dynamics were monitored using specific methanogenic activity (SMA) assays, phenol conversion rate assays, volatile fatty acids permeate characterization and Illumina MiSeq analysis of 16S rRNA gene sequences. Phenol accumulation to concentrations exceeding 600 mgPh·L<sup>-1</sup> in the reactor significantly reduced methanogenesis at different phases of operation, while applying a phenol volumetric loading rate of 0.12 gPh·L<sup>-1</sup>·d<sup>-1</sup>. Stable AnMBR reactor performance could be attained by applying a sludge phenol loading rate of about 20 mgPh·gVSS<sup>-1</sup>·d<sup>-1</sup>. In-situ maximum phenol conversion rates of 21.3 mgPh·gVSS<sup>-1</sup>·d<sup>-1</sup> were achieved, whereas conversion rates of 32.8 mgPh·gVSS<sup>-1</sup>·d<sup>-1</sup> were assessed in ex-situ batch tests at the end of the operation. The absence of caproate as intermediate inferred that the phenol conversion pathway likely occurred via carboxylation to benzoate. Strikingly, the hydrogenotrophic SMA of 0.34 gCOD-CH<sub>4</sub>·gVSS<sup>-1</sup>·d<sup>-1</sup> of the AnMBR biomass significantly exceeded the acetotrophic SMA, which only reached 0.15 gCOD-CH<sub>4</sub>·gVSS<sup>-1</sup>·d<sup>-1</sup>. Our results indicated that during the course of the experiment, acetate conversion gradually changed from acetoclastic methanogenesis to acetate oxidation coupled to hydrogenotrophic methanogenesis. Correspondingly, hydrogenotrophic methanogens of the class Methanomicrobia, together with Synergistia, Thermotogae, and Clostridia classes, dominated the microbial community and were enriched during the three phases of operation, while the acetoclastic Methanosaeta species remarkably decreased. Our findings clearly showed that highly saline phenolic wastewaters could be satisfactorily treated in a thermophilic AnMBR and that the specific phenol conversion capacity was limiting the treatment process. The possibility of efficient chemical wastewater treatment under the challenging studied conditions would represent a major breakthrough for the widespread application of AnMBR technology.

## 7.1 Introduction

Phenols are major contaminants found in wastewaters of several chemical industries, which are often discharged at high temperatures (Busca et al. 2008, Rosenkranz et al. 2013, Wang et al. 2017). Additionally, closing water loops in the chemical sector often result in concentrated, highly saline wastewaters, which increases the complexity of the produced wastewater (Muñoz Sierra et al. 2017). Despite the existing physicochemical processes applied for phenol removal, i.e., membrane distillation, pervaporation, adsorption, extraction, nanofiltration, reverse osmosis, and oxidation processes (wet air, electrochemical, ozonation, UV/H<sub>2</sub>O<sub>2</sub>, Fenton) (Raza et al. 2019, Villegas et al. 2016); biological treatment processes are preferred due to its cost-effectiveness. In this regard, anaerobic treatment offers the advantages of minimal energy requirement, low sludge production, and the conversion of organic pollutants into energy-rich biogas. Under both saline and high-temperature conditions, effective biomass immobilization becomes cumbersome, constraining the application of anaerobic sludge bed systems to treat these wastewaters (Dereli et al. 2012, van Lier et al. 2015). Moreover, the phenol degrading capacity of methanogenic consortia is generally very low and is expected to develop only slowly. Therefore, combining anaerobic treatment with membrane assisted biomass separation is an attractive option when phenol conversion is required at high salinity, and thermophilic conditions (Lin et al. 2013, Muñoz Sierra et al. 2018b).

When chemical wastewaters are at high temperatures, direct thermophilic treatment becomes of interest because it reduces the need for cooling the wastewater. Particularly when process water reclamation is envisaged, maintaining the temperature reduces the overall energy requirement. Despite its potentials (van Lier 2008), thus far, full-scale anaerobic membrane bioreactors (AnMBRs) are not applied for high-temperature chemical wastewater treatment (Duncan et al. 2017). Only a few previous studies have shown the potential of thermophilic conditions for treating phenolic compounds in continuous reactors (Ramakrishnan and Surampalli 2013, Wang et al. 2011). Wang et al. (2011) compared UASB reactors under mesophilic and thermophilic conditions and concluded that thermophilic anaerobic digestion improves about 30% the degradation of phenolic compounds. Likewise, Ramakrishnan and Surampalli (2013) suggested that thermophilic conversion of phenolic wastewater in an anaerobic hybrid reactor is superior to mesophilic in terms of methane yield, effluent quality, and stability.

Conversely, other studies have also found drawbacks of treating phenol containing wastewater under thermophilic conditions. Fang et al. (2006) indicated that the phenol conversion rate at 55 °C in a UASB reactor was significantly lower than under mesophilic conditions. Furthermore, Levén and Schnürer (2005) concluded that phenolics are mineralized to methane and carbon dioxide under mesophilic conditions, whereas under thermophilic conditions, only benzoic acid is degraded. Muñoz Sierra et al. (2018b) suggested that under mesophilic and hyper-mesophilic conditions (42–45 °C), the phenol conversion capacity of an AnMBR at high salinity is more stable compared to thermophilic conditions. However, because the operation at 55 °C in that study was carried out only during a short-term, it remains unclear whether or not a stable phenol degrading methanogenic consortium may develop. Therefore, this study aims to determine the maximum conversion capacity of a laboratory-scale AnMBR during a long-term operation at 55 °C, treating phenol-containing

wastewater at  $18 \text{ gNa}^+\cdot\text{L}^{-1}$ . Moreover, the microbial community activity and structure in response to increasing phenol loading rates along with three phases of operation were evaluated.

## 7.2 Materials and methods

### 7.2.1 Experimental set-up and operation

The experiments were performed by using a 6.5 L laboratory-scale AnMBR reactor, equipped with an ultra-filtration (UF) side-stream membrane module (Figure 7.1.). A tubular polyvinylidene fluoride membrane (X-flow, Pentair, The Netherlands) with 5.2 mm inner diameter, 0.64 m length and 30 nm nominal pore size was used. The reactor was equipped with feed, recycle, and effluent pumps with 4-20 mA variable speed (120U/DV, 220Du, Watson-Marlow, The Netherlands), pH, and temperature sensors (Memosens, Endress & Hauser, Germany), and a biogas meter (Milligas Counter MGC-1 PMMA, Ritter, Germany). Transmembrane pressure (TMP) was measured by using three pressure sensors (AE Sensors ATM, The Netherlands). The temperature of the jacketed reactor was controlled under thermophilic conditions by a thermostatic water bath (Tamson Instruments, The Netherlands). The entire set-up was controlled by a programmable logic controller (PLC) connected to a PC with LabVIEW software (version 15.0.1f1, National Instruments, USA).

The AnMBR was operated at  $55.0 \pm 0.8 \text{ }^\circ\text{C}$  for 388 days. During this time, the reactor was fed with synthetic phenolic wastewater with phenol concentration between  $50 - 800 \text{ mgPh}\cdot\text{L}^{-1}$  and a sodium concentration of  $18 \text{ gNa}^+\cdot\text{L}^{-1}$ . The experiment was divided into three phases (I, II, and III). In all of the phases, the phenol concentration was increased step-wise to determine the maximum conversion capacity and the attainable phenol loading rate of the AnMBR. The applied total organic loading rates (OLR) were between  $2.0 \text{ gCOD}\cdot\text{L}^{-1}\cdot\text{d}^{-1}$  and  $4.0 \text{ gCOD}\cdot\text{L}^{-1}\cdot\text{d}^{-1}$  during all phases (Table 1). The organic loading rates were calculated as  $\text{OLR} = \text{influent COD (g}\cdot\text{L}^{-1}) \cdot \text{Flow rate (L}\cdot\text{d}^{-1}) / \text{AnMBR volume (L)}$ . The applied flow rate was  $1.0 \text{ L}\cdot\text{d}^{-1}$ . An average solids retention time (SRT) of about  $1200 \pm 130$  days was maintained. The average solids retention time was calculated periodically as  $\text{SRT}_{\text{av}} = X (\text{g VSS in the AnMBR})_{\text{av}} / X_{\text{removed,net}} (\text{gVSS}\cdot\text{d}^{-1})$ , where  $X_{\text{removed,net}}$  resulted from the biomass removed.day<sup>-1</sup> (sampling for tests) and the biomass returned.day<sup>-1</sup> (after some tests).

The AnMBR was completely mixed applying a turnover of 170 times.d<sup>-1</sup>. The membrane unit was operated at a cross-flow velocity of  $0.65 \text{ m s}^{-1}$ . A cyclic membrane filtration operation was carried out, consisting of 500 s filtration and 30 s backwash. Backwash was done by reversing the permeate pump flow. An operational flux of  $4.0 \text{ L}\cdot\text{m}^{-2}\cdot\text{h}^{-1}$  was applied as a result of the experimental settings. The permeate flow was controlled with the variable speed of the effluent and influent pumps, and it was regularly double-checked manually. An average transmembrane pressure (TMP) of  $177 \pm 92 \text{ mbar}$  and a total membrane filtration resistance of  $9.77 \times 10^{12} \text{ [1/m]}$  could be maintained during the AnMBR long-term operation.

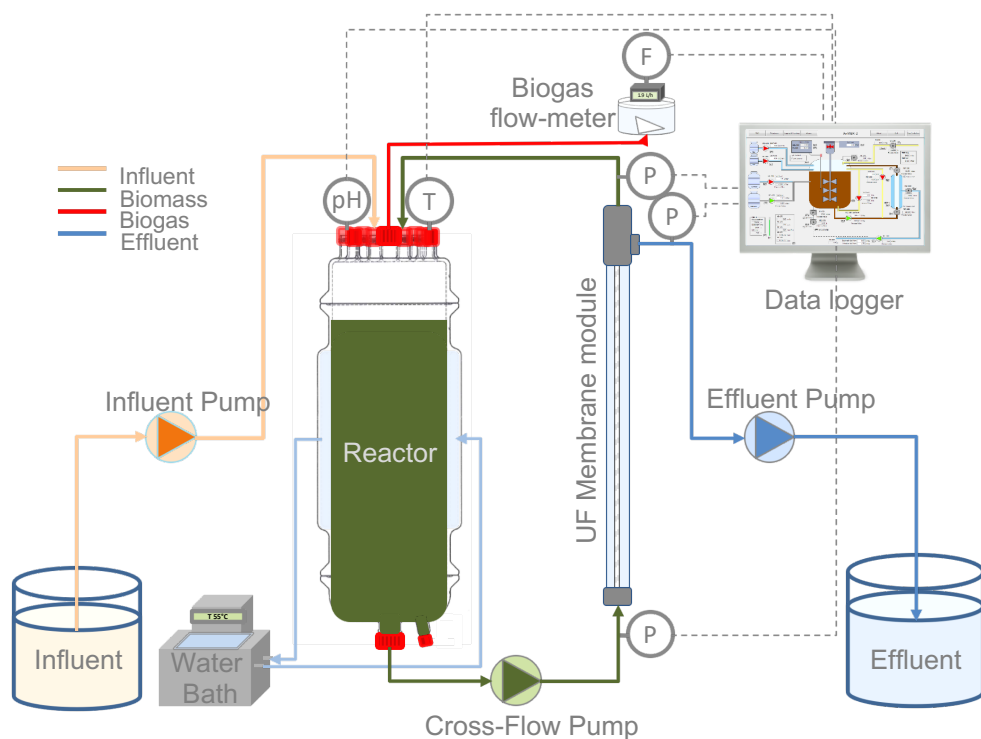


Figure 7.1 Schematic representation of the thermophilic AnMBR.

## 7.2.2 Inoculum and wastewater composition

The reactor was initially inoculated with mesophilic anaerobic biomass obtained from a full-scale UASB reactor at  $8 \text{ gNa}^+\cdot\text{L}^{-1}$  (Shell, Moerdijk, The Netherlands) and subjected to hyper-mesophilic and thermophilic conditions at  $16 \text{ gNa}^+\cdot\text{L}^{-1}$  before the start of the experiment. The synthetic phenolic wastewater consisted of phenol ( $0.1 - 0.8 \text{ gPh}\cdot\text{L}^{-1}$ ), acetate ( $10\text{-}20 \text{ g}\cdot\text{L}^{-1}$ ), yeast extract ( $2.0 \text{ g}\cdot\text{L}^{-1}$ ), NaCl,  $\text{K}_2\text{HPO}_4$ ,  $\text{KH}_2\text{PO}_4$ , varying according to the applied organic and phenol loading rates (Table 1.), while maintaining  $18 \text{ gNa}^+\cdot\text{L}^{-1}$  and a  $\text{K}^+:\text{Na}^+$  ratio of 0.05. Macronutrients ( $9 \text{ mL}\cdot\text{L}^{-1}$ ), and micronutrients ( $4.5 \text{ mL}\cdot\text{L}^{-1}$ ) solutions were added. Macronutrients solution contained (in  $\text{g}\cdot\text{L}^{-1}$ ):  $\text{NH}_4\text{Cl}$  (170),  $\text{CaCl}_2\cdot 2\text{H}_2\text{O}$  (8), and  $\text{MgSO}_4\cdot 7\text{H}_2\text{O}$  (9); micronutrients solution contained (in  $\text{g}\cdot\text{L}^{-1}$ ):  $\text{FeCl}_3\cdot 6\text{H}_2\text{O}$  (2),  $\text{CoCl}_2\cdot 6\text{H}_2\text{O}$  (2),  $\text{MnCl}_2\cdot 4\text{H}_2\text{O}$  (0.5),  $\text{CuCl}_2\cdot 2\text{H}_2\text{O}$  (0.03),  $\text{ZnCl}_2$  (0.05),  $\text{H}_3\text{BO}_3$  (0.05),  $(\text{NH}_4)_6\text{Mo}_7\text{O}_{24}\cdot 4\text{H}_2\text{O}$  (0.09),  $\text{Na}_2\text{SeO}_3$  (0.1),  $\text{NiCl}_2\cdot 6\text{H}_2\text{O}$  (0.05), EDTA (1),  $\text{Na}_2\text{WO}_4$  (0.08). The chemical reagents were of analytical grade.

## 7.2.3 Volatile Fatty Acids

Prior analysis, 10 mL of the AnMBR permeate samples was filtrated over  $0.45 \mu\text{m}$  filter paper. The filtrated liquid was diluted with pentanol ( $300 \text{ mg}\cdot\text{L}^{-1}$ ).  $10 \mu\text{L}$  of formic acid (purity >99%) was added into the final 1.5 mL vials. VFAs were measured by gas chromatography (GC) using an

Agilent 19091F-112, 25 m × 320 μm × 0.5 μm column and an FID detector (Agilent 7890A, USA). The sample injection volume was 1 μL. Helium was used as carrier gas with a total flow rate of 67 mL/min and a split ratio of 25:1. The GC oven temperature was programmed to increase from 80 to 180 °C in 10.5 min. The temperatures of the injector and detector were 80 and 240 °C, respectively.

#### 7.2.4 Permeate characterization

Phenol concentrations were measured using high-performance liquid chromatography HPLC LC-20AT (Shimadzu, Japan) equipped with a 4.6 mm reversed-phase C18 column (Phenomenex, The Netherlands) and a UV detector at a wavelength of 280 nm. The mobile phase used was 25% (v/v) acetonitrile at a flow rate of 0.95 mL·min<sup>-1</sup>. The column oven was set at 30°C. Fast phenol measurements were also carried out by Merck – Spectroquant® Phenol cell kits by using a spectrophotometer NOVA60 (Merck, Germany). Hach Lange kits were used to measure chemical oxygen demand (COD). The COD was measured using a VIS - spectrophotometer (DR3900, Hach Lange, Germany) making proper dilutions to minimize interference by high chloride concentrations, without compromising the accuracy of the measurement.

#### 7.2.5 Anaerobic phenol conversion rates

Batch tests were conducted in triplicate at the end of phase II to assess the phenol conversion recovery after AnMBR performance perturbation. The volatile suspended solid (VSS) were analyzed according to standard protocols using the lowest possible sample volume (APHA 2005). Biomass samples were taken with a 150 ml syringe and transferred to 500 mL Schott glass bottles. The bottles were filled to a volume of 400 ml with AnMBR biomass (0.68 g VSS), and a medium containing acetate (3.1 – 4.6 g·L<sup>-1</sup>), phenol (60 - 109 mgPh·L<sup>-1</sup>), 6 mL·L<sup>-1</sup> macro- and 0.6 mL·L<sup>-1</sup> micronutrients solution, 10 mM phosphate buffer solution, and 18 gNa<sup>+</sup>·L<sup>-1</sup>. Three consecutive feedings of the medium were applied. Initial COD and phenol concentrations varied between 3.4 - 5.1 gCOD·L<sup>-1</sup> and 60 - 109 mgPh·L<sup>-1</sup>, respectively. Temperature and mixing were controlled in an orbital incubator shaker (New Brunswick™ Biological Shakers Innova® 44/44R, USA) at 55°C and 120 rpm respectively. Periodically, liquid samples were taken, and phenol and COD concentrations were measured. Phenol conversion rates [mgPh·gVSS<sup>-1</sup>·d<sup>-1</sup>] were calculated by using the slope of the phenol concentration vs time curve in each bottle. After the batch tests were finished, the supernatant was removed and biomass was returned to the AnMBR. Similarly, at the end of the AnMBR operation at day 388, biomass samples were taken, and phenol conversion batch tests were carried out with initial phenol concentrations of 40 and 60 mgPh·L<sup>-1</sup>.

#### 7.2.6 Specific acetotrophic and hydrogenotrophic methanogenic activity

Specific acetotrophic methanogenic activity (SMA) tests were performed in triplicate using an automated methane potential test system (AMPTS, Bioprocess Control, Sweden). All the SMA tests were carried out at 55°C, following the method described by Spanjers and Vanrolleghem (2016).

For the hydrogenotrophic methanogenic activity, 250 ml Schott glass bottles were filled with biomass (0.57 g VSS) and medium (6 and 0.6 mL·L<sup>-1</sup> macro- and micronutrients solution,

respectively and 10 mM phosphate buffer solution at pH 7.0) to a liquid volume of 200 mL. The gas-phase of the bottles was exchanged by using a gas exchange board (G.R Instruments B.V., The Netherlands) with a gas mixture of 80% CO<sub>2</sub> and 20% H<sub>2</sub> to an end pressure of 0.5 bar during 5 continuous automated cycles to ensure the complete absence of oxygen. Bottles were incubated in an orbital shaker (New Brunswick™ Biological Shakers Innova® 44/44R, USA) at 55°C and 120 rpm for 10 days, and biogas production was calculated using the exact headspace volume and the drop in headspace pressure versus time. The headspace pressure was measured as described by Coates et al. (1996) using a pressure transducer. The methane content of the biogas was analyzed by using a gas chromatograph 7890A (GC) (Agilent Technologies, US) equipped with a front thermal conductivity detector (TCD). The temperature of the oven was 45 °C for 6 min, then 25°C/min to 100 °C. The temperatures of the front inlet, and a front detector were both 200 °C.

### 7.2.7 Microbial community analysis

Biomass samples were taken from the AnMBR on days 88, 241 and 376 to evaluate the microbial community. The DNA extraction was performed from 0.5 g of biomass by using the DNeasy UltraClean Microbial Kit (Qiagen, Hilden, Germany). Agarose gel electrophoresis and Qubit3.0 DNA detection (Qubit® dsDNA HS Assay Kit, Life Technologies, U.S.) were used for quality and quantity control of the DNA. The amplification of the 16S rRNA gene (V3-V4 region) was performed and followed by high throughput sequencing using the MiSeq Illumina platform (BaseClear, Leiden, The Netherlands) using the primers 341F (5'-CCTACGGGNGGCWGCAG-3') and 785R (5'-GACTACHVGGGTATCTAATCC-3'). The Illumina fastq reads (2x250) were processed in the QIIME2 pipeline (2018.7) (Bolyen et al. 2019). Reads were quality filtered, denoised, and the amplicon sequences variants (ASVs) were resolved with the DADA2 plugin (Callahan et al. 2016), removing chimeras with the “consensus” method. The taxonomic classification of the representative sequences of ASVs was performed with the “classify-consensus-vsearch” plugin (Rognes et al. 2016) using the SILVA (132) database as a reference. The representative sequences were aligned with the MAFFT algorithm (Kato and Standley 2013), and a phylogenetic tree was constructed with FastTree (Price et al. 2010). The feature table and tree were exported to the R environment. Differential abundance analyses between reactor operation phases were performed with the DESeq2 library (Love et al. 2014). The abundance and the tree were visualized with the phyloseq library (McMurdie and Holmes 2013). ASVs with differential abundances within the operational phases were analyzed with BLAST against the refseq rna database to identify the closest related species. The sequences reported in this paper have been deposited at ENA under the study accession number PRJEB38467.

## 7.3 Results and Discussion

### 7.3.1 Thermophilic AnMBR performance

Influent and effluent phenol and COD concentrations during the long-term thermophilic AnMBR operation are shown in Figure 7.2. During days 0-96 in phase I, the effluent COD concentrations were in the range of 2.0-10.0 gCOD·L<sup>-1</sup>, and the corresponding removal efficiencies were between

59.0%-92.3% (Figure 7.2 B) at an average organic loading rate (OLR) of 3.8 gCOD·L<sup>-1</sup>·d<sup>-1</sup>. The increase in the phenol loading rate (Table 7.1.) from 0.01 gPh L<sup>-1</sup>·d<sup>-1</sup> to 0.09 gPh L<sup>-1</sup>·d<sup>-1</sup> concomitantly increased the phenol removal efficiency from 54% to 95% (Figure 7.2 A). At the end of phase I, the phenol concentration in the reactor reached about 738 mgPh·L<sup>-1</sup> (Figure 7.2 A).

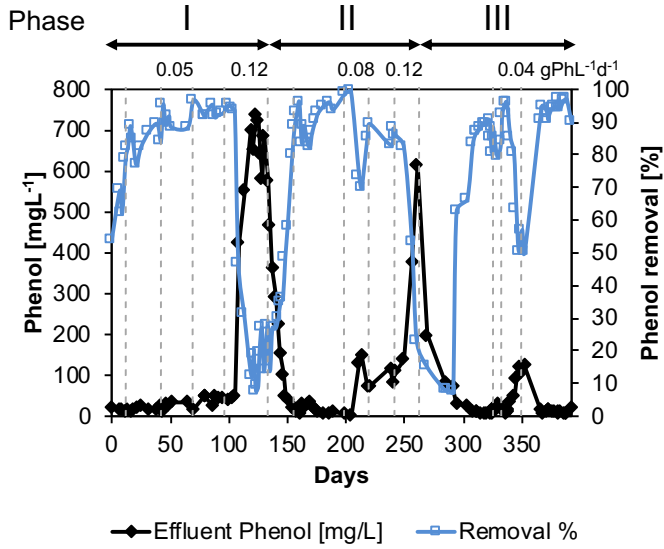
Table 7.1 Operational organic and phenol loading rates of the thermophilic AnMBR.

Phase	Days	OLR [gCOD·L <sup>-1</sup> ·d <sup>-1</sup> ]	Phenol loading rate [gPh·L <sup>-1</sup> ·d <sup>-1</sup> ]	Phenol influent concentration [g·L <sup>-1</sup> ]
I	0-12	3.7	0.01	0.05
	13-42	3.7	0.02	0.1
	43-69	3.8	0.05	0.3
	70-96	3.9	0.09	0.6
	97-108	4.0	0.12	0.8
	109-133	2.3	0.12	0.8
II	134-155	2.0	0.02	0.1
	156-198	2.1	0.03	0.2
	199-219	2.2	0.08	0.5
	220-241	2.3	0.11	0.7
	242-262	2.3	0.12	0.8
III	263-325	2.0	0.01	0.08
	326-332	2.1	0.02	0.15
	333-349	2.1	0.04	0.25
	350-388	2.1	0.03	0.2

The COD removal efficiency started to decrease at the end of the applied phenol loading rate of 0.09 gPh·L<sup>-1</sup>·d<sup>-1</sup> (Figure 7.2 B), i.e., before day 96 in phase I, and subsequently acetate concentration increased (Figure 7.3.). The observed deterioration possibly can be ascribed to an accumulation of a phenol conversion intermediate, such as benzoate (Tay et al. 2001, Wang and Barlaz 1998), impacting acetoclastic methanogens or syntrophic acetate oxidizers. After the phenol loading rate was further increased to 0.12 gPh·L<sup>-1</sup>·d<sup>-1</sup>, equivalent to a sludge phenol loading rate of 22.6 mgPh·gVSS<sup>-1</sup>·d<sup>-1</sup>, the OLR was decreased to 2.3 gCOD·L<sup>-1</sup>·d<sup>-1</sup> to avoid high volatile fatty acids concentrations in the reactor. The increase in phenol loading rate at the end of phase I, severely impacted COD and phenol conversion, resulting in removal efficiencies below 10%. The phenol concentration in the reactor broth reached 738 mgPh·L<sup>-1</sup> (Figure 7.2 A), which apparently inhibited both phenol conversion and methanogenesis. Similarly, Madigou et al. (2016) reported inhibition of phenol conversion at a concentration of 600 mgPh·L<sup>-1</sup> and biogas production nearly stopped when phenol reached 895 mgPh·L<sup>-1</sup>. In order to reduce the phenol concentration in the AnMBR,



A



B

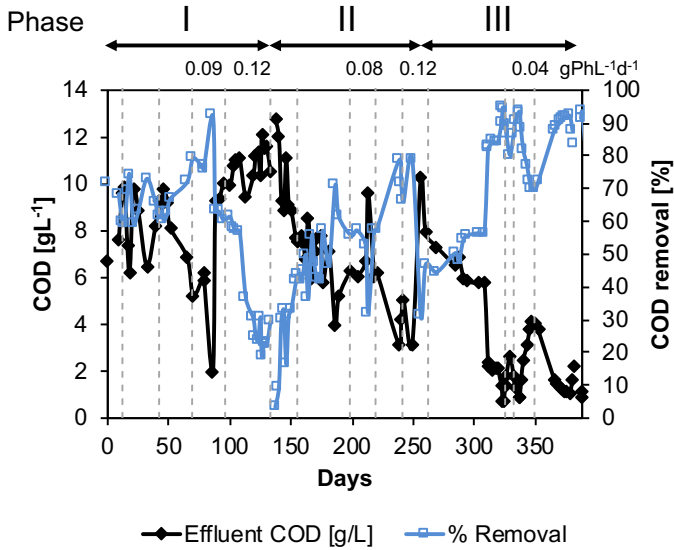


Figure 7.2 (A). Phenol removal efficiency and phenol concentration in the effluent and (B). COD removal efficiency and COD concentration in the effluent during the long-term thermophilic (55°C) condition. The vertical dotted lines indicate the changes in phenol loading rate (gPhL<sup>-1</sup>.d<sup>-1</sup>).

the phenol loading rate was decreased to  $0.02 \text{ gPh}\cdot\text{L}^{-1}\cdot\text{d}^{-1}$  ( $3.8 \text{ mgPh}\cdot\text{gVSS}^{-1}\cdot\text{d}^{-1}$ ) on day 133 to prevent further intoxication, while the OLR was reduced to  $2.0 \text{ gCOD}\cdot\text{L}^{-1}\cdot\text{d}^{-1}$ .

On day 199 in phase II, the phenol loading rate was increased from  $0.03 \text{ gPh}\cdot\text{L}^{-1}\cdot\text{d}^{-1}$  ( $6.5 \text{ mgPh}\cdot\text{gVSS}^{-1}\cdot\text{d}^{-1}$ ) to  $0.08 \text{ gPh}\cdot\text{L}^{-1}\cdot\text{d}^{-1}$  ( $17.4 \text{ mgPh}\cdot\text{gVSS}^{-1}\cdot\text{d}^{-1}$ ) which resulted in an increase in converted phenol from  $188 \text{ mgPh}\cdot\text{L}^{-1}$  to  $349 \text{ mgPh}\cdot\text{L}^{-1}$ . Concomitantly, the phenol removal efficiency dropped to 24% (Figure 7.2 A) and the COD removal efficiency to 32% (Figure 7.2 B). However, on day 240 in phase II, the phenol removal efficiency increased to 88%, while applying a phenol loading rate of  $0.11 \text{ gPh}\cdot\text{L}^{-1}\cdot\text{d}^{-1}$  ( $18.4 \text{ mgPh}\cdot\text{gVSS}^{-1}\cdot\text{d}^{-1}$ ). When the phenol loading rate was further increased to  $0.12 \text{ gPh}\cdot\text{L}^{-1}\cdot\text{d}^{-1}$  ( $20.1 \text{ mgPh}\cdot\text{gVSS}^{-1}\cdot\text{d}^{-1}$ ) the reactor performance again deteriorated, resulting in a decrease in both the COD and phenol removal efficiencies to 31% and 23%, respectively. Consequently, biogas production almost ceased on day 260 when the reactor phenol concentration reached  $616 \text{ mgPh}\cdot\text{L}^{-1}$ , inhibiting the methanogenic consortium. By decreasing the phenol loading rate back to  $0.01 \text{ gPh}\cdot\text{L}^{-1}\cdot\text{d}^{-1}$  ( $2.2 \text{ mgPh}\cdot\text{gVSS}^{-1}\cdot\text{d}^{-1}$ ), the COD and phenol removal efficiencies were gradually recovered during phase III. Surprisingly in phase III, by applying a phenol loading rate of  $0.04 \text{ gPh}\cdot\text{L}^{-1}\cdot\text{d}^{-1}$  ( $9.3 \text{ mgPh}\cdot\text{gVSS}^{-1}\cdot\text{d}^{-1}$ ) on day 352, phenol and COD removal efficiencies decreased to 50% and 80%, respectively. The latter indicates an increased sensitivity of the biomass to phenol compared to phase I.

### 7.3.2 Volatile fatty acids (VFAs) spectrum

Throughout the entire thermophilic operation, VFAs were detected in the AnMBR permeate (Figure 7.3.), indicating a limiting methanogenic conversion capacity. The effluent COD mainly consisted of acetate ( $0.02\text{-}9.6 \text{ g}\cdot\text{L}^{-1}$ ), which peaked at almost  $9.6 \text{ g}\cdot\text{L}^{-1}$  between 133-144 days when phenol accumulation occurred. VFA concentrations in the permeate, mainly acetate, indicated a limiting methanogenic conversion capacity for the organic loading rate applied. The high observed acetate concentration reaching  $9.6 \text{ g}\cdot\text{L}^{-1}$  (Figure 7.3.) when phenol accumulation occurred, could have caused a secondary inhibitory effect to the anaerobic microorganisms such as propionate-oxidizing bacteria (Van Lier et al. 1993). Concomitantly, the butyrate concentration increased to  $616 \text{ mg}\cdot\text{L}^{-1}$  in this period. In phase II, high concentrations of acetate ( $5.2 \text{ g}\cdot\text{L}^{-1}$ ) and to a lesser extent butyrate ( $295 \text{ mg}\cdot\text{L}^{-1}$ ) were found at day 260 when phenol again accumulated after an increase in the PhLR. Propionate was most of the time present in the reactor effluent with an average concentration of  $129 \pm 57 \text{ mg}\cdot\text{L}^{-1}$ . The valerate concentration increased to  $254 \text{ mg}\cdot\text{L}^{-1}$  and  $156 \text{ mg}\cdot\text{L}^{-1}$  when the reactor performance deteriorated in phases I and II, respectively. In phase III, on day 350, an increase in all VFAs was observed when reactor phenol concentration increased to  $124 \text{ mgPh}\cdot\text{L}^{-1}$ .

Despite the peaks of  $620 \text{ mg}\cdot\text{L}^{-1}$  and  $300 \text{ mg}\cdot\text{L}^{-1}$  of butyrate during the phenol accumulation events, all VFA concentrations (propionate, butyrate and valerate) remained at a relatively low level, commonly observed in anaerobic reactors under anaerobic thermophilic conditions (Van Lier et al. 1993). Caproate always remained below detection level throughout the entire thermophilic AnMBR operation. Previous studies inferred that at  $55^\circ\text{C}$ , phenol-degrading biomass might degrade phenol via n-caproate (Evans and Fuchs 1988, Fang et al. 2006). On the other hand, Hoyos-Hernandez et al. (2014) have demonstrated that thermophilic phenol degradation is possible via the benzoate

conversion route, similar to mesophilic conditions, contrasting these previous studies. Even though benzoate was not determined analytically in the AnMBR, the absence of caproate in any of the VFA analyses strongly suggests that the prevailing phenol conversion pathway was likely via benzoate carboxylation at 55°C. Following the proposed pathway, benzoate is subsequently de-aromatized to form cyclohexane carboxylic acid, which is cleaved to heptanoate, degraded further through  $\beta$ -oxidation to form valerate, propionate, and acetate, or directly to propionate and butyrate, which are further degraded to acetate (Liang and Fang 2010).

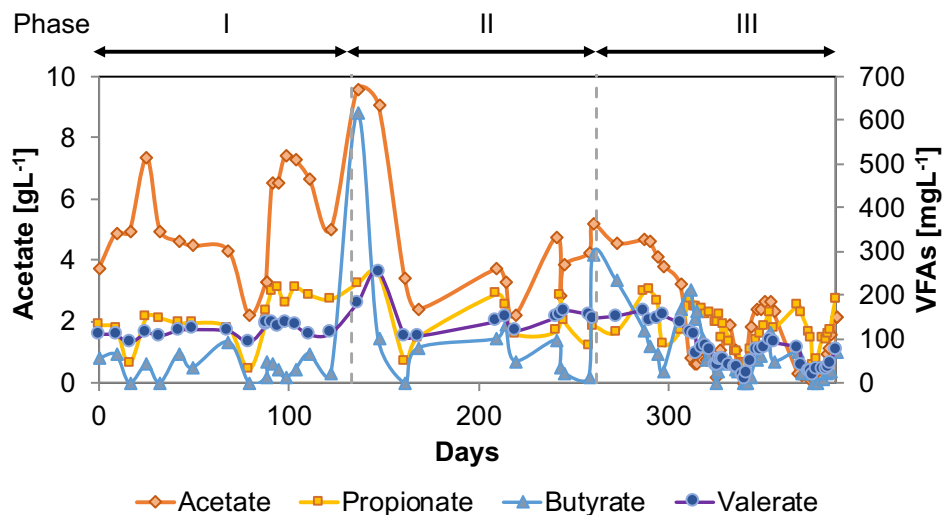


Figure 7.3 VFAs concentrations during the AnMBR long-term operation at 55°C and 18 gNa<sup>+</sup>·L<sup>-1</sup>. Acetate (left y-axis), Propionate, Butyrate, and Valerate (right y-axis). Note: The decrease of VFAs concentration values on day 79 is due to a stop of feeding.

### 7.3.3 Conversion rates and methanogenic activity

#### 7.3.3.1 Specific methanogenic activity and phenol conversion rates

SMA tests using acetate as the substrate showed a drop in the methanogenic activity of the phenol-degrading biomass in phase I, meanwhile, an increase in the specific phenol conversion rates was observed (Table 7.2). During phase II the lowest observed SMA was  $0.04 \pm 0.02$  gCOD-CH<sub>4</sub>·gVSS<sup>-1</sup>·d<sup>-1</sup>, following phenol accumulation at the end of phase I. In phase III when the influent phenol concentration was decreased to 0.2 gPh·L<sup>-1</sup>, the SMA of the phenol-degrading biomass increased to 0.13 gCOD-CH<sub>4</sub>·gVSS<sup>-1</sup>·d<sup>-1</sup>, which was similar to the value observed at the beginning of phase I.

The assessed SMA values found are similar to those reported elsewhere for phenol degrading biomass under thermophilic conditions, i.e., 0.1 gCOD-CH<sub>4</sub>·gVSS<sup>-1</sup>·d<sup>-1</sup> (Fang et al. 2006).

Table 7.2 also shows the calculated maximum in-reactor phenol conversion rates in the different phases. At the end of phase I, the phenol conversion rate had increased from an initial value of 1.3

mgPh·gVSS<sup>-1</sup>·d<sup>-1</sup> to 21.3±0.2 mgPh·gVSS<sup>-1</sup>·d<sup>-1</sup>. During the recovery periods of perturbation, i.e., days 156–198, the phenol conversion rate was 5.9±0.3 mgPh·gVSS<sup>-1</sup>·d<sup>-1</sup>. From days 220 to 262, the phenol loading rate increased until an average of 16.9 ±0.6 mgPh·gVSS<sup>-1</sup>·d<sup>-1</sup>. In phase III, the phenol conversion rate decreased to the range 2.6±0.1 - 7.6±1.6 mgPh·gVSS<sup>-1</sup>·d<sup>-1</sup>.

Table 7.2 SMA (acetate as the substrate) and phenol conversion rates at different phases of the AnMBR operation under thermophilic conditions.

Phase	Days	SMA [gCOD-CH <sub>4</sub> gVSS <sup>-1</sup> ·d <sup>-1</sup> ]	AnMBR phenol conversion rate [mgPh·gVSS <sup>-1</sup> ·d <sup>-1</sup> ]
I	0-12	0.13 ± 0.05	1.3 ± 0.6
	43-69	0.08 ± 0.05	8.4 ± 0.3
	100-133	N.D*	21.3 ± 0.2
II	156-198	0.04 ± 0.02	5.9 ± 0.3
	220-241	N.D*	16.0 ± 0.6
	242-262	N.D*	16.9 ± 0.6
III	326-332	0.09 ± 0.07	2.6 ± 0.1
	333-349	N.D	7.6 ± 1.6
	350-388	0.13 ± 0.10	6.3 ± 0.2

\*N.D = Not Determined

The observed maximum phenol conversion rate of 21.3±0.2 mgPh·gVSS<sup>-1</sup>·d<sup>-1</sup> in the AnMBR at the phenol loading rate of 0.12 gPh·L<sup>-1</sup>·d<sup>-1</sup> (22.6 mgPh·gVSS<sup>-1</sup>·d<sup>-1</sup>) at 55 °C and 18 gNa<sup>+</sup>·L<sup>-1</sup> was substantially higher than the observed phenol conversion rate of 1.7 mgPh·gVSS<sup>-1</sup>·d<sup>-1</sup> at a loading rate of 0.02 gPh·L<sup>-1</sup>·d<sup>-1</sup> (3.9 mgPh·gVSS<sup>-1</sup>·d<sup>-1</sup>), which was observed in Chapter 6 after shifting the AnMBR operation from 35°C to 55°C at a sodium concentration of 16 gNa<sup>+</sup>·L<sup>-1</sup> (Muñoz Sierra et al. 2018b). However, it is lower than the 81.3 mgPh·gVSS<sup>-1</sup>·d<sup>-1</sup> found by others (Wang et al. (2011)). It should be noted that in our present work, the AnMBR was exposed to more extreme conditions, combining high phenol concentrations, high temperature, and high salinity (18 gNa<sup>+</sup>·L<sup>-1</sup>) compared to the previous thermophilic studies (see Table 7.5.). Still, our observed phenol conversion rates can be considered low when compared to the 52.7 - 489 mgPh·gVSS<sup>-1</sup>·d<sup>-1</sup> that was achieved with thermophilic phenol degrading methanogenic enriched consortia (Chen et al. 2008).

### 7.3.3.2 Ex-situ phenol conversion rate after reactor perturbation

After reactor perturbation at the end of phase II, the phenol conversion rate was assessed in a batch test. Three different feedings were applied with different initial phenol concentrations (see Table 7.3). After the first feed, the phenol conversion rate was calculated as 4.0 ± 1.4 mgPh·gVSS<sup>-1</sup>·d<sup>-1</sup> after seven days of incubation. The phenol conversion rate increased to 9.6±2.6 and 10.5±3.3 mgPh·gVSS<sup>-1</sup>·d<sup>-1</sup> after the second and third consecutive feeding respectively, inferring a 62% recovery of the conversion capacity after about 17 days of incubation. Interestingly, also Chen et al. (2008) found a maximum phenol conversion rate after 10 to 14 days of incubation. The ex-situ assessed phenol conversion rate at the end of the batch tests was about 61% of the AnMBR conversion rate before phenol accumulation occurred (see Table 7.3). Apparently, the phenol-

degrading biomass could recover from the phenol shocks after a relatively short recovery period, while being exposed to low phenol concentrations in the reactor ( $< 100 \text{ mgPh L}^{-1}$ ).

Table 7.3. Phenol conversion rate during three consecutive feedings in the batch test.

Feed	Phenol conversion rate [ $\text{mgPh}\cdot\text{gVSS}^{-1}\cdot\text{d}^{-1}$ ]	Initial phenol concentration [ $\text{mgPh}\cdot\text{L}^{-1}$ ]	Initial COD concentration (phenol+acetate) [ $\text{gCOD}\cdot\text{L}^{-1}$ ]
1 <sup>st</sup>	$4.0 \pm 1.4$	$109 \pm 12$	$5.1 \pm 0.3$
2 <sup>nd</sup>	$9.6 \pm 2.6$	$60 \pm 3$	$3.4 \pm 0.0$
3 <sup>rd</sup>	$10.5 \pm 3.3$	$89 \pm 25$	$3.6 \pm 0.1$

### 7.3.3.3 Specific methanogenic activity and phenol conversion rates at the end of the long-term operation

Since low acetate-fed SMA values at the end of the long-term thermophilic operation period were observed of  $0.13 \pm 0.10 \text{ gCOD}\cdot\text{CH}_4\cdot\text{gVSS}^{-1}\cdot\text{d}^{-1}$ , SMA tests were performed with both acetate and hydrogen as electron donor. Likewise, the phenol conversion rate was measured in batch test with an initial phenol concentration of 40 and 60  $\text{mgPh}\cdot\text{L}^{-1}$  (Table 7.4). The acetate-fed SMA obtained was  $0.15 \pm 0.04 \text{ gCOD}\cdot\text{CH}_4\cdot\text{gVSS}^{-1}\cdot\text{d}^{-1}$  similar to what was observed at the beginning of phase I and at the end of phase III. Remarkably, the hydrogenotrophic methanogenic activity was a factor 2.3 higher ( $0.34 \pm 0.08 \text{ g COD}\cdot\text{CH}_4 \text{ gVSS}^{-1} \text{ d}^{-1}$ ), which made us hypothesize that methanogenesis of acetate proceeded via syntrophic acetate oxidation coupled to hydrogenotrophic methanogenesis, rather than acetoclastic methanogenesis.

Table 7.4 Acetate-fed and hydrogen-fed specific methanogenic activities, as well as phenol conversion rates assessed at two different initial phenol concentrations.

	SMA [ $\text{gCOD}\cdot\text{CH}_4\cdot\text{gVSS}^{-1}\cdot\text{d}^{-1}$ ]	Phenol conversion rates [ $\text{mgPh}\cdot\text{gVSS}^{-1}\cdot\text{d}^{-1}$ ]	
		[ $40 \text{ mgPh}\cdot\text{L}^{-1}$ ] <sub>initial</sub>	[ $60 \text{ mgPh}\cdot\text{L}^{-1}$ ] <sub>initial</sub>
Acetate	$0.15 \pm 0.04$	$29.2 \pm 0.1$	$32.8 \pm 0.5$
H <sub>2</sub> /CO <sub>2</sub>	$0.34 \pm 0.08$		

A maximum phenol conversion rate of  $32.8 \pm 0.5 \text{ mgPh}\cdot\text{gVSS}^{-1}\cdot\text{d}^{-1}$  was found, applying an initial phenol concentration of  $60 \text{ mgPh}\cdot\text{L}^{-1}$ . This value is higher than the maximum observed phenol conversion rate in the AnMBR during phase I, which likely can be attributed to long-term adaptation of the biomass to phenol after three phases. Of interest is the relatively high hydrogenotrophic SMA, which indicates that acetate is possibly syntrophically methanised via oxidation to hydrogen and carbon dioxide. Note that syntrophic acetate oxidation is energetically more favorable at elevated temperature and high acetate concentration and is more often observed as the dominant pathway in a large number of thermophilic anaerobic reactors (Li et al. 2020, van Lier 1996, Westerholm et al. 2016). Moreover, hydrogenotrophic methanogenesis is commonly observed at elevated salt concentrations (De Vrieze et al. 2016).

Table 7.1 Anaerobic phenol conversion in continuous flow reactor systems operated at different temperatures.

Temperature [°C]	Reactor [Volume L]	Operation time [d]	Substrate	Phenol [mgPh·L <sup>-1</sup> ]	OLR [gCOD·L <sup>-1</sup> ·d <sup>-1</sup> ]	Specific phenol conversion rate [mgPh/gVSS·d <sup>-1</sup> ]	Removal [%]	Reference
15 - 18	EGSB-AF [3.5]	415	Phenol, ethanol, butyrate, propionate and acetate	400 - 1200	5 - 10	15.4-88.9 (ex-situ)	> 80 (as COD)	(Collins et al. 2005)
9.5 - 15	EGSB-AF [3.5]	673	Phenol, ethanol, butyrate, propionate and acetate	500-1000	1 - 2 (COD <sub>Ph</sub> )	up to 68, 43-137(15°C, ex-situ)	50-98	(Scully et al. 2006)
26	UASB [2.8]	512	Phenol	1260	6	N.A	33 - 100	(Fang et al. 2004)
37	ASBR [5]	281	Phenol/phenol,glucose	120 - 1200	N.D	11 - 27	>90	(Rosenkranz et al. 2013)
37	ASBR [5]	200	Phenol	120- 1200	N.D	11 - 31	>90	(Franchi et al. 2020)
35 - 55	AnMBR [6.5]	270	Phenol, acetate (high salinity)	100 - 500	1.86 - 4.35	1.2-3.5	40 - 100	(Muñoz Sierra et al. 2018b)
55	UASB [2.8]	224	Phenol	630	0.9	N.A	59-99	(Fang et al. 2006)
55	UASB [1]	303	Phenol, phenolites, CGWW	300-500 (total phenols)	1.5 - 2.5	30.5-81.3 (ex-situ)	50-60 (total phenols)	(Wang et al. 2011)
55	AnMBR [6.5]	388	Phenol, acetate (high salinity)	50-800	2 - 4	21.3, 32.8 (ex-situ)	≤ 95	This study

N.A: not available, N.D: not determined, CGWW: coal gasification wastewater.

Comparing our present results with the different studies summarized in Table 7.5, which are performed in a broad range of temperatures, the observed maximum phenol conversion rates are comparable to those obtained under both mesophilic (Franchi et al. 2020, Rosenkranz et al. 2013) and psychrophilic (Collins et al. 2005, Scully et al. 2006) conditions, using other anaerobic high-rate reactors configurations. Nonetheless, it should be recalled that our present results were obtained under extreme salinity conditions applying sodium concentrations of  $18 \text{ gNa}^+\text{L}^{-1}$ .

Based on our results, follow-up research in a thermophilic AnMBR should reveal the minimum acetate concentration that is required to enhance phenol conversion and to avoid high VFA concentrations in the permeate. In such research, concentrations in the range of  $0.3\text{-}1.0 \text{ gCOD}\cdot\text{L}^{-1}$  acetate, and  $500\text{-}800 \text{ mgPh}\cdot\text{L}^{-1}$  phenol are recommended. Applying similar salinity conditions, we propose an OLR of  $2.0\text{--}2.2 \text{ gCOD}\cdot\text{L}^{-1}\cdot\text{d}^{-1}$  and phenol loading rates of  $15\text{-}20 \text{ mgPh}\cdot\text{gVSS}^{-1}\cdot\text{d}^{-1}$  in order to maximize the phenol conversion capacity, without compromising the methanogenic activity.

### 7.3.4 Microbial community structure analysis

The microbial community analysis revealed a total of 141 amplicon sequences variants (ASVs) with differential abundance across samples. Figure 7.4 shows the genera from both bacteria and archaea domains with main population changes in relative abundance at the different phases of the thermophilic AnMBR at  $18 \text{ gNa}^+\text{L}^{-1}$ . *Petrotoga* (Thermotogae class) was enriched along with the long-term operation up to 21.1% in phase III. This bacteria has been enriched under anaerobic thermophilic conditions from an oil reservoir containing mostly halophilic species (Dellagnèz et al. 2016). *Thermovirga* (Synergistia class) increased from 8.0% to 14.1% from phase I to II and then decreased to 7.95% relative abundance in phase III. High salinity conditions will enrich for salt-tolerant and halophilic *Thermovirga* and *Clostridium* species (Muñoz Sierra et al. 2018a). *Acetomicrobium* also belonging to phylum *Synergistetes* (see Supplementary information Figure S7.1.) increased from 0.35% during phase I to 3.93% during phase III. This genus is found in oil production water and is capable of producing hydrogen. Some species required NaCl for growth (Cook et al. 2018). A 100% similarity was found with the specie *Acetomicrobium hydrogeniformans* sp. (see Supplementary information Table S7.1). *Syntrophobacter* affiliated to the class Deltaproteobacteria increased from 0.1% to 0.5% in relative abundance from phase I to phase II; however it was not detected in phase III. A hit of 100% similarity was found for the halophilic bacteria *Syntrophobacter sulfatireducens* sp. Similarly, the relative abundance of WS6 bacterium decreased during the long-term operation. In the case of the Clostridia class, the major abundance decrease was observed with the genera *Caldicoprobacter* and *Tepidimicrobium*, whereas an increase was observed for *Syntrophaceticus* (3.3%), *Pelotomaculum* (1.2%) and *Proteiniclasticum* (2.4%). The genera found *Syntrophaceticus* are known for their capability of syntrophic acetate oxidation, and *Pelotomaculum* play an important role in the conversion of phenol and benzoate under methanogenic conditions (Chen et al. 2008). Also, *Corynebacterium* and *Enterococcus* genera belonging to Actinobacteria and Bacilli class increased significantly to 6.6% and 1.8%, respectively, in phase III.

*Methanosaeta* was about 19.7% in relative abundance in phase I decreasing to 11.4% in phase II, while it almost disappeared in phase III. The halotolerant *Methanosaeta harundinacea* sp. obtained a

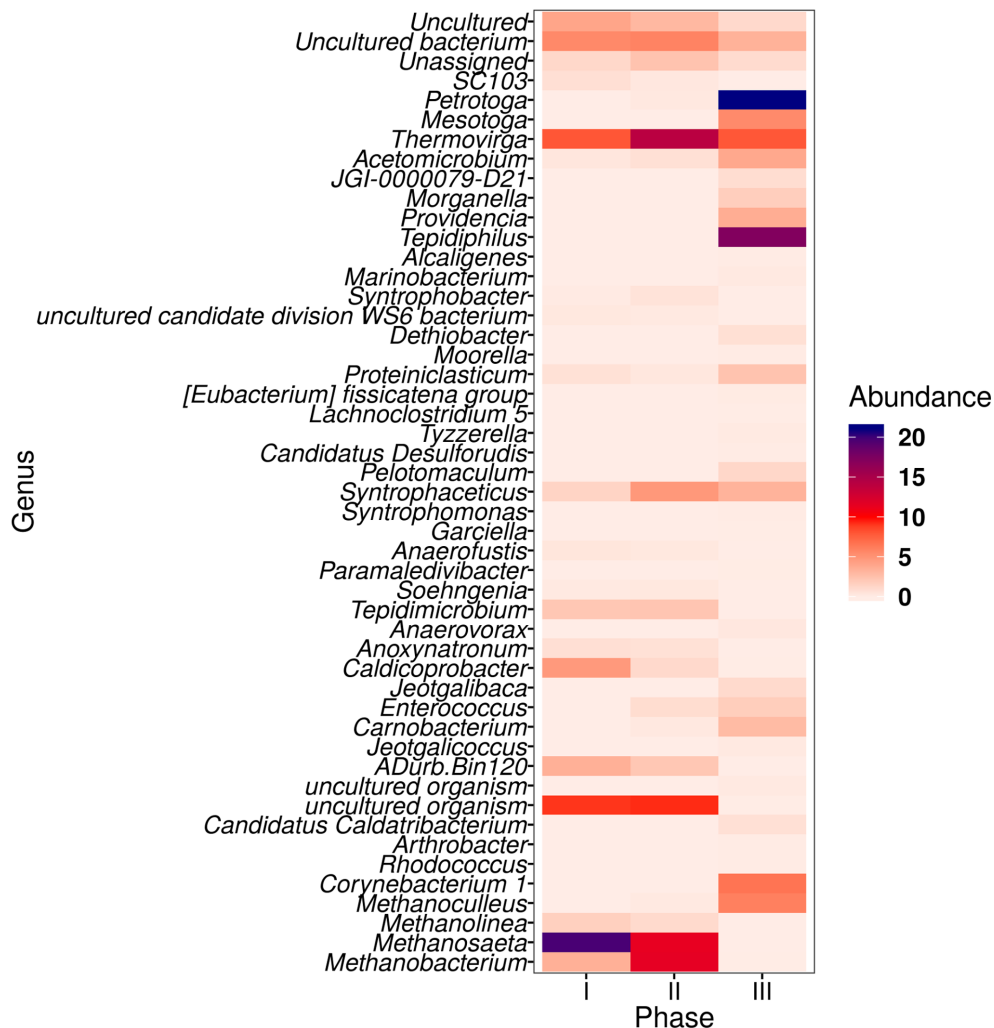


Figure 7.4 Heatmap of the genera from bacteria and archaea domains in the thermophilic AnMBR that were positive after differential abundance analysis (DESeq2) among the three phases of reactor operation. The color scale ranges from 0 to 22% relative abundance.

100% similarity on this genus. Concomitantly, *Methanobacterium* increased from 3.5% in phase I to 11.5% in phase II, but significantly dropped in phase III. In phase III, the hydrogenotrophic methanogens *Methanoculleus* increased to 6.1% in relative abundance becoming the dominant archaea while *Methanolinea* decreased significantly.

Figure 7.4 also illustrates that the most prominent amplicon sequence variants belong to 15 and 2 different classes in the bacterial and archaeal domain, respectively.



For the bacteria microbial community, the abundance of microorganisms of the class Actinobacteria, Bacilli, Synergistia, Gammaproteobacteria, and Thermotogae increased correspondingly to 6.8%, 5.9%, 22.9%, 12.6% and 26.6% at the end of the long-term thermophilic operation. Microorganisms corresponding to these classes have been found in thermophilic saline environments. Clostridia class remained in a comparable relative abundance along with the phases, but with changes at genus level. Especially, microorganisms that belong to this class have been reported as the most essential fermentative bacteria and syntrophic phenol degraders as *Pelotomaculum* (Chen et al. 2009, Muñoz Sierra et al. 2019).

Our results showed a high relative abundance of uncultured microorganisms in the AnMBR. Bacteria belonging to the class JS1, and the candidate phylum Atribacteria (see Supplementary Information Figure S7.1.) were dominant during phases I (9.15%) and II (9.41%). Microorganisms belonging to Atribacteria, mostly have been found in deep-sea methane-rich sediments (Carr et al. 2015). Lee et al. (2018) suggested a fermentative role of these microorganisms, capable of using various substrates, and syntrophic acetate oxidation coupled with hydrogen scavenging methanogens. Recently, the first culturable representative strain of this phylum was isolated and it was confirmed that it plays a role in hydrogenogenic fermentative metabolism (Katayama et al. 2019). In our case, the highest species similarity found was *Bacillus alkalitolerans* strain T3-209, with only 83%.

In the archaea domain, the microbial dynamics indicated a clear switch from acetotrophic to hydrogenotrophic methanogens in the class Methanomicrobia. Both the microbial community structure and the observation that at the end of the experiment the biomass hydrogenotrophic methanogenic activity was substantially higher than the acetate-fed methanogenic activity, support our hypothesis that acetate conversion switched from aceticlastic methanogenesis to acetate oxidation coupled to hydrogenotrophic methanogenesis.

## 7.4 Perspectives and further research

The observed AnMBR performance perturbation following phenol accumulation indicated that the cultivated thermophilic phenol-degrading biomass was dependent on the presence of active methanogens. A drop in the hydrogenotrophic methanogenic activity may have led to the observed reduced phenol conversion capacity. It should be noted that the entire experiment was performed under high salinity ( $18 \text{ gNa}^+\cdot\text{L}^{-1}$ ) conditions. Further research will focus on the role of syntrophic acetate oxidation and phenol degradation intermediates (e.g., benzoate). Our present study showed that highly saline phenolic wastewaters indeed could be treated in a thermophilic AnMBR. However, the achievable phenol conversion capacity was restricted to  $20 \text{ mgPh}\cdot\text{gVSS}^{-1}\cdot\text{d}^{-1}$ , determining an applicable phenol loading rate of about  $0.12 \text{ gPh}\cdot\text{L}^{-1}\cdot\text{d}^{-1}$ . Although thermophilic operation will bring operational energy benefits when treating high-temperature industrial wastewaters with the target of process water reuse, the phenol conversion capacity of the reactor will be lower than when opting for mesophilic operation.

## 7.5 Conclusions

Maximum COD and phenol removal efficiencies of about 95% were achieved during the long-term thermophilic AnMBR operation at  $18 \text{ gNa}^+\cdot\text{L}^{-1}$ . However, severe perturbations occurred following relatively small increments in the phenol loading rate from  $0.01$  to  $0.12 \text{ gPh}\cdot\text{L}^{-1}\cdot\text{d}^{-1}$ . Moreover, by exceeding a sludge phenol loading rate of  $20 \text{ mgPh}\cdot\text{gVSS}^{-1}\cdot\text{d}^{-1}$  the system immediately responded in phenol build-up to concentrations higher than  $600 \text{ mgPh}\cdot\text{L}^{-1}$  leading to significant deterioration of methanogenesis. The observed maximum phenol conversion rates were  $21.3\pm 0.2$  and  $32.8\pm 0.5 \text{ mgPh}\cdot\text{gVSS}^{-1}\cdot\text{d}^{-1}$  in the AnMBR, and in ex-situ batch test at the end of the reactor operation, respectively. The absence of caproate in the VFAs spectrum inferred that the phenol conversion pathway was likely via benzoate carboxylation. The assessed hydrogenotrophic SMA was a factor 2.3 higher than the acetate-fed SMA. Correspondingly, microbial population dynamics indicated that hydrogenotrophic methanogens were enriched during the long-term operation and *Clostridia* class was dominant. Overall, thermophilic AnMBR operation under high salinity seemed to be susceptible to sudden increase in phenol loading rate or phenol shocks, indicating that the specific phenol conversion capacity under the studied conditions was limiting the treatment process.

## Supplementary Information

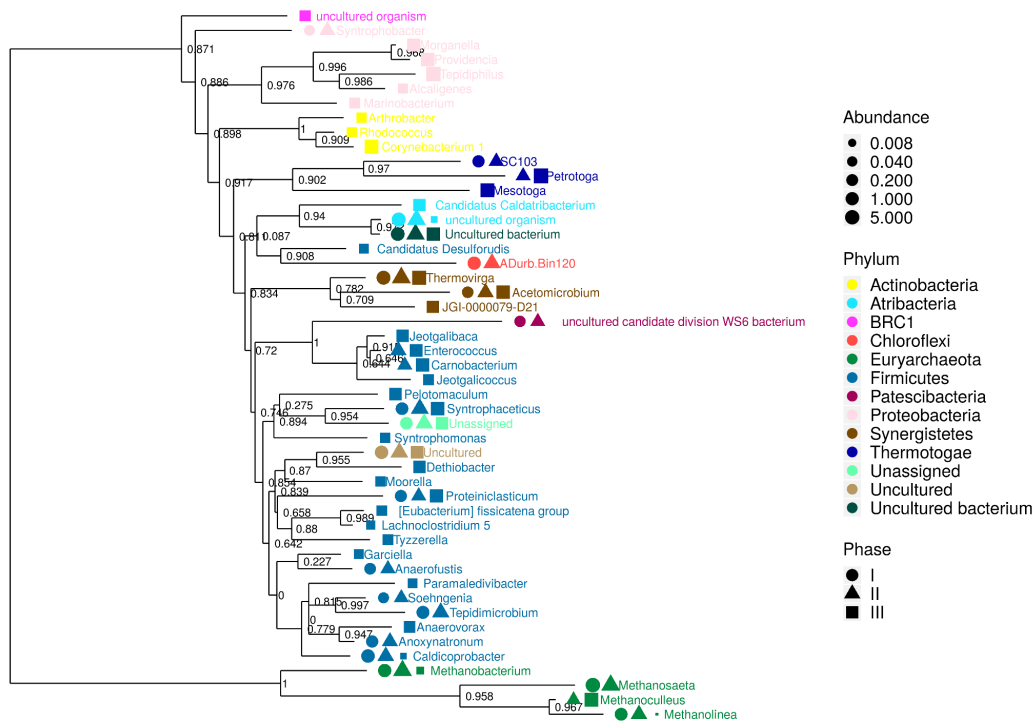


Figure S7.1. Phylogenetic tree after differential abundance analysis (DESeq2), indicating the relative abundance of bacteria and archaea genera belonging to their respective phylum at phases I (circle), II (triangle) and III (square) during the long-term thermophilic AnMBR operation. The size of circle, triangle, and square represent the relative abundance, which is presented in Log<sub>2</sub> scale (0–5) to facilitate the comparison among phases.

Table S7.1. ASVs with differential abundances within the operational phase (I, II, III) and their closest related species hits based on similarity. RA: relative abundance

RA	RA	RA	Phylum	Class	Genus	NCBI_ID	Similarity	Specie_NCBI
I	II	III						
0,00	0,00	0,11	Firmicutes	Clostridia	[Eubacterium] fissicatena group	NR_144617.1	99,00	<i>Marricoccus intestini</i> strain 2PC-424-CC-1
0,00	0,17	2,02	Synergistetes	Synergistia	Acetomicrobium	NR_116842.1	<b>99,26</b>	<i>Acetomicrobium hydrogeniformans</i> ATCC B-4A-1850 strain OS1
0,35	0,55	1,91	Synergistetes	Synergistia	Acetomicrobium	NR_116842.1	<b>100,00</b>	<i>Acetomicrobium hydrogeniformans</i> ATCC B-4A-1850 strain OS1
0,82	0,67	0,00	Chloroflexi	Anaerolineae	ADurb.Bin120	NR_041354.1	91,77	<i>Bellilinea caldijulcae</i> strain GOMI-1
2,36	1,27	0,00	Chloroflexi	Anaerolineae	ADurb.Bin120	NR_041355.1	90,52	<i>Longilinea arnyozae</i> strain KOME-1
0,28	0,21	0,00	Chloroflexi	Anaerolineae	ADurb.Bin120	NR_040972.1	92,25	<i>Levilinea sacharomytica</i> strain KIBI-1
0,00	0,00	0,07	Proteobacteria	Gammaproteobacteri	Alcaligenes	NR_114959.1	<b>100,00</b>	<i>Alcaligenes aquatilis</i> strain LMG 22996
0,39	0,27	0,00	Firmicutes	Clostridia	Anaerofustis	NR_027562.1	93,05	<i>Anaerofustis stercorihominis</i> strain W/AL 14563
0,00	0,00	0,30	Firmicutes	Clostridia	Anaerovorax	NR_159296.1	97,02	<i>Aminipila buyrica</i> strain FH042
0,32	0,35	0,00	Firmicutes	Clostridia	Anoxynatronum	NR_043664.1	<b>99,50</b>	<i>Tindallia texanensis</i> strain IMP-300
0,45	0,32	0,00	Firmicutes	Clostridia	Anoxynatronum	NR_043664.1	98,50	<i>Tindallia texanensis</i> strain IMP-300
0,00	0,00	0,08	Actinobacteria	Actinobacteria	Arthrobacter	NR_116375.1	<b>100,00</b>	<i>Arthrobacter halodurans</i> strain JSM 078085
4,73	1,11	0,00	Firmicutes	Clostridia	Caldicoprobacter	NR_117466.1	90,35	<i>Caldicoprobacter algeriensis</i> strain TH7C1
0,00	0,00	0,33	Atribacteria	Caldatribacteria	Candidatus	NR_133741.1	82,98	<i>Enterococcus xiangfangensis</i> strain 11097
0,00	0,00	0,10	Atribacteria	Caldatribacteria	Candidatus	NR_126262.1	83,18	<i>Melghirimyces profundicolus</i> strain SCSIO 11153
0,00	0,00	0,29	Atribacteria	Caldatribacteria	Candidatus	NR_133741.1	82,98	<i>Enterococcus xiangfangensis</i> strain 11097
0,00	0,00	0,06	Firmicutes	Clostridia	Candidatus Desulforudis	NR_159908.1	86,39	<i>Desulfotermobacter acidiphilus</i> strain 3408-1
0,00	0,00	0,21	Firmicutes	Bacilli	Carnobacterium	NR_040926.1	<b>99,53</b>	<i>Carnobacterium mobile</i> strain DSM 4848
0,00	0,00	0,75	Firmicutes	Bacilli	Carnobacterium	NR_042093.1	<b>99,53</b>	<i>Carnobacterium gallinarum</i> strain DSM 4847
0,00	0,25	1,90	Firmicutes	Bacilli	Carnobacterium	NR_040926.1	<b>99,77</b>	<i>Carnobacterium mobile</i> strain DSM 4848

0,00	0,00	1,27	Actinobacteria	Actinobacteria	Corynebacterium 1	NR_074663.1	99,27	<i>Corynebacterium glutamicum</i> strain ATCC 13032
0,00	0,00	4,48	Actinobacteria	Actinobacteria	Corynebacterium 1	NR_074663.1	99,76	<i>Corynebacterium glutamicum</i> strain ATCC 13032
0,00	0,00	0,88	Actinobacteria	Actinobacteria	Corynebacterium 1	NR_074663.1	99,51	<i>Corynebacterium glutamicum</i> strain ATCC 13032
0,00	0,00	0,74	Firmicutes	Clostridia	Dethiobacter	NR_117747.2	89,19	<i>Desulfotomaculum thermocisternus</i> DSM 10259
0,00	0,14	0,30	Firmicutes	Bacilli	Enterococcus	NR_117976.1	99,77	<i>Enterococcus nikkeiensis</i> strain IE3.2
0,00	0,79	1,49	Firmicutes	Bacilli	Enterococcus	NR_114453.1	100,00	<i>Enterococcus malodoratus</i> strain ATCC 43197
0,00	0,00	0,05	Firmicutes	Clostridia	Garciella	NR_144613.1	95,78	<i>Irregularibacter muris</i> strain 2PG-426-CC-4.2
0,00	0,00	0,95	Firmicutes	Bacilli	Jeogalibaca	NR_125553.1	100,00	<i>Jeogalibaca danbookensis</i> strain EX-07
0,00	0,00	0,10	Firmicutes	Bacilli	Jeogalibaca	NR_156899.1	98,12	<i>Jeogalibaca arbutidis</i> strain 1805-02
0,00	0,00	0,18	Firmicutes	Bacilli	Jeogalibacoccus	NR_025644.1	100,00	<i>Jeogalibacoccus psychrophilus</i> strain YKJ-115
0,00	0,00	0,31	Synergistetes	Synergistia	JGI-0000079-D21	NR_116842.1	89,95	<i>Acetomicrobium hydrogeniformans</i> ATCC BAA-1850 strain OS1
0,00	0,00	0,55	Synergistetes	Synergistia	JGI-0000079-D21	NR_116842.1	90,20	<i>Acetomicrobium hydrogeniformans</i> ATCC BAA-1850 strain OS1
0,00	0,00	0,02	Firmicutes	Clostridia	Lachnoclostridium 5	NR_112174.1	99,75	[ <i>Clostridium</i> ] <i>sphenoides</i> JCM 1415 strain ATCC 19403
0,00	0,00	0,18	Proteobacteria	Gammaproteobacteria	Marinobacterium	NR_114163.1	99,06	<i>Marinobacterium goongense</i> strain NBRC 102606
0,00	0,00	5,42	Thermotogae	Thermotogae	Mesotoga	NR_117646.2	100,00	<i>Mesotoga infera</i> strain VYN100
0,00	0,00	0,10	Thermotogae	Thermotogae	Mesotoga	NR_117755.1	99,77	<i>Mesotoga prima</i> MesG1.Ag.4.2 strain mesG1.Ag.4.2
0,29	1,03	0,00	Euryarchaeota	Methanobacteria	Methanobacterium	NR_042895.1	100,00	<i>Methanobacterium aarhusense</i> strain H2-LR
3,16	10,4	0,01	Euryarchaeota	Methanobacteria	Methanobacterium	NR_028247.1	99,74	<i>Methanobacterium subterraneum</i> strain A8p
0,00	0,18	5,40	Euryarchaeota	Methanomicrobia	Methanoculleus	NR_043961.1	100,00	<i>Methanoculleus neptacali</i> strain ZC-2
0,00	0,00	0,66	Euryarchaeota	Methanomicrobia	Methanoculleus	NR_116881.1	99,74	<i>Methanoculleus hydrogeniphilus</i> strain HC
1,66	1,07	0,00	Euryarchaeota	Methanomicrobia	Methanolinea	NR_028163.1	96,84	<i>Methanolinea larla</i> strain NOBI-1
0,39	0,34	0,00	Euryarchaeota	Methanomicrobia	Methanosacta	NR_043203.1	100,00	<i>Methanosacta horridinacea</i> strain 8.Ac
18,7	10,6	0,00	Euryarchaeota	Methanomicrobia	Methanosacta	NR_043203.1	98,18	<i>Methanosacta horridinacea</i> strain 8.Ac
0,60	0,40	0,00	Euryarchaeota	Methanomicrobia	Methanosacta	NR_043203.1	98,70	<i>Methanosacta horridinacea</i> strain 8.Ac
0,00	0,00	0,07	Firmicutes	Clostridia	Moorella	NR_113196.1	94,10	<i>Moorella thamoactica</i> strain JCM 9319

0,00	0,00	0,18	Proteobacteria	Gammaproteobacteri a	Morganella	NR_043751.1	99,53	<i>Morganella morganii</i> subsp. <i>sibonii</i> strain DSM 14850
0,00	0,00	0,17	Proteobacteria	Gammaproteobacteri a	Morganella	NR_043751.1	99,77	<i>Morganella morganii</i> subsp. <i>sibonii</i> strain DSM 14850
0,00	0,00	1,25	Proteobacteria	Gammaproteobacteri a	Morganella	NR_043751.1	99,29	<i>Morganella morganii</i> subsp. <i>sibonii</i> strain DSM 14850
0,00	0,00	0,14	Proteobacteria	Gammaproteobacteri a	Morganella	NR_043751.1	99,77	<i>Morganella morganii</i> subsp. <i>sibonii</i> strain DSM 14850
0,00	0,00	0,05	Firmicutes	Clostridia	Paramaledivibacter	NR_152683.1	92,50	<i>Paramaledivibacter batliensis</i> strain DY30321
0,00	0,00	1,23	Firmicutes	Clostridia	Pelotomaculum	NR_041320.1	96,02	<i>Pelotomaculum isophthalicacum</i> J1
0,00	0,18	20,9	Thermotogae	Thermotogae	Petrogoga	NR_169443.1	99,76	<i>Petrogoga japonica</i> strain AR80
0,00	0,08	0,18	Thermotogae	Thermotogae	Petrogoga	NR_169443.1	99,29	<i>Petrogoga japonica</i> strain AR80
0,00	0,00	2,39	Firmicutes	Clostridia	Proteiniclasticum	NR_118108.1	96,25	<i>Youngibacter fragilis</i> 232.1
0,68	0,31	0,00	Firmicutes	Clostridia	Proteiniclasticum	NR_115875.1	99,00	<i>Proteiniclasticum ruminis</i> DSM 24773 strain D3RC-2
0,00	0,00	1,23	Proteobacteria	Gammaproteobacteri a	Providencia	NR_115880.1	99,77	<i>Providencia rettgeri</i> strain NCTC 11801
0,00	0,00	1,24	Proteobacteria	Gammaproteobacteri a	Providencia	NR_104913.1	100,00	<i>Providencia sneebia</i> DSM 19967 strain A
0,00	0,00	1,18	Proteobacteria	Gammaproteobacteri a	Providencia	NR_115880.1	99,53	<i>Providencia rettgeri</i> strain NCTC 11801
0,00	0,00	0,06	Actinobacteria	Actinobacteria	Rhodococcus	NR_104776.1	100,00	<i>Nocardia codata</i> strain DSM 44595
0,76	0,30	0,00	Thermotogae	Thermotogae	SC103	NR_025969.1	80,00	<i>Pseudothermotoga subterranea</i> strain SLJ
0,18	0,27	0,00	Firmicutes	Clostridia	Soehngenia	NR_117382.1	100,00	<i>Soehngenia saccharolytica</i> strain DSM 12858
1,43	4,81	3,30	Firmicutes	Clostridia	Syntrophaceticus	NR_110297.1	97,02	<i>Syntrophaceticus schinkii</i> strain Sp3
0,13	0,52	0,00	Proteobacteria	Deltaproteobacteria	Syntrophobacter	NR_043073.1	100,00	<i>Syntrophobacter sulfidireducens</i> strain TB8106
0,00	0,00	0,03	Firmicutes	Clostridia	Syntrophomonas	NR_122058.1	93,71	<i>Syntrophomonas wolfei</i> strain Goettingen G311
0,00	0,00	0,04	Firmicutes	Clostridia	Syntrophomonas	NR_122058.1	93,47	<i>Syntrophomonas wolfei</i> strain Goettingen G311
0,94	0,89	0,00	Firmicutes	Clostridia	Tepidimicrobium	NR_117380.1	99,75	<i>Tepidimicrobium ferriphilum</i> strain DSM 16624
0,43	0,40	0,00	Firmicutes	Clostridia	Tepidimicrobium	NR_116042.1	97,24	<i>Tepidimicrobium sylvaniticum</i> strain PML14
0,26	0,18	0,00	Firmicutes	Clostridia	Tepidimicrobium	NR_117379.1	97,00	[ <i>Clostridium</i> ] <i>ulbinense</i> DSM 10521

0,54	0,80	0,00	Firmicutes	Clostridia	Tepidimicrobium	NR_117379.1	96,75	<i>[Clostridium] ultanense</i> DSM 10521
0,00	0,00	4,29	Proteobacteria	Gammaproteobacteri a	Tepidiphilus	NR_025556.1	<b>99,06</b>	<i>Tepidiphilus margaritiflor</i> strain N2-214
0,00	0,00	12,9	Proteobacteria	Gammaproteobacteri a	Tepidiphilus	NR_025556.1	<b>99,29</b>	<i>Tepidiphilus margaritiflor</i> strain N2-214
3,76	5,89	4,56	Synergistetes	Synergistia	Thermovirga	NR_074606.1	93,30	<i>Thermovirga lienii</i> strain DSM 17291
0,17	0,32	0,00	Synergistetes	Synergistia	Thermovirga	NR_074606.1	93,56	<i>Thermovirga lienii</i> strain DSM 17291
0,67	1,29	0,00	Synergistetes	Synergistia	Thermovirga	NR_074606.1	93,81	<i>Thermovirga lienii</i> strain DSM 17291
0,26	0,35	0,00	Synergistetes	Synergistia	Thermovirga	NR_074606.1	93,05	<i>Thermovirga lienii</i> strain DSM 17291
0,00	0,00	0,57	Synergistetes	Synergistia	Thermovirga	NR_074606.1	92,80	<i>Thermovirga lienii</i> strain DSM 17291
2,58	5,39	0,03	Synergistetes	Synergistia	Thermovirga	NR_074606.1	93,56	<i>Thermovirga lienii</i> strain DSM 17291
0,35	0,74	0,00	Synergistetes	Synergistia	Thermovirga	NR_074606.1	93,09	<i>Thermovirga lienii</i> strain DSM 17291
0,00	0,00	1,08	Synergistetes	Synergistia	Thermovirga	NR_074606.1	92,80	<i>Thermovirga lienii</i> strain DSM 17291
0,22	0,12	0,00	Synergistetes	Synergistia	Thermovirga	NR_074606.1	91,87	<i>Thermovirga lienii</i> strain DSM 17291
0,00	0,00	1,70	Synergistetes	Synergistia	Thermovirga	NR_074606.1	93,55	<i>Thermovirga lienii</i> strain DSM 17291
0,00	0,00	0,14	Firmicutes	Clostridia	Tyzzerella	NR_113408.1	<b>99,50</b>	<i>Anaerovirgum propionicum</i> strain JCM 1430
0,00	0,00	0,04	Bacteroidetes	Bacteroidia	Unassigned	NR_042987.1	92,86	<i>Petrimonas sulfariphila</i> strain BN3
0,00	0,00	0,34	BRC1	Unassigned	Unassigned	NR_104861.1	82,01	<i>Caldanaebacter subterraneus</i> strain DSM 13054
0,00	0,00	0,03	Firmicutes	Clostridia	Unassigned	NR_102767.2	97,88	<i>Syntrophothermus lipocalidus</i> strain DSM 12680
0,00	0,00	0,07	Firmicutes	Clostridia	Unassigned	NR_120221.1	88,76	<i>Desulfaribacillus alkalisarsenatis</i> strain_AHT28
0,00	0,00	0,07	Firmicutes	Clostridia	Unassigned	NR_108634.1	89,18	<i>Moorella hamiferrea</i> strain 64-FGQ
0,15	0,17	0,00	Patescibacteria	Microgenomatia	Unassigned	NR_150873.1	78,35	<i>Actinophytocola xanthii</i> strain KCTC 39690
0,22	1,84	0,01	Firmicutes	Clostridia	Unassigned	NR_114349.1	85,98	<i>Calditerribacillus maritimus</i> strain KKC1
0,00	0,00	0,12	Planctomycetes	Phycisphaerae	Unassigned	NR_164615.1	81,64	<i>Sedimentisphaera salicampi</i> strain ST-Pulz/AB-D4
0,21	0,12	0,00	Acidobacteria	c5LKS83	Unassigned	NR_152720.1	80,98	<i>Manniibaculum humilum</i> strain H2
0,00	0,00	0,13	Proteobacteria	Gammaproteobacteri a	Unassigned	NR_025510.1	99,29	<i>Alicyclophilus dentirificans</i> K601
0,00	0,00	0,02	Firmicutes	Clostridia	Unassigned	NR_119284.1	96,53	<i>Pseudoclostridium thermosaccinigenes</i> strain DSM 5807

0,59	0,24	0,00	Thermotogae	Thermotogae	Unassigned	NR_044583.2	90,68	90,68	<i>Kosmotoga olearia</i> TBF 19.5.1
0,00	0,00	0,16	Firmicutes	Clostridia	Unassigned	NR_041236.1	89,08	89,08	<i>Lactispora thermophila</i> DSM 19022 strain EBR46
3,16	2,44	0,00	Firmicutes	Clostridia	uncultured	NR_044205.1	88,59	88,59	<i>Dehalobacter alkalicophilus</i> AHT 1
0,21	0,22	0,00	Chloroflexi	Anaerolineae	uncultured	NR_109544.1	89,53	89,53	<i>Ornatilinea apprima</i> strain P3M-1
0,00	0,00	0,04	Firmicutes	Clostridia	uncultured	NR_125623.1	88,81	88,81	<i>Proteinivorax tanatarense</i> strain Z-910
0,24	0,21	0,00	Chloroflexi	Anaerolineae	uncultured	NR_109544.1	89,03	89,03	<i>Ornatilinea apprima</i> strain P3M-1
0,50	0,15	0,00	Firmicutes	Clostridia	uncultured	NR_125623.1	88,31	88,31	<i>Proteinivorax tanatarense</i> strain Z-910
0,00	0,00	1,07	Deferribacteres	Deferribacteres	uncultured	NR_158118.1	93,68	93,68	<i>Petrothermobacter organivorans</i> strain ANA
4,98	4,45	0,00	Attribacteria	JS1	uncultured bacterium	NR_163643.1	82,90	82,90	<i>Bacillus alkalicolerans</i> strain T3-209
0,15	0,15	0,00	Tenericutes	Mollicutes	uncultured bacterium	NR_042955.1	83,41	83,41	<i>Acholeplasma brassicae</i> 0502
0,13	0,81	0,00	Firmicutes	Clostridia	uncultured bacterium	NR_117466.1	90,82	90,82	<i>Caldicoprobacter algeriensis</i> strain TH7C1
0,12	0,33	0,00	Firmicutes	Clostridia	uncultured bacterium	NR_117466.1	87,56	87,56	<i>Caldicoprobacter algeriensis</i> strain TH7C1
0,20	0,16	0,00	Aegirbacteria	uncultured bacterium	uncultured bacterium	NR_159236.1	83,57	83,57	<i>Desulfonatronum purunguonense</i> strain P-AR180
0,00	0,00	0,02	Proteobacteria	Deltaproteobacteria	uncultured bacterium	NR_025746.1	86,95	86,95	<i>Desulfoloba fastidiosa</i> strain P2
0,00	0,00	2,70	Bacteroidetes	Bacteroidia	uncultured bacterium	NR_156071.1	80,47	80,47	<i>Lobithiobacter aurantiacus</i> strain HQYD1
0,00	0,00	0,53	Chloroflexi	Anaerolineae	uncultured bacterium	NR_117865.1	88,42	88,42	<i>Thermanaerobrix duxensis</i> strain GNS-1
0,00	0,00	0,11	Actinobacteria	Coriobacteria	uncultured bacterium	NR_146815.1	89,93	89,93	<i>Oligella multihensis</i> strain KHD7
0,28	0,19	0,00	Patescibacteria	WS6 (Dojkabacteria)	uncultured candidate	NR_044490.1	79,85	79,85	<i>Butyrivibrio pullicaeorum</i> strain 25-3
6,05	5,58	0,00	Attribacteria	JS1	division WS6 bacterium	NR_163643.1	82,90	82,90	<i>Bacillus alkalicolerans</i> strain T3-209
3,10	3,82	0,00	Attribacteria	JS1	uncultured organism	NR_163643.1	83,14	83,14	<i>Bacillus alkalicolerans</i> strain T3-209
0,00	0,00	0,18	BRC1	uncultured organism	uncultured organism	NR_136805.1	84,43	84,43	<i>Marinithermophilum abyssi</i> strain SCYIO 11157
0,00	0,00	0,11	Firmicutes	Clostridia	[Eubacterium] fissicatena group	NR_144617.1	99,00	99,00	



## References

- APHA (2005) Standard Methods for the Examination of Water and Wastewater, American Public Health Association, Washington, DC. USA
- Bolyen, E., Rideout, J.R., Dillon, M.R., Bokulich, N.A., Abnet, C.C., Al-Ghalith, G.A., Alexander, H., Alm, E.J., Arumugam, M., Asnicar, F., Bai, Y., Bisanz, J.E., Bittinger, K., Brejnrod, A., Brislawn, C.J., Brown, C.T., Callahan, B.J., Caraballo-Rodríguez, A.M., Chase, J., Cope, E.K., Da Silva, R., Diener, C., Dorrestein, P.C., Douglas, G.M., Durall, D.M., Duvallet, C., Edwardson, C.F., Ernst, M., Estaki, M., Fouquier, J., Gauglitz, J.M., Gibbons, S.M., Gibson, D.L., Gonzalez, A., Gorlick, K., Guo, J., Hillmann, B., Holmes, S., Holste, H., Huttenhower, C., Huttley, G.A., Janssen, S., Jarmusch, A.K., Jiang, L., Kaehler, B.D., Kang, K.B., Keefe, C.R., Keim, P., Kelley, S.T., Knights, D., Koester, I., Kosciulek, T., Kreps, J., Langille, M.G.I., Lee, J., Ley, R., Liu, Y.-X., Loftfield, E., Lozupone, C., Maher, M., Marotz, C., Martin, B.D., McDonald, D., McIver, L.J., Melnik, A.V., Metcalf, J.L., Morgan, S.C., Morton, J.T., Naimey, A.T., Navas-Molina, J.A., Nothias, L.F., Orchanian, S.B., Pearson, T., Peoples, S.L., Petras, D., Preuss, M.L., Pruesse, E., Rasmussen, L.B., Rivers, A., Robeson, M.S., Rosenthal, P., Segata, N., Shaffer, M., Shiffer, A., Sinha, R., Song, S.J., Spear, J.R., Swafford, A.D., Thompson, L.R., Torres, P.J., Trinh, P., Tripathi, A., Turnbaugh, P.J., Ull-Hasan, S., van der Hooft, J.J.J., Vargas, F., Vázquez-Baeza, Y., Vogtmann, E., von Hippel, M., Walters, W., Wan, Y., Wang, M., Warren, J., Weber, K.C., Williamson, C.H.D., Willis, A.D., Xu, Z.Z., Zaneveld, J.R., Zhang, Y., Zhu, Q., Knight, R. and Caporaso, J.G. (2019) Reproducible, interactive, scalable and extensible microbiome data science using QIIME 2. *Nature Biotechnology* 37(8), 852-857.
- Busca, G., Berardinelli, S., Resini, C. and Arrighi, L. (2008) Technologies for the removal of phenol from fluid streams: A short review of recent developments. *Journal of Hazardous materials* 160(2), 265-288.
- Callahan, B.J., McMurdie, P.J., Rosen, M.J., Han, A.W., Johnson, A.J.A. and Holmes, S.P. (2016) DADA2: High-resolution sample inference from Illumina amplicon data. *Nature Methods* 13, 581.
- Carr, S.A., Orcutt, B.N., Mandernack, K.W. and Spear, J.R. (2015) Abundant Atribacteria in deep marine sediment from the Adélie Basin, Antarctica. *Frontiers in Microbiology* 6(872).
- Chen, C.-L., Wu, J.-H. and Liu, W.-T. (2008) Identification of important microbial populations in the mesophilic and thermophilic phenol-degrading methanogenic consortia. *Water Research* 42(8), 1963-1976.
- Chen, C.-L., Wu, J.-H., Tseng, I.C., Liang, T.-M. and Liu, W.-T. (2009) Characterization of Active Microbes in a Full-Scale Anaerobic Fluidized Bed Reactor Treating Phenolic Wastewater. *Microbes and Environments* 24(2), 144-153.
- Coates, J.D., Coughlan, M.F. and Colleran, E. (1996) Simple method for the measurement of the hydrogenotrophic methanogenic activity of anaerobic sludges. *Journal of Microbiological Methods* 26(3), 237-246.
- Collins, G., Foy, C., McHugh, S., Mahony, T. and O'Flaherty, V. (2005) Anaerobic biological treatment of phenolic wastewater at 15–18°C. *Water Research* 39(8), 1614-1620.
- Cook, L.E., Gang, S.S., Ihlan, A., Maune, M., Tanner, R.S., McInerney, M.J., Weinstock, G., Lobos, E.A. and Gunsalus, R.P. (2018) Genome Sequence of *Acetomicrobium hydrogeniformans* OS1. *Genome announcements* 6(26), e00581-00518.
- De Vrieze, J., Raport, L., Roume, H., Vilchez-Vargas, R., Jáuregui, R., Pieper, D.H. and Boon, N. (2016) The full-scale anaerobic digestion microbiome is represented by specific marker populations. *Water Research* 104, 101-110.

- Dellagneze, B.M., Vasconcellos, S.P.d., Melo, I.S.d., Santos Neto, E.V.D. and Oliveira, V.M.d. (2016) Evaluation of bacterial diversity recovered from petroleum samples using different physical matrices. *Brazilian journal of microbiology* : [publication of the Brazilian Society for Microbiology] 47(3), 712-723.
- Dereli, R.K., Ersahin, M.E., Ozgun, H., Ozturk, I., Jeison, D., van der Zee, F. and van Lier, J.B. (2012) Potentials of anaerobic membrane bioreactors to overcome treatment limitations induced by industrial wastewaters. *Bioresource Technology* 122, 160-170.
- Duncan, J., Bokhary, A., Fatehi, P., Kong, F., Lin, H. and Liao, B. (2017) Thermophilic membrane bioreactors: A review. *Bioresource Technology* 243(Supplement C), 1180-1193.
- Evans and Fuchs, G. (1988) Anaerobic Degradation of Aromatic Compounds. *Annual Review of Microbiology* 42(1), 289-317.
- Fang, H.H.P., Liang, D.W., Zhang, T. and Liu, Y. (2006) Anaerobic treatment of phenol in wastewater under thermophilic condition. *Water Research* 40(3), 427-434.
- Fang, H.H.P., Liu, Y., Ke, S.Z. and Zhang, T. (2004) Anaerobic degradation of phenol in wastewater at ambient temperature. *Water Science and Technology* 49(1), 95-102.
- Franchi, O., Cabrol, L., Chamy, R. and Rosenkranz, F. (2020) Correlations between microbial population dynamics, bamA gene abundance and performance of anaerobic sequencing batch reactor (ASBR) treating increasing concentrations of phenol. *Journal of Biotechnology* 310, 40-48.
- Hoyos-Hernandez, C., Hoffmann, M., Guenne, A. and Mazeas, L. (2014) Elucidation of the thermophilic phenol biodegradation pathway via benzoate during the anaerobic digestion of municipal solid waste. *Chemosphere* 97, 115-119.
- Katayama, T., Nobu, M.K., Kusada, H., Meng, X.-Y., Yoshioka, H., Kamagata, Y. and Tamaki, H. (2019) Membrane-bounded nucleoid discovered in a cultivated bacterium of the candidate phylum 'Atribacteria'. *bioRxiv*, 728279.
- Katoh, K. and Standley, D.M. (2013) MAFFT multiple sequence alignment software version 7: Improvements in performance and usability. *Molecular Biology and Evolution* 30(4), 772-780.
- Lee, Y.M., Hwang, K., Lee, J.I., Kim, M., Hwang, C.Y., Noh, H.-J., Choi, H., Lee, H.K., Chun, J., Hong, S.G. and Shin, S.C. (2018) Genomic Insight Into the Predominance of Candidate Phylum Atribacteria JS1 Lineage in Marine Sediments. *Frontiers in Microbiology* 9(2909).
- Levén, L. and Schnürer, A. (2005) Effects of temperature on biological degradation of phenols, benzoates and phthalates under methanogenic conditions. *International Biodeterioration & Biodegradation* 55(2), 153-160.
- Li, Q., Liu, Y., Yang, X., Zhang, J., Lu, B. and Chen, R. (2020) Kinetic and thermodynamic effects of temperature on methanogenic degradation of acetate, propionate, butyrate and valerate. *Chemical Engineering Journal* 396, 125366.
- Liang, D. and Fang, H.H.P. (2010) *Environmental Anaerobic Technology*, pp. 185-205.
- Lin, H., Peng, W., Zhang, M., Chen, J., Hong, H. and Zhang, Y. (2013) A review on anaerobic membrane bioreactors: Applications, membrane fouling and future perspectives. *Desalination* 314, 169-188.
- Love, M.I., Huber, W. and Anders, S. (2014) Moderated estimation of fold change and dispersion for RNA-seq data with DESeq2. *Genome Biology* 15(12).

- Madigou, C., Poirier, S., Bureau, C. and Chapleur, O. (2016) Acclimation strategy to increase phenol tolerance of an anaerobic microbiota. *Bioresource Technology* 216, 77-86.
- McMurdie, P.J. and Holmes, S. (2013) Phyloseq: An R Package for Reproducible Interactive Analysis and Graphics of Microbiome Census Data. *PLoS ONE* 8(4).
- Muñoz Sierra, J.D., Lafita, C., Gabaldón, C., Spanjers, H. and van Lier, J.B. (2017) Trace metals supplementation in anaerobic membrane bioreactors treating highly saline phenolic wastewater. *Bioresource Technology* 234, 106-114.
- Muñoz Sierra, J.D., Oosterkamp, M.J., Wang, W., Spanjers, H. and van Lier, J.B. (2018a) Impact of long-term salinity exposure in anaerobic membrane bioreactors treating phenolic wastewater: Performance robustness and endured microbial community. *Water Research* 141, 172-184.
- Muñoz Sierra, J.D., Oosterkamp, M.J., Wang, W., Spanjers, H. and van Lier, J.B. (2019) Comparative performance of upflow anaerobic sludge blanket reactor and anaerobic membrane bioreactor treating phenolic wastewater: Overcoming high salinity. *Chemical Engineering Journal* 366, 480-490.
- Muñoz Sierra, J.D., Wang, W., Cerqueda-García, D., Oosterkamp, M.J., Spanjers, H. and van Lier, J.B. (2018b) Temperature susceptibility of a mesophilic anaerobic membrane bioreactor treating saline phenol-containing wastewater. *Chemosphere* 213, 92-102.
- Price, M.N., Dehal, P.S. and Arkin, A.P. (2010) FastTree 2 - Approximately maximum-likelihood trees for large alignments. *PLoS ONE* 5(3).
- Ramakrishnan, A. and Surampalli, R.Y. (2013) Performance and energy economics of mesophilic and thermophilic digestion in anaerobic hybrid reactor treating coal wastewater. *Bioresource Technology* 127, 9-17.
- Raza, W., Lee, J., Raza, N., Luo, Y., Kim, K.-H. and Yang, J. (2019) Removal of phenolic compounds from industrial waste water based on membrane-based technologies. *Journal of Industrial and Engineering Chemistry* 71, 1-18.
- Rognes, T., Flouri, T., Nichols, B., Quince, C. and Mahé, F. (2016) VSEARCH: A versatile open source tool for metagenomics. *PeerJ* 2016(10).
- Rosenkranz, F., Cabrol, L., Carballa, M., Donoso-Bravo, A., Cruz, L., Ruiz-Filippi, G., Chamy, R. and Lema, J.M. (2013) Relationship between phenol degradation efficiency and microbial community structure in an anaerobic SBR. *Water Research* 47(17), 6739-6749.
- Scully, C., Collins, G. and O'Flaherty, V. (2006) Anaerobic biological treatment of phenol at 9.5–15°C in an expanded granular sludge bed (EGSB)-based bioreactor. *Water Research* 40(20), 3737-3744.
- Spanjers, H. and Vanrolleghem, P. (2016) In: van Loosdrecht et al. *Experimental methods in wastewater treatment* Online, W.I. (ed), p. 360, Water Intell. Online.
- Tay, J.-H., He, Y.-X. and Yan, Y.-G. (2001) Improved Anaerobic Degradation of Phenol with Supplemental Glucose. *Journal of Environmental Engineering* 127(1), 38-45.
- van Lier, J.B. (1996) Limitations of thermophilic anaerobic wastewater treatment and the consequences for process design. *Antonie van Leeuwenhoek* 69(1), 1-14.

- van Lier, J.B. (2008) High-rate anaerobic wastewater treatment: diversifying from end-of-the-pipe treatment to resource-oriented conversion techniques. *Water Science and Technology* 57(8), 1137-1148.
- Van Lier, J.B., Grolle, K.C., Frijters, C.T., Stams, A.J. and Lettinga, G. (1993) Effects of acetate, propionate, and butyrate on the thermophilic anaerobic degradation of propionate by methanogenic sludge and defined cultures. *Applied and environmental microbiology* 59(4), 1003-1011.
- van Lier, J.B., van der Zee, F.P., Frijters, C.T.M.J. and Ersahin, M.E. (2015) Celebrating 40 years anaerobic sludge bed reactors for industrial wastewater treatment. *Reviews in Environmental Science and Bio/Technology* 14(4), 681-702.
- Villegas, L.G.C., Mashhadi, N., Chen, M., Mukherjee, D., Taylor, K.E. and Biswas, N. (2016) A Short Review of Techniques for Phenol Removal from Wastewater. *Current Pollution Reports* 2(3), 157-167.
- Wang, W., Ma, W., Han, H., Li, H. and Yuan, M. (2011) Thermophilic anaerobic digestion of Lurgi coal gasification wastewater in a UASB reactor. *Bioresource Technology* 102(3), 2441-2447.
- Wang, W., Yang, K., Muñoz Sierra, J., Zhang, X., Yuan, S. and Hu, Z. (2017) Potential impact of methyl isobutyl ketone (MIBK) on phenols degradation in an UASB reactor and its degradation properties. *Journal of Hazardous materials* 333, 73-79.
- Wang, Y.-S. and Barlaz, M.A. (1998) Anaerobic biodegradability of alkylbenzenes and phenol by landfill derived microorganisms. *FEMS Microbiology Ecology* 25(4), 405-418.
- Westerholm, M., Moestedt, J. and Schnürer, A. (2016) Biogas production through syntrophic acetate oxidation and deliberate operating strategies for improved digester performance. *Applied Energy* 179, 124-135.





# 8

## Conclusions and Outlook

## 8.1 Main Conclusions

The research presented in this thesis demonstrates the potential of the application of anaerobic membrane bioreactor (AnMBR) technology for chemical wastewaters under high salinity and high-temperature conditions. The performed long-term evaluation brought novel insights into the feasibility and limitations of anaerobic bioconversion of a model aromatic compound, i.e. phenol, under these conditions, meanwhile applying ultrafiltration membranes to ensure complete biomass retention. Phenol toxicity was exhibited depending on prevailing concentration and applied specific phenol loading rate, leading to the deterioration of methanogenesis under thermophilic and high salinity conditions. The developed AnMBR technology opens interesting perspectives for such chemical wastewaters that can be hardly treated in conventional anaerobic reactors. In this section, the main findings are integrated and discussed following the corresponding extreme conditions assessed.

### 8.1.1 High and fluctuating salinity

#### 8.1.1.1 Biomass methanogenic activity and trace metals bioavailability

High sodium concentrations caused a poor performance during the start-up of the AnMBRs, concomitantly decreasing the biomass particle size. Sodium accumulation in the biomass matrix occurred and led to solubilization of trace metals (TM), becoming more soluble and prone to wash-out. Although the supplied TM cocktail provided adequate metal concentrations, the metals might not have been present in a bioavailable form that can be taken up by the microorganisms. An increase in TM concentration avoided depletion of bioavailable metals, preventing ions exchange, or displacement of TM by sodium. In this thesis, a sodium concentration of  $23 \text{ gNa}^+\cdot\text{L}^{-1}$  decreased the specific methanogenic activity of adapted biomass to salinity to half of the maximum value and was regarded as the 50% inhibition concentration ( $\text{IC}_{50}$ ). At  $34 \text{ gNa}^+\cdot\text{L}^{-1}$  almost complete inhibition was found (**Chapter 2**). While sodium concentration increased from 14 to  $20 \text{ gNa}^+\cdot\text{L}^{-1}$ , a decrease of 24% in the specific methanogenic activity was observed (**Chapter 3**). Despite the findings in **Chapter 2**, the achieved results in **Chapter 4**, by applying a step-wise salinity increase, showed that methanogenesis still occurred at  $36 \text{ gNa}^+\cdot\text{L}^{-1}$  but the specific methanogenic activity (SMA) decreased by 70%. Nonetheless, the observed SMA was approximately ten times higher than the expected activity based on the reported sodium response curve in **Chapter 2**, indicating endurance and net growth of the relevant microbial consortia (**Chapter 4**).

#### 8.1.1.2 AnMBR performance

The impact of a long-term salinity increase to  $20 \text{ gNa}^+\cdot\text{L}^{-1}$  on the AnMBR conversion performance was assessed. Phenol removal efficiencies of up to 99.9% were obtained. A phenol conversion rate of  $11.7 \text{ mgPh}\cdot\text{gVSS}^{-1}\cdot\text{d}^{-1}$  was achieved at  $20 \text{ gNa}^+\cdot\text{L}^{-1}$ . Flow cytometry indicated that raising the sodium concentration compromised the cell membranes. However, the AnMBR performance was not affected by short-term step-wise salinity fluctuations of  $2 \text{ gNa}^+\cdot\text{L}^{-1}$  in the reactor bulk liquid (**Chapter 3**). An increase in sodium concentration exceeding  $26 \text{ gNa}^+\cdot\text{L}^{-1}$ , and applied large fluctuations between 8 and  $34 \text{ gNa}^+\cdot\text{L}^{-1}$ , reduced the phenol and COD removal



efficiency significantly. Nonetheless, the AnMBR biomass was able to maintain phenol conversion rates between  $6.9 \text{ mgPh}\cdot\text{gVSS}^{-1}\cdot\text{d}^{-1}$  and  $25.5 \text{ mgPh}\cdot\text{gVSS}^{-1}\cdot\text{d}^{-1}$  (**Chapter 4**).

Contrarily, membrane filtration was adversely affected by salinity increase, e.g., from  $14 \text{ gNa}^+\cdot\text{L}^{-1}$  to  $20 \text{ gNa}^+\cdot\text{L}^{-1}$ , which was confirmed by an increase in the transmembrane pressure to about 350 mbar, and a concomitant increase in the membrane resistance to filtration. This was attributed to a substantial 92% reduction in biomass particle size (**Chapter 3**). Similarly, an overall reduction of about 80% in biomass particle size was found when large salinity fluctuations were applied. The fluctuations hampered the membrane filtration performance and induced transmembrane pressures of above 400 mbar and membrane resistance to filtration to  $25 \times 10^{12} \text{ m}^{-1}$ . The high sodium concentration and large fluctuations induced a high biomass stress index, transiently reducing the microbial activity of the sludge and the cells membrane integrity (**Chapter 4**).

### 8.1.1.3 Microbial community

The adaptation of the microbial community to salinity changes resulted in higher removal efficiencies of phenol. *Clostridium* genus (up to 54% relative abundance) dominated the bacterial community and archaea were dominated by *Methanobacterium* and *Methanosaeta* genus. Syntrophic phenol-degrading bacteria, such as *Pelotomaculum* showed an increased relative abundance after adaptation of the microbial community to high salinity together with a higher phenol conversion (**Chapter 3**). Likewise, the dominant bacteria found in the AnMBR during large salinity fluctuations belong to the Clostridiales and Synergistales order, whereas archaea belonged to both Methanosarcinales and Methanobacteriales decreased in relative abundance. Microbial richness and diversity were reduced substantially by sodium concentration changes in the bulk liquid larger than  $14 \text{ gNa}^+\cdot\text{L}^{-1}$  (**Chapter 4**).

### 8.1.1.4 The role of other cations: $\text{K}^+:\text{Na}^+$ ratio effect on methane production and $\text{Ca}^{2+}$ leaching

COD and phenol removal rates at 16, 20, and  $24 \text{ gNa}^+\cdot\text{L}^{-1}$ , applying a fixed  $\text{K}^+:\text{Na}^+$  ratio of 0.05, showed the best performance at  $16 \text{ gNa}^+\cdot\text{L}^{-1}$ , i.e., COD removal efficiency of 93.6% and phenol removal efficiency of 99.9%. The methane production rates were highest at a  $\text{K}^+:\text{Na}^+$  ratio of 0.05, indicating the importance of the  $\text{K}^+:\text{Na}^+$  ratio to maintain the methanogenic activity under saline conditions (**Chapter 3**).

At high sodium concentrations, calcium displacement from the biomass was observed in both the AnMBR and the UASB reactor under the same loading conditions. The amount of  $\text{Ca}^{2+}$  washed out from the UASB biomass was high at  $26 \text{ gNa}^+\cdot\text{L}^{-1}$ . Our results showed that  $\text{Ca}^{2+}$  leaching is related to the applied salinity level and biomass properties rather than to reactor configuration. However, in the UASB the  $\text{Ca}^{2+}$  leaching led to deflocculation and failure of the treatment system. Results clearly showed that an AnMBR with full biomass retention exhibited higher stability than the UASB under high salinity stress (**Chapter 5**).

## 8.1.2 High temperature: from mesophilic to thermophilic operation

### 8.1.2.1 Temperature susceptibility

Besides high salinity and the presence of toxic compounds, high temperature is similarly a challenging extreme condition for industrial chemical wastewater treatment. The temperature susceptibility of an AnMBR to stepwise temperature increase by 5°C from 35 °C to 55 °C at 16 gNa<sup>+</sup>·L<sup>-1</sup> showed that the phenol conversion process was less susceptible than methanogenesis. Phenol conversion rate dropped from 3.2 at 35 °C to 1.7 mgPh·gVSS<sup>-1</sup>·d<sup>-1</sup> at 55 °C, while the overall COD removal efficiency decreased from about 99.8% at 35°C to 38.0% at 55°C. Apparently, the phenol converting bacteria have a wider upward temperature span than the methanogenic Archaea. The upper-temperature limit (45°C) for mesophilic operation was associated with the decrease in microbial abundance of the phyla Firmicutes and Proteobacteria, which are linked to syntrophic phenol degradation. Eleven operational taxonomic units from the reactor's microbial community, which are linked to the degradation of aromatics, showed temperature differential abundance.

Furthermore, the membrane filtration performance was negatively affected by the temperature increase concomitant with a 77% decrease in biomass mean particle size and a higher content of microbial protein-like substances. Under mesophilic and hyper-mesophilic conditions (42-45°C), the phenol conversion rate of the AnMBR at high salinity was more stable than under thermophilic conditions. Our findings indicated that at high salinity a mesophilic AnMBR can tolerate a temperature of up to 45 °C without being limited in the phenol conversion capacity (**Chapter 6**).

### 8.1.2.2 Thermophilic long-term operation

Few studies investigated the conversion of phenolic wastewaters under thermophilic conditions with anaerobic reactors. Because it is unclear whether or not a stable phenol-degrading methanogenic consortium may develop at 55 °C, the maximum conversion capacity of an AnMBR during long-term operation at 55°C, at 18 gNa<sup>+</sup>·L<sup>-1</sup> was determined. COD and phenol removal efficiencies of about 95% were achieved. However, by exceeding a phenol loading rate of 20 mgPh·gVSS<sup>-1</sup>·d<sup>-1</sup> the phenol concentration increased in the reactor, leading to substantial deterioration of methanogenesis.

Our work was the first to investigate the limits of the phenol conversion capacity for suspended biomass under thermophilic conditions in an AnMBR. Moreover, it linked the microbial community structure and thermophilic degradation activity of phenol at high salinity. The hydrogenotrophic methanogenic activity was 2.3 times higher than the acetate-fed methanogenic activity. Correspondingly, hydrogenotrophic methanogens were enriched, while the aceticlastic *Methanoseta* species decreased in relative abundance (**Chapter 7**). Our findings showed that highly saline phenolic wastewaters could be treated in a thermophilic AnMBR. Additionally, the thermophilic operation of AnMBR could bring operational energy benefits, when treating high-temperature industrial wastewaters with the target of process water reuse towards a more circular chemical industry. The possibility of efficient chemical wastewater treatment under the studied challenging

conditions would represent a major breakthrough for the widespread application of AnMBR technology

In summary, the results from this thesis provide a solid basis for further research and application of the AnMBR for treating chemical wastewaters with high salinity, high temperature and presence of toxic compounds, overcoming the limitations of conventional high-rate anaerobic sludge bed reactors.

However promising, research of phenolic-rich industrial wastewaters with AnMBRs is still very limited. Despite recent progress, applicability and reliability with more complex wastewaters need further research, focusing on other phenolic or aromatic compounds, to ensure a satisfactory reactor conversion capacity as well as strategies to maintain sustainable filtration performance for large-scale applications when extreme conditions deteriorate the biomass characteristics.

## 8.2 Perspectives and Recommendations for future research

Pilot and full-scale plants treating industrial wastewater have demonstrated higher COD to methane conversion efficiencies in AnMBRs in comparison to commonly applied sludge bed reactors (Bianco et al. 2021, Christian et al. 2011, Futselaar et al. 2013, van Lier et al. 2015). The challenge for future research is to find the optimum operational conditions for enhanced bioconversion under extreme conditions without being limited by low membrane fluxes. This will increase the feasibility of AnMBR technology, thereby accelerating its full-scale application. Applying the AnMBR may distinctly reduce treatment costs of extreme chemical wastewaters. Moreover, particularly in those countries where surface water protection laws are limitedly developed or not effectively enforced, pollution by industrial chemical effluents can be reduced, and the treated water can be easily reclaimed as process water, being an alternative source for existing freshwater resources in industrial processes.

Based on the findings described in this dissertation, aspects that deserve attention and require further research are proposed as following:

- The maximum bioconversion capacity of an AnMBR should be further assessed, applying high specific phenol loading rates and low hydraulic retention times. Moreover, investigating further the effects of co-substrates, such as volatile fatty acids (VFAs), could open opportunities for the use of low-value biodegradable waste streams as additional carbon and energy sources. Co-substrates can enhance the phenol conversion when dealing with chemical wastewaters, and promote the development of a highly active phenol degrading biomass (García Rea et al. 2020).
- The research conducted in this thesis used phenol as a model compound representing aromatic compounds in industrial chemical wastewaters. However, most of the waste streams in the petrochemical sector contain besides phenol, other aromatics such as its derivatives cresol and resorcinol, that are regarded as toxic or inhibitory compounds. Therefore, multi-component research of phenolics (Chen et al. 2016, Franchi et al. 2018, Garcia Rea et al. 2021,

Guiot et al. 2000, Razo-Flores et al. 2003, Ren et al. 2019, Wang and Han 2012), that not necessarily share the same degradation pathways as phenol should be carried out. Research focusing on loading thresholds and inhibitory concentrations of more complex multicomponent wastewaters in AnMBRs is required. Therefore, pilot and feasibility studies of AnMBR applications for the treatment of real phenolic wastewaters, considering pretreatment as well as post-treatment, are encouraged to be carried out for further optimization. Concomitantly, the predictive value of laboratory research using synthetic wastewater could be verified.

- When phenol shocks were present and caused reactor performance perturbation, differences between permeate and reactor broth phenol concentrations of more than 5% were observed, suggesting a likely contribution in bioconversion of the formed cake layer on the membrane surface. Consequently, the contribution of the cake layer to the overall phenolic conversion under extreme conditions should be further investigated. The latter may imply that the application of anaerobic dynamic membrane bioreactors (AnDMBRs) could become important, especially when high fluxes are not required for chemical wastewaters. Thus far, AnDMBRs studies for the treatment of high-strength wastewaters are still very limited (Ersahin et al. 2014).
- Previous studies have shown that under thermophilic conditions anaerobic phenol conversion might occur via *n*-caproate (Evans and Fuchs 1988, Fang et al. 2006). In contrast, other studies have demonstrated (Hoyos-Hernandez et al. 2014) and suggested (Limam et al. 2013, Muñoz Sierra et al. 2020) that phenol degradation via benzoate is possibly similar under both thermophilic and mesophilic conditions. Because this is still an ongoing debate, further research should determine analytically benzoate and other phenol degradation intermediates in the AnMBR. In such research, elucidating the rate-limiting step is crucial, especially when intermediates accumulation is the cause for low phenolic removal performance.
- Bioaugmentation has been extensively documented in relation to anaerobic digestion and municipal wastewater treatment. However, few comprehensive studies have been conducted on its application in industrial chemical wastewater treatment (Fang et al. 2013, Park et al. 2008, Wu et al. 2019). In AnMBRs, bioaugmentation could be enhanced in-situ because the membrane effectively retains all biomass, thereby keeping specialized microbial populations for proper augmentation. It is therefore recommended to further investigate the potentials for bioaugmentation using AnMBRs in industrial wastewater treatment to meet specific challenges, such as the degradation of refractory organics.
- As an alternative to syntrophic metabolism via interspecies hydrogen or formate transfer, direct interspecies electron transfer (DIET) could effectively maintain the methanogenic consortia stable under stress conditions (Jin et al. 2019). Conductive materials to promote DIET, including metal-based materials such as zero-valent iron (ZVI), have been used as a reductive agent to treat refractory organic pollutants including phenolics (Wang et al. 2016,

Xiao et al. 2013, Xu et al. 2020). Also, magnetite ( $\text{Fe}_3\text{O}_4$ ) has shown to enhance DIET (Huang et al. 2018, Lei et al. 2018, Ma et al. 2021, Zhao et al. 2018), and, in combination with ZVI, magnetite has shown to stimulate syntrophic acetate oxidation combined with hydrogenotrophic methanogenesis to enhance phenol conversion to methane under mesophilic conditions (He et al. 2019). Other conductive carbon-based materials also have been shown to improve the efficiency of anaerobic digestion by promoting DIET (Li et al. 2020, Martins et al. 2018). Therefore, the stimulation of DIET to enhance the degradation of phenolic compounds in chemical wastewaters under high temperature and high salinity conditions should be investigated.

- Even though NaCl is the most widely apparent salt in chemical industry wastewaters, other salts can also contribute to the salinity of the wastewater (De Vrieze et al. 2016). In order to compare results across different studies, it is recommended that further research at high and fluctuating salinity includes measured osmotic pressure and electrical conductivity, rather than only sodium concentrations or total dissolved solids. In addition, further research should include salinity fluctuations at a lower HRT in the AnMBR, meaning more severe changes in osmotic pressure. The latter will also provide insight in research of AnMBRs coupled to forward osmosis as a pre-concentration step, with high reverse solute fluxes (Vinardell et al. 2020).
- The impact of large salinity fluctuations on biomass characteristics, such as the decrease in particle size, increase in capillary suction time, or increase in soluble microbial products (SMP), should be minimized. Quorum quenching promotes enzymatic and bacterial degradation in the reactor. This technique shows potential in controlling fouling by degrading EPS and SMP (De Vela 2021, Liu et al. 2021, Shahid et al. 2020). It is also recommended to further investigate the addition of certain flux enhancers to guarantee sustainable fluxes at full-scale applications thereby maintaining high microbial activity (Odriozola et al. 2021, Odriozola et al. 2020). Short-term cross-flow filtration tests using the anaerobic Delft filtration characterization method (AnDFCm) (Lousada-Ferreira et al. 2017) with biomass at different salinities or osmotic pressure could be used to study the relationship between filterability and biomass characteristics, and introduce a control strategy for optimal online flux enhancer dosage to maintain fluxes and resistance to filtration. Further research is needed to find practical solutions to mitigate membrane fouling (Sohn et al. 2021) and improve fluxes.
- Trace metals supplementation in anaerobic reactors is a critical, complex, and technical challenge. Despite the recognized importance of trace elements for successful anaerobic degradation (Fermoso et al. 2019), the chemistry and speciation behind the accessibility of trace elements for biological uptake is poorly understood. Because extreme conditions such as high temperature demand trace metals optimization (Hendriks et al. 2018), further research is required to focus on an efficient trace metals dosing strategy (Weiss et al. 2019) taking into account the AnMBR operating conditions and the wastewater characteristics such as high salinity and toxicity.

## References

- Bianco, F., Race, M., Forino, V., Pacheco-Ruiz, S. and Rene, E.R. (2021) Waste Biorefinery. Bhaskar, T., Varjani, S., Pandey, A. and Rene, E.R. (eds), pp. 103-124, Elsevier.
- Chen, Y., He, J., Wang, Y.-Q., Kotsopoulos, T.A., Kaparaju, P. and Zeng, R.J. (2016) Development of an anaerobic co-metabolic model for degradation of phenol, m-cresol and easily degradable substrate. *Biochemical Engineering Journal* 106, 19-25.
- Christian, S., Grant, S., McCarthy, P., Wilson, D. and Mills, D. (2011) The First Two Years of Full-Scale Anaerobic Membrane Bioreactor (AnMBR) Operation Treating High-Strength Industrial Wastewater. *Water Practice and Technology* 6(2).
- De Vela, R.J. (2021) A review of the factors affecting the performance of anaerobic membrane bioreactor and strategies to control membrane fouling. *Reviews in Environmental Science and Bio/Technology*.
- De Vrieze, J., Coma, M., Debeuckelaere, M., Van der Meeren, P. and Rabaey, K. (2016) High salinity in molasses wastewaters shifts anaerobic digestion to carboxylate production. *Water Research* 98, 293-301.
- Ersahin, M.E., Ozgun, H., Tao, Y. and van Lier, J.B. (2014) Applicability of dynamic membrane technology in anaerobic membrane bioreactors. *Water Research* 48, 420-429.
- Evans, W.C. and Fuchs, G. (1988) Anaerobic degradation of aromatic compounds. *Annu Rev Microbiol* 42, 289-317.
- Fang, F., Han, H., Zhao, Q., Xu, C. and Zhang, L. (2013) Bioaugmentation of biological contact oxidation reactor (BCOR) with phenol-degrading bacteria for coal gasification wastewater (CGW) treatment. *Bioresource Technology* 150, 314-320.
- Fang, H.H.P., Liang, D.W., Zhang, T. and Liu, Y. (2006) Anaerobic treatment of phenol in wastewater under thermophilic condition. *Water Research* 40(3), 427-434.
- Fermoso, F.G., van Hullebusch, E., Collins, G., Roussel, J., Mucha, A.P. and Esposito, G. (2019) *Trace Elements in Anaerobic Biotechnologies*, IWA Publishing.
- Franchi, O., Rosenkranz, F. and Chamy, R. (2018) Key microbial populations involved in anaerobic degradation of phenol and p-cresol using different inocula. *Electronic Journal of Biotechnology* 35, 33-38.
- Futselaar, H., Rosink, R., Smith, G. and Koens, L. (2013) The anaerobic MBR for sustainable industrial wastewater management. *Desalination and Water Treatment* 51(4-6), 1070-1078.
- García Rea, V.S., Egerland-Bueno, B., Cerqueda-García, D., Muñoz Sierra, J.D., Spanjers, H. and van Lier, J.B. (2021) Degradation of p-cresol, resorcinol, and phenol in anaerobic membrane bioreactors under saline conditions. *Chemical Engineering Journal*, 132672.
- García Rea, V.S., Muñoz Sierra, J.D., Fonseca Aponte, L.M., Cerqueda-García, D., Spanjers, H. and Van Lier, J.B. (2020) Enhancing phenol conversion rates in saline anaerobic membrane bioreactor using acetate and butyrate as additional carbon and energy sources. *Frontiers in Microbiology* 11, 2958.
- Guiot, S.R., Tawfik-Hájjí, K. and Lépine, F. (2000) Immobilization strategies for bioaugmentation of anaerobic reactors treating phenolic compounds. *Water Science and Technology* 42(5-6), 245-250.
- He, C., Lin, W., Zheng, X., Wang, C., Hu, Z. and Wang, W. (2019) Synergistic effect of magnetite and zero-valent iron on anaerobic degradation and methanogenesis of phenol. *Bioresource Technology* 291, 121874.
- Hendriks, A.T.W.M., van Lier, J.B. and de Kreuk, M.K. (2018) Growth media in anaerobic fermentative processes: The underestimated potential of thermophilic fermentation and anaerobic digestion. *Biotechnology Advances* 36(1), 1-13.
- Hoyos-Hernandez, C., Hoffmann, M., Guenne, A. and Mazeas, L. (2014) Elucidation of the thermophilic phenol biodegradation pathway via benzoate during the anaerobic digestion of municipal solid waste. *Chemosphere* 97, 115-119.

- Huang, B., Wang, H.-C., Cui, D., Zhang, B., Chen, Z.-B. and Wang, A.-J. (2018) Treatment of pharmaceutical wastewater containing  $\beta$ -lactams antibiotics by a pilot-scale anaerobic membrane bioreactor (AnMBR). *Chemical Engineering Journal* 341, 238-247.
- Jin, Z., Zhao, Z. and Zhang, Y. (2019) Potential of direct interspecies electron transfer in synergetic enhancement of methanogenesis and sulfate removal in an up-flow anaerobic sludge blanket reactor with magnetite. *Science of The Total Environment* 677, 299-306.
- Lei, Y., Wei, L., Liu, T., Xiao, Y., Dang, Y., Sun, D. and Holmes, D.E. (2018) Magnetite enhances anaerobic digestion and methanogenesis of fresh leachate from a municipal solid waste incineration plant. *Chemical Engineering Journal* 348, 992-999.
- Li, Q., Gao, X., Liu, Y., Wang, G., Li, Y.-Y., Sano, D., Wang, X. and Chen, R. (2020) Biochar and GAC intensify anaerobic phenol degradation via distinctive adsorption and conductive properties. *Journal of Hazardous Materials*, 124183.
- Limam, I., Mezni, M., Guenne, A., Madigou, C., Driss, M.R., Bouchez, T. and Mazéas, L. (2013) Evaluation of biodegradability of phenol and bisphenol A during mesophilic and thermophilic municipal solid waste anaerobic digestion using  $^{13}\text{C}$ -labeled contaminants. *Chemosphere* 90(2), 512-520.
- Liu, J., Sun, F., Zhang, P. and Zhou, Y. (2021) Integrated powdered activated carbon and quorum quenching strategy for biofouling control in industrial wastewater membrane bioreactor. *Journal of Cleaner Production* 279, 123551.
- Lousada-Ferreira, M., Odriozola, M., Spanjers, H. and van Lier, J.B. (2017) On-line filterability measurements in anaerobic membrane bioreactors, Québec City, Québec, Canada.
- Ma, W., Li, J., Zhong, D., Ge, X., Li, K., Dai, C. and Gao, Y. (2021) New insights into enhanced anaerobic degradation of coal gasification wastewater (CGW) with the assistance of magnetite nanoparticles. *Chemosphere* 262, 127872.
- Martins, G., Salvador, A.F., Pereira, L. and Alves, M.M. (2018) Methane Production and Conductive Materials: A Critical Review. *Environmental Science & Technology* 52(18), 10241-10253.
- Muñoz Sierra, J.D., García Rea, V.S., Cerqueda-García, D., Spanjers, H. and van Lier, J.B. (2020) Anaerobic Conversion of Saline Phenol-Containing Wastewater Under Thermophilic Conditions in a Membrane Bioreactor. *Frontiers in Bioengineering and Biotechnology* 8(1125).
- Odriozola, M., Lousada-Ferreira, M., Spanjers, H. and van Lier, J.B. (2021) Effect of sludge characteristics on optimal required dosage of flux enhancer in anaerobic membrane bioreactors. *Journal of Membrane Science* 619, 118776.
- Odriozola, M., Morales, N., Vazquez-Padin, J., Lousada Ferreira, M., Spanjers, H., van Lier, J. and Val del Río, Á. (2020) Fouling Mitigation by Cationic Polymer Addition into a Pilot-Scale Anaerobic Membrane Bioreactor Fed with Blackwater. *Polymers* 12, 2383.
- Park, D., Lee, D.S., Kim, Y.M. and Park, J.M. (2008) Bioaugmentation of cyanide-degrading microorganisms in a full-scale cokes wastewater treatment facility. *Bioresource Technology* 99(6), 2092-2096.
- Razo-Flores, E.a., Iniestra-González, M., Field, J.A., Olguín-Lora, P. and Puig-Grajalas, L. (2003) Biodegradation of Mixtures of Phenolic Compounds in an Upward-Flow Anaerobic Sludge Blanket Reactor. *Journal of Environmental Engineering* 129(11), 999-1006.
- Ren, J., Li, J., Li, J., Chen, Z. and Cheng, F. (2019) Tracking multiple aromatic compounds in a full-scale coking wastewater reclamation plant: Interaction with biological and advanced treatments. *Chemosphere* 222, 431 - 439.
- Shahid, M.K., Kashif, A., Rout, P.R., Aslam, M., Fuwad, A., Choi, Y., Banu J, R., Park, J.H. and Kumar, G. (2020) A brief review of anaerobic membrane bioreactors emphasizing recent advancements, fouling issues and future perspectives. *Journal of Environmental Management* 270, 110909.

- Sohn, W., Guo, W., Ngo, H.H., Deng, L., Cheng, D. and Zhang, X. (2021) A review on membrane fouling control in anaerobic membrane bioreactors by adding performance enhancers. *Journal of Water Process Engineering* 40, 101867.
- van Lier, J.B., van der Zee, F.P., Frijters, C.T.M.J. and Ersahin, M.E. (2015) Celebrating 40 years anaerobic sludge bed reactors for industrial wastewater treatment. *Reviews in Environmental Science and Bio/Technology* 14(4), 681-702.
- Vinardell, S., Astals, S., Peces, M., Cardete, M.A., Fernández, I., Mata-Alvarez, J. and Dosta, J. (2020) Advances in anaerobic membrane bioreactor technology for municipal wastewater treatment: A 2020 updated review. *Renewable and Sustainable Energy Reviews* 130, 109936.
- Wang, W. and Han, H. (2012) Recovery strategies for tackling the impact of phenolic compounds in a UASB reactor treating coal gasification wastewater. *Bioresource Technology* 103(1), 95-100.
- Wang, W., Wang, S., Zhang, J., Hu, Z., Zhang, X. and Muñoz Sierra, J. (2016) Degradation kinetics of pentachlorophenol and changes in anaerobic microbial community with different dosing modes of co-substrate and zero-valent iron. *International Biodeterioration & Biodegradation* 113, 126-133.
- Weiss, S., Ustak, S., Guibaud, G., Stamatelidou, K., Collins, G., Esposito, G., Wardak, C., Mucha, A.P., Savic, D. and Stres, B. (2019) Trace element supplementation as a management tool for anaerobic digester operation: benefits and risks: eBook.
- Wu, B., He, C., Yuan, S., Hu, Z. and Wang, W. (2019) Hydrogen enrichment as a bioaugmentation tool to alleviate ammonia inhibition on anaerobic digestion of phenol-containing wastewater. *Bioresource Technology* 276, 97-102.
- Xiao, X., Sheng, G.-P., Mu, Y. and Yu, H.-Q. (2013) A modeling approach to describe ZVI-based anaerobic system. *Water Research* 47(16), 6007-6013.
- Xu, W., Zhao, H., Cao, H., Zhang, Y., Sheng, Y., Li, T., Zhou, S. and Li, H. (2020) New insights of enhanced anaerobic degradation of refractory pollutants in coking wastewater: Role of zero-valent iron in metagenomic functions. *Bioresource Technology* 300, 122667.
- Zhao, Z., Zhang, Y., Li, Y., Quan, X. and Zhao, Z. (2018) Comparing the mechanisms of ZVI and Fe<sub>3</sub>O<sub>4</sub> for promoting waste-activated sludge digestion. *Water Research* 144, 126-133.







# Acknowledgments

It would not have been possible to publish this dissertation book without the contribution that several people had on my PhD journey. First of all, I am grateful to my promotors Prof. dr. ir. Jules van Lier and Dr. ir. Henri Spanjers for trusting me in developing my ideas and leading the Bioextreme Project. Your different approaches to carry out research contributed to enrich me as a scientist. Thank you Jules for your knowledgeable input and critical feedback. I found it always very positive to improve the quality of my research and motivate myself to strive for very good scientific journals and relevant scientific conferences. I still remember the first time we met. You were presenting in Colombia the latest advances from your research group as a total “anaerobic rockstar”. Thank you for, years later, letting me play in your “anaerobic rock band”, and enjoy being part of the international anaerobic scientific community. Thank you Henri for your efforts in keeping the project running longer than initially planned, which also broad opportunities to carry out more following-up research and extend my contribution. Thank you especially for your support to improve my writing communication skills. Your ironic remarks in each of the manuscripts have always encouraged me to communicate each message in a better way.

My sincere appreciation to the members of my defense committee for reading and assessing my PhD dissertation.

Also, I would like to thank Prof. dr. ir. Merle de Kreuk for selecting me to work on the AnMBRs research proposal. It was a pleasure to work with you during those eight months. I felt fortunate to have you around because of your enthusiasm that motivated me to continue working hard. I am grateful for your openness to scientific and personal discussions and your talent in finding the right words when facing challenges. Without a doubt, you have been the best Sinterklaas ever!

I owe special thanks to my colleagues with whom I had the pleasure to work, especially Marjet, Wei Wang, Victor, Daniel, and Carlos. Thank you all for helping me to go through the different research questions, for the support and motivation to complete the different experiments, analysis of results, and discussions. I enjoyed very much working with you and I am looking forward to collaborating with you in the future. Thanks to all the intern students who supported me in one way or another with the lab work: Emilien, Basak, Juan, Mertixell, Jonathan, Bart, and Francesc.

I would like to thank as well to the BioXtreme project steering committee, MSc. ir. Carla Frijers, Dr. ir. Niels Groot, Dr. Caroline Plugge, and Ir. Jan Willem Mulder, for your suggestions, feedback, and encouragement after each of the progress meetings.

I thank all colleagues from the Department of Water Management for the wonderful time spent throughout this long journey, for all the good vibes, lunches, trips, conferences, parties, research, and talks about life. There were a lot of people that I had the opportunity to share great moments with, without any particular order: Astrid, Mostafa, Feifei, Wilton, Maria, Xuedong, Hong-Xiao, Evren, Hale, Zhong Bo, Ran, Peng, Yu Tao, Zhe Deng, Gang Liu, Alexander, Guido, Steef, Dara, Andre, Juan Pablo, Andres, Magela, Pamela, Tales, Frans, Javier, Adrian, Sara, Niels, and Ralph.

Also to my colleagues from Environmental Biotechnology: Robbert Kleerebezem, Mark van Loodsrecht, Shiva, Emmanuella, etc. for the nice talks, advices, tennis matches, and fun around scientific life. I am very glad I got to know you guys. My sincere thanks to the Sanitary Engineering section staff for doing their best in making our PhD life easier, especially to our lab technicians Mohammed, Armand, and Tonny. Moreover, to all the support staff who were always there to help and strive for having a nice working atmosphere in our department: Mariska, Luz, Jennifer, Tamara, and Sabrina. For sure, I may forget some people that I met during these years, thank you all.

I also would like to thank all my co-authors from different institutions for trusting me in contributing with ideas, scientific input, analysis of samples, results, and discussions on different joint-research papers. I truly enjoyed collaborating with you and feeling scientifically active in broader topics than only on my PhD research. Special thanks to Ran Mei and Wei Wang for welcoming me to Urbana-Champaign, USA, and Hefei, China, respectively.

I would like to thank all the Colombian friends in Delft for being a source of joy and happiness in the Netherlands: Caro, Ana, Andrea, Jorge, Esteban, Naty, Sebastian, Fidel, Cesar, Caro L., and Liz. I treasured all the good memories we had together. Also I thank to my former professor Darío Gallego, and group fellows from the National University of Colombia, Diana, Darío and Natalia for supporting me when I dreamed about pursuing research abroad and for sharing interesting initiatives. To all my housemates and friends from different nationalities, Jesse, Thomas, Felipe, Alicia, Julien, Miguel, Raquel, thank you for your patience after some difficult days in the lab, the nice dinners together, drinks, movies, trips, and all the good moments.

Este logro no hubiera sido posible sin el amor, el apoyo y la confianza incondicional de mi familia. No se imaginan cuantos días quise tenerlos mas cerca para poder sobrepasar con mayor alegría todas aquellas dificultades que se presentaron durante estos años. Gracias Mama, Papa, Hermanita, Hermano, Valentina, Hector y Abril por toda su fortaleza, optimismo, sacrificio y compañía en la distancia. Ciertamente este éxito es también de ustedes, los amo!.

And last but not least, my truly genuine gratitude to my beloved Sandra. MOR, you kept me all the time motivated towards the completion of my dissertation. I am very fortunate to have you by my side during this journey. It was a challenge to travel regularly from Delft to Hamburg and vice versa during those years, but it was also super cool and full of terrific adventures. Your support, happiness, encouragement, patience, and true love, made this journey more joyful. Ámote moito! Grazas tamén á miña segunda familia pola boa vida e as increíbles viaxes pola fascinante Galicia.

I am fully aware that it took me a while to finally get to this page of the book. I strived to have all my chapters published, but I have never expected the process to take so long and to struggle due to the slow writing and peer-review process. In the end, I managed and despite the timeline, I am very delighted with the outcome.

All in all, I am very grateful to have spent this amazing time of my life at the Delft University of Technology, a place that truly inspired me, taught me, where I felt very happy and that allowed me to find love and accomplish the dream of becoming a Doctor. I will always be proud of being part of it.

# Publications

## Peer-reviewed journals

- Muñoz Sierra, J.D.**, Oosterkamp, M.J., Spanjers, H. and van Lier, J.B. (2021) Effects of large salinity fluctuations on an anaerobic membrane bioreactor treating phenolic wastewater. *Chemical Engineering Journal* 417, art. no. 129263. DOI: 10.1016/j.ccej.2021.129263
- Muñoz Sierra, J.D.**, García Rea, V.S., Cerqueda-García, D., Spanjers, H., and van Lier, J.B. (2020) Anaerobic Conversion of Saline Phenol-Containing Wastewater Under Thermophilic Conditions in a Membrane Bioreactor. *Frontiers in Bioengineering and Biotechnology*, 8, art. no. 565311, DOI: 10.3389/fbioe.2020.565311
- Muñoz Sierra, J.D.**, Oosterkamp, M.J., Wang, W., Spanjers, H., and van Lier, J.B. (2019) Comparative performance of upflow anaerobic sludge blanket reactor and anaerobic membrane bioreactor treating phenolic wastewater: Overcoming high salinity. *Chemical Engineering Journal*, 366, pp. 480-490. DOI: 10.1016/j.ccej.2019.02.097
- Muñoz Sierra, J.D.**, Wang, W., Cerqueda-García, D., Oosterkamp, M.J., Spanjers, H., and van Lier, J.B. (2018) Temperature susceptibility of a mesophilic anaerobic membrane bioreactor treating saline phenol-containing wastewater. *Chemosphere*, 213, pp. 92-102. DOI: 10.1016/j.chemosphere.2018.09.023
- Muñoz Sierra, J.D.**, Oosterkamp, M.J., Wang, W., Spanjers, H., and van Lier, J.B. (2018) Impact of long-term salinity exposure in anaerobic membrane bioreactors treating phenolic wastewater: Performance robustness and endured microbial community. *Water Research*, 141, pp. 172 -184. DOI: 10.1016/j.watres.2018.05.006
- Muñoz Sierra, J.D.**, Lafita, C., Gabaldón, C., Spanjers, H., and van Lier, J.B. (2017) Trace metals supplementation in anaerobic membrane bioreactors treating highly saline phenolic wastewater. *Bioresource Technology*, 234, pp. 106-114. DOI: 10.1016/j.biortech.2017.03.032
- García Rea, V.S., Egerland-Bueno, B., Cerqueda-García, D., **Muñoz Sierra, J.D.**, Spanjers, H., and van Lier, J.B. (2021) Degradation of p-cresol, resorcinol, and phenol in anaerobic membrane bioreactors under saline conditions. *Chemical Engineering Journal*, 132672. DOI: 10.1016/j.ccej.2021.132672
- García Rea, V.S., **Muñoz Sierra, J.D.**, Fonseca Aponte, L.M., Cerqueda-García, D., Quchani, K.M., Spanjers, H., and van Lier, J.B. (2020) Enhancing Phenol Conversion Rates in Saline Anaerobic Membrane Bioreactor Using Acetate and Butyrate as Additional Carbon and Energy Sources. *Frontiers in Microbiology*, 11, art. no. 604173, DOI: 10.3389/fmicb.2020.604173
- Muñoz Sierra, J.D.**, Garcia-Rea, V.S., Spanjers, H., and van Lier, J.B. (2022). Recent progress in chemical wastewater treatment by anaerobic membrane bioreactors. *In preparation*.
- García-Rea, V.S., **Muñoz Sierra, J.D.**, El-Kalliny, A.S., Cerqueda Garcia, D., Lindeboom, R.E.F., Spanjers, H., and van Lier, J. B. (2021) Enhancing phenol conversion using acetate as additional

carbon and energy source in a thermophilic anaerobic membrane bioreactor under saline conditions. *In preparation*.

Garcia Rea, V. S., Egerland Bueno, B., Lopez Prieto, I. J., **Muñoz Sierra, J. D.**, Cerqueda Garcia, D., Nair, A., van Lier, J. B., and Spanjers, H. Assessment of bitumen fume condensate degradation in anaerobic membrane bioreactor. *In preparation*.

Garcia Rea, V.S., Huisman, D., Egerland Bueno, B., **Muñoz Sierra, J.D.**, Cerqueda Garcia, D., Spanjers, H., and van Lier, J. B. Biodegradability assessment of aniline under methanogenic and saline conditions in anaerobic membrane bioreactor. *In preparation*

Lousada-Ferreira, M., **Muñoz Sierra, J.D.**, Odriozola, M., Spanjers, H., and van Lier, J.B. Flux enhancers in anaerobic membrane bioreactors. *In preparation*

## Other peer-reviewed publications

Wang, J., Wu, B., **Muñoz Sierra, J.**, He, C., Hu, Z. and Wang, W. (2020) Influence of particle size distribution on anaerobic degradation of phenol and analysis of methanogenic microbial community. *Environmental Science and Pollution Research* 27(10), 10391-10403.

Ashrafi, E., Mehrabani Zeinabad, A., Borghei, S.M., Torresi, E. and **Muñoz Sierra, J.** (2019) Optimising nutrient removal of a hybrid five-stage Bardenpho and moving bed biofilm reactor process using response surface methodology. *Journal of Environmental Chemical Engineering* 7(1), 102861.

Wang, W., Pang, C., **Muñoz Sierra, J.**, Hu, Z. and Ren, X. (2019) Performance and recovery of a completely separated partial nitrification and anammox process treating phenol-containing wastewater. *Environmental Science and Pollution Research* 26(33), 33917-33926.

Mei, R., Nobu, M.K., Narihito, T., Kuroda, K., **Muñoz Sierra, J.**, Wu, Z., Ye, L., Lee, P.K.H., Lee, P.-H., van Lier, J.B., McInerney, M.J., Kamagata, Y. and Liu, W.-T. (2017) Operation-driven heterogeneity and overlooked feed-associated populations in global anaerobic digester microbiome. *Water Research* 124, 77-84.

Wang, W., Yang, K., **Muñoz Sierra, J.**, Zhang, X., Yuan, S. and Hu, Z. (2017) Potential impact of methyl isobutyl ketone (MIBK) on phenols degradation in an UASB reactor and its degradation properties. *Journal of Hazardous Materials* 333, 73-79.

Wang, W., Wang, S., Zhang, J., Hu, Z., Zhang, X. and **Muñoz Sierra, J.** (2016) Degradation kinetics of pentachlorophenol and changes in anaerobic microbial community with different dosing modes of co-substrate and zero-valent iron. *International Biodeterioration & Biodegradation* 113, 126-133.

Wang, W., Wang, S., Feng, J., Yuan, S., Hu, Z., **Muñoz Sierra, J.** and Zhang, X. (2016) Kinetics of hydroquinone oxidation by a wire-cylinder dielectric barrier discharge reactor. *Desalination and Water Treatment* 57(60), 29212-29219.

**Muñoz Sierra, J.D.**, Picioreanu, C. and van Loosdrecht, M.C.M. (2014) Modeling phototrophic biofilms in a plug-flow reactor. *Water Science and Technology* 70(7), 1261-1270

## **Oral and poster presentations in conferences/proceedings**

van Lier, J.B., Spanjers, H., **Muñoz Sierra, J.D.**, Garcia-Rea, V.S., and Odriozola, M. (2020) Innovations in Anaerobic Membrane Bioreactor Technology. *Environmental Technology for Impact*. Wageningen, The Netherlands, June 3-4. Oral Presentation.

**Muñoz Sierra J.D.**, Spanjers, H., and van Lier, J.B. (2019) Challenging high salinity chemical wastewater treatment by applying anaerobic membrane bioreactors. In: *Proc. of 16th IWA Anaerobic Digestion World Conference*, Delft, The Netherlands, June 23-27. Oral Presentation.

Garcia Rea, V.S., Fonseca Aponte, L.M., **Muñoz Sierra, J.D.**, Garcia Cerqueda, D., Spanjers, H., and van Lier, J.B. (2019) Acetate addition enhances phenol conversion rate and recovery time after phenol shock load in an anaerobic membrane bioreactor. In: *Proc. of 16th IWA Anaerobic Digestion World Conference*, Delft, The Netherlands, June 23-27. Poster.

Garcia Rea, V.S., **Muñoz Sierra, J.D.**, Oosterkamp, M.J., Lindeboom, R., Spanjers, H., and van Lier, J.B. (2018). Enhancement of phenol conversion rate by addition of acetate in a thermophilic anaerobic membrane bioreactor. In: *Proc. of IWA XIII Latin American Workshop and Symposium on Anaerobic Digestion*. Medellin, Colombia, October 21-24. Oral Presentation.

**Muñoz Sierra J.D.**, Oosterkamp, M.J., Garcia Rea, V.S., Wang, W., Spanjers, H., and van Lier J.B. (2017) Thermophilic Anaerobic Membrane Bioreactor treating saline phenolic wastewaters: temperature transition and long-term operation. In: *Proc. of 15th IWA Anaerobic Digestion World Conference*, Beijing, China, October 18-20. Poster.

**Muñoz Sierra, J.D.**, Oosterkamp, M.J., Wang, W., Spanjers, H., and van Lier, J.B. (2017) Comparison of AnMBR and UASB reactors for treating saline phenolic wastewater: overcoming extreme salinity. In: *Proc. of IWA 15th World Conference in Anaerobic Digestion*. Beijing, China, 17-20 October. Oral Presentation + Poster.

**Muñoz Sierra, J.D.**, Oosterkamp, M.J., Wang, W., Spanjers, H., and van Lier, J.B. (2017). Bioaugmentation in anaerobic membrane bioreactors treating saline phenolic wastewater. *1st Symposium on Microbiological Methods for Waste & Water Resource Recovery*. Delft, The Netherlands, May 18-19. Poster.

Garcia Rea V.S., **Muñoz Sierra, J.D.**, Oosterkamp, M.J., Spanjers, H., and van Lier, J.B. (2017) Phenolic wastewater treatment by an anaerobic membrane bioreactor. In: *Proc. of 15th IWA Anaerobic Digestion World Conference*, Beijing, China, October 18-20. Poster.

Oosterkamp, M.J., **Muñoz Sierra, J.D.**, Wang, W., Spanjers, H., van Lier, J.B. (2017) Microbial community dynamics of an anaerobic membrane bioreactor treating phenolic wastewater with high salinity under mesophilic and thermophilic temperature conditions. In: *Proc. of 3rd*

International Conference on Biogas Microbiology. Wageningen, The Netherlands, 1-3 May. Oral Presentation.

**Muñoz Sierra, J.D.**, Oosterkamp, M.J., Spanjers, H., and van Lier, J.B. (2016) Microbial community and diversity in Anaerobic Membrane Bioreactor treating highly saline phenolic wastewater. In: Proc. of IWA Microbial Ecology in Water Engineering and Biofilms specialist conference. Copenhagen, Denmark. September 4-7. Oral Presentation

**Muñoz Sierra, J.D.**, Oosterkamp, M.J., Wang, W., Spanjers, H., and van Lier, J.B. (2016) Effect of Temperature Transition on Structure and Performance of a Microbial Community Degrading Saline Phenolic Wastewater. In: Proc. of 16th International Symposium on Microbial Ecology. Montreal, Canada. August 21-25. Poster.

**Muñoz Sierra, J.D.**, Oosterkamp, M.J., Spanjers, H., and van Lier, J.B. (2016) Impact of Salinity Fluctuations on AnMBR treating phenolic wastewater. In: Proc. of 13th IWA Leading Edge Technologies conference. Jerez de la Frontera, Spain, June 13-16. Poster.

**Muñoz Sierra J.D.**, Wang, W., Spanjers, H., van Lier, J.B. (2015) Treatment of saline phenolic wastewater applying bio-augmentation in anaerobic membrane bioreactors. In: Proc. of IWA Anaerobic Digestion World Conference, Viña del Mar, Chile, November 15-18. Oral presentation + Poster

**Muñoz Sierra, J.D.**, Donmez, B., Spanjers, H., and van Lier, J.B. (2015) Salinity fluctuations in AnMBRs treating phenolic wastewater. 4th IWA Benelux Young Water Professionals conference. Leeuwarden, The Netherlands. September. Poster + Short Abstract

**Muñoz Sierra, J.D.**, Spanjers, H., van Lier J.B. (2014). Biomass acclimation during start-up of AnMBR reactors treating saline phenolic wastewater. In: Proc. IWA 11th Latin American Workshop and Symposium on Anaerobic Digestion. La Habana, Cuba, 25-28 November. Oral Presentation.



## About the Author

Julian David Muñoz Sierra was born in Medellín, Colombia. In 2007, he completed his five years Diploma degree in Chemical Engineering at the National University of Colombia, Medellín, with a two years track on Biotechnology. His one-year thesis entitled “Evaluation of an alkaline system applied to the upgrading of biogas to natural gas” was awarded as the best Chemical Engineering thesis from that year. After his graduation, he worked in the sanitary engineering laboratory from the Faculty of Mines and also as a consultant on the design, commissioning, and start-up of two drinking water treatment plants.



In the period 2008-2010, Julian worked as a project and R&D engineer at Tecniaguas®, one of the Colombian market leaders in industrial water and wastewater treatment. His duties ranged from researching emerging treatment technologies to process design, control & automation, plant commissioning, and management of turn-key projects for food, chemical, and petroleum companies.

At the end of 2010, he came to the Netherlands to pursue a Professional Doctorate in Bioprocess Engineering at the Department of Biotechnology at Delft University of Technology. He decided to follow this program since it focuses on advanced applied techniques and bioprocess design to develop and offer innovative solutions to the industry. He worked together with companies (DSM, Corbion, Siemens Water Technologies) and scientific advisors from BE-Basic foundation partners in design projects looking at novel and eco-efficient processes for the production of dicarboxylic acids and clean water. Julian conducted his PDEng research & design project at the Environmental Biotechnology group. He successfully implemented a phototrophic biofilm model to describe the microbial dynamics within the biofilm and along the reactor that was used for the design of a novel decentralized wastewater treatment system.

Julian joined the Department of Water Management to write a research proposal for the Watertech-2013 call, which was positively granted in February 2014 by STW (NWO) and became his PhD project (BioXtreme). He focused on the application of anaerobic membrane bioreactors in chemical industrial wastewater streams under high and fluctuating salinity, and high temperature. During his doctoral trajectory, Julian published several peer-reviewed journal publications, presented at multiple international conferences, and cooperated with researchers from diverse nationalities. He was also a visiting scholar at the University of Illinois at Urbana-Champaign during summer 2017. Additionally, from January 2018 onwards, he contributed to the development of the TU Delft Professional Education online course “High-rate anaerobic wastewater treatment” by developing the course material and coordinating tasks and lectures.

Since June 2018, Julian works as a Scientific Researcher and Project Manager at KWR Water

## About the author

Research Institute. He focuses on innovative treatment concepts and technologies (e.g., mainstream Anammox, forward osmosis coupled to anaerobic digestion, anaerobic treatment of high protein and FOG wastewater, new-sanitation routes, nanofiltration), and resource recovery (water, energy, metals, and nutrients). Moreover, he carries out consultancy projects of conceptual process design, troubleshooting and optimization, feasibility studies, and strategic technology selection of wastewater treatment and water reuse systems for industrial clients and municipalities in Europe, Latin America, and the Gulf region.

Julian is a very enthusiastic researcher who is always looking at new challenges, opportunities, and international cooperation.

